

CO<sub>2</sub> Revalorization for the  
Organocatalytic Synthesis of Cyclic  
Carbonates and Vanillin-Based Non-  
Isocyanate Polyurethanes (NIPUs)

**Marcos Noé Fanjul Mosteirín**

Submitted for the degree of Doctor of Philosophy



Department of Chemistry

December 2019

# Table of Contents

<b>List of Figures, Schemes and Tables</b> .....	<b>vii</b>
Figures.....	vii
Schemes.....	ix
Tables.....	xii
<b>Acknowledgments</b> .....	<b>xiv</b>
<b>Declaration of authorship</b> .....	<b>xvi</b>
<b>List of Publications</b> .....	<b>xvii</b>
<b>List of Abbreviations</b> .....	<b>xviii</b>
<b>Abstract</b> .....	<b>xxi</b>
<b>1. Introduction</b> .....	<b>1</b>
1.1 CO <sub>2</sub> .....	2
1.1.1 CO <sub>2</sub> and the greenhouse effect.....	2
1.1.2 CO <sub>2</sub> thermodynamics.....	3
1.1.3 CO <sub>2</sub> use for chemical processes.....	4
1.1.4 Synthesis of five-membered cyclic carbonates using CO <sub>2</sub> and epoxides.....	5
1.1.5 Synthesis of five-membered cyclic carbonates promoted by organometallic catalysts.....	6
1.1.6 Synthesis of five-membered cyclic carbonates promoted by organocatalysts...7	
1.1.6.1 Synthesis of five-membered cyclic carbonates promoted by nitrogen-based heterocycles.....	7
1.1.6.2 Synthesis of five-membered cyclic carbonates promoted by organic salts, molten salts and ionic liquids.....	10
1.1.6.3 Synthesis of five-membered cyclic carbonates promoted by polyphenolic and polyhydroxy compounds.....	12
1.2 Synthesis of non-isocyanate polyurethanes (NIPU).....	13

1.2.1 Synthesis of poly(hydroxyurethanes) by step-growth polymerization of bis-cyclic carbonates and bis-amines.....	16
1.3 Renewable polymer feedstock.....	20
1.3.1 Feedstocks derived from cellulose and hemicellulose.....	21
1.3.1.1 5-Hydroxymethylfurfural (HMF).....	22
1.3.1.2 Lactic acid.....	23
1.3.2 Feedstocks derived from lignin.....	25
1.3.2.1 Vanillin.....	26
1.4 Conclusions.....	29
1.5 References.....	30
<b>2. Organocatalytic synthesis of cyclic carbonates using DBU derivatives.....</b>	<b>40</b>
2.1 Introduction.....	41
2.2 Results and discussion.....	44
2.2.1 Synthesis of DBU salts.....	44
2.2.2 Catalyst screening, optimization and synthesis of functional cyclic carbonates.....	45
2.2.3 Computational calculations.....	51
2.3 Conclusions.....	54
2.4 References.....	55
<b>3. Novel guanidinium salts as organocatalysts for the synthesis of cyclic carbonates from epoxides and CO<sub>2</sub>.....</b>	<b>58</b>
3.1 Introduction.....	59
3.2 Results and discussion.....	63
3.2.1 Synthesis of guanidinium iodide salts.....	63
3.2.2 Catalyst screening and optimization.....	64
3.2.3 Anion influence study.....	68
3.2.4 Reaction mechanism.....	70

3.3 Conclusions.....	73
3.4 References.....	73
<b>4. Synthesis of non-isocyanate poly(hydroxy urethane) (NIPU) from vanillin.....</b>	<b>76</b>
4.1 Introduction.....	77
4.2 Results and discussion.....	79
4.2.1 Dakin oxidation of vanillin.....	79
4.2.2 Glycidylation reactions.....	81
4.2.3 Organocatalytic CO <sub>2</sub> insertion into bis-glycidyl intermediates.....	83
4.2.4 Synthesis of NIPUs from bis-carbonate vanillin derivatives.....	85
4.3 Conclusions.....	91
4.4 References.....	91
<b>5. Waterborne synthesis of non-isocyanate poly(hydroxy urethanes) thermo-responsive hydrogels.....</b>	<b>94</b>
5.1 Introduction.....	95
5.2 Results and discussion.....	98
5.2.1 Synthesis of five and eight-membered cyclic carbonate and kinetic study of their reactivity with PEG diamines in water.....	98
5.2.2 Gelation process.....	100
5.2.3 Water influence in the gelation process.....	102
5.2.4 Crosslinker-PEG diamine ratio influence.....	104
5.2.5 Temperature influence study.....	105
5.2.6 Thermo responsive behaviour and 3D printing.....	106
5.2.7 3D printing.....	108
5.3 Conclusions.....	109
5.4 References.....	109
<b>6. Experimental.....</b>	<b>112</b>
6.1 Materials.....	113

6.2 Instrumentation.....	113
6.3 Experimental protocols for Chapter 2.....	114
6.3.1 General procedure for the synthesis of [HDBU]X X = Halide salts.....	114
6.3.2 General procedure for the synthesis of [HDBU]X (X = BF <sub>4</sub> , PhCO <sub>2</sub> , MsO, TfO, TsO) salts.....	115
6.3.3 General procedure for the synthesis of [R-DBU]X salts.....	117
6.3.4 General method for the synthesis of five-membered cyclic carbonates.....	120
6.3.5 Computational details.....	122
6.4 Experimental protocols for Chapter 3.....	122
6.4.1 General procedure for the synthesis of guanidines.....	122
6.4.2 General procedure for the synthesis of guanidinium salts.....	124
6.4.3 General method for the synthesis of five-membered cyclic carbonates.....	128
6.5 Experimental protocols for Chapter 4.....	129
6.5.1 Synthesis of methoxyhydroquinone (2).....	129
6.5.2 Synthesis of vanillyl alcohol (4).....	129
6.5.3 General method for synthesis of bis epoxides.....	130
6.5.4 General method for the synthesis of bis carbonates.....	132
6.5.5 General method for the synthesis of NIPUs.....	134
6.6 General protocols for Chapter 5.....	137
6.6.1 Synthesis of bis cyclic carbonates.....	137
6.6.1.1 Synthesis of 6,6'-(ethane-1,2-diyl)bis(1,3,6-dioxazocan-2-one) (1).....	137
6.6.1.2 Synthesis of 4,4'-(oxybis(methylene))bis(1,3-dioxolan-2-one) (2).....	138
6.6.2 Synthesis of linear poly(hydroxy urethane).....	138
6.6.3 Synthesis of poly(hydroxy urethane) hydrogels.....	138
6.6.4 3D printing of hydrogels.....	139
6.7 References.....	139

<b>A. Appendix: Supplementary Information.....</b>	<b>141</b>
A.1 Supplementary NMR spectra for Chapter 2.....	142
A.2 Supplementary NMR spectra for Chapter 3.....	164
A.3 Supplementary NMR spectra for Chapter 4.....	178
A.4 Supplementary NMR spectra for Chapter 5.....	192

# List of Figures, Schemes and Tables

## Figures

- Figure 1.1.** Keeling curve representing the carbon dioxide concentration in Earth's atmosphere.....2
- Figure 1.2.** Solar radiation spectrum (adapted from Ref 2).....3
- Figure 1.3.** Gibbs free energy of formation of depicted chemicals (*left*), thermodynamics of some CO<sub>2</sub> reactions (*right*) (adapted from Refs 4 and 5).....4
- Figure 1.4.** Most representative imidazolium-based catalysts for the synthesis of five-membered cyclic carbonates.....9
- Figure 1.5.** Examples of organic salts and ionic salts catalysts used for the synthesis of five-membered cyclic carbonates (adapted from Ref 29).....10
- Figure 1.6.** Examples of polyphenolic and polyalcohol compounds as organocatalysts for CO<sub>2</sub> insertion reaction into epoxides.....13
- Figure 1.7.** Components of lignocellulose.....20
- Figure 2.1.** <sup>1</sup>H NMR spectra of DBU (*top*) and the resultant [HDBU]I catalyst (*bottom*). (300 MHz, 298 K, CDCl<sub>3</sub>).....44
- Figure 2.2.** <sup>1</sup>H NMR spectrum of crude reaction for the synthesis of styrene carbonate from styrene oxide using 10 mol% of [HDBU]I at 70 °C for 4 hours (\* corresponds to [HDBU]I) (300 MHz, 298 K, CDCl<sub>3</sub>).....46
- Figure 2.3.** <sup>1</sup>H NMR spectrum of isolated styrene carbonate by flash column chromatography in silica gel (*top*) (300 MHz, 298 K, CDCl<sub>3</sub>). <sup>13</sup>C APT NMR spectrum of isolated styrene carbonate by flash column chromatography in silica gel (*bottom*) (75 MHz, 298 K, CDCl<sub>3</sub>).....49
- Figure 2.4.** Conversion of allyl glycidyl ether from recycled catalyst.....51
- Figure 2.5.** Energy profile for TS1 considering mechanism pathway (a). In the left, comparison between attack 1 and 2 when reaction is catalysed using [HDBU]I. In the right, comparison between [HDBU]Cl, [HDBU]Br and [HDBU]I for attack 1.....53

<b>Figure 2.6.</b> Energy profile for the formation of 4-methyl-1,3-dioxolan-2-one from propylene oxide and CO <sub>2</sub> catalysed by [HDBU]I considering pathway (a) and attack 1	54
<b>Figure 3.1.</b> Examples of relevant guanidine-containing molecules present in nature	59
<b>Figure 3.2.</b> <sup>1</sup> H NMR spectra of DCC ( <i>top</i> ), the resultant guanidine <b>4</b> after reaction with imidazole ( <i>middle</i> ) and guanidinium salt <b>9</b> catalyst ( <i>bottom</i> ). (400 MHz, 298 K, DMSO)	64
<b>Figure 3.3.</b> <sup>1</sup> H NMR spectrum of crude reaction for the synthesis of styrene carbonate from styrene oxide using 1 mol% of <b>9</b> at 90 °C for 24 hours (* corresponds to <b>9</b> ) (300 MHz, 298 K, CDCl <sub>3</sub> )	67
<b>Figure 3.4.</b> <sup>1</sup> H NMR spectrum of crude reaction for the synthesis of styrene carbonate from styrene oxide using 1 mol% of <b>14</b> at 90 °C for 24 hours ( <i>top</i> ) (* corresponds to <b>14</b> ) (300 MHz, 298 K, CDCl <sub>3</sub> ). <sup>1</sup> H NMR spectrum of crude reaction for the synthesis of styrene carbonate from styrene oxide using 1 mol% of <b>15</b> at 90 °C for 24 hours ( <i>bottom</i> ) (* corresponds to <b>15</b> ) (300 MHz, 298 K, CDCl <sub>3</sub> )	70
<b>Figure 3.5.</b> Possible geometrical conformations for catalyst <b>9</b> . In red, conformations with a low influence in the reaction mechanism, in blue, conformations with a moderate influence in the reaction mechanism, in green, conformations with a high influence in the reaction mechanism	71
<b>Figure 4.1.</b> Monolignol precursors for the biosynthesis of lignin	78
<b>Figure 4.2.</b> <sup>1</sup> H NMR spectrum of compound <b>6</b> (300 MHz, 298 K, CDCl <sub>3</sub> ) ( <i>top</i> ). <sup>13</sup> C APT NMR spectrum of compound <b>6</b> (75 MHz, 298 K, CDCl <sub>3</sub> ) ( <i>bottom</i> )	82
<b>Figure 4.3.</b> <sup>1</sup> H NMR spectrum of epoxide <b>6</b> (300 MHz, 298 K, CDCl <sub>3</sub> ) ( <i>top</i> ) and the resultant carbonate <b>9</b> after cyclocarbonation reaction between <b>6</b> and CO <sub>2</sub> (300 MHz, 298 K, DMSO) ( <i>bottom</i> )	84
<b>Figure 4.4.</b> <sup>1</sup> H NMR spectrum of monomer <b>9</b> ( <i>top</i> ) and the resultant NIPU <b>13</b> ( <i>bottom</i> ) by reaction of <b>9</b> and hexamethylenediamine in DMSO at 80 °C for 24 h (300 MHz, 298 K, DMSO)	87
<b>Figure 4.5.</b> FTIR spectrum of NIPUs <b>14</b> and <b>13</b> prepared from monomer <b>9</b> ( <i>left</i> ), zoom in carbonyl stretching region of NIPUs <b>14</b> and <b>13</b> prepared from monomer <b>9</b> ( <i>right</i> )	88
<b>Figure 4.6.</b> GPC traces of the different NIPUs obtained from functionalised vanillin bis-carbonates	89



<b>Figure 4.7.</b> DSC curves of the different NIPUs obtained from functionalised vanillin bis-carbonates.....	90
<b>Figure 4.8.</b> TGA curves of the different NIPUs obtained from functionalised vanillin bis-carbonates.....	90
<b>Figure 5.1.</b> <sup>1</sup> H NMR spectrum of formation of <b>2</b> at R.T overnight. The conversion was calculated with the following equation: % conversion = $\frac{b}{(b+\frac{c}{2})}$ . Final conversion was 91% (top). <sup>1</sup> H NMR spectrum of formation of <b>4</b> at R.T overnight. The conversion was calculated with the following equation: % conversion = $\frac{c}{(c+d)}$ . In this case, the final conversion was 12% (bottom). (300 MHz, 298 K, DMSO- <i>d</i> <sub>6</sub> ).....	100
<b>Figure 5.2.</b> Synthesised water solution of <b>2</b> and cross-linked poly(hydroxyurethane) hydrogel <b>5</b> (left) and rheological characterization of both materials by frequency sweep experiments (right).....	101
<b>Figure 5.3.</b> FTIR spectra of compound <b>1</b> (bottom) and a lyophilised hydrogel formulation of <b>5</b> .....	102
<b>Figure 5.4.</b> Evolution of the storage (G') and loss (G'') moduli for a representative crosslinking formation of <b>5</b> at 25 °C using different amounts of water.....	103
<b>Figure 5.5.</b> Frequency sweep test for hydrogel <b>5</b> using different amounts of water.....	104
<b>Figure 5.6.</b> Evolution of the cross-linking reaction for hydrogel formulations <b>5</b> , <b>6</b> and <b>7</b> .....	105
<b>Figure 5.7.</b> Modulus evolution at different temperatures for hydrogel <b>5</b> formulation.....	106
<b>Figure 5.8.</b> Temperature sweep-experiments for formulations <b>6</b> , <b>7</b> and <b>8</b> .....	106
<b>Figure 5.9.</b> DSC heating (a) and cooling (b) scans for the hydrogel formulation <b>5</b> with different water contents. Evolution of the melting enthalpy as a function of the water content in the sample (c).....	108
<b>Figure 5.10.</b> Freshly prepared hydrogel <b>5</b> (left) and 3D printed scaffolds after the heat treatment (right).....	109
 Schemes	
<b>Scheme 1.1.</b> Industrialised examples of CO <sub>2</sub> utilization for the synthesis of various chemicals.....	5

<b>Scheme 1.2.</b> Traditional synthesis of functionalised cyclic carbonates using phosgene from functionalised 1,2-diols.....	6
<b>Scheme 1.3.</b> Proposed mechanism for the metalorganic catalysed synthesis of functionalised five-membered cyclic carbonates (adapted from Ref 34).....	7
<b>Scheme 1.4.</b> Synthesis of zwitterionic NHC-CO <sub>2</sub> and their use for the preparation of five-membered cyclic carbonates from epoxides.....	8
<b>Scheme 1.5.</b> Carbamate salts obtained by the coupling of CO <sub>2</sub> with organic superbases.....	9
<b>Scheme 1.6.</b> General reaction mechanism for the synthesis of five-membered cyclic carbonates catalysed by an organic salt or ionic liquid.....	11
<b>Scheme 1.7.</b> Methodologies reported inspired on the work of Fanizzi and coworkers for the synthesis of five-membered cyclic carbonates.....	12
<b>Scheme 1.8.</b> Traditional syntheses of isocyanates.....	14
<b>Scheme 1.9.</b> Alternative isocyanate-free approaches for the synthesis of polyurethanes...	16
<b>Scheme 1.10.</b> Proposed mechanism for the aminolysis of five-membered cyclic carbonates.....	17
<b>Scheme 1.11.</b> Reactivity order of various amines vs cyclic carbonates (adapted from Ref 121).....	18
<b>Scheme 1.12.</b> Catalysis types for the aminolysis of cyclic carbonates a), different organocatalysts tested for aminolysis of cyclic carbonates b).....	19
<b>Scheme 1.13.</b> Side reactions in the aminolysis of cyclic carbonates (Adapted from Ref 123).....	19
<b>Scheme 1.14.</b> Targeted chemical building blocks from depolymerization of cellulose and hemicellulose.....	22
<b>Scheme 1.15.</b> Added-value platform chemicals derived from HMF (Adapted from Ref 136).....	23
<b>Scheme 1.16.</b> Added-value platform chemicals derived from lactic acid.....	24
<b>Scheme 1.17.</b> Added-value platform chemicals obtained from lignin depolymerization...	25
<b>Scheme 1.18.</b> Industrial synthetic routes for the synthesis of vanillin.....	26
<b>Scheme 1.19.</b> Targeted monomers prepared from vanillin (adapted from Ref 165).....	27

<b>Scheme 1.20.</b> Synthesis of vanillin-based epoxy resins a), synthesis of vanillin-based polycarbonates b).....	29
<b>Scheme 2.1.</b> DBU carbamate salt when reacting with CO <sub>2</sub> .....	41
<b>Scheme 2.2.</b> Proposed organocatalytic mechanisms for the synthesis of five-membered cyclic carbonates using DBU as catalyst (left pathway) and DBU salts (right pathway)....	43
<b>Scheme 2.3.</b> Synthesis of protic <b>1-8</b> (a) and <i>N</i> -alkyl <b>9-14</b> (b) DBU based catalysts.....	45
<b>Scheme 2.4.</b> Synthesis of styrene carbonate using different DBU salts.....	45
<b>Scheme 2.5.</b> Proposed mechanism for the cycloaddition of CO <sub>2</sub> into methyl oxirane.....	52
<b>Scheme 3.1.</b> Guanidine synthesis using guanylation agents.....	60
<b>Scheme 3.2.</b> Proposed mechanism for the cycloaddition of CO <sub>2</sub> into propylene oxide catalysed by [HTBD]Br.....	62
<b>Scheme 3.3.</b> Synthesis of guanidines <b>1-5</b> and guanidinium iodide salts <b>6-12</b> based around DCC.....	63
<b>Scheme 3.4.</b> Synthesis of styrene carbonate using different guanidinium based salts.....	64
<b>Scheme 3.5.</b> Synthesis of chloride and bromide imidazole based guanidinium salts.....	68
<b>Scheme 3.6.</b> Anion influence study for the synthesis of styrene carbonate using imidazole based guanidinium halide salts.....	69
<b>Scheme 3.7.</b> Proposed mechanism for the cycloaddition of CO <sub>2</sub> into styrene oxide catalysed by <b>9</b> .....	72
<b>Scheme 4.1.</b> Vanillin transformation for potential monomers (adapted from Ref 28).....	79
<b>Scheme 4.2.</b> Reaction scheme for the synthesis of <b>2</b> ( <i>top</i> ). <sup>1</sup> H and <sup>13</sup> C APT NMR spectrum of compound <b>2</b> in DMSO ( <i>bottom</i> ).....	80
<b>Scheme 4.3.</b> Mechanism of vanillin oxidation <i>via</i> Dakin reaction.....	81
<b>Scheme 4.4.</b> Synthesis of glycidyl ethers <b>5-7</b> .....	81
<b>Scheme 4.5.</b> Aromatic glycidyl ether formation mechanism.....	83
<b>Scheme 4.6.</b> Synthetic route for the synthesis of functional bis-carbonates derived from vanillin.....	85
<b>Scheme 4.7.</b> Synthesis of vanillin based non-isocyanate poly(hydroxyurethanes).....	86

<b>Scheme 5.1.</b> Formation of urea <i>via</i> reaction of isocyanate with water.....	96
<b>Scheme 5.2.</b> Different approaches for the synthesis of NIPUs.....	97
<b>Scheme 5.3.</b> a) Gennen <i>et al.</i> synthesis of five-membered poly(hydroxy urethanes), b) Yuen <i>et al.</i> aminolysis reaction study of five, six and eight-membered cyclic carbonates.....	98
<b>Scheme 5.4.</b> Synthesis of precursors <b>1</b> and <b>3</b> for the preparation of hydrogels and subsequent synthesis of waterborne NIPUs <b>2</b> and <b>4</b> with PEG-1,000 diamine at room temperature.....	99
<b>Scheme 5.5.</b> Synthesis of waterborne hydrogels at room temperature.....	100

## Tables

<b>Table 2.1.</b> Literature catalyst screening for the synthesis of styrene carbonate from styrene oxide and CO <sub>2</sub> using DBU derivatives.....	42
<b>Table 2.2.</b> Reaction studies for styrene oxide and CO <sub>2</sub> cycloaddition catalysed by DBU salts.....	47
<b>Table 2.3.</b> Screening catalysts loading for the synthesis of styrene carbonate.....	48
<b>Table 2.4.</b> Cycloaddition of CO <sub>2</sub> to different functional epoxides catalysed by [HDBU]I.....	50
<b>Table 3.1.</b> Literature screening for the synthesis of styrene carbonate from styrene oxide and CO <sub>2</sub> using guanidine-based derivatives.....	61
<b>Table 3.2.</b> Reaction studies for styrene oxide and CO <sub>2</sub> cycloaddition catalysed by guanidinium based salts.....	65
<b>Table 3.3.</b> Imidazole and benzimidazole guanidinium iodide catalyst screening for the synthesis of styrene carbonate.....	66
<b>Table 3.4.</b> Time influence for the synthesis of styrene carbonate catalysed by <b>9</b> .....	67
<b>Table 3.5.</b> Temperature influence for the synthesis of styrene carbonate catalysed by <b>9</b> ...	68
<b>Table 3.6.</b> Anion influence study for the synthesis of styrene carbonate using imidazole based guanidinium halide salts.....	69

**Table 4.1.** Summary of molecular weight distributions and  $T_g$  registered from SEC and DSC calorimetry respectively of vanillin NIPUs.....89

**Table 5.1.** Synthesis of different PHU using different ratios of PEG diamine and TAEA.....104

# Acknowledgements

First, I would like to thank Professor Andrew Dove for giving me the opportunity to do a PhD under his supervision in his group. His support, advice, motivation and patience have represented the four main pillars for getting this piece of work done. Next, I would like to give thanks to all the members of the Dove group that I had the opportunity to work with. Your help on the last four years of my doctoral studies meant a lot to me.

Todo tiene un principio y un fin, y esta etapa que he vivido los últimos cuatro años no iba a resultar diferente. Ha sido un episodio en el que han ocurrido muchísimas cosas, muy probablemente las que me han enriquecido como persona y de las que más he aprendido no figuran en este manuscrito y si tuviera que relatar todas ellas seguramente tendrían una extensión más grande que mi tesis. Hay una gran cantidad de gente a la que me gustaría agradecerles todo su ánimo, sin todos y cada una de las personas mencionadas a continuación no hubiera sido capaz de llevar esto a buen puerto.

A la primera persona a la que me gustaría agradecer haber llegado a este punto es a mi difunto padre, del cual la vida me ha hecho no poder disfrutar de él todo lo que me hubiera gustado. Aún así, el escaso tiempo que hemos pasado juntos me ha servido para que me inculcará una serie de valores imprescindibles para haber logrado llegar hasta donde he llegado. Su mentalidad de trabajador incansable y esa pasión que siempre tuvo por aprender ha estado muy presente en mí todos estos años. Allá donde estés solo quiero darte las gracias y espero que estés orgulloso de en lo que me he convertido y ha donde he llegado.

Quisiera seguir dándole las gracias por su amor y apoyo a mi madre, Úrsula y a mis hermanos, Tono e Iván, sin vosotros tampoco hubiera sido capaz de estar escribiendo estas líneas ahora mismo. Mamá, siempre has estado ahí, apoyándome incansablemente y siempre has sido un ejemplo para mi de no rendirse jamás sin importar las adversidades por las que uno tiene que pasar en la vida. Tono, en realidad, no hay mucho que tenga que decir que a estas alturas ya no sepas, por circunstancias de la vida te ha tocado hacer de padre, de hermano y de amigo al mismo tiempo. Has sido y siempre serás un espejo donde me veo reflejado y no

podría estar más orgulloso de todo lo que he aprendido de ti y de la persona en la que me he convertido, y todo ello, es sin duda gracias a ti.

Siguiendo con los agradecimientos hay una persona que, a pesar de que nuestras vidas tomaron caminos diferentes no sería para nada justo no mencionar aquí. Gracias Lucía por el tiempo que hemos estado juntos, las cosas no terminaron del modo que a mi me hubiera gustado, pero a pesar de ello estuviste a mi lado durante mucho tiempo y sin tu apoyo no hubiera logrado terminar este trabajo.

Me gustaría también aprovechar estas líneas para darle las gracias a mi mentor, el Dr. Vicente del Amo. Sin todo lo aprendido por ti antes de haber empezado esta andadura hubiera sido imposible haber logrado finalizar esta tesis doctoral. Muchas gracias por todo Vicen.

Quisiera también darle las gracias a mi otra familia, mis amigos. Gracias a todos y a cada uno de vosotros por haber estado siempre ahí. Gracias por haber hecho que, a pesar de la distancia de estos últimos años, todas y cada una de las veces que nos hemos vuelto a ver, me habéis hecho sentir como si el tiempo no hubiera pasado y nos hubiéramos visto ayer mismo. Soy un gran afortunado de teneros a mi lado y nuestros inquebrantables lazos no hay dinero en el mundo que lo pague.

Muchas gracias a mi codirector de tesis, Haritz Sardón. Gracias por haber supervisado mi trabajo estos años y haber creído siempre en mí. Gracias por tu paciencia y apoyo durante las dos estancias en las que estuve en Donosti.

Agradecer también a todos mis buenos amigos de San Sebastián. Ha sido un enorme placer trabajar con todos vosotros y me habéis hecho sentir como en mi propia casa.

Finalmente quisiera dar las gracias a Jorge y a Judith por ese último y muy necesario empujón para terminar este duro trabajo. Gracias Judith por tu incalculable apoyo en estos últimos meses. Sin duda alguna tenerte a mi lado estos últimos meses ha significado muchísimo para mí. Como bien sabes, no puedo asegurarte nada con respecto a nuestro futuro, lo único que te puedo asegurar es que sin tu ayuda y apoyo esto no lo hubiera terminado y que espero ayudarte en los meses venideros del mismo modo que tú lo has hecho conmigo.

# Declaration of authorship

This thesis is submitted to the University of Warwick in support of my application for the degree of Doctor of Philosophy. It has been composed by myself and has not been submitted for any previous for any degree. The work presented (included data generated and data analysis) was carried out by the author expect in the cases outlined below:

- Computational calculations depicted in Chapter 2 were carried out by Dr. Coralie Jehanno at the University of the Basque Country.
- Rheological testing depicted in Chapter 6 was carried out by Dr. Roberto H. Aguirresarobe at the University of the Basque Country.
- 3D printed hydrogel scaffolds depicted in Chapter 6 were carried out by Naroa Sadaba.



# List of Publications

(1) Rational study of DBU salts for the CO<sub>2</sub> insertion into epoxides for the synthesis of cyclic carbonates, Noé Fanjul-Mosteirín, Coralie Jehanno, Fernando Ruipérez, Haritz Sardon and Andrew P. Dove. **ACS Sustainable Chem. Eng.** 2019, 7, 12, 10633-10640.

# List of abbreviations

8MCC	Eight-membered cyclic carbonate
Å	Amstrong
APT	Attached proton test
Atm	Atmosphere
Bn	Benzyl
DBU	1,8-Diazabicyclo[5.4.0]undec-7-ene
DCC	<i>N,N'</i> -Dicyclohexylcarbodiimide
DFT	Density functional theory
$D_M$	Dispersity
DMF	Dimethylformamide
DMSO	Dimethylsulfoxide
DSC	Differential scanning calorimetry
ESI-TOF	Electrospray ionization time of flight
Et	Ethyl
EtOAc	Ethyl acetate
FTIR	Fourier-transform infrared spectroscopy
$G'$	Storage modulus
$G''$	Loss modulus
GC-MS	Gas chromatography–mass spectrometry
h	Hours
HMDA	Hexamethylenediamine
HP	High pressure
HRMS	High resolution mass spectroscopy

Hx	Hexyl
Hz	Hertz
<i>J</i>	Coupling constant
K	Kelvin
kcal	Kilocalories
L-Arg	L-arginine
Me	Methyl
MeOH	Methanol
MHz	Megahertz
mL	Mililitre
mm	Milimetre
MPa	Megapascal
Ms	Mesyl
MTBD	7-Methyl-1,5,7-triazabicyclo[4.4.0]dec-5-ene
NIPU	Non-isocyanate poly(hydroxyurethane)
NMR	Nuclear magnetic resonance
PEG	Polyethylene glycol
Ph	Phenyl
PHU	Poly(hydroxyurethane)
ppm	Parts per million
ppmv	Parts per million in volume
PS	Poly(styrene)
R.T	Room temperature
RBF	Round bottom flask

RI	Refractive indeex
SAOS	Small amplitude oscillatory experiments
SEC	Size exclusion chromatography
S <sub>N</sub> 2	Bimolecular nucleophilic substitution
TAEA	Tris(2-aminoethyl)amine
TBD	1,5,7-Triazabicyclo[4.4.0]dec-5-ene
TEBAC	Benzyltriethylammonium chloride
Tf	Triflyl
T <sub>g</sub>	Glass transition temperature
TGA	Thermogravimetric analysis
THF	Tetrahydrofuran
TLC	Thin layer chromatography
TMS	Trimethylsilane
TOF	Turnover frequency
Ts	Tosyl
TS	Transition state
TTX	Tetrodotoxin
ZPVE	Zero-point vibrational energy
$\delta$	Chemical shift
$\mu$ L	Microlitre
$\mu$ M	Micromolar

# Abstract

**Chapter 1** describes a general introduction to all the contents exhibited in this thesis. In this chapter the CO<sub>2</sub> potential for the synthesis of added-value chemicals is explored. A strong survey is made in the organocatalytic methodologies for the synthesis of five-membered cyclic carbonates. Later, the synthesis of non-isocyanate polyurethanes (NIPUs) is discussed. One of the most used methods for the synthesis of the aforementioned polymers is by the step-growth polymerization of bis-cyclic carbonates with amines. This approach links with the CO<sub>2</sub> revalorization above discussed and gives a more sustainable approach for the production of polyurethanes since this method bypasses the use of toxic isocyanates. Finally, a survey of the renewable polymer feedstock is done with special emphasis in vanillin, a key renewable building block obtained from lignin.

**Chapter 2** shows a rational study for the organocatalysed synthesis of five-membered cyclic carbonates from CO<sub>2</sub> and epoxides. Several alkylated and protonated DBU-based catalysts were prepared and tested for the synthesis of five-membered cyclic carbonates. A relationship between structure and reactivity is established, showing the importance of hydrogen bond donor moieties in the DBU core revealing that iodide salt of DBU, *i.e.* [HDBU]I, exhibited the highest activity for the cyclocarboxylation of a battery of terminal functionalised epoxides. The influence of the anion was studied displaying iodide the highest performance. In addition, the catalyst was recycled up to six times without significant losses of activity. Finally, DFT calculations further support the influence of the nucleophilicity and leaving ability of the counter anion and corroborates the experimental observations.

**Chapter 3** describes a preliminary study for the cycloaddition of CO<sub>2</sub> into epoxides using novel guanidinium halide salts based around DCC. Inspired on the findings of chapter 2, a battery of guanidinium iodide salts were synthesised and fully characterised. Then, they were tested for the synthesis of styrene carbonate from styrene oxide and CO<sub>2</sub>. The incorporation of an imidazole moiety in the guanidinium core improved the catalytic activity in comparison with the other catalysts tested. A systematic optimization of the reaction parameters was

described, rendering so, an efficient methodology for the synthesis of five-membered cyclic carbonates. Finally, a discussion of the mechanism is described, the C2 proton of the imidazole ring is proposed to make a very efficient epoxide activation *via* hydrogen bond interactions compared to the other tested guanidinium salts.

**Chapter 4** explores the synthesis of non-isocyanate polyurethanes (NIPUS) based around vanillin. Several modifications of the vanillin functionalities were performed rendering three different bis-cyclic carbonates. Subsequently, each of those monomers were reacted with two different bis-amines to yield six different NIPUs which were fully characterised by  $^1\text{H}$  and  $^{13}\text{C}$  NMR spectroscopy, FTIR and SEC. Furthermore, their thermal properties were characterised by DSC analysis and TGA.

**Chapter 5** describes the synthesis of waterborne thermo-responsive non-isocyanate poly(hydroxyurethane) hydrogels. Those materials were prepared by the reaction of a bis-eight membered cyclic carbonate, a PEG bis-amine and a tris-amine which was used as a cross-linker. The presence of hydrophilic PEG moieties and the tuning of ratios of PEG bis-amine and cross-linker rendered materials able to be printed as a consequence of their reversible moduli decay when they are heated up and their subsequent moduli increase when they are cooled down.

**Chapter 6** shows experimental protocols plus spectroscopy data presented in this thesis.

A final appendix is provided showing all the  $^1\text{H}$  and  $^{13}\text{C}$  NMR spectroscopy data in all chapters.

*Dedicado a la memoria de mi padre.*

# **1. Introduction**



## 1.1 CO<sub>2</sub>

### 1.1.1 CO<sub>2</sub> and the greenhouse effect

CO<sub>2</sub> represents the fourth most abundant gas in the atmosphere, its concentration is around 0.04% (410 ppmv), therefore it is considered a trace gas. CO<sub>2</sub> concentration remained almost constant until the mid-18<sup>th</sup> century, around 280 ppm. Since then, coinciding with the industrial revolution in which, the development of the steam machine along with steam locomotive and subsequently the internal combustion engine, and its inherent increase of coal use and fossil fuels respectively, resulted in an exponential growth in the CO<sub>2</sub> atmospheric concentration (Figure 1.1).<sup>1</sup> In addition, CO<sub>2</sub> is along with water vapour (H<sub>2</sub>O), methane (CH<sub>4</sub>), nitrous oxide (N<sub>2</sub>O), ozone (O<sub>3</sub>), chlorofluorocarbons (CFCs) and hydrochlorofluorocarbons (HCFCs) considered as a greenhouse effect gas. The greenhouse effect is the responsible of making the Earth habitable, as those gases play a critical role in the planetary equilibrium temperature. Without the existence of those gases it is estimated that the average surface temperature on Earth would be - 18 °C, instead of the current 14 °C.

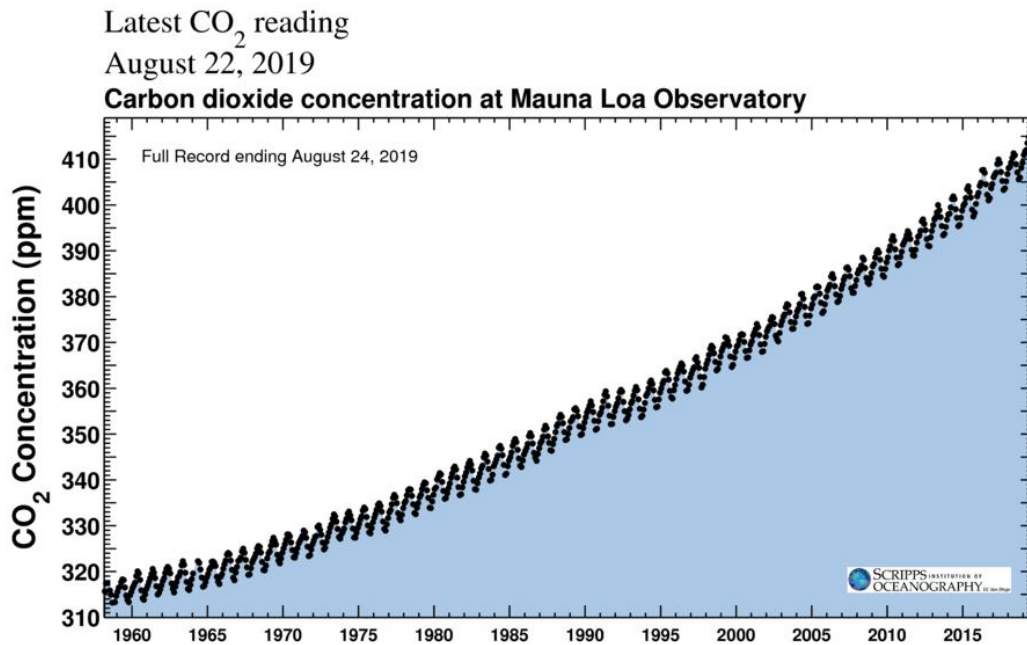


**Figure 1.1.** Keeling curve representing the carbon dioxide concentration in Earth's atmosphere.

Solar radiation falls upon the Earth scattered in the form of ultraviolet, visible and near-infrared radiation (Figure 1.2).<sup>2</sup> Only a small percentage of the most energetic radiation *i.e.* ultraviolet, reach the Earth surface, as it is absorbed by the oxygen and the ozone, the remaining radiation is partially absorbed in the Earth surface and subsequently reflected to the atmosphere. This reflected radiation, mainly infrared, responsible of rotation and vibration of molecules, interacts with the greenhouse effect gases and that excess of kinetic energy is transferred in the form of heat, which eventually implies rising the air temperature.

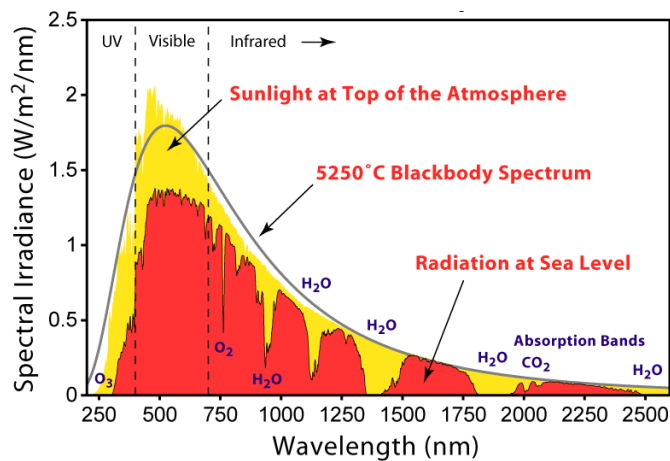


**Figure 1.2.** Solar radiation spectrum (adapted from Ref 2).

The aforementioned mechanism relies on the balanced amount of greenhouse effect gases. As a consequence, there's a directly proportional relationship between greenhouse effect gases and temperature. The increase on greenhouse effect gases by anthropogenic activities, leads to a decrease of infrared radiation energy leaving the atmosphere. In turn it translates on an increase of the average temperature on Earth. The surface of our planet, in order to keep the energy balance between absorbed and emitted solar radiation, warms up emitting a larger amount of infrared radiation to balance the effect of the increase of greenhouse effect gases. This phenomenon is well-known as global warming.<sup>3</sup>

### 1.1.2 CO<sub>2</sub> thermodynamics

As a consequence of the increase of the emissions of greenhouse effect gases in the atmosphere, and their direct relationship with the climate change, strategies not only for capturing CO<sub>2</sub> but for its revalorization *i.e.* using it in the development of added-value products have emerged in the last decades. CO<sub>2</sub> represents an inexhaustible

non-toxic and cheap C1 synthon. Moreover, it represents a safer alternative in certain synthetic routes to toxic reagents such phosgene, carbon monoxide and isocyanates. However, the main drawback in the use of CO<sub>2</sub> is its low reactivity. The standard Gibbs free energy of formation ( $\Delta G_f^\circ = -394$  kJ/mol) is quite high, which means that formation of CO<sub>2</sub> is thermodynamically favoured, and also, any transformation of a this molecule, will require high amounts of energy and the use of optimised catalytic systems (Figure 1.3).<sup>4, 5</sup>

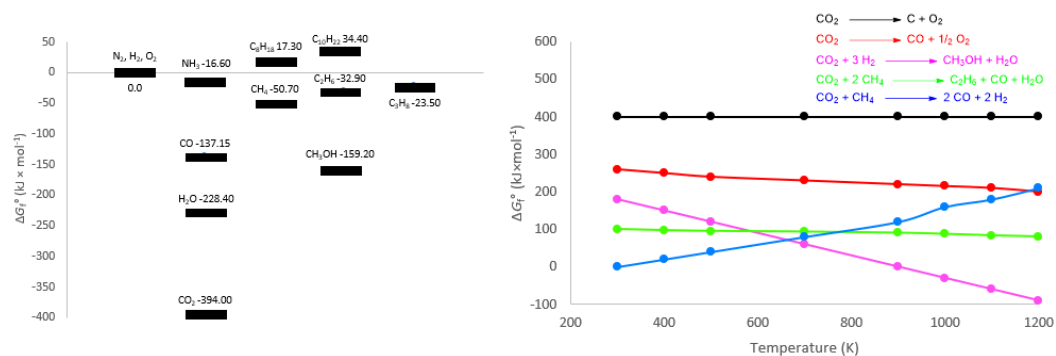
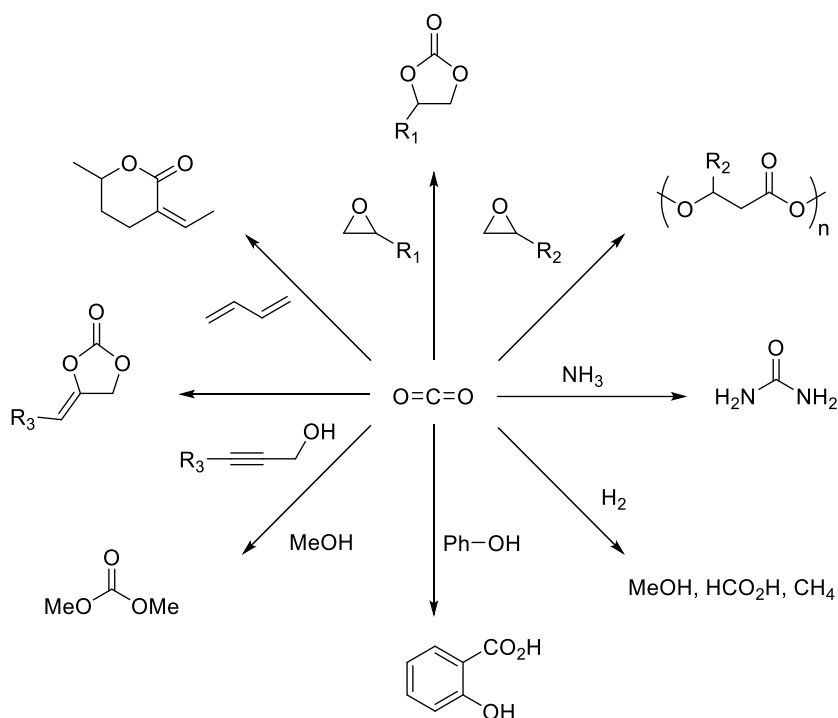


**Figure 1.3.** Gibbs free energy of formation of depicted chemicals (*left*), thermodynamics of some CO<sub>2</sub> reactions (*right*) (adapted from Refs 4 and 5).

### 1.1.3 CO<sub>2</sub> use for chemical processes

There is a plethora of organic reactions in which CO<sub>2</sub> is used. Despite its low reactivity as a consequence of thermodynamic aspects commented above, many methodologies have been extensively developed for the synthesis of added-value chemicals. Some of those processes have been industrialised (Scheme 1.1).<sup>4-8</sup>

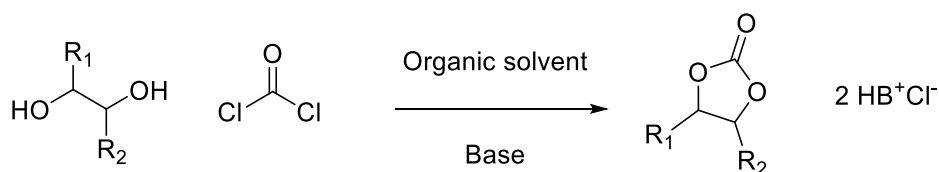
CO<sub>2</sub> is used in the production of *syngas* in the so-called dry reforming process. This reaction consists in reacting CO<sub>2</sub> with methane in the presence of a metallic-based catalyst to yield H<sub>2</sub> and CO.<sup>9-11</sup> Subsequently *syngas* can be converted through the Fischer-Tropsch process into a large variety of hydrocarbons such liquefied petroleum gas, a mixture of propane and butane, naphtha, diesel and wax. The reaction takes place in a temperature range between 150-300 °C, however, the temperature is kept in the low range to avoid the formation of methane. Several metal-based catalysts have been developed including Co, Ni, Fe or Ru.<sup>8, 12-14</sup>



**Scheme 1.1.** Industrialised examples of CO<sub>2</sub> utilization for the synthesis of various chemicals.

#### 1.1.4 Synthesis of five-membered cyclic carbonates using CO<sub>2</sub> and epoxides

Cyclic carbonates are one of the many high added-value products that can be prepared using CO<sub>2</sub> as a reagent. This kind of compound are of great interest as they are widely used in many different applications such as non-toxic polar solvents for organic synthesis,<sup>15</sup> battery electrolytes,<sup>16, 17</sup> and as intermediates for a vast number of products like polycarbonates<sup>18-21</sup> and non-isocyanate polyurethanes (NIPUs).<sup>22-24</sup> Five-membered cyclic carbonates have been traditionally prepared using 1,2-diols and phosgene dissolved in an organic solvent, in the presence of a base to quench the HCl formed (Scheme 1.2).<sup>25</sup> Even though the reaction is quite efficient and takes place under energetically mild conditions, the use of phosgene, a chemical forbidden in several countries, along with the production of chlorinated residues and the use of organic solvents, has led to the development of alternative synthetic routes for the preparation of five-membered cyclic carbonates. One of the most exploited methodologies is the use of CO<sub>2</sub> as a greener and safer alternative for the use of toxic phosgene.



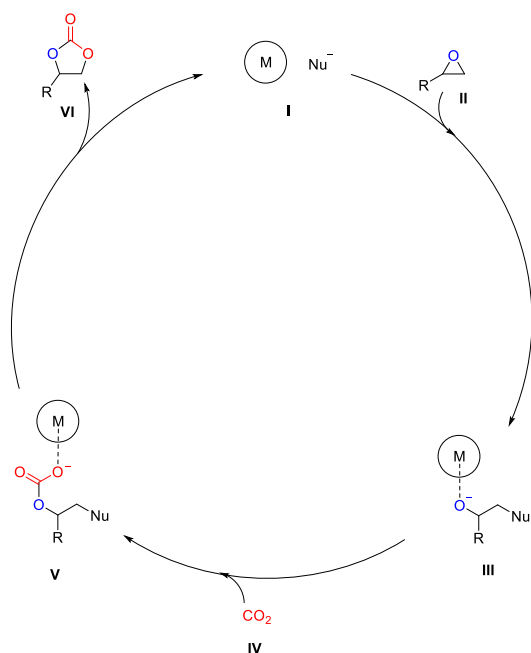
**Scheme 1.2.** Traditional synthesis of functionalised cyclic carbonates using phosgene from functionalised 1,2-diols.

Along with 1,2-diols, five-membered cyclic carbonates can also be prepared from epoxides. There is a vast amount of reported methodologies in the literature for this transformation employing either organometallic or organocatalysts, as well as consisting on homogeneous or heterogeneous systems.<sup>26-31</sup>

### 1.1.5 Synthesis of five-membered cyclic carbonates promoted by organometallic catalysts

Organometallic catalysts represent the most efficient type of catalysts as they can fix CO<sub>2</sub> into epoxides rendering functionalised terminal cyclic carbonates under very mild reaction conditions, very low catalyst loading, room temperature and low CO<sub>2</sub> pressure. Despite their high efficiency and high selectivity, organometallic catalysts exhibit several drawbacks. Typically, they are moisture and air sensitivity, so the reactions must be carried out under anhydrous conditions. Additionally, from the point of view of sustainability, the use of organometallic compounds is undesirable as a consequence of their intrinsic toxicity.

The reaction mechanism for the synthesis of five-membered cyclic carbonates has been extensively studied. In general, it is accepted as follows:<sup>32-34</sup> the metal complex **I** activates the epoxide **II** by the interaction of the oxygen atom of the epoxide with a Lewis acid centre. Most of the metal-based systems need a nucleophilic cocatalyst to ring-open the epoxide *e.g.* TBAB, TBAI, PPN-Cl. These cocatalysts are responsible for opening the epoxide through a nucleophilic attack on its less-substituted carbon atom. Then, a halo-alkoxide **III** is obtained. It suffers CO<sub>2</sub> insertion to render a linear halo-carboxylate, **V**, which is stabilised by the metal centre. Finally, an intramolecular ring-closing substitution yielding the desired cyclic carbonate **VI** and releasing the halide anion (Scheme 1.3).



**Scheme 1.3.** Proposed mechanism for the metalorganic catalysed synthesis of functionalised five-membered cyclic carbonates (adapted from Ref 34).

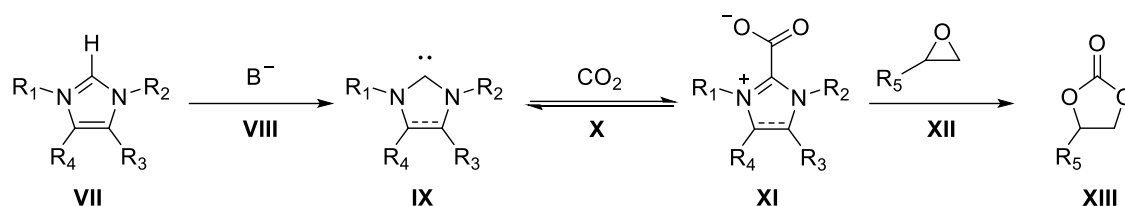
### 1.1.6 Synthesis of five-membered cyclic carbonates promoted by organocatalysts

Organocatalysts are cheap, non-toxic and non-sensitive catalysts utilised on the synthesis of five-membered cyclic carbonates. There are a huge amount of methodologies described all across the literature.<sup>35</sup> The nature of these catalysts is based around three main different types of compounds: a) nitrogen-based heterocycles, b) organic salts, molten salts and ionic liquids and c) polyphenolic and polyhydroxy compounds. Despite their advantages, organocatalytic systems remain less active than their organometallic homologous. Indeed, the reaction conditions in terms of pressure, temperature, time and catalyst loading are usually significantly higher in the case of organocatalytic methodologies.

#### 1.1.6.1 Synthesis of five-membered cyclic carbonates promoted by nitrogen-based heterocycles

Organic bases, such as amines, represent one of the cheapest and simplest organocatalysts used for the synthesis of five-membered cyclic carbonates. Their reactivity relies on their ability to reversibly react with CO<sub>2</sub> rendering carbamates.<sup>36</sup> <sup>37</sup> *N*-Heterocyclic carbenes (NHCs) have been reported as efficient organocatalysts for the synthesis of five-membered cyclic carbonates. NHCs can be prepared by the

treatment of a functionalised imidazole, **VII**, with a strong base, **VIII**, the so-obtained NHC, **IX**, indeed reacts with CO<sub>2</sub>, **X**, forming a NHC-CO<sub>2</sub> zwitterionic species, **XI**, capable of reacting with an epoxide, **XII**, to render the corresponding five-membered cyclic carbonate, **XIII** (Scheme 1.4).<sup>38-40</sup> However, as a consequence of their high reactivity they are moisture and air sensitive. Moreover, NHCs have been reported to decompose under high temperatures, which represents a major drawback for the development of efficient methodologies for the synthesis of functionalised five-membered cyclic carbonates.



**Scheme 1.4.** Synthesis of zwitterionic NHC-CO<sub>2</sub> and their use for the preparation of five-membered cyclic carbonates from epoxides.

Imidazolium ionic liquids are one of the most exploited organocatalysts for the synthesis of five-membered cyclic carbonates as a consequence of their unique ability for dissolving CO<sub>2</sub><sup>41</sup> (Figure 1.4).<sup>42-55</sup> In contrast to NHCs, imidazolium ionic liquids are robust and stable against air humidity, hence, easier to handle. In addition, the positions 1, 2 and 3 of the heteroaromatic ring can be functionalised with a plethora of different functional groups in order to tune their performance. The increase of alkyl chain substituents under supercritical conditions has been demonstrated to improve the performance of these catalysts, as a consequence of the improved solubility of scCO<sub>2</sub> in less polar catalytic species.<sup>54</sup> Regarding the influence of the anion, the catalytic activity is similar when bromide and iodide are used, but chloride is less active. This fact is explained by the necessity of a nucleophilic species with a good leaving ability.<sup>46, 47</sup> The incorporation of hydrogen bond donor moieties in the imidazolium core has been demonstrated to have a positive impact on the performance of the imidazolium-based catalysts.<sup>44, 45, 48, 50-53,</sup>

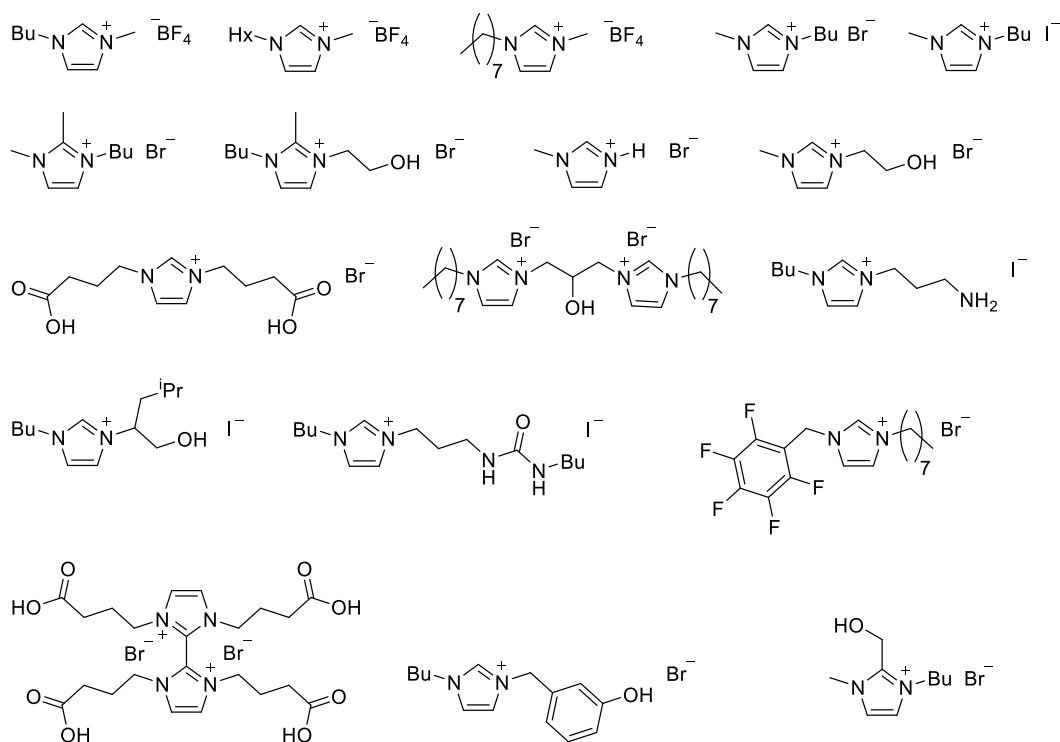
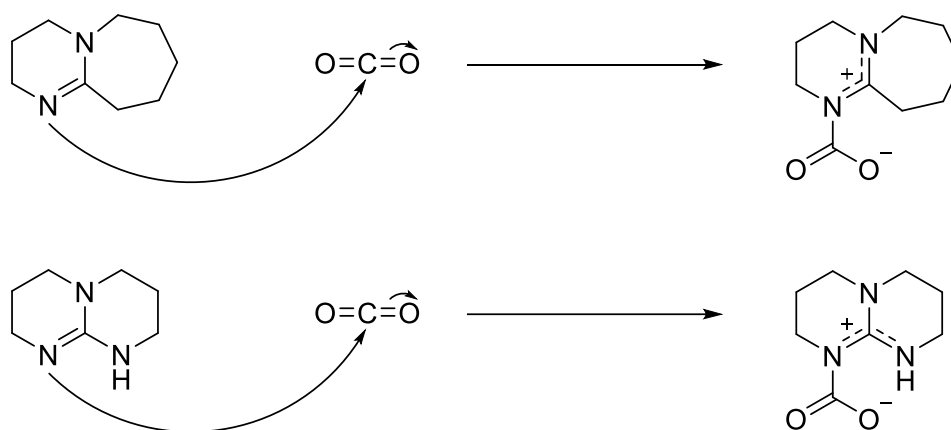


**Figure 1.4.** Most representative imidazolium-based catalysts for the synthesis of five-membered cyclic carbonates.

Organic superbases such as amidines, like DBU, and guanidines, like TBD, have been exploited on developing organocatalytic syntheses of five-membered cyclic carbonates. Both organic superbases have been demonstrated to be able to activate  $\text{CO}_2$ .<sup>56-58</sup> These organic superbases reacts with  $\text{CO}_2$  rendering a stable carbamate species (Scheme 1.5).



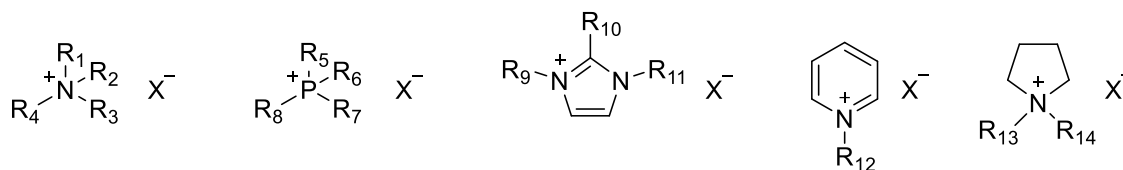
**Scheme 1.5.** Carbamate salts obtained by the coupling of  $\text{CO}_2$  with organic superbases.



Therefore, multiple methodologies based around organic superbases like DBU and TBD have been developed taking advantage of the unique ability of these superbases to activate CO<sub>2</sub>. In addition, the aforementioned capability of TBD to react with CO<sub>2</sub> has also been used for the synthesis of methanol by the reductive coupling of CO<sub>2</sub> with organosilanes<sup>59</sup> and organoboranes.<sup>60</sup>

### 1.1.6.2 Synthesis of five-membered cyclic carbonates promoted by organic salts, molten salts and ionic liquids

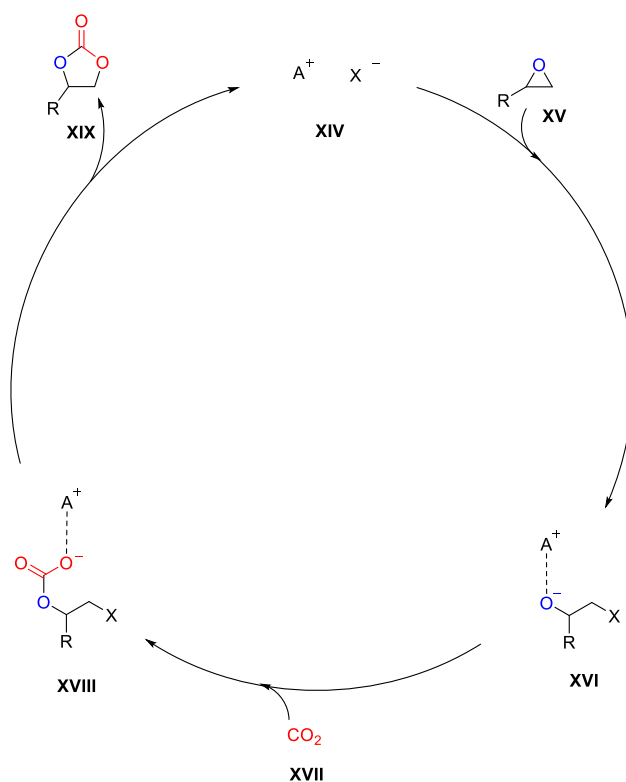
Organic salts, molten salts and ionic liquids represent by far, the organocatalysts most used on the cycloaddition reaction of CO<sub>2</sub> into epoxides. In industry, an ammonium salt, tetraethylammonium bromide has been used as catalyst since the 1950s for the synthesis of ethylene and propylene carbonate from CO<sub>2</sub> and either ethylene and propylene oxide respectively.<sup>61, 62</sup> Since then, a huge amount of methodologies based around ammonium, phosphonium, imidazolium (above discussed), pyridinium and pyrrolidinium salts has been developed (Figure 1.5).<sup>42, 63-72</sup>



X = Cl, Br, I, BF<sub>4</sub>, PF<sub>6</sub>, OH, AcO, HCO<sub>3</sub>, HSO<sub>4</sub>

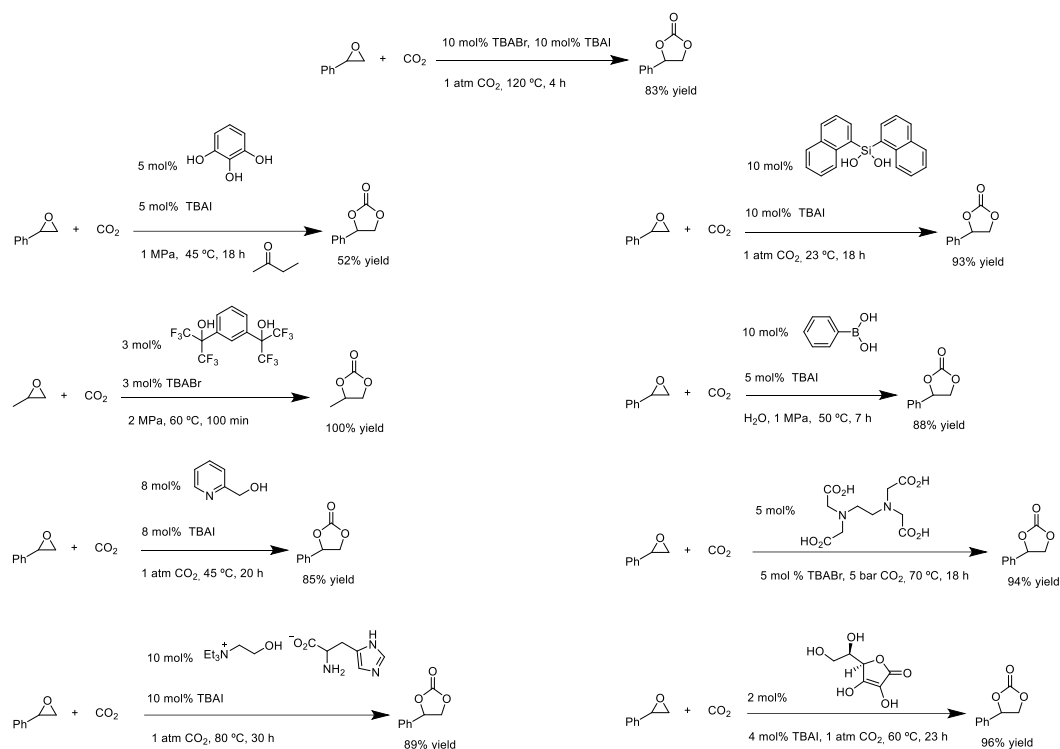
**Figure 1.5.** Examples of organic salts and ionic salts catalysts used for the synthesis of five-membered cyclic carbonates (adapted from Ref 29).

One of the advantages of these organocatalysts is their stability towards harsh conditions and their commercially availability. The reaction mechanism when this type of catalysts is used relies on the nucleophilic attack of the anionic part of the catalytic species, **XIV**, to the less substituted carbon of the epoxide, **XV**, to yield an alkoxide intermediate, **XVI**, which is stabilised by the cationic part of the catalyst. Subsequently CO<sub>2</sub> insertion takes place to render a linear carbonate, **XVIII**, which spontaneously undertakes an intramolecular ring-closure substitution to obtain the desired cyclic carbonate, **XIX**, and regenerates the catalyst (Scheme 1.6).



**Scheme 1.6.** General reaction mechanism for the synthesis of five-membered cyclic carbonates catalysed by an organic salt or ionic liquid.

Fanizzi and coworkers set a cornerstone on this area when they reported the synthesis of several functionalised five-membered cyclic carbonates using a binary system of equal weight percentage made of molten tetrabutylammonium bromide (TBABr) and tetrabutylammonium iodide (TBAI). This methodology was found to be efficient under mild pressure *i.e.* 1 atm. A battery of epoxides could be converted into their corresponding cyclic carbonates in 1 to 24 h at 120 °C.<sup>63</sup> The use of TBAI and TBABr was then exploited for the development of a large range of different binary catalytic systems in which a hydrogen bond donor species is included. The latter activates the epoxide through a hydrogen bond interaction, thus polarizing its C-O bond and facilitating the ring-opening of the epoxide by the halide anion. Moreover, the obtained reaction intermediate, a halo-alkoxide, is stabilised by both hydrogen bond donor co-catalyst and the tetrabutylammonium cation. The cooperative action mode of these binary catalytic systems allowed for the development of more efficient methodologies which operate under milder conditions to those reported by Fanizzi and coworkers (Scheme 1.7).<sup>63, 73-80</sup>



**Scheme 1.7.** Methodologies reported inspired on the work of Fanizzi and coworkers for the synthesis of five-membered cyclic carbonates.

### 1.1.6.3 Synthesis of five-membered cyclic carbonates promoted by polyphenolic and polyhydroxy compounds

Polyphenolic and polyhydroxy compounds represent an interesting tuneable platform for the development of organocatalytic methodologies for the synthesis of five-membered cyclic carbonates. Many of them, *i.e.* saccharides, pyrogallol, catechol, tannic acid, gallic acid result to be very attractive as they are widely present in nature (Figure 1.6).<sup>73, 75, 81-87</sup> Mechanistically, it is thought that the hydroxyl groups interact with epoxides through hydrogen bond interactions.

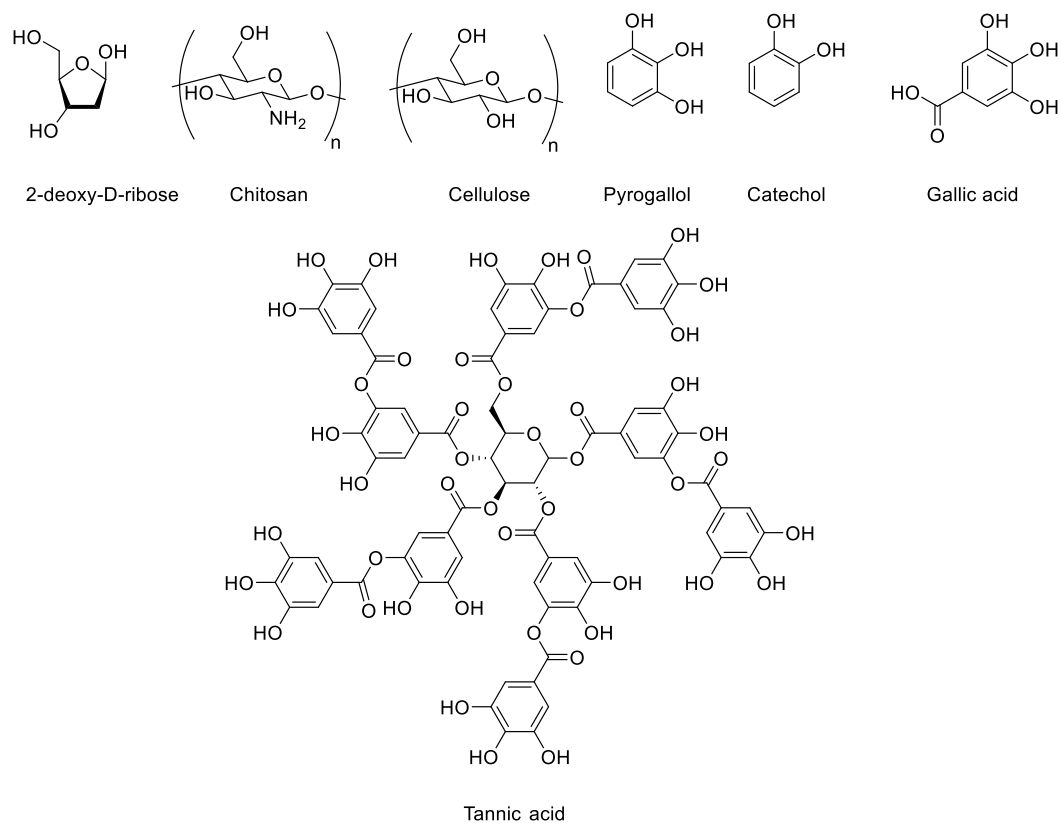
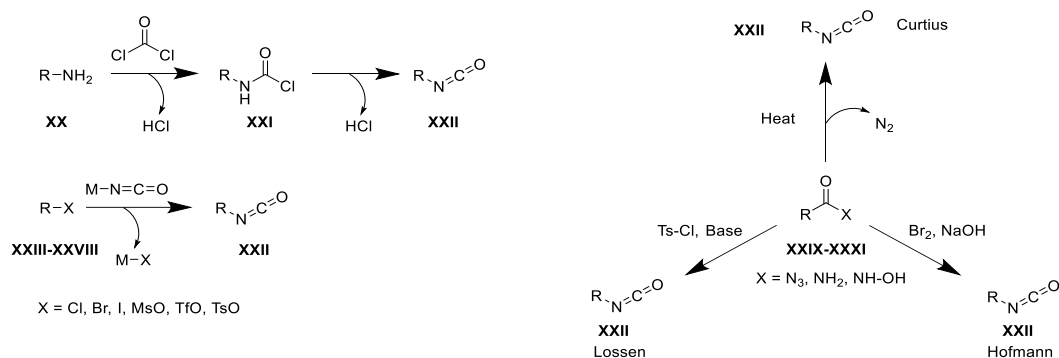


**Figure 1.6.** Examples of polyphenolic and polyalcohol compounds as organocatalysts for CO<sub>2</sub> insertion reaction into epoxides.

### 1.2 Synthesis of non-isocyanate polyurethanes (NIPU)

Polyurethanes represent the 6<sup>th</sup> most produced type of polymer in the world, with an 18 million tons produced in 2016, estimations reveal an upward trend for the next years. Otto Bayer and coworkers reported the first synthesis of polyurethanes back in 1937 by polyaddition of a diol in the presence of a diisocyanate.<sup>88</sup> In the beginning polyurethanes were developed as an alternative to polyolefins, polyesters and polyamides. Nowadays polyurethanes represent one of the most versatile materials produced in the world as a consequence of their good physical and mechanical properties, therefore they are widely found in a large number of different applications such as rigid and soft foams, coatings, adhesive, sealants, elastomers and in biomedical applications.<sup>89-93</sup> Despite of all the advantages of polyurethanes, some challenges remains unsolved, particularly in terms of sustainability: a) replacement of metal-based catalysts and organic solvents; b) avoiding the use of toxic isocyanates. The use of metal-based catalysts, mainly tin-based catalysts<sup>94</sup> jeopardises the potential use of the prepared polyurethanes by this

means in biomedical applications, since the total remove of the metal in the final polymer cannot be guaranteed.<sup>95</sup> Also, organic solvents are needed for the polyurethane formation as their presence solves the issue of viscosity increase occurring along with the polymerization process, therefore a large amount of volatile organic compounds (VOCs) and hazardous air pollutants (HAPs) are used. Exposure to the aforementioned species is undesirable and indeed they have been reported to be related with health issues.<sup>96</sup> Moreover, isocyanates are highly toxic compounds. The Bhopal disaster in which a methyl isocyanate leak killed thousands of people was a tragic example of how hazardous this kind of compounds are.<sup>97</sup> The conventional synthesis of isocyanates also involves the use of other highly toxic compounds (Scheme 1.8).<sup>98</sup>



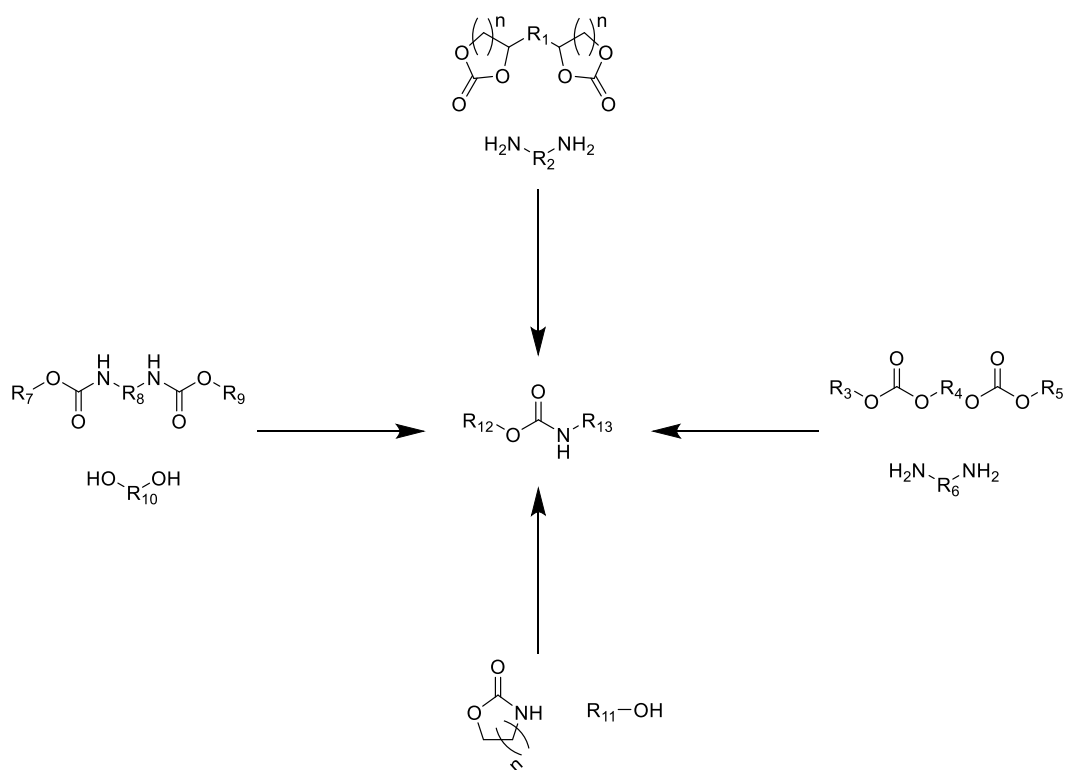
**Scheme 1.8.** Traditional syntheses of isocyanates.

The most extended one is phosgene utilised in the presence of a primary amine, **XX**.<sup>99</sup> In the first step of this process, a carbamoyl chloride intermediate, **XXI**, is formed and HCl is released. This intermediate evolves rendering the desired isocyanate, **XXII**, and a second equivalent of HCl is extruded. Other phosgene derivatives, *i.e.* diphosgene and triphosgene are less toxic and easier to handle alternative to phosgene.<sup>100</sup> The nucleophilic substitution of alkyl halides, tosylates, mesylates or triflates, **XXIII-XXVIII**, with metal cyanates has also been used, however side reactions are reported to take place, which lower the yield in which isocyanate, **XXII**, can be isolated.<sup>101-103</sup> Another strategy for the preparation of isocyanates are rearrangement reactions. The Curtius rearrangement consists in an anhydrous heat treatment of an acyl azide, **XXIX**, to yield an isocyanate, **XXII**, and release nitrogen. This reaction is highly efficient as the obtained yields are high, however, the use of toxic and explosives azide compounds is not desirable for industrial purposes.<sup>104</sup> The Hofmann rearrangement in which an amide, **XXX**,

reacts under basic conditions with bromine affords isocyanate, **XXII**, as a reaction intermediate. Nevertheless, this reaction is envisaged for the synthesis of primary amines instead of isocyanates.<sup>105</sup> The same scenario is observed for the Lossen rearrangement, in this case an *N*-hydroxyamide, **XXXI**, is reacted with an acyl or aryl chloride in the presence of a base yielding an isocyanate, **XXII**, that evolves to render a primary amine. Yet, other modified methodologies based on the Hofmann and Lossen rearrangements have been reported for the preparation of isocyanates.<sup>106, 107</sup>

As a consequence of the aforementioned sustainable related issues featured on the synthesis of isocyanates and the subsequent use of later mentioned precursors for the preparation of polyurethanes, both the European Union and the United States Environmental Protection Agency (EPA) have led to the implementation of regulations to reduce the usage of VOCs and diisocyanates.<sup>108</sup> In this scenario, alternative synthetic routes for the synthesis of non-isocyanates polyurethanes (NIPUs) have drawn large attention in recent years.<sup>23, 24, 109-111</sup>

Four main different approaches have been employed for the synthesis of NIPUs (Scheme 1.9): a) the step-growth polyaddition of bis-cyclic carbonates and bis-amines; b) the step-growth polycondensation of linear bis-carbonates and bis-amines; c) the step-growth polycondensation of linear bis-carbamates and diols; d) the ring opening polymerization of cyclic carbamates. The most employed strategy is the reaction between five-, six-, seven- and eight-membered bis-cyclic carbonates with bis-amines. There is a linear correlation between ring size and reactivity *vs* bis-amines. The higher reactivity of the cyclic carbonate with a bigger ring size, can be explained by its ring strain. The reactivity of these systems have been extensively studied by Tomita *et al.* and further supported by computational calculations.<sup>112-114</sup> Usually, the syntheses of six-, seven- and eight-membered bis-cyclic carbonates requires the use of phosgene or derivatives, like alkyl chloroformates, while, the synthesis of five-membered cyclic carbonates can be performed efficiently by organocatalysed methodologies.

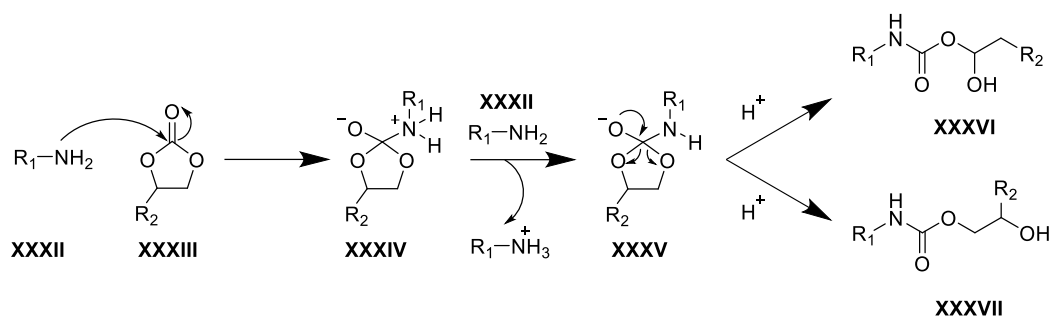


**Scheme 1.9.** Alternative isocyanate-free approaches for the synthesis of polyurethanes.

### 1.2.1 Synthesis of poly(hydroxyurethanes) by step-growth polymerization of bis-cyclic carbonates and bis-amines

Aminolysis of five-membered cyclic carbonates renders two different species, 1-hydroxyalkyl carbamates and 2-hydroxyalkyl carbamates. This reaction has a 100% atom efficiency, therefore it has been exploited for the synthesis of poly(hydroxyurethanes). Indeed, as it was mentioned above, is the most used strategy for the synthesis of NIPUs. Its reaction mechanism has been studied by many authors.<sup>115, 116</sup> In the first step, which is considered the limiting step of the reaction, a nucleophilic attack of the amine **XXXII** on the carbonyl atom of the cyclic carbonate **XXXIII** takes place rendering a tetrahedral intermediate, **XXXIV**. Then, a second equivalent of the amine **XXXII** deprotonates the ammonium moiety of intermediate **XXXIV**, yielding **XXXV**. The final step of the reaction mechanism involves two different carbon-oxygen cleavages leading to **XXXVI** and **XXXVII** (Scheme 1.10). According to Tomita *et al.*<sup>112</sup> and Steblyanko *et al.*<sup>117</sup> the formation of secondary alcohols is usually favoured, as they present a lower potential energy. However, some other parameters in the reactivity, like the nature of the solvent, the

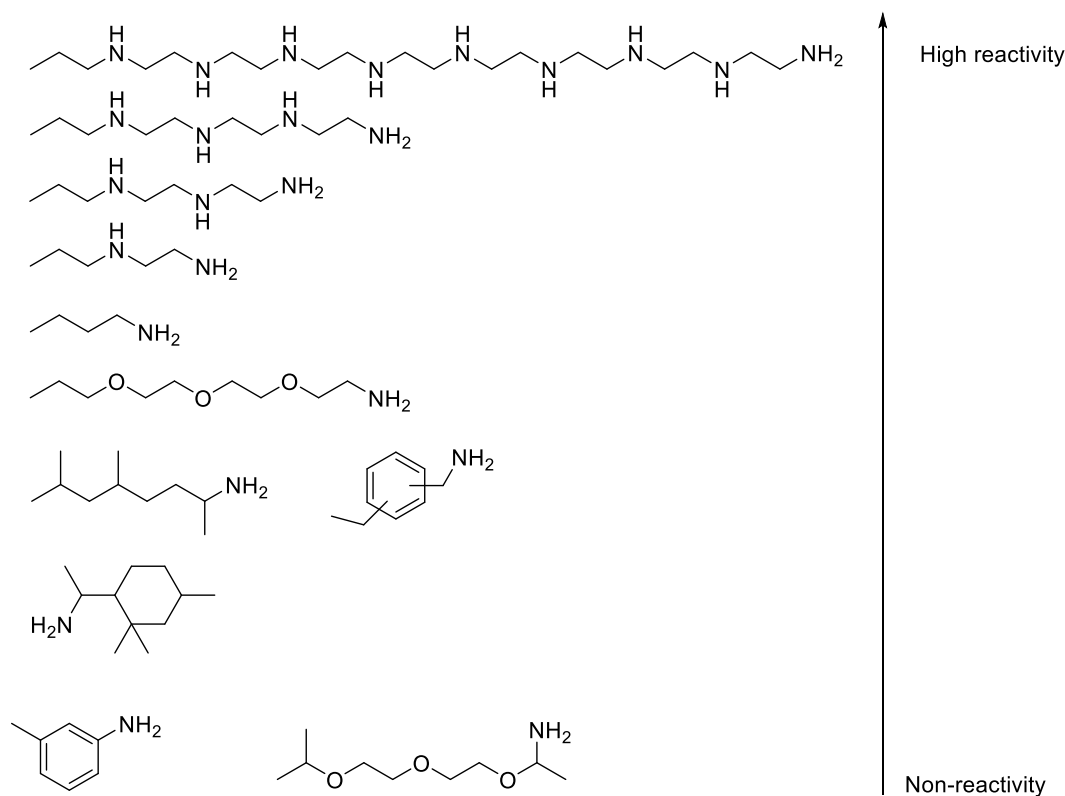
substituents on the carbonate and on the amine, and the catalysis approach have to be taken in account.



**Scheme 1.10.** Proposed mechanism for the aminolysis of five-membered cyclic carbonates.

The influence of the solvent was studied by Garipov *et al.*<sup>118</sup> According to their findings, when the reaction is carried out in a protic solvent, the kinetics are more rapid as the electrophilicity of the cyclic carbonate is increased by the hydrogen bond interactions between the cyclic carbonate and the protic solvent. The nature of the cyclic carbonates has a big influence in the kinetics reaction, two approaches have been made: a) ring size of the cyclic carbonate. The reactivity was found to be higher in the case of eight-, seven- and six-membered cyclic carbonates compared to five-membered ones, which are less reactive. This phenomenon is explained as a consequence of the ring strain of the cyclic carbonate. Five-membered cyclic carbonates have a lower ring strain, thus, they are more stable which makes their reactivity lower towards the aminolysis reaction;<sup>112, 116, 119</sup> b) influence of the cyclic carbonate substituents. The presence of electron-withdrawing groups substituents increases the electrophilicity of carbonyl group of the cyclic carbonate, which translates in an increase of reactivity towards amines. Electron-donating substituents makes the contrary effect, as they decrease the electrophilicity of the carbonyl and the aminolysis reaction is disfavoured.<sup>115, 118, 120</sup> The influence of the amine structure has been studied by Diakoumakos *et al.*<sup>121</sup> In this case it was concluded that aromatic primary amines along with secondary amines exhibit low reactivity as a consequence of their poor nucleophilicity. On the contrary, primary amines with low steric hindrance show higher reactivities. Also, they demonstrated that the amine substituents also play an important role on their reactivity, electron-withdrawing groups in  $\alpha$  and  $\beta$  position or imino and amino groups enhances the reactivity (Scheme 1.11).

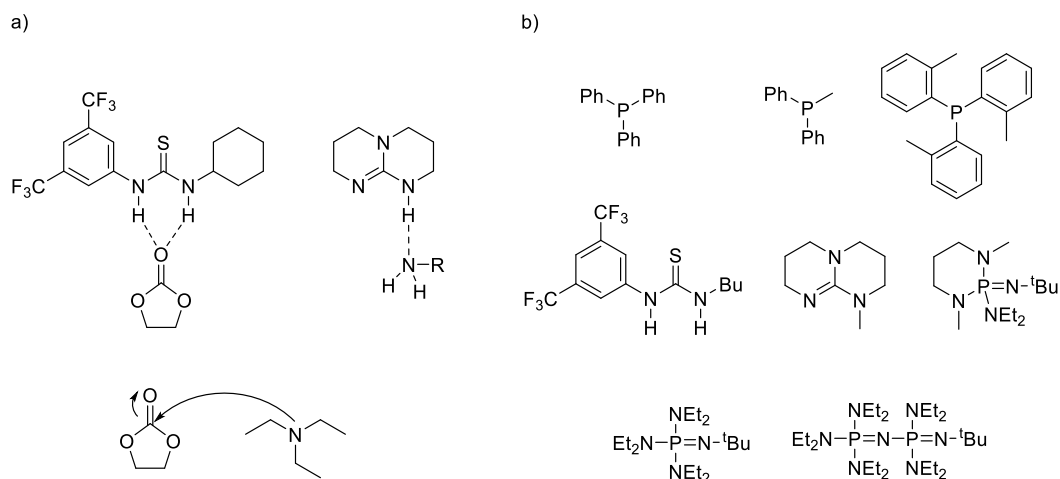




**Scheme 1.11.** Reactivity order of various amines vs cyclic carbonates (adapted from Ref 121).

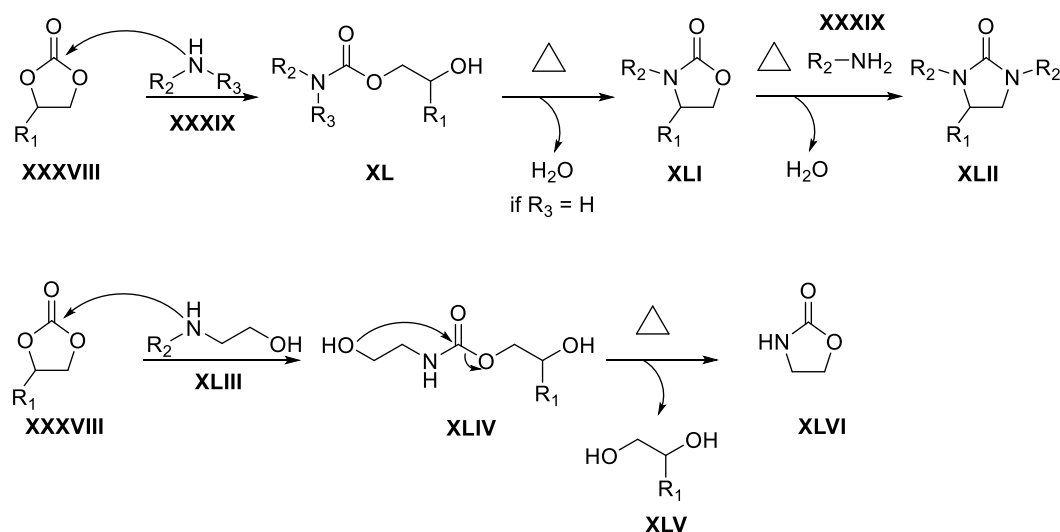
Three different outlooks have been proposed for the types of catalysis for the aminolysis of cyclic carbonates (Scheme 1.12a): a) increase of electrophilicity of carbonyl of cyclic carbonate; b) increase of nucleophilicity of amine; c) ring-opening of cyclic carbonate with a nucleophilic catalyst. Among all the different catalysts tested, TBD and 1-(3,5-bis(trifluoromethyl)phenyl)-3-cyclohexylthiourea exhibited the best performance (Scheme 1.12b).

One of the biggest limitations of the synthesis of PHU, is the difficulty of obtaining high molecular weights in order to get access to materials with good thermal and mechanical properties.<sup>122</sup> The rupture of stoichiometry by side reactions occurring during the polymerization prevents the obtention of polymers with high molecular weights. Clements reported the occurring side reactions in the aminolysis of cyclic carbonates by primary, secondary and  $\beta$ -hydroxyalkylamines. When a primary amine **XXXIX** reacts with a cyclic carbonate **XXXVIII**, aminolysis reaction takes place to render a hydroxylcarbamate **XL**. If this reaction is performed in the presence of a primary amine, and the intermediate **XL** is heated up, an intramolecular elimination takes place, where



**Scheme 1.12.** Catalysis types for the aminolysis of cyclic carbonates a), different organocatalysts tested for aminolysis of cyclic carbonates b).

water is eliminated and an oxazolidinone, **XLVI**, is obtained. In addition, this oxazolidinone can react further under the presence of **XLV** and heat, eliminating a second equivalent of water to afford an urea, **XLII**. Another scenario was studied by Clemens when employing a  $\beta$ -hydroxyalkylamine, **XLIII**, as an aminolysis reagent. A bis- $\beta$ -hydroxyalkylamine intermediate **XLIV** is obtained when **XLIII** is reacted with a cyclic carbonate, **XXXVIII**. Then, if **XLIV** is heated up, an intramolecular attack of hydroxyl group takes place eliminating an equivalent of 1,2-diol **XLV** and an oxazolidinone, **XLVI**, is obtained (Scheme 1.13).<sup>123</sup>



**Scheme 1.13.** Side reactions in the aminolysis of cyclic carbonates (Adapted from Ref 123).

Subsequently Lamarzelle *et al.*<sup>120</sup> confirmed that under harsh reaction conditions, the aminolysis of five-membered cyclic carbonates lead to side reactions and to the formations of undesired by-products like ureas, glycols, amides and oxazolidinones.

### 1.3 Renewable polymer feedstock

The current depletion of fossil fuels mainly used for the production of energy and chemical products is becoming an environmental and economic issue.<sup>124-126</sup> Therefore, the alternative use of renewable resources and sustainable methodologies has attracted many attention in the last decade.<sup>127, 128</sup> Biomass represent an inexhaustible renewable source of carbon which is available all over the planet, while oil is only available in very specific locations. The main raw materials that are available in the biomass are cellulose, hemicellulose and lignin (Figure 1.7). The main drawback of biomass revalorization is about optimising the chemical process to isolate the desired building blocks as a consequence of the high heterogeneity of biomass.

A first approach to by-pass this issue, is to separate the aliphatic portion of biomass, *i.e.* cellulose and hemicellulose from the aromatic one, *i.e.* lignin. For such purpose, both mechanical and chemical processes have been developed, following two different approaches. In the first one cellulose and hemicellulose are isolated *via* solubilization, leaving lignin as an insoluble residue. The second one is the opposite, lignin is dissolved and both cellulose and hemicellulose remain as insoluble residues.

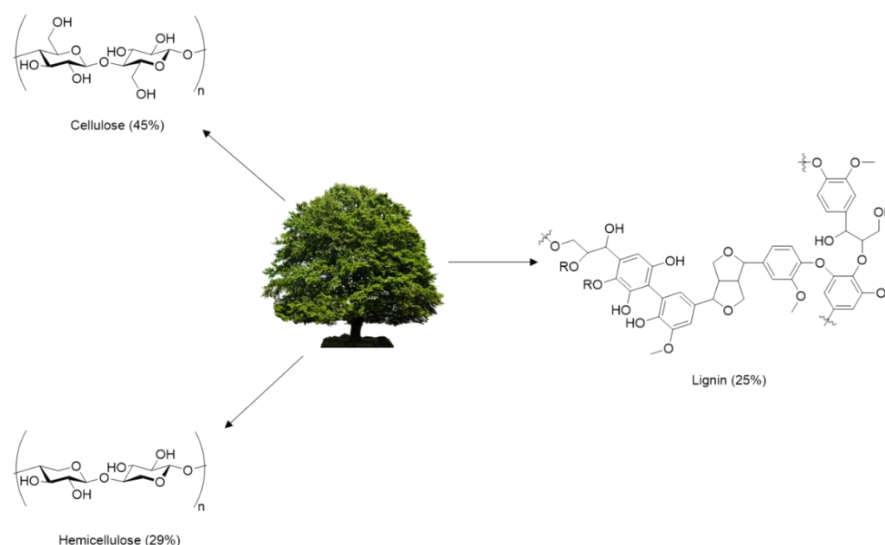
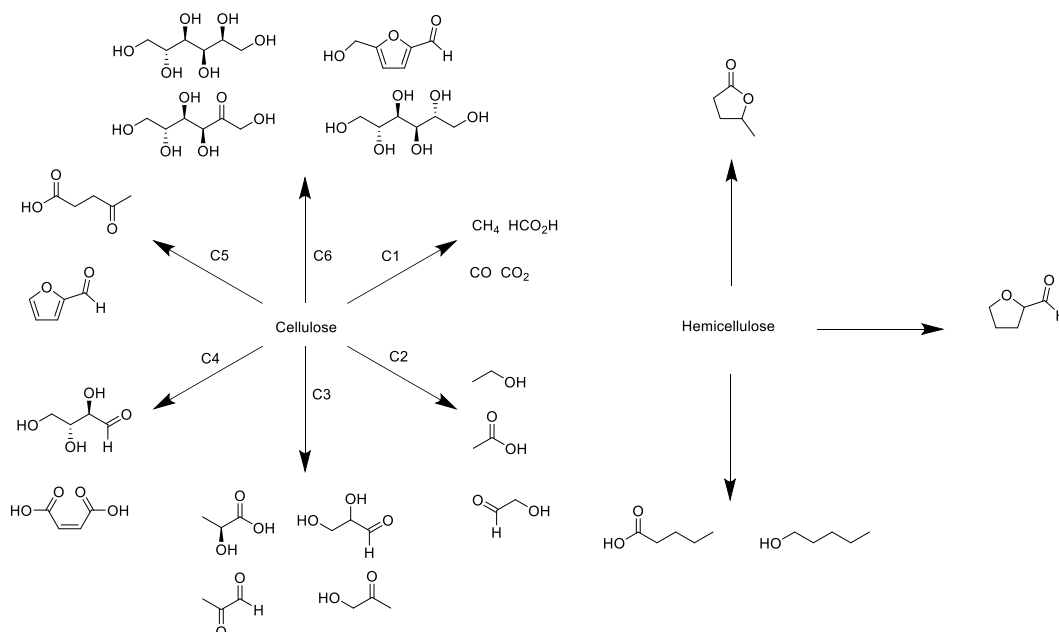


**Figure 1.7.** Components of lignocellulose.

### 1.3.1 Feedstocks derived from cellulose and hemicellulose

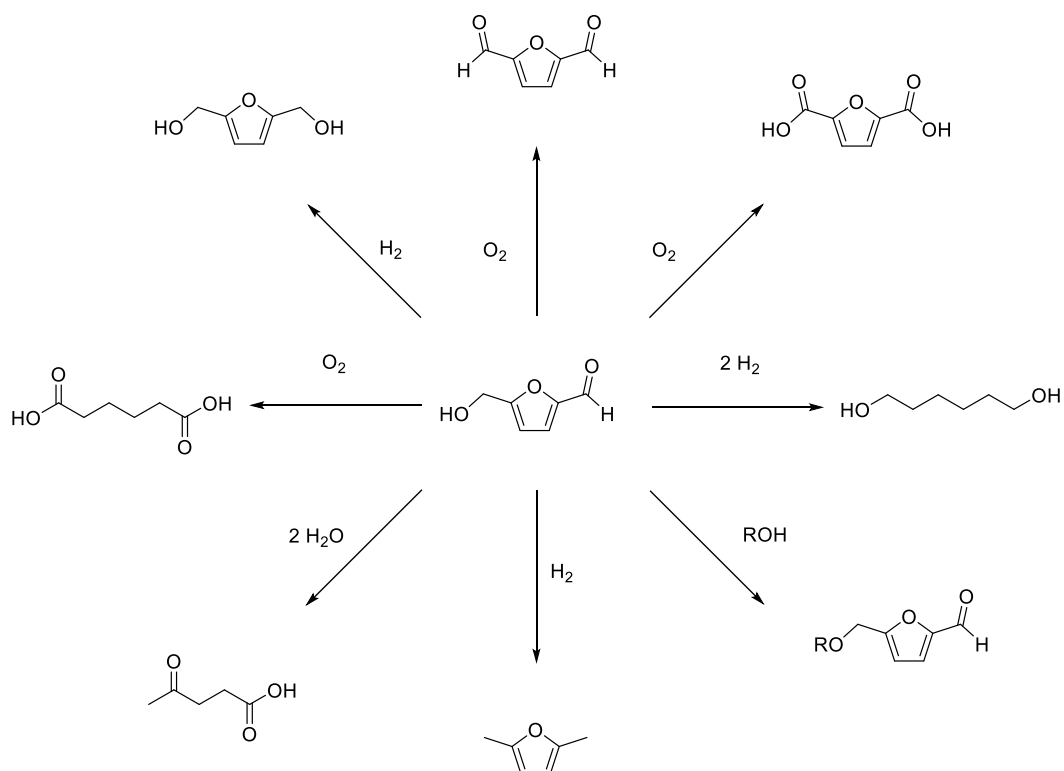
Cellulose and hemicellulose represent the aliphatic portion of lignocellulose and the most abundant, approximately 75%. On the one hand, cellulose is a C6 polysaccharide made of anhydrous D-glucose units linked by  $\beta$ -1-4 linkages. On the other hand hemicellulose is a C5 heteropolysaccharide composed by different sugars such as xylan, galactose, mannose and arabinose linked by  $\beta$ -1-4 linkages. Depending on the chemical processing of the aforementioned polysaccharides, *i.e.* dehydration, hydrogenation or hydrodeoxygenation, different building blocks can be targeted (Scheme 1.14).<sup>129</sup> Among all the different building blocks that can be isolated from cellulose and hemicellulose, stands out hydroxymethylfurfural (HMF), a very promising chemical platform for the synthesis of a plethora of renewable added-value products as a consequence of its heterocyclic nature along with the presence of high reactive functionalities like hydroxyl and aldehyde.<sup>130</sup> Levulinic acid is indeed obtained from the acid aqueous hydrolysis of HMF and it is currently used in a wide range of applications such as preparation of lubricants, chiral reagents, resins, adsorbents, batteries and electronic devices.<sup>131</sup> Furfural represents a C5 building block that can be isolated from hemicellulose as it contains a large amount of xylose and arabinose.<sup>132</sup> Furfural is a critical intermediate for other widely used chemicals like furan, tetrahydrofuran or furfuryl alcohol.<sup>133</sup> Lactic acid has applications in different areas like the alimentary industry and the elaboration of pharmaceuticals and cosmetics.<sup>134</sup> However, the most interesting application of lactic acid arises from its polymerization. So, polylactide (PLA) represents one of the most emerging bio-plastic used nowadays as a consequence of its biodegradability and their good mechanical properties.<sup>135</sup>



**Scheme 1.14.** Targeted chemical building blocks from depolymerization of cellulose and hemicellulose.

### 1.3.1.1 5-Hydroxymethylfurfural (HMF)

5-Hydroxymethylfurfural (HMF) has been considered as a versatile added-value chemical as a consequence of the large amount of different chemicals that can be prepared from it (Scheme 1.15).<sup>136</sup> A large amount of different methodologies has been reported for the isolation of HMF.<sup>137</sup> Briefly, cellulose is hydrolysed to render glucose, then this saccharide is isomerised to obtain fructose and finally, a series of different dehydration reactions take place to yield the desired HMF monomer. The catalysts used for the synthesis of HMF can be divided in four different kinds: a) solid acid catalyst; b) polymeric ion-exchange resins; c) heteropoly acid salts; d) metal-organic frameworks.<sup>136</sup> Despite the large amount of methodologies reported in the literature, profitable synthesis of HMF still remains quite challenging, especially in terms of catalyst recycling and also because of the inherent complexity of lignocellulose. The precursors prepared from HMF have been used for the synthesis of several different kinds of polymers like polyesters, polyamides or polyurethanes.<sup>138</sup> Burgess *et al.* synthesised a poly(ethylene furanoate)



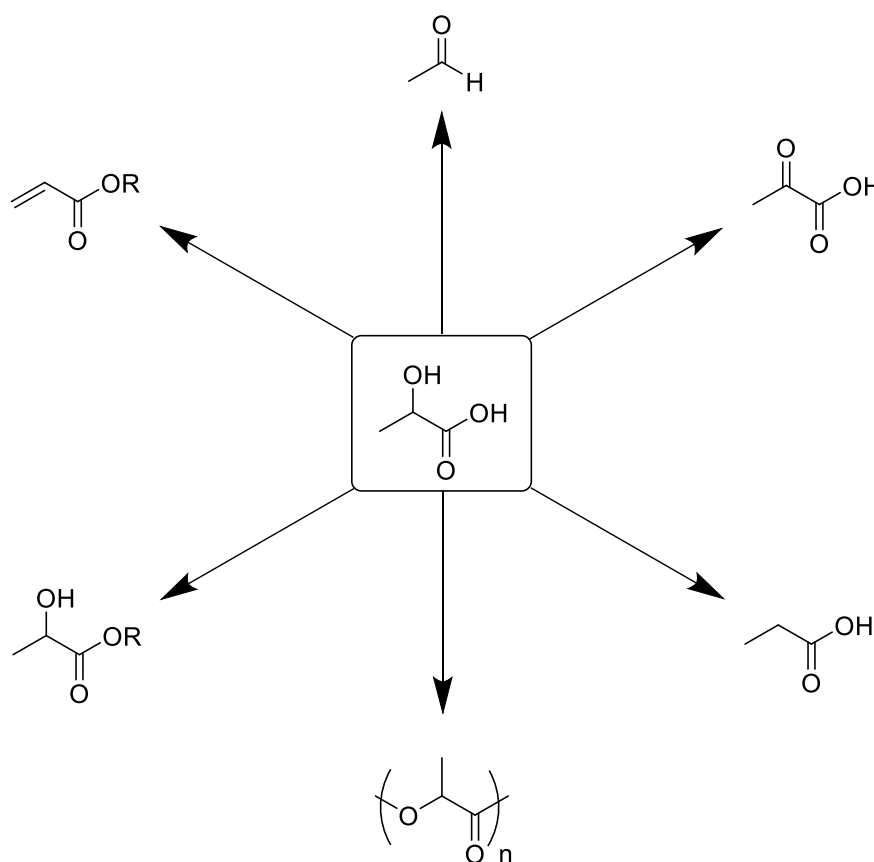
**Scheme 1.15.** Added-value platform chemicals derived from HMF (Adapted from Ref 136).

(PEF) from 2,5-furandicarboxylic acid. They studied its thermal and mechanical properties and compared them to the analogous poly(ethylene terephthalate) (PET). It was reported that the renewable bio-based PEF exhibits improved mechanical and thermal properties compared to the PET counterpart. The authors attributed the enhanced properties to the higher rigidity of the PEF, so demonstrating that polyesters prepared around HMF derivatives have a high potential to replace the petroleum-based polyesters obtained from dimethyl terephthalate or terephthalic acid.<sup>139</sup>

### 1.3.1.2 Lactic acid

Lactic acid has been conventionally produced from the fermentation of carbohydrates. However, as a consequence of the low efficiency of this process, different metal-based methodologies, both homogeneous and heterogeneous, have been reported for the synthesis of lactic acid from biomass.<sup>140</sup> Apart from cellulose, glycerol is another recurrent starting material for the preparation of lactic acid. Indeed, Hanefeld and co-workers reported a methodology based on the use of a

heterogeneous catalyst. Glycerol was converted with a 54% selectivity for lactic acid using Pt/CaCO<sub>3</sub> as catalyst and a borate ester as additive at 200 °C.<sup>141</sup> Among all the chemicals that can be obtained from lactic acid (Scheme 1.16), PLA is the most exploited one. Indeed, PLA is one of the most studied polymers for biomedical applications as a consequence of its biocompatibility, and the fact that this material is innocuous (the product obtained from its degradation is lactic acid, a metabolite of the Cori cycle). Due to its good mechanical and thermal properties, merged with its previously mentioned biocompatibility, PLA is an excellent polymer used in the development of 3D printed scaffolds, such as stents, surgical sutures, surgical screws for bone fixation, soft-tissue implants and drug delivery.<sup>142</sup>



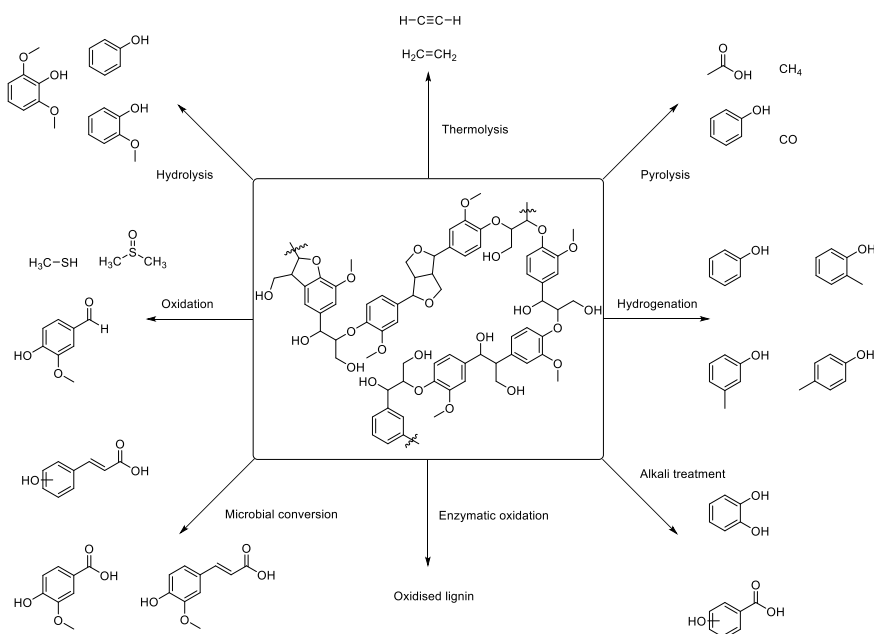
**Scheme 1.16.** Added-value platform chemicals derived from lactic acid.

PLA is obtained by two means, polycondensation of lactic acid or by ring-opening polymerization of lactide.<sup>143</sup> The first route was discovered by Carothers in 1932,<sup>144</sup> the PLA obtained had a low  $M_w$  since the water obtained as a by-product had to be removed in order to force the equilibrium to the obtention of PLA. The ring-opening polymerization of lactide represents a more efficient way to obtain PLA.<sup>145</sup> In industry, PLA is obtained by polymerization of lactide using an organotin catalyst.

By this route, the PLA obtained has a higher molecular weight and smaller dispersity ( $D_M$ ), hence, it displays better thermal and mechanical properties. Lactic acid is a chiral molecule, with two different enantiomers. Accordingly, two different polymers can be obtained from the polymerization of lactic acid. Polymer stereocomplexation consists in the mixing of two different enantiomers yielding a polymer with enhanced properties compared to their sole counterparts.<sup>146</sup> This phenomenon firstly reported by Ikada *et al.*,<sup>147</sup> has been widely exploited for the preparation of nanostructures for several biomedical applications.<sup>148, 149</sup>

### 1.3.2 Feedstocks derived from lignin

Lignin is the bio-polymer responsible of the structural and mechanical integrity of plants. It is constituted by three different phenylpropanoid units: *p*-coumaryl alcohol, coniferyl alcohol and sinapyl alcohol. These three monolignols are produced in the cytoplasm *via* the shikimate pathway, a metabolic pathway present in bacteria, fungi and plants. The composition of lignin varies from plants to plants, which means that the distribution of the three different monolignols is not uniform. Despite its heterogeneity, lignin is envisaged as the largest bio-based aromatic feedstock in nature. Depending on the depolymerization process, a large variety of different added value chemicals can be isolated from the depolymerization of lignin (Scheme 1.17).<sup>150</sup>

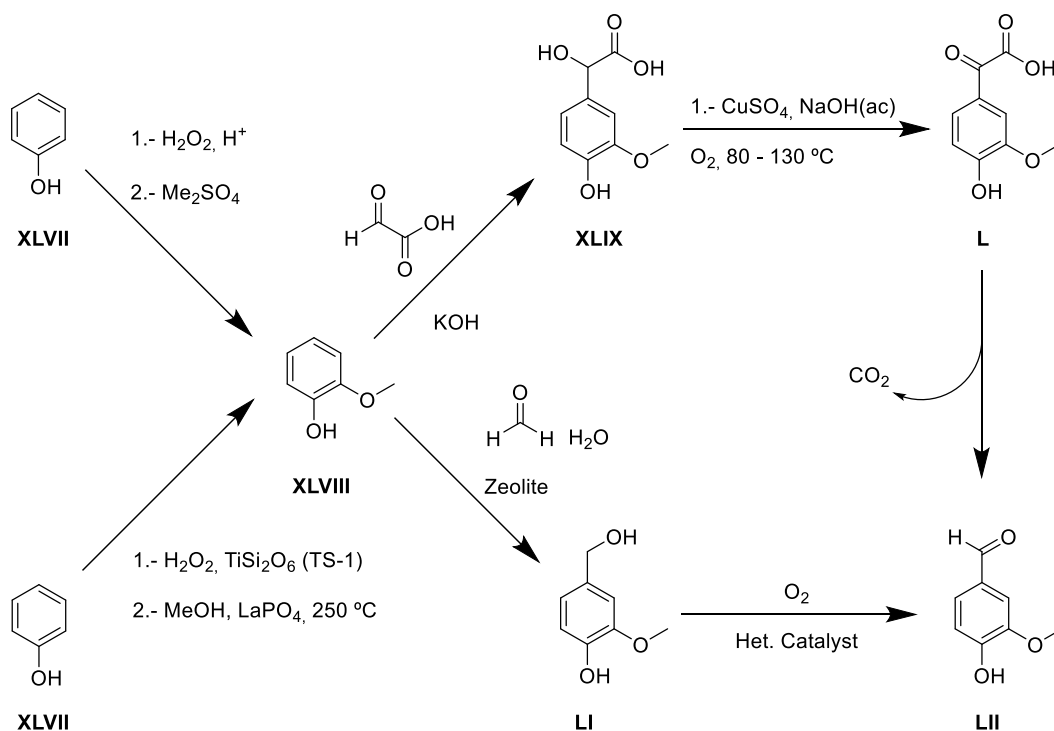


**Scheme 1.17.** Added-value platform chemicals obtained from lignin depolymerization.



### 1.3.2.1 Vanillin

Vanillin (4-hydroxy-3-methoxybenzaldehyde) represents a key renewable aromatic building block.<sup>151</sup> Vanillin worldwide production is estimated around 20.000 tons per year<sup>152</sup>, distributed in three main sources, scilicet, oil (85%), lignin (15%) and vanilla (<1%). Natural vanillin comes from the vanilla plant. This species grows in both tropical and subtropical areas. Vanillin is isolated from vanilla beans through a curing process in which the vanillin glucoside present on the vanilla bean is enzymatically hydrolysed to glucose and vanillin.<sup>153</sup> Synthetic vanillin represents 85% of worldwide production. Two different synthetic routes have been developed by Rhône Poulenc using phenol as starting material (Scheme 1.18).<sup>154</sup> In the first route, phenol, **XLVII**, is oxidised by sodium peroxide in acidic media. Subsequently a monomethylation takes place using  $\text{Me}_2\text{SO}_4$  to render guaiacol, **XLVIII**. It is then reacted with glyoxylic acid under basic media in the so called Riedel process to obtain intermediate **XLIX**, which is oxidised using a cooper salt yielding **L**, which eventually suffers a decarboxylation reaction to obtain vanillin, **LII**.

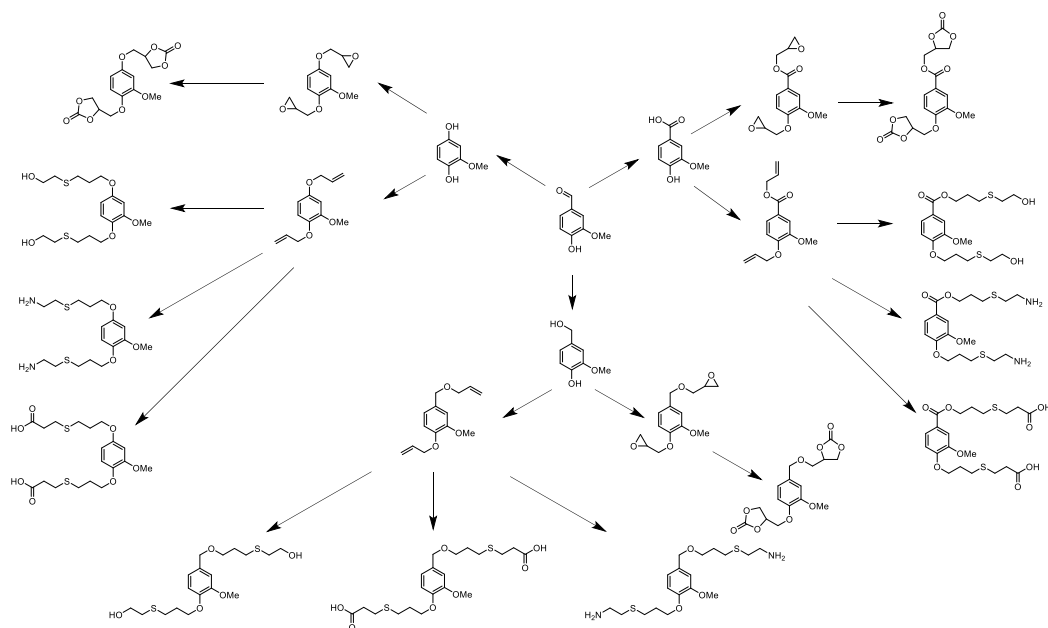


**Scheme 1.18.** Industrial synthetic routes for the synthesis of vanillin.

The second route circumvents the use of toxic  $\text{Me}_2\text{SO}_4$  and satisfactorily improves the atom efficiency by using a gas-phase methylation with methanol and a  $\text{LaPO}_4$  catalyst to obtain **XLVIII**, then the route was modified due to the low yield in the

formylation reaction using glyoxylic acid, the aforementioned low yield can be explained by the Cannizzaro reaction<sup>155</sup>, which involves the disproportionation of a non-enolizable aldehyde under basic media to give an alcohol and a carboxylic acid. To by-pass this inefficient step, a zeolite-catalysed hydroxymethylation was performed using formaldehyde yielding vanillyl alcohol, **LI**. In the final step, intermediate **LI** is oxidised to give vanillin, **LII**.

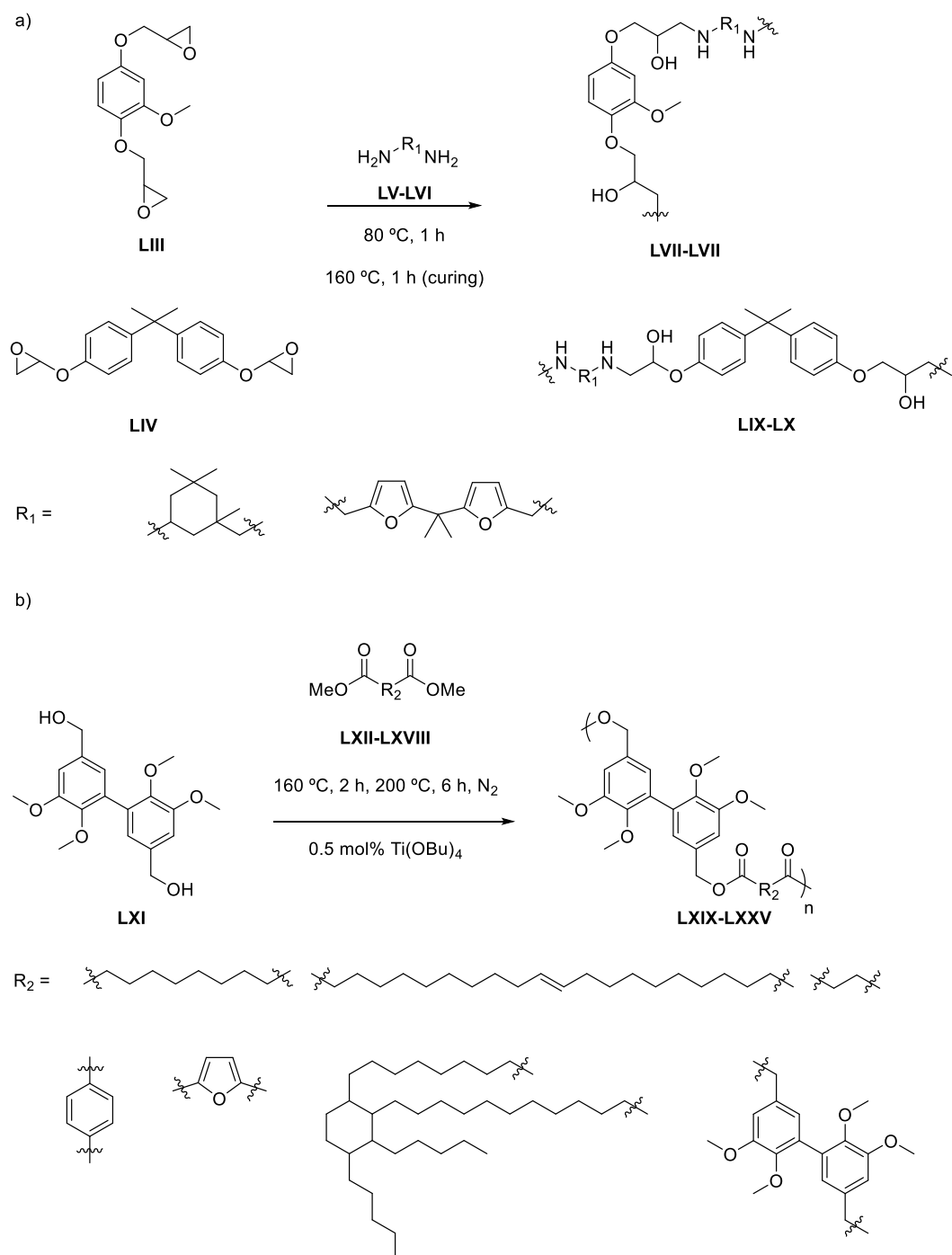
The third source for vanillin production is lignin. As discussed above, lignin represents 25% of hemicellulose, moreover, lignin is one of the three kinds of renewable aromatic building blocks along with tannins<sup>156</sup> which is obtained from wood, and cashew nutshell liquid.<sup>157</sup> The isolated types of lignin can be classified depending on the physicochemical method applied for its isolation.<sup>158</sup> There are three different types of lignin which are classified based on the chemical processes applied for the production of wood pulp, scilicet, sulfite, kraft and soda.<sup>159, 160</sup> Depolymerization of lignin to isolate vanillin involves a process in which a series of oxidations of lignin in an aqueous media under high pressures and temperatures take place. As a consequence of the complex heterogeneity of lignin, different mechanisms have been proposed for the transformation of lignin in to vanillin.<sup>161-164</sup> Vanillin indeed represents a very interesting building block as Fache *et al.* reported.<sup>165</sup> The presence of an aromatic aldehyde moiety along with a phenol offers huge opportunities for targeting specific monomers for the synthesis of a plethora of different kinds of polymers (Scheme 1.19).



**Scheme 1.19.** Targeted monomers prepared from vanillin (adapted from Ref 165).

The huge potential of vanillin-based monomers has been exploited by several authors to prepare different kinds of polymers.<sup>166</sup> For example, Caillol and co-workers reported the synthesis of a fully bio-based epoxy thermosets prepared from vanillin and furfural derivatives (Scheme 1.20a).<sup>167</sup> Epoxy thermosets were prepared by reaction of a vanillin-based epoxide, **LIII**, with different amines, **LV-LVI**. The thermomechanical properties of the prepared materials, **LVII-LVIII**, were studied and compared with the analogous epoxy thermoset prepared around diglycidylether of bisphenol A (DGEBA), **LIX-LX**. To the delight of the authors, the properties of the bio-based polymers exhibited improved properties compared to the oil-based, DGEBA, **LIV**. Their findings revealed the high potential that vanillin-based polymers have for the substitution of bisphenol A-based polymers, which indeed is a known endocrine disruptor and it is suspected to produce reproductive harmful effects.

Vanillin-based monomers have also been reported in the synthesis of polyesters (Scheme 1.20b).<sup>168</sup> Llevot *et al.* synthesised a symmetrical vanillin-based diol, **LXI**, using an enzymatic pathway. Then, **LXI** was reacted with a series of different diesters, **LXII-LXVIII**. The polymerization was carried out in bulk and catalysed by an organotin compound. The so obtained polyesters, **LXIX-LXXV**, showed high molar masses, up to 65,000 g/mol. Thermo-mechanical properties were studied by dynamical mechanical analysis (DMA) and the battery of polyesters exhibited a storage modulus ranging from 0.1 to 8.1 GPa.



**Scheme 1.20.** Synthesis of vanillin-based epoxy resins a), synthesis of vanillin-based polycarbonates b).

## 1.4 Conclusions

In conclusion, despite its low reactivity, CO<sub>2</sub> represents an inexhaustible C1 synthon for the synthesis of a broad range of different chemicals. As a consequence of its straight influence in the global warming phenomenon, many studies are being conducted in order to find methodologies to not only capture and reduce CO<sub>2</sub>

emissions, but to revalorise it. Among the CO<sub>2</sub> revalorization technologies, the synthesis of cyclic carbonates from epoxides is one of the most studied ones. For that goal, both metal-based and organocatalytic methodologies have been described. Despite the higher efficiency of metal-based methods, nowadays it is in fashion finding novel organocatalysts more sustainable, able to perform chemical transformations with the same efficiency that their organometallic analogous. Following the pursuit of fully green and sustainable methodologies for the synthesis of added-value chemicals, biomass can be envisaged as a renewable substitute for fossil fuels resources. Lignocellulose is the most abundant renewable raw material on Earth and biofuels *e.g.* bio-ethanol. One of the three components that lignocellulose is composed of is lignin. This aromatic biopolymer represents one main source of renewable aromatic compounds. Vanillin is one of the highlighted aromatic compounds that can be isolated from lignin. Its phenol and aromatic aldehyde functionalities are unique platforms for the synthesis of a plethora of potential monomers with different bis-functionalities. One of those functionalities are cyclic carbonates. As discussed above cyclic carbonates can be prepared by cycloaddition of CO<sub>2</sub> to epoxides. Moreover bis-cyclic carbonates are the most used type of monomers for the synthesis of non-isocyanate poly(hydroxyurethanes), This strategy has the great advantage of by-passing the use of toxic isocyanates in the synthesis of polyurethanes. Investigations around the preparation of NIPUs are indeed attracting lots of interest in both industry and academia.

### 1.5 References

1. The Early Keeling Curve. Scripps CO<sub>2</sub> Program, [http://scrippsco2.ucsd.edu/history\\_legacy/early\\_keeling\\_curve](http://scrippsco2.ucsd.edu/history_legacy/early_keeling_curve)).
2. D. J. Jacob, *Introduction to atmospheric chemistry*, Princeton University Press, 1999.
3. T. F. Stocker, D. Qin, G. K. Plattner, M. M. B. Tignor, S. K. Allen, J. Boschung, A. Nauels, Y. Xia, V. Bex and P. M. Midgley, *IPCC 2013: Summary for Policy Makers* Cambridge Univ. Press, 2013.
4. F. T. Zangeneh, S. Sahebdehfar and M. T. Ravanchi, *J. Nat. Gas Chem.*, 2011, **20**, 219-231.
5. A. A. Olajire, *J. CO<sub>2</sub> Util.*, 2013, **3-4**, 74-92.

6. S.-i. Fujita, H. Yoshida, R. Liu and M. Arai, in *New and Future Developments in Catalysis*, ed. S. L. Luib, Elsevier, Amsterdam, 2013, ch. 5, pp. 149-169.
7. Q. Liu, L. Wu, R. Jackstell and M. Beller, *Nat Commun.*, 2015, **6**, 5933.
8. A. Rafiee, K. Rajab Khalilpour, D. Milani and M. Panahi, *J. Environ. Chem. Eng.*, 2018, **6**, 5771-5794.
9. M. M. Halmann, *Chemical Fixation of Carbon Dioxide: Methods for Recycling CO<sub>2</sub> Into Useful Products*, CRC Press, Boca Raton, 1993.
10. S. B. Wang, G. Q. M. Lu and G. J. Millar, *Energy Fuels*, 1996, **10**, 896-904.
11. D. Pakhare and J. Spivey, *Chem. Soc. Rev.*, 2014, **43**, 7813-7837.
12. H. Schulz, *Appl. Catal., A*, 1999, **186**, 3-12.
13. A. Y. Khodakov, W. Chu and P. Fongarland, *Chem. Rev.*, 2007, **107**, 1692-1744.
14. A. de Klerk, in *Kirk-Othmer Encyclopedia of Chemical Technology*, Wiley-VCH, Weinheim, 2013, pp. 1-36.
15. B. Schöffner, F. Schöffner, S. P. Verevkin and A. Börner, *Chem. Rev.*, 2010, **110**, 4554-4581.
16. M. WH, *Adv. Mater.*, 1998, **10**, 439-448.
17. S. S. Zhang, *J. Power Sources*, 2006, **162**, 1379-1394.
18. G. W. Coates and D. R. Moore, *Angew. Chem. Int. Ed.*, 2004, **43**, 6618-6639.
19. D. J. Darensbourg, *Chem. Rev.*, 2007, **107**, 2388-2410.
20. M. R. Kember, A. Buchard and C. K. Williams, *Chem. Commun.*, 2011, **47**, 141-163.
21. S. J. Poland and D. J. Darensbourg, *Green Chem.*, 2017, **19**, 4990-5011.
22. H. Blattmann, M. Fleischer, M. Bahr and R. Mulhaupt, *Macromol. Rapid Commun.*, 2014, **35**, 1238-1254.
23. G. Rokicki, P. G. Parzuchowski and M. Mazurek, *Polym. Adv. Technol.*, 2015, **26**, 707-761.
24. L. Maisonneuve, O. Lamarzelle, E. Rix, E. Grau and H. Cramail, *Chem. Rev.*, 2015, **115**, 12407-12439.
25. N. Kindermann, T. Jose and A. W. Kleij, *Top. Curr. Chem.*, 2017, **375**, 15.
26. A. Decortes, A. M. Castilla and A. W. Kleij, *Angew. Chem. Int. Ed.*, 2010, **49**, 9822-9837.

27. Q. He, J. W. O'Brien, K. A. Kitselman, L. E. Tompkins, G. C. T. Curtis and F. M. Kerton, *Catal. Sci. Technol.*, 2014, **4**, 1513-1528.
28. R. R. Shaikh, S. Pornpraprom and V. D'Elia, *ACS Catal.*, 2017, **8**, 419-450.
29. M. Alves, B. Grignard, R. Mereau, C. Jerome, T. Tassaing and C. Detrembleur, *Catal. Sci. Technol.*, 2017, **7**, 2651-2684.
30. H. Buttner, L. Longwitz, J. Steinbauer, C. Wulf and T. Werner, *Top. Curr. Chem.*, 2017, **375**, 50.
31. R. Dalpozzo, N. Della Ca', B. Gabriele and R. Mancuso, *Catalysts*, 2019, **9**.
32. J. W. Comerford, I. D. V. Ingram, M. North and X. Wu, *Green Chem.*, 2015, **17**, 1966-1987.
33. C. Martín, G. Fiorani and A. W. Kleij, *ACS Catal.*, 2015, **5**, 1353-1370.
34. V. D'Elia, J. D. A. Pelletier and J.-M. Basset, *ChemCatChem*, 2015, **7**, 1906-1917.
35. G. Fiorani, W. Guo and A. W. Kleij, *Green Chem.*, 2015, **17**, 1375-1389.
36. J. C. Hicks, J. H. Drese, D. J. Fauth, M. L. Gray, G. G. Qi and C. W. Jones, *J. Am. Chem. Soc.*, 2008, **130**, 2902-2903.
37. H. Yang, Z. Xu, M. Fan, R. Gupta, R. B. Slimane, A. E. Bland and I. Wright, *J. Environ. Sci.*, 2008, **20**, 14-27.
38. Y. Kayaki, M. Yamamoto and T. Ikariya, *Angew. Chem. Int. Ed.*, 2009, **48**, 4194-4197.
39. H. Zhou, Y.-M. Wang, W.-Z. Zhang, J.-P. Qu and X.-B. Lu, *Green Chem.*, 2011, **13**, 644-650.
40. M. J. Ajitha and C. H. Suresh, *Tetrahedron Lett.*, 2011, **52**, 5403-5406.
41. C. Cadena, J. L. Anthony, J. K. Shah, T. I. Morrow, J. F. Brennecke and E. J. Maginn, *J. Am. Chem. Soc.*, 2004, **126**, 5300-5308.
42. J. Peng and Y. Deng, *New J. Chem.*, 2001, **25**, 639-641.
43. H. Kawanami, A. Sasaki, K. Matsui and Y. Ikushima, *Chem. Commun.*, 2003, 896-897.
44. J. Sun, S. Zhang, W. Cheng and J. Ren, *Tetrahedron Lett.*, 2008, **49**, 3588-3591.
45. J. Sun, L. Han, W. Cheng, J. Wang, X. Zhang and S. Zhang, *ChemSusChem*, 2011, **4**, 502-507.

46. A.-L. Girard, N. Simon, M. Zanatta, S. Marmitt, P. Gonçalves and J. Dupont, *Green Chem.*, 2014, **16**, 2815-2825.
47. L. Xiao, D. Su, C. Yue and W. Wu, *J. CO<sub>2</sub> Util.*, 2014, **6**, 1-6.
48. C. Yue, D. Su, X. Zhang, W. Wu and L. Xiao, *Catal. Lett.*, 2014, **144**, 1313-1321.
49. M. H. Anthofer, M. E. Wilhelm, M. Cokoja, I. I. E. Markovits, A. Pöthig, J. Mink, W. A. Herrmann and F. E. Kühn, *Catal. Sci. Technol.*, 2014, **4**, 1749-1758.
50. J.-Q. Wang, W.-G. Cheng, J. Sun, T.-Y. Shi, X.-P. Zhang and S.-J. Zhang, *RSC Adv.*, 2014, **4**, 2360-2367.
51. M. H. Anthofer, M. E. Wilhelm, M. Cokoja, M. Drees, W. A. Herrmann and F. E. Kühn, *ChemCatChem*, 2015, **7**, 94-98.
52. M. Feng, G. Zhao, H. Gao and S. Zhang, *Aust. J. Chem.*, 2015, **68**, 1513-1517.
53. S. Denizaltı, *RSC Adv.*, 2015, **5**, 45454-45458.
54. P. Jaiswal and M. N. Varma, *J. CO<sub>2</sub> Util.*, 2016, **14**, 93-97.
55. S. Wu, B. Wang, Y. Zhang, E. H. M. Elageed, H. Wu and G. Gao, *J. Mol. Catal. A-Chem.*, 2016, **418-419**, 1-8.
56. E. R. Pérez, R. H. A. Santos, M. T. P. Gambardella, L. G. M. d. Macedo, U. P. Rodrigues-Filho, J.-C. Launay and D. W. Franco, *J. Org. Chem*, 2004, **69**, 8005-8011.
57. J. Ma, X. Zhang, N. Zhao, A. S. N. Al-Arifi, T. Aouak, Z. A. Al-Othman, F. Xiao, W. Wei and Y. Sun, *J. Mol. Catal. A. Chem.*, 2010, **315**, 76-81.
58. F. S. Pereira, E. R. deAzevedo, E. F. da Silva, T. J. Bonagamba, D. L. da Silva Agostíni, A. Magalhães, A. E. Job and E. R. Pérez González, *Tetrahedron*, 2008, **64**, 10097-10106.
59. C. Das Neves Gomes, O. Jacquet, C. Villiers, P. Thuery, M. Ephritikhine and T. Cantat, *Angew. Chem. Int. Ed.*, 2012, **51**, 187-190.
60. C. Das Neves Gomes, E. Blondiaux, P. Thuery and T. Cantat, *Chem. Eur. J.*, 2014, **20**, 7098-7106.
61. J. F. Cooper and L. Myri, 1956, *U.S. Patent No 2773070*.
62. W. J. Peppel, *Ind. Eng. Chem. Res.*, 1958, **50**, 767-770.
63. V. Caló, A. Nacci, A. Monopoli and A. Fanizzi, *Org. Lett.*, 2002, **4**, 2561-2563.



64. J. Song, B. Zhang, P. Zhang, J. Ma, J. Liu, H. Fan, T. Jiang and B. Han, *Catal. Today*, 2012, **183**, 130-135.
65. T. Ema, K. Fukuhara, T. Sakai, M. Ohbo, F.-Q. Bai and J.-y. Hasegawa, *Catal. Sci. Technol.*, 2015, **5**, 2314-2321.
66. J. Sun, J. Ren, S. Zhang and W. Cheng, *Tetrahedron Lett.*, 2009, **50**, 423-426.
67. T. Takahashi, T. Watahiki, S. Kitazume, H. Yasuda and T. Sakakura, *Chem. Commun.*, 2006, 1664-1666.
68. N. Aoyagi, Y. Furusho and T. Endo, *Tetrahedron Lett.*, 2013, **54**, 7031-7034.
69. M. Galvan, M. Selva, A. Perosa and M. Noè, *Asian J. Org. Chem.*, 2014, **3**, 504-513.
70. J. Tharun, A. C. Kathalikkattil, R. Roshan, D.-H. Kang, H.-C. Woo and D.-W. Park, *Catal. Commun.*, 2014, **54**, 31-34.
71. W. L. Wong, P. H. Chan, Z. Y. Zhou, K. H. Lee, K. C. Cheung and K. Y. Wong, *ChemSusChem*, 2008, **1**, 67-70.
72. A. R. Hajipour, Y. Heidari and G. Kozehgary, *RSC Adv.*, 2015, **5**, 61179-61183.
73. C. J. Whiteoak, A. Nova, F. Maseras and A. W. Kleij, *ChemSusChem*, 2012, **5**, 2032-2038.
74. A. M. Hardman-Baldwin and A. E. Mattson, *ChemSusChem*, 2014, **7**, 3275-3278.
75. M. Alves, B. Grignard, S. Gennen, R. Mereau, C. Detrembleur, C. Jerome and T. Tassaing, *Catal. Sci. Technol.*, 2015, **5**, 4636-4643.
76. V. B. Saptal and B. M. Bhanage, *ChemSusChem*, 2017, **10**, 1145-1151.
77. L. Wang, G. Zhang, K. Kodama and T. Hirose, *Green Chemistry*, 2016, **18**, 1229-1233.
78. J. Wang and Y. Zhang, *ACS Catal.*, 2016, **6**, 4871-4876.
79. X.-F. Liu, Q.-W. Song, S. Zhang and L.-N. He, *Catal. Today*, 2016, **263**, 69-74.
80. S. Arayachukiat, C. Kongtes, A. Barthel, S. V. C. Vummaleti, A. Poater, S. Wannakao, L. Cavallo and V. D'Elia, *ACS Sustainable Chem. Eng*, 2017, **5**, 6392-6397.

81. J. Sun, W. Cheng, Z. Yang, J. Wang, T. Xu, J. Xin and S. Zhang, *Green Chem.*, 2014, **16**.
82. W. Cheng, F. Xu, J. Sun, K. Dong, C. Ma and S. Zhang, *Synth. Commun.*, 2016, **46**, 497-508.
83. K. R. Roshan, T. Jose, A. C. Kathalikkattil, D. W. Kim, B. Kim and D. W. Park, *Appl. Catal., A*, 2013, **467**, 17-25.
84. J. Sun, J. Wang, W. Cheng, J. Zhang, X. Li, S. Zhang and Y. She, *Green Chem.*, 2012, **14**, 654-660.
85. V. Besse, N. Illy, G. David, S. Caillol and B. Boutevin, *ChemSusChem*, 2016, **9**, 2167-2173.
86. J. Q. Wang, J. Sun, W. G. Cheng, K. Dong, X. P. Zhang and S. J. Zhang, *Phys. Chem. Chem. Phys.*, 2012, **14**, 11021-11026.
87. S. Sopena, G. Fiorani, C. Martin and A. W. Kleij, *ChemSusChem*, 2015, **8**, 3248-3254.
88. O. Bayer, *Angew. Chem.*, 1947, **59**, 257-272.
89. Z. S. Petrovic and J. Ferguson, *Prog. Polym. Sci.*, 1991, **16**, 695-836.
90. R. B. Seymour and G. B. Kauffman, *J. Chem. Educ.*, 1992, **69**, 909-910.
91. D. K. Chattopadhyay and K. V. S. N. Raju, *Prog. Polym. Sci.*, 2007, **32**, 352-418.
92. E. Delebecq, J. P. Pascault, B. Boutevin and F. Ganachaud, *Chem. Rev.*, 2013, **113**, 80-118.
93. H. W. Engels, H. G. Pirkl, R. Albers, R. W. Albach, J. Krause, A. Hoffmann, H. Casselmann and J. Dormish, *Angew. Chem. Int. Ed.*, 2013, **52**, 9422-9441.
94. R. Devendra, N. R. Edmonds and T. Söhnel, *J. Mol. Catal. A-Chem.*, 2013, **366**, 126-139.
95. Y. Salánki, Y. D'eri, A. Platokhin and K. Sh-Rózsa, *Neurosci. Behav. Physiol.*, 2000, **30**, 63-73.
96. L. Møhlhave, B. Bach and O. F. Pedersen, *Environ. Int.*, 1986, **12**, 167-175.
97. E. Broughton, *Environ. Health*, 2005, **4**, 6.
98. O. Kreyc, H. Mutlu and M. A. R. Meier, *Green Chem.*, 2013, **15**.
99. H. J. Twitchett, *Chem. Soc. Rev.*, 1974, **3**, 209-230.
100. W. Su, W. Zhong, G. Bian, X. Shi and J. Zhang, *Org. Prep. Proced. Int.*, 2004, **36**, 499-547.

101. A. Wurtz, *Liebigs Ann.*, 1849, **71**, 326-342.
102. A. W. Hofmann, *Liebigs Ann.*, 1850, **74**, 1-33.
103. K. H. Slotta and L. Lorenz, *Chem. Ber.*, 1925, **58**, 1320-1323.
104. S. Brase, C. Gil, K. Knepper and V. Zimmermann, *Angew. Chem. Int. Ed.*, 2005, **44**, 5188-5240.
105. A. W. Hofmann, *Ber. Dtsch. Chem. Ges.*, 1881, **14**, 2725-2736.
106. W. J. Middleton, *J. Org. Chem.*, 1984, **49**, 4541-4543.
107. P. Dubé, N. F. Fine Nathel, M. Vetelino, M. Couturier, C. Larrivé Aboussafy, S. Pichette, M. L. Jorgensen and M. Hardink, *Org. Lett.*, 2009, **11**, 5622-5625.
108. S. Merenyi, *REACH: Regulation (EC) No 1907/2006: Consolidated version (June 2012) with an introduction and future prospects regarding the area of Chemicals legislation*, 2012.
109. H. Sardon, A. Pascual, D. Mecerreyes, D. Taton, H. Cramail and J. L. Hedrick, *Macromolecules*, 2015, **48**, 3153-3165.
110. A. Cornille, R. Auvergne, O. Figovsky, B. Boutevin and S. Caillol, *Eur. Polym. J.*, 2017, **87**, 535-552.
111. V. Froidevaux, C. Negrell, S. Caillol, J. P. Pascault and B. Boutevin, *Chem. Rev.*, 2016, **116**, 14181-14224.
112. H. Tomita, F. Sanda and T. Endo, *J. Polym. Sci. A Polym. Chem.*, 2001, **39**, 162-168.
113. H. Tomita, F. Sanda and T. Endo, *J. Polym. Sci. A Polym. Chem.*, 2001, **39**, 860-867.
114. H. Tomita, F. Sanda and T. Endo, *J. Polym. Sci. A Polym. Chem.*, 2001, **39**, 4091-4100.
115. H. Tomita, F. Sanda and T. Endo, *J. Polym. Sci. A Polym. Chem.*, 2001, **39**, 3678-3685.
116. A. Yuen, A. Bossion, E. Gómez-Bengoia, F. Ruipérez, M. Isik, J. L. Hedrick, D. Mecerreyes, Y. Y. Yang and H. Sardon, *Polym. Chem.*, 2016, **7**, 2105-2111.
117. A. Steblyanko, W. Choi, F. Sanda and T. Endo, *J. Polym. Sci. A Polym. Chem.*, 2000, **38**, 2375-2380.

118. R. M. Garipov, V. A. Sysoev, V. V. Mikheev, A. I. Zagidullin, R. Y. Deberdeev, V. I. Irzhak and A. A. Berlin, *Dokl. Phys. Chem.*, 2003, **393**, 289-292.
119. L. Maisonneuve, A.-L. Wirotius, C. Alfos, E. Grau and H. Cramail, *Polym. Chem.*, 2014, **5**, 6142-6147.
120. O. Lamarzelle, P.-L. Durand, A.-L. Wirotius, G. Chollet, E. Grau and H. Cramail, *Polym. Chem.*, 2016, **7**, 1439-1451.
121. C. D. Diakoumakos and D. L. Kotzev, *Macromol. Symp.*, 2004, **216**, 37-46.
122. V. Besse, F. Camara, F. Méchin, E. Fleury, S. Caillol, J.-P. Pascault and B. Boutevin, *Eur. Polym. J.*, 2015, **71**, 1-11.
123. J. H. Clements, *Ind. Eng. Chem. Res.*, 2003, **42**, 663-674.
124. A. J. Ragauskas, C. K. Williams, B. H. Davison, G. Britovsek, J. Cairney, C. A. Eckert, W. J. Frederick, Jr., J. P. Hallett, D. J. Leak, C. L. Liotta, J. R. Mielenz, R. Murphy, R. Templer and T. Tschaplinski, *Science*, 2006, **311**, 484-489.
125. A. Demirbas, *Prog. Energy Combust. Sci.*, 2007, **33**, 1-18.
126. M. Höök and X. Tang, *Energy Policy*, 2013, **52**, 797-809.
127. D. Esposito and M. Antonietti, *Chem. Soc. Rev.*, 2015, **44**, 5821-5835.
128. N. Brun, P. Hesemann and D. Esposito, *Chem. Sci.*, 2017, **8**, 4724-4738.
129. K. Kohli, R. Prajapati and B. Sharma, *Energies*, 2019, **12**, 233.
130. A. Gandini and T. M. Lacerda, *Prog. Polym. Sci.*, 2015, **48**, 1-39.
131. J. J. Bozell, L. Moens, D. C. Elliott, Y. Wang, G. G. Neuenschwander, S. W. Fitzpatrick, R. J. Bilski and J. L. Jarnefeld, *Resour. Conserv. Recycl.*, 2000, **28**, 227-239.
132. Y. Luo, Z. Li, X. Li, X. Liu, J. Fan, J. H. Clark and C. Hu, *Catal. Today*, 2019, **319**, 14-24.
133. F. W. Lichtenthaler, *Acc. Chem. Res.*, 2002, **35**, 728-737.
134. R. Datta and M. Henry, *J. Chem. Technol. Biotechnol.*, 2006, **81**, 1119-1129.
135. M. Jamshidian, E. A. Tehrany, M. Imran, M. Jacquot and S. Desobry, *Compr. Rev. Food Sci. Food Saf.*, 2010, **9**, 552-571.
136. B. Agarwal, K. Kailasam, R. S. Sangwan and S. Elumalai, *Renew. Sustain. Energ. Rev.*, 2018, **82**, 2408-2425.
137. F. Menegazzo, E. Ghedini and M. Signoretto, *Molecules*, 2018, **23**, 2201.

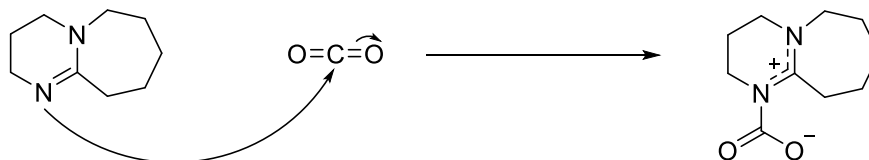
138. D. Zhang and M.-J. Dumont, *J. Polym. Sci. A Polym. Chem.*, 2017, **55**, 1478-1492.
139. S. K. Burgess, J. E. Leisen, B. E. Kraftschik, C. R. Mubarak, R. M. Kriegel and W. J. Koros, *Macromolecules*, 2014, **47**, 1383-1391.
140. K. Madhavan Nampoothiri, N. R. Nair and R. P. John, *Bioresour. Technol.*, 2010, **101**, 8493-8501.
141. J. Ten Dam, F. Kapteijn, K. Djanashvili and U. Hanefeld, *Catal. Commun.*, 2011, **13**, 1-5.
142. S. Farah, D. G. Anderson and R. Langer, *Adv. Drug. Deliv. Rev.*, 2016, **107**, 367-392.
143. R. Mehta, V. Kumar, H. Bhunia and S. N. Upadhyay, *Macromol. Sci, Part C: Polym. Rev.*, 2005, **45**, 325-349.
144. W. H. Carothers, G. L. Dorough and F. J. v. N. J., *J. Am. Chem. Soc.*, 1932, **54**, 761-772.
145. B. Lin and R. M. Waymouth, *J. Am. Chem. Soc.*, 2017, **139**, 1645-1652.
146. J. C. Worch, H. Prydderch, S. Jimaja, P. Bexis, M. L. Becker and A. P. Dove, *Nat. Rev. Chem.*, 2019, **3**, 514-535.
147. Y. Ikada, K. Jamshidi, H. Tsuji and S. H. Hyon, *Macromolecules*, 1987, **20**, 904-906.
148. M. Brzeziński and T. Biela, *Polym. Int.*, 2015, **64**, 1667-1675.
149. H. Soleymani Abyaneh, M. R. Vakili, A. Shafaati and A. Lavasanifar, *Mol. Pharm.*, 2017, **14**, 2487-2502.
150. J. E. Holladay, J. F. White, J. J. Bozell and D. Johnson, *Top Value Added Chemicals from Biomass. Vol II: Results of Screening for Potential Candidates from Biorefinery Lignin*, Washington DC, USA, 2007.
151. M. Fache, B. Boutevin and S. Caillol, *ACS Sustainable Chem. Eng*, 2015, **4**, 35-46.
152. M. M. Bomgardner, *Chem. Eng. News*, 2014, **92**, 14.
153. M. B. Hocking, *J. Chem. Educ.*, 1997, **74**, 1055-1059.
154. B. Schaefer, *Natural Products in the Chemical Industry*, Springer, 2014.
155. S. Cannizzaro, *Justus Liebigs Ann. Chem.*, 1853, **88**, 129-130.
156. A. Pizzi, in *Monomers Polymers and Composites from Renewable Resources*, eds. M. N. Belgacem and A. Gandini, Elsevier, Amsterdam, 2008, ch. 8, pp. 179-199.

157. V. S. Balachandran, S. R. Jadhav, P. K. Vemula and G. John, *Chem. Soc. Rev.*, 2013, **42**, 427-438.
158. J. R. Obst and T. K. Kirk, *Methods Enzymol.*, 1988, **161**, 3-12.
159. J. Lora, in *Monomers Polymers and Composites from Renewable Resources*, eds. M. N. Belgacem and A. Gandini, Elsevier, Amsterdam, 2008, ch. 10.
160. A. Vishtal and A. Kraslawski, *BioResources*, 2011, **6**, 3547-3568.
161. V. Tarabanko, D. Petukhov and G. Selyutin, *Kinet. Catal.*, 2004, **45**, 569-577.
162. P. C. Rodrigues Pinto, E. A. Borges da Silva and A. E. Rodrigues, in *Biomass Conversion: The Interface of Biotechnology, Chemistry and Materials Science*, eds. C. Baskar, S. Baskar and R. S. Dhillon, Springer, Berlin, 2012, ch. 12.
163. A. W. Pacek, P. Ding, M. Garrett, G. Sheldrake and A. W. Nienow, *Ind. Eng. Chem. Res.*, 2013, **52**, 8361-8372.
164. Q. Mei, X. Shen, H. Liu and B. Han, *Chin. Chem. Lett.*, 2019, **30**, 15-24.
165. M. Fache, E. Darroman, V. Besse, R. Auvergne, S. Caillol and B. Boutevin, *Green Chem.*, 2014, **16**, 1987-1998.
166. A. Llevot, E. Grau, S. Carlotti, S. Grelier and H. Cramail, *Macromol. Rapid Commun.*, 2016, **37**, 9-28.
167. M. Fache, C. Mont er mal, B. Boutevin and S. Caillol, *Eur. Polym. J.*, 2015, **73**, 344-362.
168. A. Llevot, E. Grau, S. Carlotti, S. Grelier and H. Cramail, *Polym. Chem.*, 2015, **6**, 6058-6066.

## **2. Organocatalytic synthesis of cyclic carbonates using DBU derivatives**

## 2.1 Introduction

As described in chapter 1, emissions of CO<sub>2</sub> to the atmosphere have been proven to be one of the most important factors of the greenhouse effect and therefore responsible for climate change.<sup>1</sup> However, CO<sub>2</sub> can be pictured as an inexhaustible, cheap and non-toxic C1 synthon and hence it can be exploited for the synthesis of a broad range of added-value products.<sup>2-8</sup> One of the products that can be prepared using CO<sub>2</sub>, is the synthesis of cyclic carbonates from epoxides.<sup>9-13</sup> Cyclic carbonates are found as intermediates for fine chemical synthesis, electrolytes in Li-ion batteries,<sup>14, 15</sup> monomers for the synthesis of polycarbonates and non-isocyanate poly(hydroxyurethanes) (NIPUs)<sup>16-20</sup> and as non-toxic polar solvents in synthesis and catalysis.<sup>21</sup> In this chapter, the relationship between structure and catalytic performance of different protic and alkyl DBU derivatives, for the synthesis of functional five-membered cyclic carbonates is studied. DBU unique ability to activate CO<sub>2</sub> forming a zwitterionic species has been extensively studied (Scheme 2.1)<sup>22</sup>, therefore DBU has been extensively exploited as platform for developing methodologies for the synthesis of five-membered cyclic carbonates (Table 2.1).



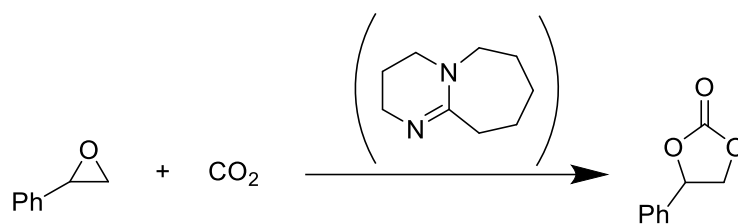
**Scheme 2.1.** DBU carbamate salt when reacting with CO<sub>2</sub>.

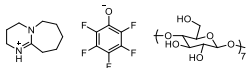
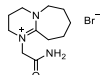
There are two different approaches to develop DBU-based methodologies for the synthesis of five-membered cyclic carbonates from epoxides according to the mechanisms reported to date (Scheme 2.2). In the first case DBU **I** is combined with a separate epoxide activating species (*e.g. via* hydrogen bond or acid-base Lewis interaction) in a binary system, CO<sub>2</sub> **II**, is activated by DBU forming a zwitterionic species **III**, thereupon, epoxide **IV** is ring-opened by **III** through a nucleophilic attack on the less substituted carbon to afford **V**, which undertakes an intramolecular ring-closure to obtain the desired five-membered carbonate **VI** (Table 2.1, entries 1 to 10).<sup>23-29</sup> Alternatively, DBU can be derivatised by either



protonation or alkylation of the basic nitrogen atom in position 1 (Table 2.1, entries 11 to 16).<sup>29-34</sup> This modification of the DBU renders a salt **VII** where the anion opens the epoxide ring *via* nucleophilic attack and the so obtained halo-alkoxide intermediate **VIII** is stabilised by the cation, subsequently CO<sub>2</sub> is added rendering an halo-carboxylate species **IX**. In the final step an intramolecular ring-closure of **IX** affords the desired five-membered cyclic carbonate **VI** and regenerates the corresponding catalyst.

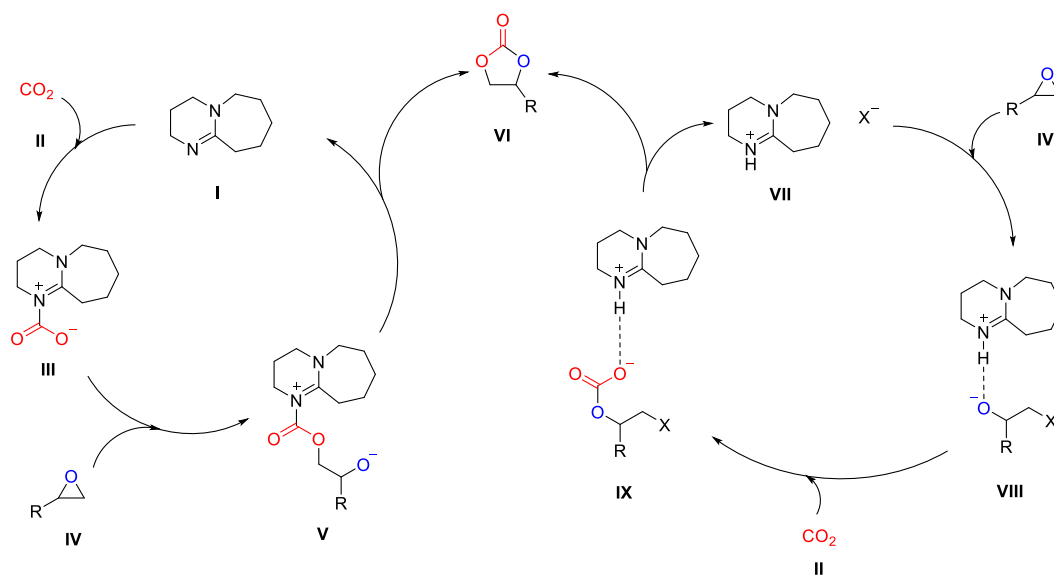
**Table 2.1.** Literature catalyst screening for the synthesis of styrene carbonate from styrene oxide and CO<sub>2</sub> using DBU derivatives.



Entry	Catalyst	Cat. Loading (%)	Pressure (bar)	Temperature (°C)	Time (h)	Yield (%)	TOF <sup>f</sup> (h <sup>-1</sup> )
1	DBU/Cellulose	15/1	20	120	2	85 <sup>a</sup>	42.5
2	DBU/2-deoxy-D-ribose	15/1	20	120	2	82 <sup>b</sup>	41.0
3	DBU/L-Histidine	10/2	20	120	2	85 <sup>b</sup>	21.2
4	DBU/CaBr <sub>2</sub>	5/5	1	100	12	90 <sup>b, c</sup>	1.50
5	DBU/BnBr	5/5	1	65	22	82 <sup>a</sup>	0.74
6	DBU/I <sub>2</sub>	5/5	1	65	4.75	96 <sup>b, d</sup>	4.04
7	DBU/Succinimide	5/5	1	100	10	18 <sup>b, e</sup>	0.36
8	DBU/ <i>N</i> -chlorosuccinimide	5/5	1	100	10	59 <sup>b, e</sup>	1.18
9	DBU/ <i>N</i> -bromosuccinimide	5/5	1	100	10	89 <sup>b, e</sup>	1.78
10	DBU/ <i>N</i> -iodosuccinimide	5/5	1	100	10	98 <sup>b, e</sup>	1.96
11	[HDBU]succinimide	5	1	100	10	8 <sup>b, e</sup>	0.16
12	[HDBU]Cl	1	10	140	2	81 <sup>b</sup>	40.5
13	[HDBU]I	5	1	25	24	64 <sup>b</sup>	0.53
14		1.5/1.5	30	130	10	96 <sup>b</sup>	6.40
15	2[HDBU]tartrate/ZnI <sub>2</sub>	0.64/0.96	30	80	5	95 <sup>b</sup>	29.7
16		2	20	120	3	90 <sup>b</sup>	15.0

<sup>a</sup> Yield was calculated by isolation of the cyclic carbonates by flash column silica chromatography. <sup>b</sup> Yield was calculated by GC-MS or <sup>1</sup>H NMR. <sup>c</sup> DMF was used as solvent. <sup>d</sup> 1,2-epoxybutane used as substrate. <sup>e</sup> 1,2-epoxyhexane used as substrate. <sup>f</sup> TOF = moles of product/(moles of catalyst × time).

Table 2.1 summarises the methodologies reported in the literature using DBU along with a cocatalyst or a DBU modified species, however the reaction conditions in most of the cases are not unified, therefore is not simple how to evaluate the structure-performance relationship upon preparation of an efficient DBU catalyst for the cyclocarbonation reaction of terminal epoxides to prepare five-membered cyclic carbonates.



**Scheme 2.2.** Proposed organocatalytic mechanisms for the synthesis of five-membered cyclic carbonates using DBU as catalyst (left pathway) and DBU salts (right pathway).

Herein, we describe a rational and systematic study of the relationship between structure and reactivity for protic and alkyl DBU derivatives in the cycloaddition of CO<sub>2</sub> to epoxides under solvent-free mild conditions, the optimal experimental conditions were extended to different functional epoxides and recyclability of the catalyst was tested. To corroborate the experimental data a computational study is reported.

## 2.2 Results and discussion

### 2.2.1 Synthesis of DBU salts

DBU has been reported as a CO<sub>2</sub> activator that can form a reversible carbamate species.<sup>22</sup> Despite this, DBU is not an efficient catalyst for the synthesis of five-membered cyclic carbonates from epoxides under mild conditions. Therefore, DBU derivatives were synthesised in order to improve its activity for the later mentioned process. Two different types of DBU based catalysts can be distinguished, a) protic DBU salts, **1-8**, which were prepared by simply protonation of the amidine using an acid or an ammonium halide (Figure 2.1); and b) *N*-alkyl derivatives, **9-14**, prepared *via* a bimolecular nucleophilic substitution (S<sub>N</sub>2) reaction between DBU and different functional alkyl halides (Scheme 2.3). The whole battery of catalysts, **1-14**, was characterised by <sup>1</sup>H and <sup>13</sup>C NMR spectroscopy. For novel compounds, HRMS and elemental analysis were also performed.

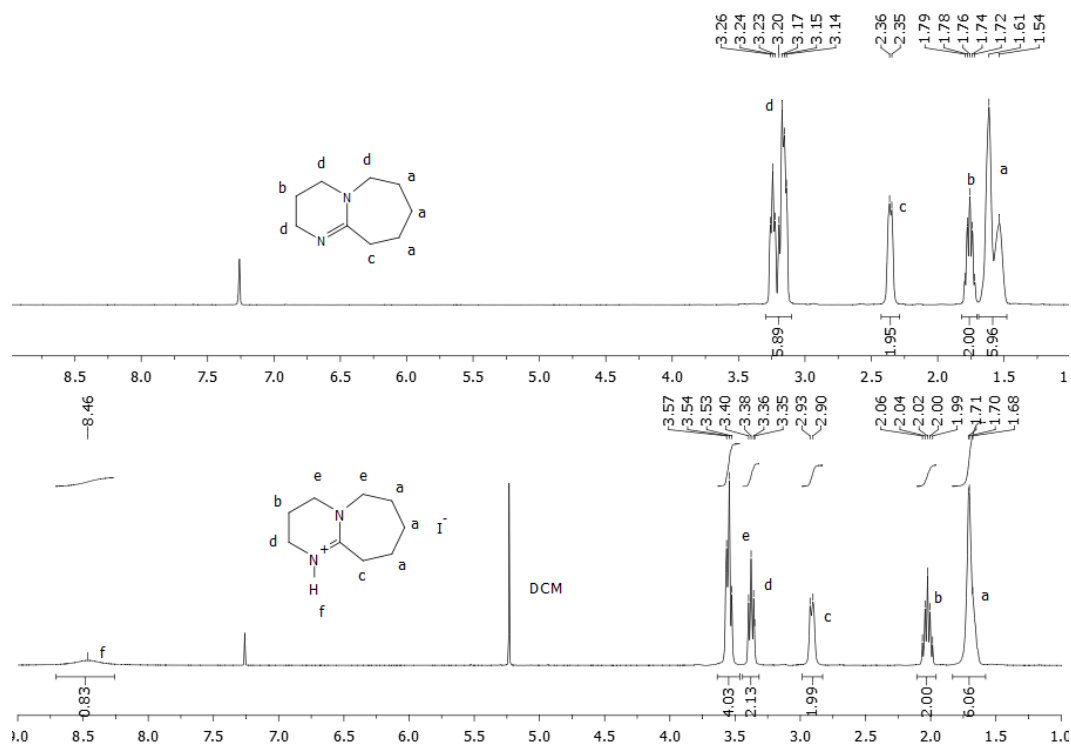
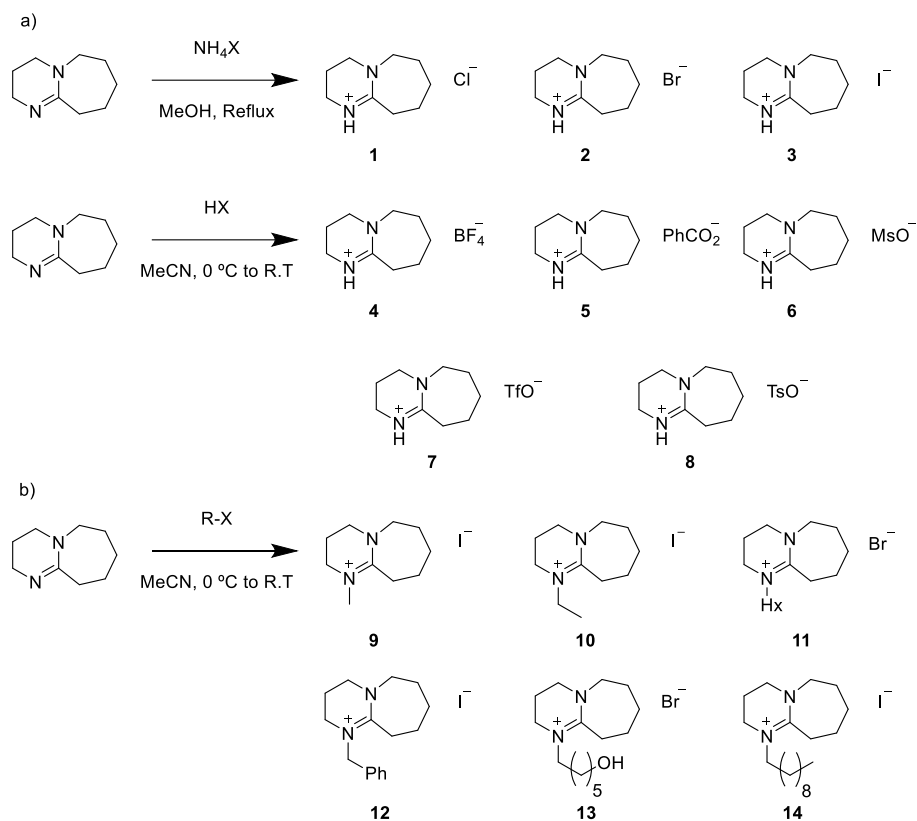


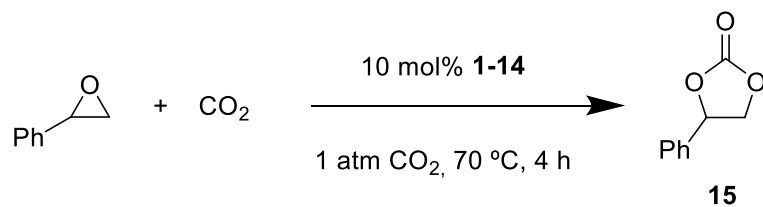
**Figure 2.1.** <sup>1</sup>H NMR spectra of DBU (*top*) and the resultant [HDBU]I catalyst (*bottom*). (300 MHz, 298 K, CDCl<sub>3</sub>).



**Scheme 2.3.** Synthesis of protic **1-8** (a) and *N*-alkyl **9-14** (b) DBU based catalysts.

### 2.2.2 Catalyst screening, optimization and synthesis of functional cyclic carbonates

All the catalysts were tested using styrene oxide as model substrate. The temperature was set at 70 °C far below from the boiling point of styrene oxide, and a pressure of 1 atm CO<sub>2</sub> was used (Scheme 2.4).



**Scheme 2.4.** Synthesis of styrene carbonate using different DBU salts.

Protic DBU catalysts **1-8** bearing halide anions showed moderate to high conversions with the iodide catalyst **3** performing the highest activity (Table 2.2, entries 1 to 3) (Figure 2.2). The remaining protic catalysts **4-8** showed none (Table 2.2, entries 4, 6 and 8) or very low activities (Table 2.2, entries 5 and 7). This low activity can be attributed to the poor nucleophilicity of the corresponding anions compared to the halide analogues. *N*-Alkyl DBU derivatives **9-14** didn't exhibit better performance compared to [HDBU]I, nevertheless certain tendencies were observed: a) an increase of the alkyl chain rendered higher conversions (Table 2.2, entries 13 and 14 vs 9 and 10); b) the incorporation of a phenyl ring didn't entail any significant improvement in the catalytic activity compared with the methyl and ethyl examples (Table 2.2, entry 11 vs 9 and 10); c) the presence of a hydroxyl group, which are known to interact with the epoxide *via* hydrogen bond

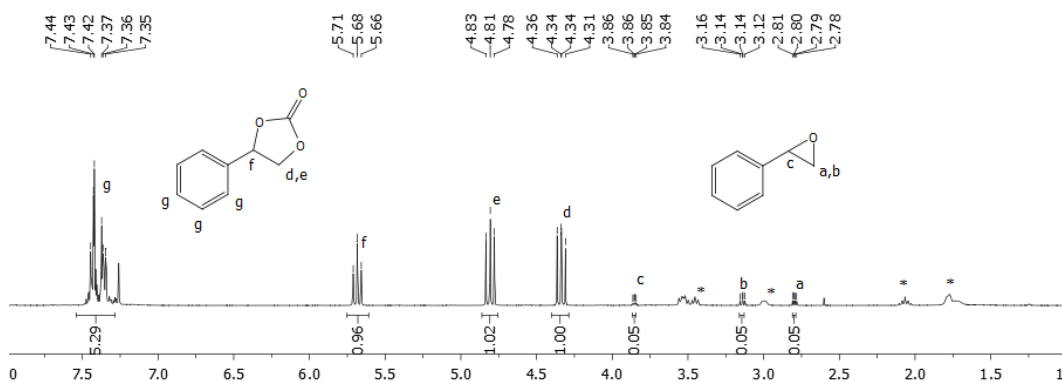


**Figure 2.2.** <sup>1</sup>H NMR spectrum of crude reaction for the synthesis of styrene carbonate from styrene oxide using 10 mol% of [HDBU]I at 70 °C for 4 hours (\* corresponds to [HDBU]I) (300 MHz, 298 K, CDCl<sub>3</sub>).

interaction, showed a significant improvement in the conversion compared with the non-hydroxylated analogue (Table 2.2, entry 12 vs 14). Finally, in order to demonstrate the synergistic effect of the DBU moiety and the halide anion, precursors of the best example observed were tested in their own as control experiments. Very low (3%) and no conversions were obtained when DBU and NH<sub>4</sub>I were tested under optimal conditions (Table 2.2, entries 15 and 16). Hydrogen bond donors are known to activate epoxides as they make the methylene and methene carbons more electrophilic. This fact explains the results observed, protic catalysts and the *N*-alkyl ones bearing hydrogen bond donor moieties showed the

best performances. According to proposed mechanisms found in the literature,<sup>35-37</sup> there is a compromise between nucleophilicity and leaving group ability. It is proposed that a halo-alkoxide intermediate is obtained once the epoxide ring is opened. Then, CO<sub>2</sub> is inserted and subsequently a ring-closure occurs rendering the cyclic carbonate, revealing the importance of having a good leaving group present on this last intermediate. Next, the effect of the catalyst loading was investigated for the best performing catalyst [HDBU]I (**3**). Unsurprisingly there is a linear correlation between the conversion obtained and the catalyst loading used (Table 2.3).

**Table 2.2.** Reaction studies for styrene oxide and CO<sub>2</sub> cycloaddition catalysed by DBU salts.<sup>a</sup>

Entry	R	X	Conv. <sup>b</sup> (%)	TOF <sup>c</sup> (h <sup>-1</sup> )
1	H	Cl	60	1.50
2	H	Br	77	1.93
3	H	I	96	2.40
4	H	BF <sub>4</sub>	0	0
5	H	PhCO <sub>2</sub>	13	0.33
6	H	MsO	0	0
7	H	TfO	5	0.13
8	H	TsO	0	0
9	Me	I	40	1.00
10	Et	I	36	0.90
11	Bn	I	41	1.03
12	HO-(CH <sub>2</sub> ) <sub>6</sub>	Br	71	1.78
13	CH <sub>3</sub> -(CH <sub>2</sub> ) <sub>9</sub>	I	75	1.88
14	Hx	Br	50	1.25
15 <sup>d</sup>	N.A	N.A	3	0.08
16 <sup>e</sup>	N.A	N.A	0	0

<sup>a</sup> Reactions carried out at 70 °C and 1 bar of pressure for 4 hours using 10 mol% of catalyst. <sup>b</sup> Conversion determined by <sup>1</sup>H NMR spectroscopy on the crude reaction mixture. <sup>c</sup> TOF = moles of product / (moles of catalyst × time). <sup>d</sup> DBU used as catalyst. <sup>e</sup> NH<sub>4</sub>I used as catalyst.

To prove the substrate versatility of the methodology, different terminal epoxides were tested under the optimal experimental conditions and isolated by flash column chromatography in silica gel (Figure 2.3). High conversions were obtained for

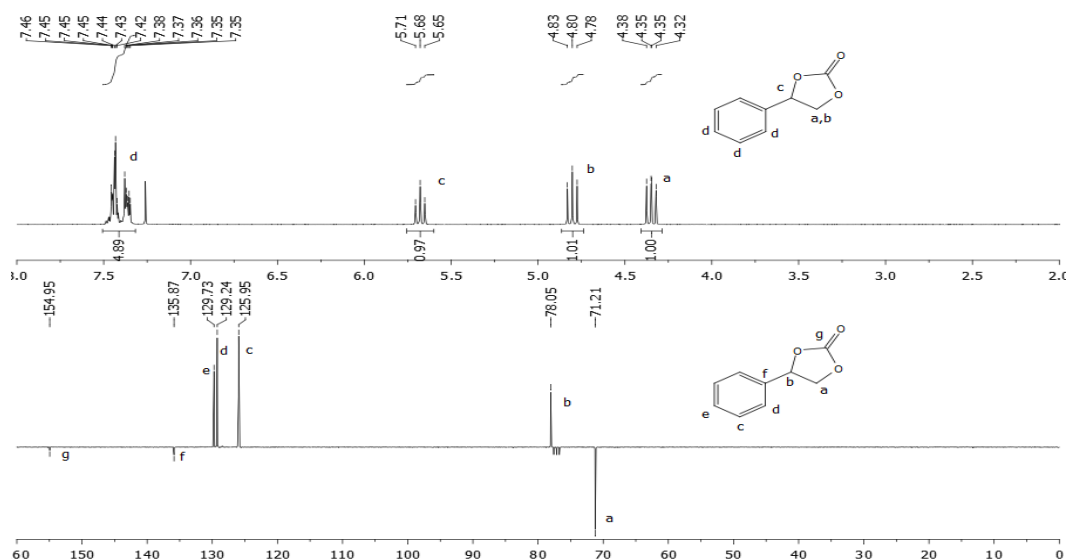
epoxides with several different functionalities, epichlorohydrin, allyl glycidyl ether, benzyl glycidyl ether and glycidol (Table 2.4, entries 2, 3, 4 and 5). However, in the cases of epoxides bearing saturated alkyl chains *i.e.* 1,2-epoxyoctane and 1,2-epoxybutane, the reaction mixtures were not homogeneous as [HDBU]I was insoluble in these substrates, (Table 2.4, entries 6 and 8).

**Table 2.3.** Screening catalysts loading for the synthesis of styrene carbonate.<sup>a</sup>

Entry	Catalyst Loading (%)	Conv. <sup>b</sup> (%)
1	1	54
2	2.5	66
3	5	80
4	10	96

<sup>a</sup> Reactions carried out at 70 °C and 1 bar of pressure for 4 hours. <sup>b</sup> Conversion determined by <sup>1</sup>H NMR spectroscopy on the crude reaction mixture.

As a consequence of these poor solubility, DMF, a solvent known to enhance reaction rates for this process,<sup>38,39</sup> was used, revealing full conversion in both cases (Table 2.4, entries 7 and 9). Finally, the cycloaddition of cyclohexene oxide was investigated. It is a non-terminal epoxide reported in the literature to be one of the most challenging substrates<sup>40</sup> as a consequence of its steric hindrance, that requires harsher reaction conditions to render the desired carbonate. Indeed, when cyclohexene oxide was tested under the optimal experimental conditions for the remaining epoxides, no cyclohexene carbonate was obtained (Table 2.4, entry 10). To obtain the carbonate **22**, the reaction was requested to be conducted in a high pressure reactor using 3 MPa of CO<sub>2</sub> at 140 °C to ensure full conversion. Beyond the harsher reaction conditions that were used, DMF was also required to enhance the reaction rate (Table 2.4, entry 11).

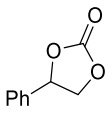
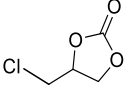
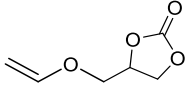
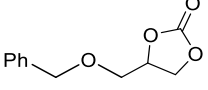
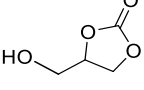
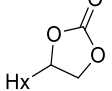
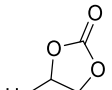
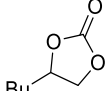
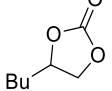
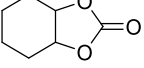
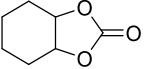


**Figure 2.3.**  $^1\text{H}$  NMR spectrum of isolated styrene carbonate by flash column chromatography in silica gel (*top*) (300 MHz, 298 K,  $\text{CDCl}_3$ ).  $^{13}\text{C}$  APT NMR spectrum of isolated styrene carbonate by flash column chromatography in silica gel (*bottom*) (75 MHz, 298 K,  $\text{CDCl}_3$ ).

To wrap up the study, the recyclability of the catalyst was studied using allyl glycidyl ether as model substrate since the corresponding carbonate **17** has a relatively low boiling point and the recyclability could be conducted more efficiently and under milder conditions. After five runs, no significant decrease on the conversion was observed, remaining between 99-97 %. The catalyst is highly efficient even after six runs in which conversion slightly decreased to 93 % (Figure 2.4).



**Table 2.4.** Cycloaddition of CO<sub>2</sub> to different functional epoxides catalysed by [HDBU]I.

Entry	Cyclic carbonate	Compound	Conv. <sup>a</sup> (%)	Yield <sup>d</sup> (%)
1		<b>15</b>	96	85
2		<b>16</b>	96	73
3		<b>17</b>	99	87
4		<b>18</b>	91	82
5		<b>19</b>	90	65
6		<b>20</b>	59	
7		<b>20</b>	100 <sup>b</sup>	83
8		<b>21</b>	14	
9		<b>21</b>	100 <sup>b</sup>	87
10		<b>22</b>	0	0
11		<b>22</b>	100 <sup>c</sup>	79

<sup>a</sup> Conversion determined by <sup>1</sup>H NMR spectroscopy on the crude reaction mixture. <sup>b</sup> DMF used as solvent. <sup>c</sup> 3MPa, 140 °C, 48 hours in DMF. <sup>d</sup> Product was isolated by flash column chromatography on silica gel.

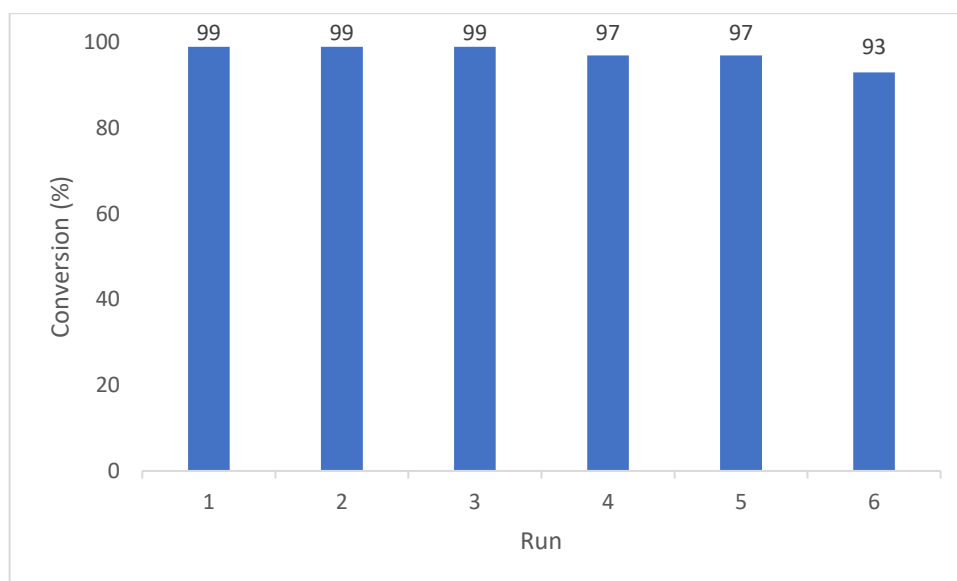
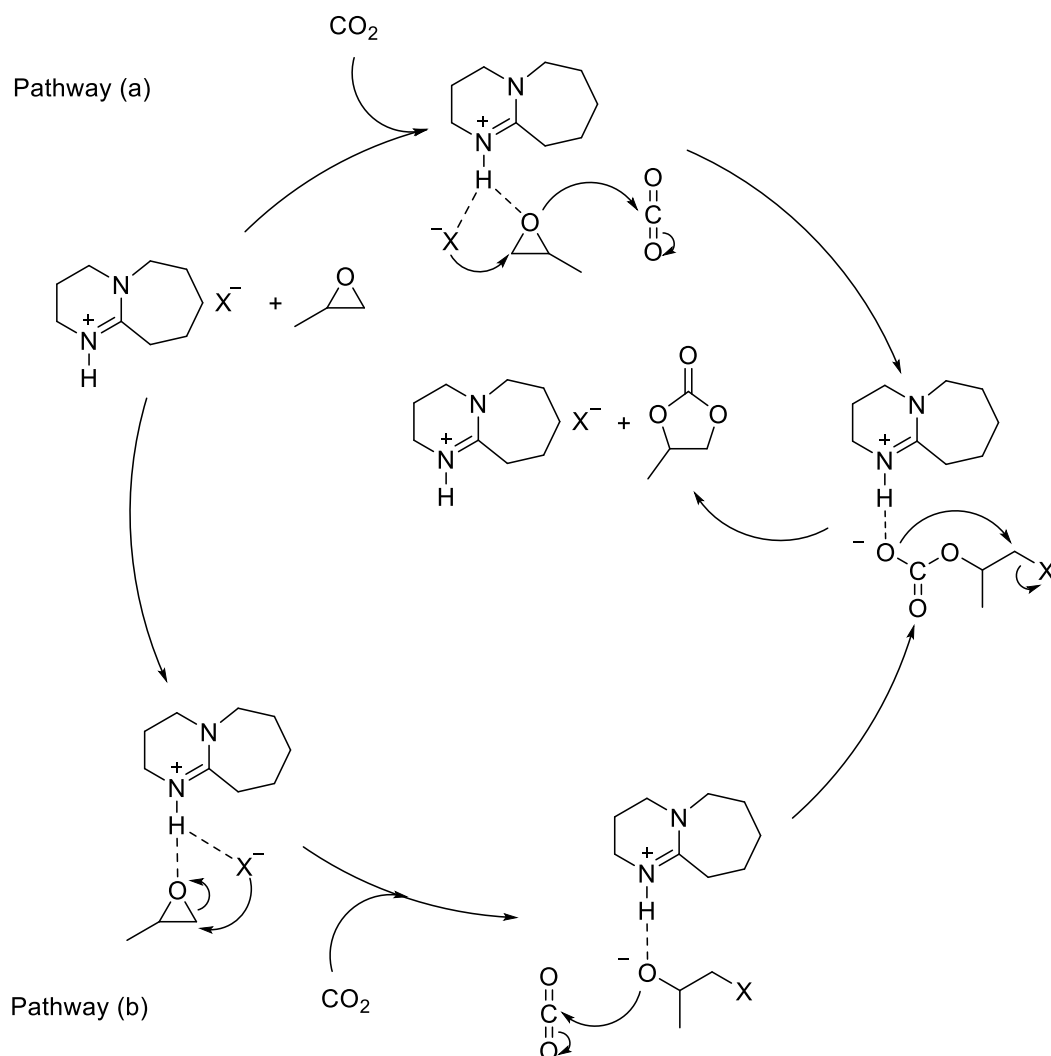


**Figure 2.4.** Conversion of allyl glycidyl ether from recycled catalyst.

### 2.2.3 Computational calculations

Density Functional Theory (DFT) was performed to envisage which is the reaction mechanism and to corroborate the premises discussed previously, hydrogen bond donor moieties promoting the ring-opening of the epoxide, plus the compromise between nucleophilicity and leaving group ability of the anion. Propylene oxide was used as model substrate and the protonated halide salts: [HDBU]Cl (**1**), [HDBU]Br (**2**) and [HDBU]I (**3**) as catalysts. Inspired by previous computational calculations reported in the literature literature,<sup>35-37</sup> two different mechanistic routes were suggested (Scheme 2.5). In the first one, epoxide and CO<sub>2</sub> activation occur simultaneously (Scheme 2.5, pathway (a)), whereas in the second one there is a stepwise activation of the epoxide before CO<sub>2</sub> is added (Scheme 2.5, pathway (b)). Calculations disclosed [HDBU]I (**3**) as the catalyst with the most favourable energetic profile corroborating the experimental results observed. The first transition state (TS1) involves the ring opening of the epoxide and corresponds to the rate-determining step in both reaction pathways. Energetic barriers for TS1 are for pathway (a), 20.9 kcal·mol<sup>-1</sup> and 30.9 kcal·mol<sup>-1</sup> for pathway (b) respectively when [HDBU]I (**3**) was used as catalyst (Figure 2.5). The difference of reaction barriers of 10 kcal·mol<sup>-1</sup> suggests that statistically this reaction is more likely to proceed through pathway (a), simultaneous activation of the CO<sub>2</sub> along with the

epoxide, since the energy required for the obtention of the cyclic carbonate is lower than the one calculated for pathway (b). The energy barriers obtained for (TS1) for the other halide salts were 26.7 kcal·mol<sup>-1</sup> and 26.1 kcal·mol<sup>-1</sup> for [HDBU]Cl (**1**) and [HDBU]Br (**2**) respectively (Figure 2.5). This result confirms that [HDBU]I (**3**) is more efficient to carry out the reaction when compared with the other two halide salts. Nucleophilic attack of the anion was calculated for the substituted and non-substituted carbons adjacent to the oxygen atom. As expected, the attack on the less steric hindered carbon (attack 1), was more energetically favoured since the values for the energy barriers value, when [HDBU]I (**3**) was used as catalyst, were 20.9 kcal·mol<sup>-1</sup> for the attack on the less substituted carbon and 26.3 kcal·mol<sup>-1</sup> for the attack on the more steric hindered carbon (attack 2) (Figure 2.5).



**Scheme 2.5.** Proposed mechanism for the cycloaddition of CO<sub>2</sub> into methyl oxirane.

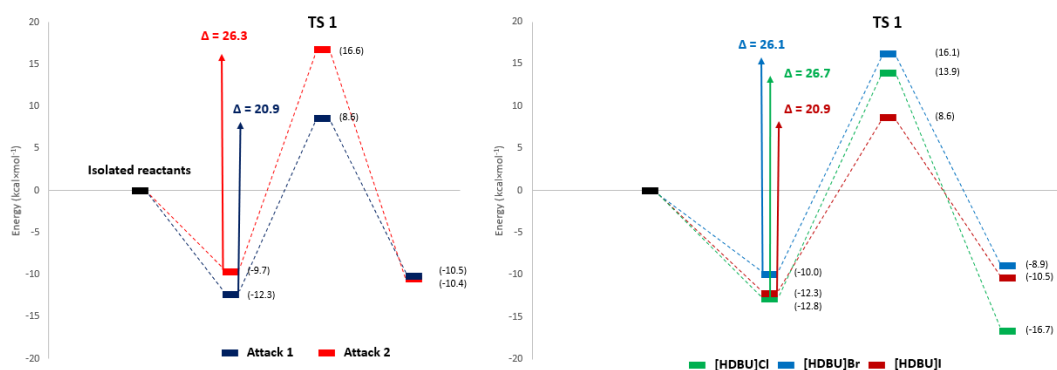


**Figure 2.5.** Energy profile for TS1 considering mechanism pathway (a). In the left, comparison between attack 1 and 2 when reaction is catalysed using [HDBU]I. In the right, comparison between [HDBU]Cl, [HDBU]Br and [HDBU]I for attack 1.

TS2 (TS3 in the pathway (b)) consists in the intramolecular ring-closure of the  $\beta$ -halocarbonate intermediate to render the desired cyclic carbonate with the concomitant regeneration of the protic DBU halide derivative. Catalyst [HDBU]I (**3**) exhibits the lowest energetic barrier value,  $15.7 \text{ kcal}\cdot\text{mol}^{-1}$  of the three catalyst. Energetic barriers values are lower compared to the ones calculated for TS1. This confirms that the rate-determining step in the reaction is TS1. The observed trend for the energetic barrier values for TS2 were,  $[\text{HDBU}]\text{I} < [\text{HDBU}]\text{Br} < [\text{HDBU}]\text{Cl}$ . The energetic barrier for [HDBU]Cl was  $19.9 \text{ kcal}\cdot\text{mol}^{-1}$  whereas for [HDBU]Br was  $16.7 \text{ kcal}\cdot\text{mol}^{-1}$ , slightly lower. This energetic difference can justify the experimental catalytical activity observed. In this respect the conversion obtained when [HDBU]Br was used as a catalyst, is higher than the conversion registered when [HDBU]Cl was employed instead (77 vs 60%) (Figure 2.6). In conclusion, the comparative study of halide salts ( $[\text{HDBU}]\text{X}$ ) revealed the following catalytic reactivity:  $[\text{HDBU}]\text{I} > [\text{HDBU}]\text{Br} > [\text{HDBU}]\text{Cl}$ , DFT calculations fully support the experimental results observed and demonstrate the postulated anion influence.

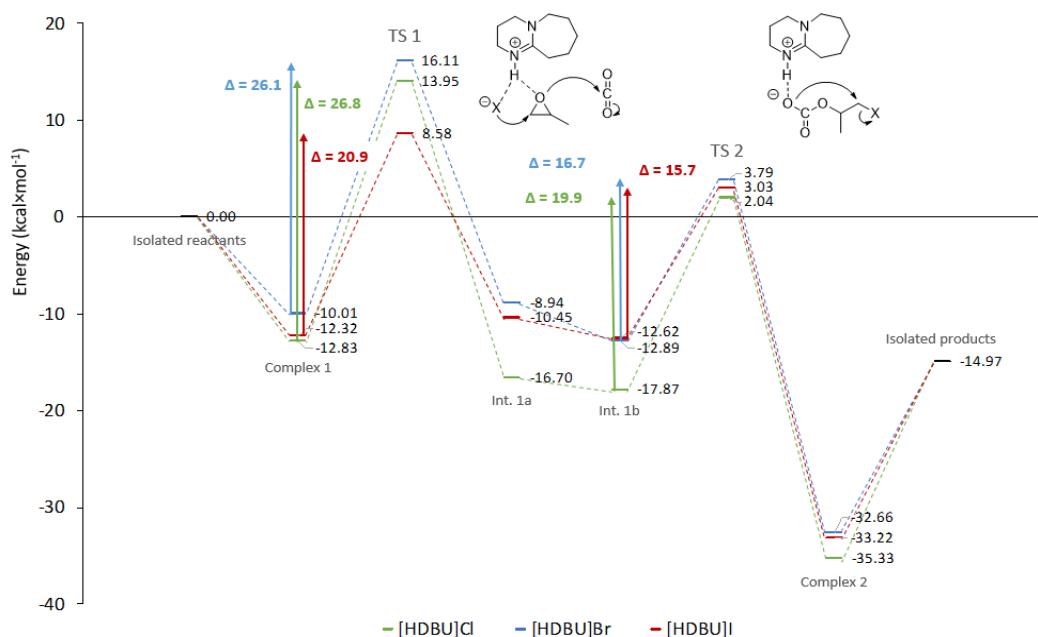


**Figure 2.6.** Energy profile for the formation of 4-methyl-1,3-dioxolan-2-one from propylene oxide and CO<sub>2</sub> catalysed by [HDBU]I considering pathway (a) and attack 1.

## 2.3 Conclusions

A systematic and rational study for the cycloaddition of CO<sub>2</sub> into epoxides has been developed for the organocatalytic synthesis of functional five-membered cyclic carbonates using DBU derivatives bearing protic or *N*-alkyl substituents, both types exhibiting a wide range of anions. The reaction proceeds with moderate to high yields under very mild conditions when protonated DBU salts were used, while *N*-alkylated DBU salts result in a decrease of catalytic performance. DFT calculations have corroborated the experimental data and confirmed the importance of hydrogen bond donor moieties to activate the epoxide along with the compromise of nucleophilicity and leaving group ability of the counter anion with the iodide exhibiting the best activity.

## 2.4 References

1. S. Solomon, G. K. Plattner, R. Knutti and P. Friedlingstein, *Proc. Natl. Acad. Sci. U.S.A.*, 2009, **106**, 1704-1709.
2. M. A. Courtemanche, M. A. Legare, L. Maron and F. G. Fontaine, *J. Am. Chem. Soc.*, 2013, **135**, 9326-9329.
3. J. Kothandaraman, A. Goeppert, M. Czaun, G. A. Olah and G. K. Prakash, *J. Am. Chem. Soc.*, 2016, **138**, 778-781.
4. S. Moret, P. J. Dyson and G. Laurenczy, *Nat. Commun.*, 2014, **5**, 4017.
5. W. Leitner, *Angew. Chem., Int. Ed. Engl.*, 1995, **30**, 2207-2221.
6. M. Aresta, A. Dibenedetto and A. Angelini, *Chem. Rev.*, 2014, **114**, 1709-1742.
7. S.-i. Fujita, H. Yoshida, R. Liu and M. Arai, in *New and future development in catalysis. Activation of Carbon Dioxide*, ed. S. L. Luib, Elsevier, Amsterdam, 2013, ch. 5, pp. 149-169.
8. Q. Liu, L. Wu, R. Jackstell and M. Beller, *Nat. Commun.*, 2015, **6**, 5933.
9. M. Alves, B. Grignard, R. Mereau, C. Jerome, T. Tassaing and C. Detrembleur, *Catal. Sci. Technol.*, 2017, **7**, 2651-2684.
10. Q. He, J. W. O'Brien, K. A. Kitselman, L. E. Tompkins, G. C. T. Curtis and F. M. Kerton, *Catal. Sci. Technol.*, 2014, **4**, 1513-1528.
11. D.-H. Lan, N. Fan, Y. Wang, X. Gao, P. Zhang, L. Chen, C.-T. Au and S.-F. Yin, *Chin. J. Catal.*, 2016, **37**, 826-845.
12. G. Fiorani, W. Guo and A. W. Kleij, *Green Chem.*, 2015, **17**, 1375-1389.
13. T. M. McGuire, E. M. López-Vidal, G. L. Gregory and A. Buchard, *J. CO<sub>2</sub> Util.*, 2018, **27**, 283-288.
14. M. WH, *Adv Mater*, 1998, **10**, 439-448.
15. S. S. Zhang, *J. Power Sources*, 2006, **162**, 1379-1394.
16. H. Blattmann, M. Fleischer, M. Bahr and R. Mulhaupt, *Macromol. Rapid Commun.*, 2014, **35**, 1238-1254.
17. G. Rokicki, P. G. Parzuchowski and M. Mazurek, *Polym. Adv. Technol.*, 2015, **26**, 707-761.
18. L. Maisonneuve, O. Lamarzelle, E. Rix, E. Grau and H. Cramail, *Chem. Rev.*, 2015, **115**, 12407-12439.
19. S. J. Poland and D. J. Darensbourg, *Green Chem.*, 2017, **19**, 4990-5011.

20. D. J. Darensbourg, *Chem. Rev.*, 2007, **107**, 2388-2410.
21. F. S. B. Schöffner, S. P. Verevkin, A. Börner, *Chem. Rev.*, 2010, **110**, 4554-4581.
22. E. R. S. Perez, R. H. A.; Gambardella, M. T. P.; de Macedo, L. G. M.; Rodrigues-Filho, U. P.; Launay, J.-C.; Franco, D. W., *J. Org. Chem.*, 2004, **69**, 8005-8011.
23. J. Sun, W. Cheng, Z. Yang, J. Wang, T. Xu, J. Xin and S. Zhang, *Green Chem.*, 2014, **16**, 3071-3078.
24. W. Cheng, F. Xu, J. Sun, K. Dong, C. Ma and S. Zhang, *Synth. Commun.*, 2016, **46**, 497-508.
25. Y. Qi, W. Cheng, F. Xu, S. Chen and S. Zhang, *Synth. Commun.*, 2018, **48**, 876-886.
26. X. Liu, S. Zhang, Q.-W. Song, X.-F. Liu, R. Ma and L.-N. He, *Green Chem.*, 2016, **18**, 2871-2876.
27. L. Wang, K. Kodama and T. Hirose, *Catal. Sci. Technol.*, 2016, **6**, 3872-3877.
28. O. Coulembier, S. Moins, V. Lemaure, R. Lazzaroni and P. Dubois, *J. CO<sub>2</sub> Util.*, 2015, **10**, 7-11.
29. R. Ma, L.-N. He, X.-F. Liu, X. Liu and M.-Y. Wang, *J. CO<sub>2</sub> Util.*, 2017, **19**, 28-32.
30. Z.-Z. Yang, L.-N. He, C.-X. Miao and S. Chanfreau, *Adv. Synth. Catal.*, 2010, **352**, 2233-2240.
31. N. Aoyagi, Y. Furusho and T. Endo, *Chem. Lett.*, 2012, **41**, 240-241.
32. K. Li, X. Wu, Q. Gu, X. Zhao, M. Yuan, W. Ma, W. Ni and Z. Hou, *RSC Adv.*, 2017, **7**, 14721-14732.
33. C. Yang, M. Liu, J. Zhang, X. Wang, Y. Jiang and J. Sun, *Mol. Catal.*, 2018, **450**, 39-45.
34. W. Li, W. Cheng, X. Yang, Q. Su, L. Dong, P. Zhang, Y. Yi, B. Li and S. Zhang, *Chin. J. Chem.*, 2018, **36**, 293-298.
35. A.-L. Girard, N. Simon, M. Zanatta, S. Marmitt, P. Gonçalves and J. Dupont, *Green Chem.*, 2014, **16**, 2815-2825.
36. S. Foltran, R. Mereau and T. Tassaing, *Catal. Sci. Technol.*, 2014, **4**, 1585-1597.

37. J.-Q. Wang, K. Dong, W.-G. Cheng, J. Sun and S.-J. Zhang, *Catal. Sci. Technol.*, 2012, **2**, 1480-1484.
38. L. Wang, L. Lin, G. Zhang, K. Kodama, M. Yasutake and T. Hirose, *Chem. Commun.*, 2014, **50**, 14813-14816.
39. J. L. Jiang and R. Hua, *Synth. Commun.*, 2006, **36**, 3141-3148.
40. T. Hirose, S. Qu, K. Kodama and X. Wang, *J. CO<sub>2</sub> Util.*, 2018, **24**, 261-265.



**3. Novel guanidinium salts as  
organocatalysts for the synthesis of  
cyclic carbonates from epoxides and  
CO<sub>2</sub>**

### 3.1 Introduction

The guanidine functionality consists in a  $\text{CN}_3$ , Y-shaped core containing an imine ( $\text{C}=\text{N}$ ) along with two amines. Guanidines are considered as superbases, since they have a  $\text{p}K_{\text{a}}$  value higher than the proton sponge.<sup>1</sup> These kind of compounds are widely present in natural products, therefore the guanidine moiety plays a critical role in several biological interactions. The most representative example containing a guanidine functionality is L-arginine, one of the twenty proteinogenic amino acids. In addition, guanidines like tetrodotoxin (TTX), a highly potent neurotoxin has been identified from fishes and other aquatic animals.<sup>2</sup> The guanidine functionality is also present in streptomycin, the first aminoglycoside antibiotic discovered by Albert Schatz and extensively used in the treatment of tuberculosis (Figure 3.1).<sup>3</sup>

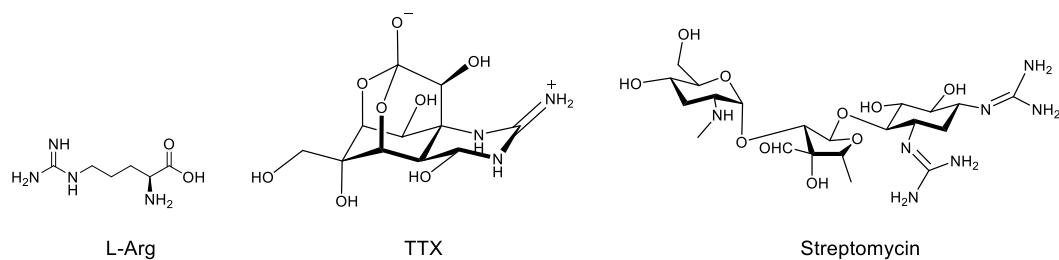
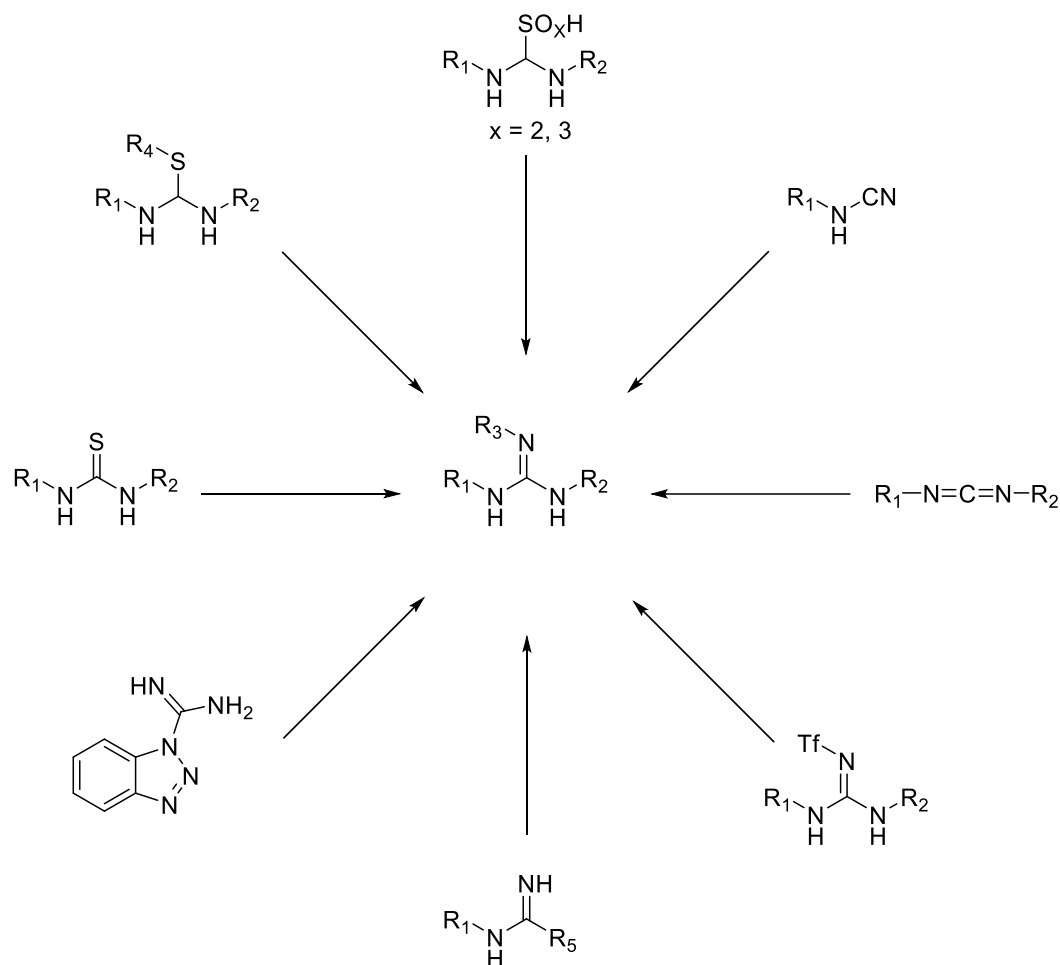


**Figure 3.1.** Examples of relevant guanidine-containing molecules present in nature.

Apart from their role and presence in nature, guanidines have been extensively exploited, as a consequence of its basicity, as chiral organocatalysts in a plethora or different asymmetric organic reactions such as, the Henry reaction,<sup>4</sup> the aldol reaction,<sup>5</sup> the Strecker reaction,<sup>6</sup> several different types of Michael reaction,<sup>7-10</sup> the Diels-Alder cycloaddition,<sup>11</sup> ring-opening polymerization,<sup>12</sup> the Claisen rearrangement,<sup>13</sup> nucleophilic epoxidation reactions<sup>14</sup> and the Mannich reaction.<sup>15</sup> Guanidines can be prepared using the so called, guanylating agents,<sup>16</sup> which include a wide variety of precursors, *i.e* thioureas, isothioureas, amidine sulfonic and sulfinic acids, cyanamides, carbodiimides, triflyl guanidines, carboximidamides, and benzotriazole containing moieties (Scheme 3.1). Among the aforementioned guanylating agents, thiourea is one of the most used, as a consequence of its availability and ready preparation. Thioureas can be treated with an oxidant resulting in a desulfurisation, and a carbodiimide intermediate is obtained,<sup>17</sup> this

intermediate suffers a nucleophilic attack by an amine, rendering so a substituted guanidine.<sup>18</sup>

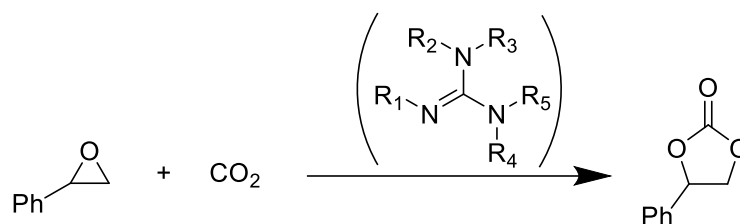


**Scheme 3.1.** Guanidine synthesis using guanylating agents.

Similarly to DBU, guanidines have been reported as CO<sub>2</sub> activators.<sup>19</sup> Indeed, the well-known zwitterionic carbamate species has been properly characterised by several spectroscopic techniques.<sup>20</sup> Therefore guanidines have been extensively reported and exploited as platforms for the design of organocatalysts used in the synthesis of five-membered cyclic carbonates from epoxides and CO<sub>2</sub> (Table 3.1).<sup>21-30</sup> However, in contrast to DBU based methodologies for the synthesis of five-membered cyclic carbonates, very few methodologies using a guanidine along with a cocatalyst have been reported (Table 3.1, entries 1 and 9). Unlike, functionalised guanidinium salts, whether, protonated or alkylated were reported as catalysts for the synthesis of five-membered cyclic carbonates (Table 3.1, entries 2,

4, 5, 6, 7 and 10) and also has been reported guanidinium salts used in a binary system with zinc halides (Table 3.1, entries 3 and 8). With regard to the reaction mechanism, most authors have proposed the same mechanism, however Foltran *et al.* reported a thorough study supported on both spectroscopic results and computational calculations.<sup>26</sup> The epoxide **I** is activated through a hydrogen bond

**Table 3.1.** Literature screening for the synthesis of styrene carbonate from styrene oxide and CO<sub>2</sub> using guanidine-based derivatives.

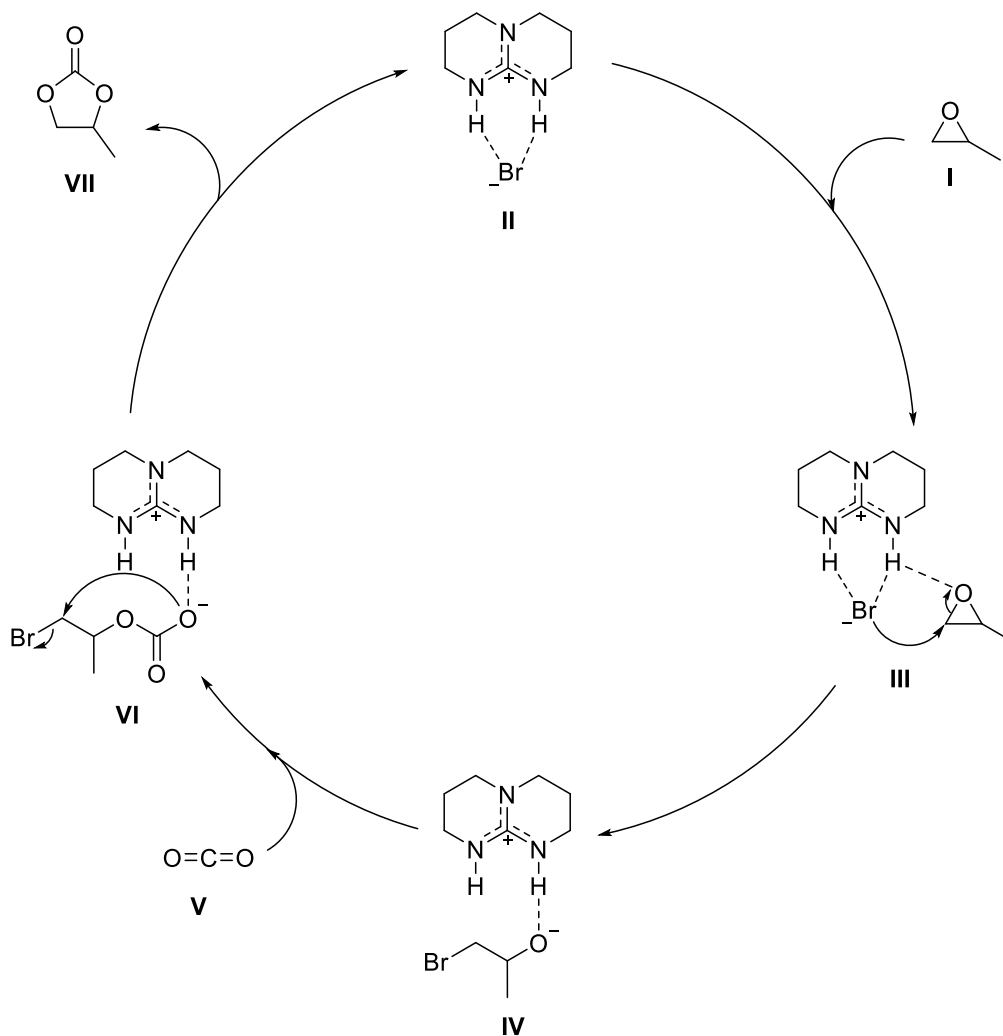


Entry	Catalyst	Cat. Loading (%)	Pressure (bar)	Temperature (°C)	Time (h)	Yield (%)	TOF <sup>f</sup> (h <sup>-1</sup> )
1	MTBD	4	50	140	20	95 <sup>a, c</sup>	1.19
2		2	1	120	4	94 <sup>b</sup>	11.8
3		0.06/0.01	30	130	1	95 <sup>b</sup>	9500
4		0.5	40	110	4	97 <sup>b, d</sup>	485
5		1	1	120	8	95 <sup>b</sup>	11.9
6	[HTBD]Br	1	80	80	20	87 <sup>b, d</sup>	4.35
7		1	1	120	8	93 <sup>b</sup>	11.6
8		7.2/1.4	10	100	3	80 <sup>b</sup>	19.1
9	TBD/1-iodooctane	10/30	1	100	8	79 <sup>a, c</sup>	0.99
10		10	1	40	24	98 <sup>b</sup>	0.41

<sup>a</sup> Yield was calculated by isolation of the cyclic carbonates by flash column silica chromatography. <sup>b</sup> Yield was calculated by GC-MS or <sup>1</sup>H NMR spectroscopy. <sup>c</sup> MeCN was used as solvent. <sup>d</sup> PEG<sub>6000</sub> used as linker. <sup>e</sup> Dioxane used as solvent. <sup>f</sup> TOF = moles of product/(moles of catalyst × time).

interaction with protonated TBD **II**. This interaction renders a polarization of the C-O bond in the epoxide which makes methylene more electrophilic **III**, then,

bromide anion ring-opens the epoxide yielding a bromo-alkoxide intermediate **IV** which is stabilised by protonated TBD. Successively, CO<sub>2</sub> **V** reacts with the stabilised bromo-alkoxide rendering a bromo-carboxylate **VI** which, indeed, is also stabilised by protonated TBD. The last step of the proposed mechanism consists of a ring closure *via* nucleophilic attack of the oxygen of the carboxylate which affords the desired propylene carbonate **VII** and releases the bromide regenerating so the catalyst [HTBD]Br (Scheme 3.2).



**Scheme 3.2.** Proposed mechanism for the cycloaddition of CO<sub>2</sub> into propylene oxide catalysed by [HTBD]Br.

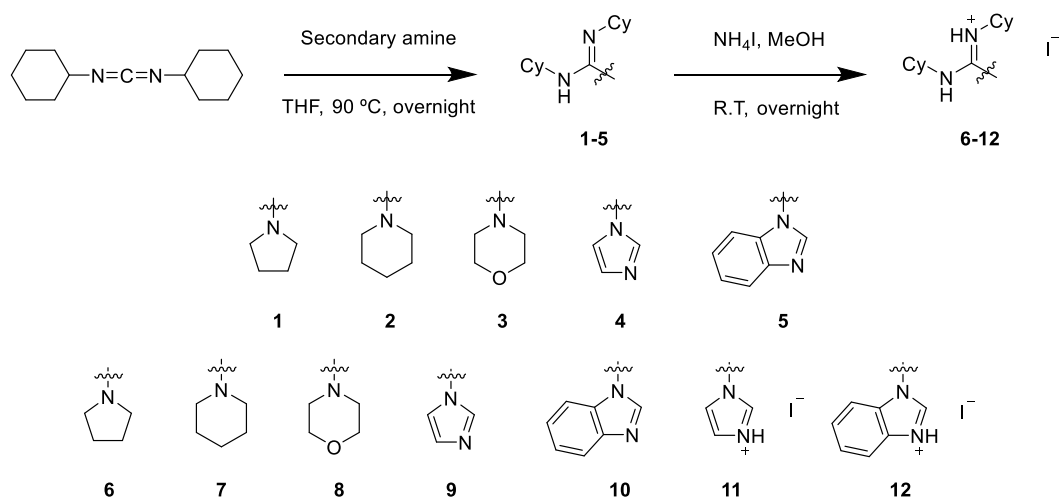
Inspired by the findings depicted in chapter 2, the synthesis of *de novo* guanidinium halide salts based around *N,N'*-dicyclohexylcarbodiimide (DCC) was performed. A structure-reactivity relationship has been established when these compounds were

tested as catalysts in the cycloaddition of CO<sub>2</sub> to styrene oxide under solvent-free conditions. In addition, reaction parameters were optimised and indeed, styrene carbonate was efficiently obtained under mild conditions using an imidazole based guanidinium iodide organocatalyst.

## 3.2 Results and discussion

### 3.2.1 Synthesis of guanidinium iodide salts

Linear guanidines **1-5** were prepared by catalyst free nucleophilic attack of cyclic secondary amines to DCC. Guanidine compounds, such TBD, reacts with CO<sub>2</sub> affording a reversible zwitterionic species,<sup>20</sup> analogously to DBU, despite of CO<sub>2</sub> activation of guanidine compounds, they are unable to yield five-membered cyclic carbonates. Herein inspired in the findings described in chapter 2, different guanidinium iodide salts, **6-10**, were prepared by protonation of the corresponding guanidine using ammonium iodide (Figure 3.2). Guanidines prepared around imidazole and benzimidazole with its nitrogen basic atom in the heterocyclic ring, allowed to prepare two more guanidinium iodide salts **11** and **12** by using two equivalents of NH<sub>4</sub>I (Scheme 3.3). The whole battery of guanidinium iodide salts was fully characterised by <sup>1</sup>H, <sup>13</sup>C NMR spectroscopy, HRMS and elemental analysis.



**Scheme 3.3.** Synthesis of guanidines **1-5** and guanidinium iodide salts **6-12** based around DCC.

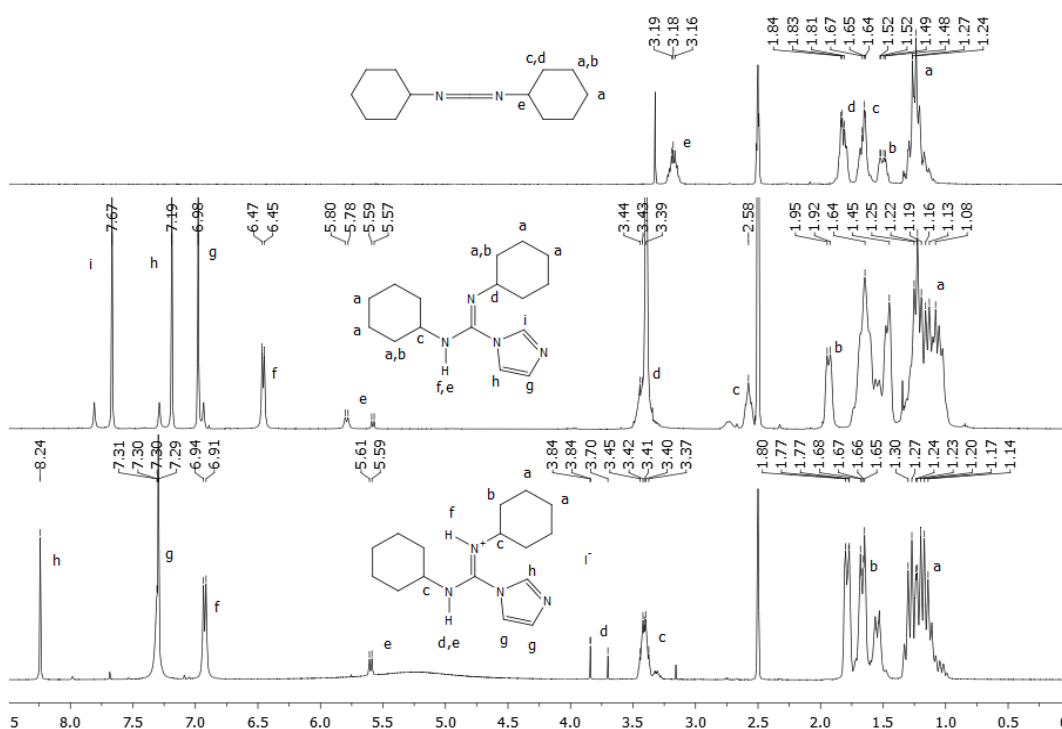
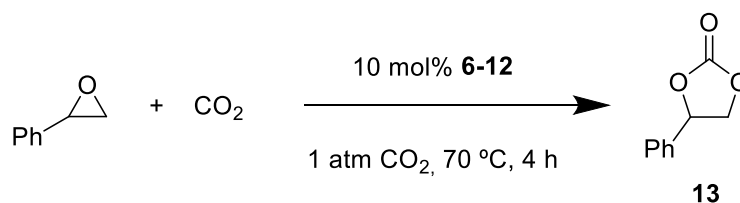


**Figure 3.2.** <sup>1</sup>H NMR spectra of DCC (*top*), the resultant guanidine **4** after reaction with imidazole (*middle*) and guanidinium salt **9** catalyst (*bottom*). (400 MHz, 298 K, DMSO).

### 3.2.2 Catalyst screening and optimization

All the novel catalysts were firstly tested under the same conditions described in chapter 2, *i.e.* styrene oxide as model substrate, 70 °C, 10 mol% catalyst and 1 atm. of CO<sub>2</sub> (Scheme 3.4). All the catalysts tested under this set conditions exhibited moderate to high conversions, *i.e.* 68 to 98% conversion (Table 3.2).



**Scheme 3.4.** Synthesis of styrene carbonate using different guanidinium based salts.

Catalyst **1** exhibited the highest conversion (Table 3.2, entry 1), however, despite their partial insolubility, the guanidinium salts based around imidazole and benzimidazole yield almost quantitative conversions (Table 3.2, entries 4 and 7). Herein, further reaction optimization parameters were performed on those imidazole and benzimidazole guanidinium based catalysts, since it was considered that as the reaction media was not homogeneous, the catalyst loading was not actually 10 mol%. Finally, in order to demonstrate the synergic effect of the guanidinium functional group along with the iodide anion, guanidine **4** and NH<sub>4</sub>I were tested as control experiments. As expected, a very low conversion of only 8% was obtained when NH<sub>4</sub>I was used as catalyst (Table 3.2, entry 9) and 6% when **4** was tested (Table 3.2, entry 10).

**Table 3.2.** Reaction studies for styrene oxide and CO<sub>2</sub> cycloaddition catalysed by guanidinium based salts.<sup>a</sup>

Entry	Catalyst	Conv. <sup>b</sup> (%)	TOF <sup>c</sup> (h <sup>-1</sup> )
1	<b>6</b>	98	2.44
2	<b>7</b>	86	2.14
3	<b>8</b>	79	1.97
4	<b>9</b>	97	2.41
5	<b>10</b>	82	2.04
6	<b>11</b>	68	1.69
7	<b>12</b>	96	2.39
8	NH <sub>4</sub> I	8	0.20
9	<b>4</b>	6	0.15

<sup>a</sup> Reactions carried out at 70 °C and 1 bar of pressure for 4 hours using 10 mol% of catalyst. <sup>b</sup> Conversion determined by <sup>1</sup>H NMR spectroscopy on the crude reaction mixture. <sup>c</sup> TOF = moles of product / (moles of catalyst × time).

Next, a catalyst loading study was performed using catalyst **9** to **12**. Reaction mixtures still remained heterogeneous even when the catalyst loading was reduced twofold. Unsurprisingly lower conversions were registered when a lower catalyst loading was used (Table 3.3, entries 1 to 4). A sensible reduction in catalytic performance was observed when **12** was used with a 5% mol of catalyst loading



since conversion decayed from 96% conversion (Table 3.2, entry 7) to 60% (Table 3.3, entry 4). In the case of **9**, this decay wasn't so significant, since 98% (Table 3.2, entry 4) vs 91% (Table 3.3, entry 1) was observed when 10 and 5% mol of catalyst were used respectively. Further decreasing the catalyst loading was studied using **9** as catalyst. As it could be expected, lower conversions were observed when lower catalyst loading were used (Table 3.3, entry 5). An increase in the reaction time led to a higher conversion (Table 3.3, entry 6), however it was observed that some catalyst remained insoluble, herein successive decrease on the catalyst loading was studied obtaining so, a moderate conversion of 64% when 1 mol% of catalyst was used for 8 h (Table 3.3, entry 9).

**Table 3.3.** Imidazole and benzimidazole guanidinium iodide catalyst screening for the synthesis of styrene carbonate.<sup>a</sup>

Entry	Catalyst	Catalyst Loading (%)	Conv. <sup>b</sup> (%)	TOF <sup>c</sup> (h <sup>-1</sup> )
1	<b>9</b>	5	91	4.98
2	<b>10</b>	5	79	4.32
3	<b>11</b>	5	60	3.28
4	<b>12</b>	5	60	3.28
5	<b>9</b>	2.5	56	5.60
6	<b>9</b>	2.5	94 <sup>d</sup>	4.70
7	<b>9</b>	1.0	64 <sup>d</sup>	8.00

<sup>a</sup> Reactions carried out at 70 °C and 1 bar of pressure for 4 hours. <sup>b</sup> Conversion determined by <sup>1</sup>H NMR spectroscopy on the crude reaction mixture. <sup>c</sup> TOF = moles of product / (moles of catalyst × time). <sup>d</sup> 8 hours reaction time.

Optimal catalyst loading was set to 1% mol, then, the influence of time was studied for the synthesis of styrene carbonate (Table 3.4). Longer reaction times resulted in higher conversions, reaction proceeded fast in the first 12 hours as 78% conversion was observed (Table 3.4, entry 2). The conversion was almost quantitative when the reaction was carried out for 24 h (Table 3.4, entry 3).

**Table 3.4.** Time influence for the synthesis of styrene carbonate catalysed by **9**.<sup>a</sup>

Entry	Time (h)	Conv. <sup>b</sup> (%)	TOF <sup>c</sup> (h <sup>-1</sup> )
1	8	64	8.00
2	12	78	6.50
3	24	93	3.88

<sup>a</sup> Reactions carried out at 70 °C and 1 bar of pressure using 1 mol% of **9**. <sup>b</sup> Conversion determined by <sup>1</sup>H NMR spectroscopy on the crude reaction mixture. <sup>c</sup> TOF = moles of product / (moles of catalyst × time).

Finally, the temperature influence for the synthesis of styrene carbonate was studied (Table 3.5). The cyclocarbonation of styrene oxide resulted to be very temperature dependent since at R.T and 40 °C, very low and low conversions were observed (Table 3.5, entries 1 and 2). In order to ensure complete conversions, an experiment at 90 °C was performed (Table 3.5, entry 4). In this case, almost quantitative conversion was obtained, furthermore it was noticed that when the reaction was carried out at 90 °C, the reaction mixture was completely homogeneous (Figure 3.3). The increase of the reaction temperature along with the reaction media homogeneity are most likely to be responsible of ensuring almost quantitative conversion for the synthesis of styrene carbonate.

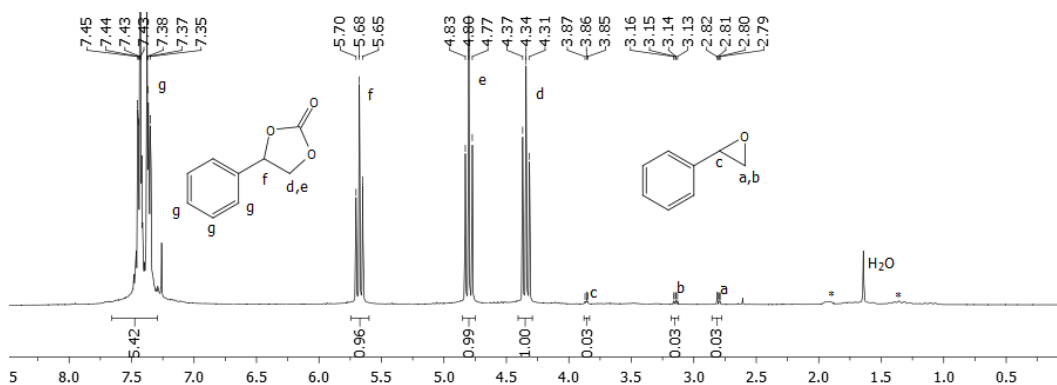


**Figure 3.3.** <sup>1</sup>H NMR spectrum of crude reaction for the synthesis of styrene carbonate from styrene oxide using 1 mol% of **9** at 90 °C for 24 hours (\* corresponds to **9**) (300 MHz, 298 K, CDCl<sub>3</sub>).

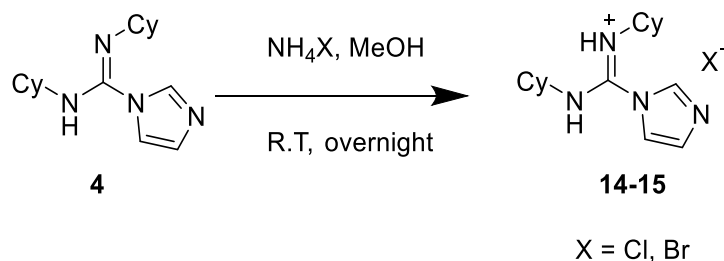
**Table 3.5.** Temperature influence for the synthesis of styrene carbonate catalysed by **9**.<sup>a</sup>

Entry	Temperature (°C)	Conv. <sup>b</sup> (%)	TOF <sup>c</sup> (h <sup>-1</sup> )
1	R.T	5	0.21
2	40	31	1.29
3	70	93	3.88
4	90	97 <sup>e</sup>	4.05

<sup>a</sup> Reactions carried out at 1 bar of pressure using 1 mol% of **9** for 24 hours. <sup>b</sup> Conversion determined by <sup>1</sup>H NMR spectroscopy on the crude reaction mixture. <sup>c</sup> TOF = moles of product / (moles of catalyst × time). <sup>e</sup> 88% isolated yield obtained after flash column chromatography in silica gel.

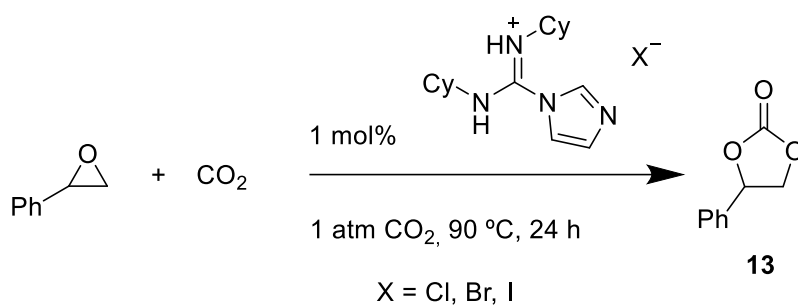
### 3.2.3 Anion influence study

In order to study the influence of the halide anion series, chloride and bromide imidazole based guanidinium salts were synthesised by mono-protonation of species **4** with ammonium chloride and ammonium bromide respectively (Scheme 3.5).



**Scheme 3.5.** Synthesis of chloride and bromide imidazole based guanidinium salts.

Those catalysts were fully characterised (<sup>1</sup>H, <sup>13</sup>C NMR spectroscopy, FTIR, HRMS and elemental analysis) and subsequently tested for the cyclocarbonation of styrene oxide under the optimal reaction parameters previously studied (Scheme 3.6).



**Scheme 3.6.** Anion influence study for the synthesis of styrene carbonate using imidazole based guanidinium halide salts.

The trend observed with the halide series was unsurprisingly, the same one observed in chapter 2, *i.e.* Cl < Br < I (Table 3.6, entries 1, 2 and 3) (Figure 3.4). According to the proposed mechanisms reported in the literature,<sup>31, 32</sup> the higher nucleophilicity and leaving group ability explain why iodide exhibits the best performance. Moreover, computational calculations reveal that for this kind of catalysts where halide atoms are involved, the calculated reaction profiles show, that transition states where iodide is present have a lower activation energy,<sup>33</sup> therefore the results observed regarding the anion influence are coherent with the results reported in the literature and supported by computational calculations.

**Table 3.6.** Anion influence study for the synthesis of styrene carbonate using imidazole based guanidinium halide salts.

Entry	Catalyst	Conv. <sup>b</sup> (%)	TOF <sup>c</sup> (h <sup>-1</sup> )
1	<b>9</b>	97	4.05
2	<b>14</b>	25	1.04
3	<b>15</b>	70	2.92

<sup>a</sup> Reactions carried out at 1 bar of pressure using 1 mol% of catalyst at 90 °C for 24 hours. <sup>b</sup> Conversion determined by <sup>1</sup>H NMR spectroscopy on the crude reaction mixture. <sup>c</sup> TOF = moles of product / (moles of catalyst × time).

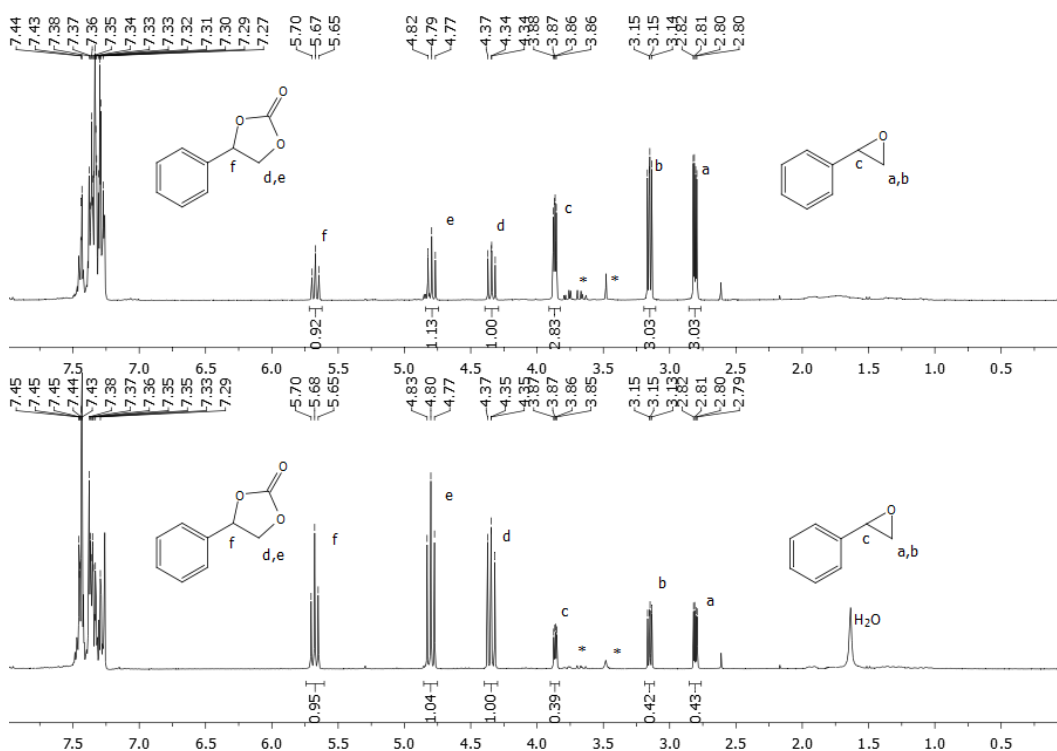


**Figure 3.4.**  $^1\text{H}$  NMR spectrum of crude reaction for the synthesis of styrene carbonate from styrene oxide using 1 mol% of **14** at 90 °C for 24 hours (*top*) (\* corresponds to **14**) (300 MHz, 298 K,  $\text{CDCl}_3$ ).  $^1\text{H}$  NMR spectrum of crude reaction for the synthesis of styrene carbonate from styrene oxide using 1 mol% of **15** at 90 °C for 24 hours (*bottom*) (\* corresponds to **15**) (300 MHz, 298 K,  $\text{CDCl}_3$ ).

### 3.2.4 Reaction mechanism

The reaction mechanism was proposed and discussed following the findings described on chapter 2. Styrene oxide was activated through the hydrogen bond interactions established between the oxygen atom of the epoxide and the hydrogen atoms of the guanidine functional group. These interactions yield a polarization between the C-O bond, which makes the carbon more electrophilic and therefore facilitates the ring-opening by the iodide through a nucleophilic attack. Imidazole and benzimidazole moieties have been widely reported as platforms for the synthesis of organocatalysts used in the cyclocarbonation reaction of terminal epoxides.<sup>31, 34, 35</sup> The proton of the C2 in the imidazole moiety indeed interacts with the epoxide in the same manner as it was described above. Therefore, it was established in the mechanism proposed that, an equilibrium between the activation

promoted by the guanidinium moiety and the activation promoted by the proton of the C2 of the imidazole and the proton of the protonated nitrogen atom is acknowledged. Moreover, linear guanidinium salts present different conformations as a consequence of its rotational freedom (Figure 3.5),<sup>36</sup> then several conformational equilibria can be postulated. However, none all the possible conformations have the same influence on the reaction pathway. Conformations **B** and **D** are highly improbable to exist, as in both cases cyclohexyl substituents are in *Z* conformation and therefore the steric impediment is the highest when all the possible conformations are considered. In the conformations **A**, **C** and **H**, cyclohexyl substituents are in the *E* conformation, which is more favourable in terms of steric hindrance, nevertheless, in none of the cases, the positive charged nitrogen, responsible of stabilising the reaction intermediates, and the proton in C2 position of the imidazole ring or the N-H moiety are properly oriented to efficiently activate, through hydrogen bond interactions, the epoxide. Conformations **E**, **F** and **G** have the cyclohexyl substituents in the *E* conformation, then, as commented above, the steric hindrance is minimal, moreover in those conformations, an optimal orientation of the moieties responsible for both epoxide activation and reaction intermediate is, indeed present.

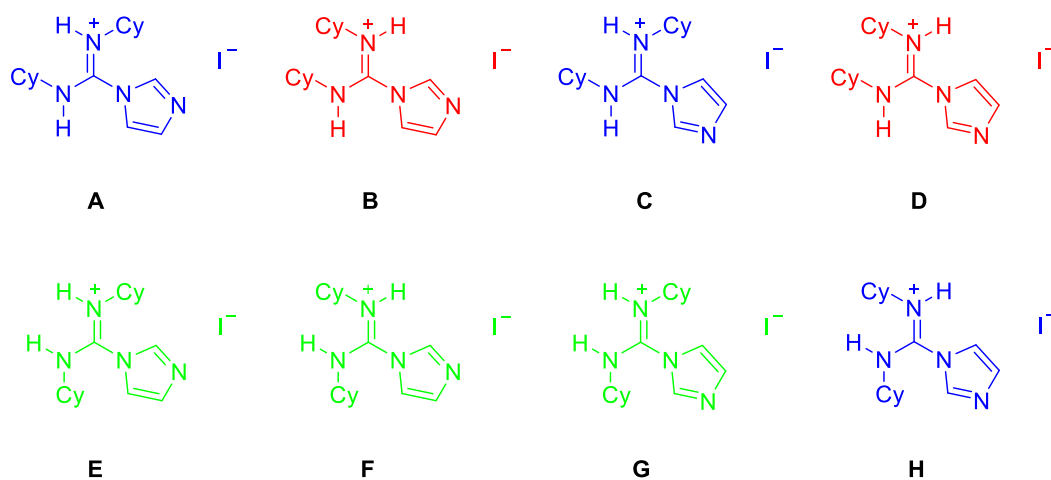
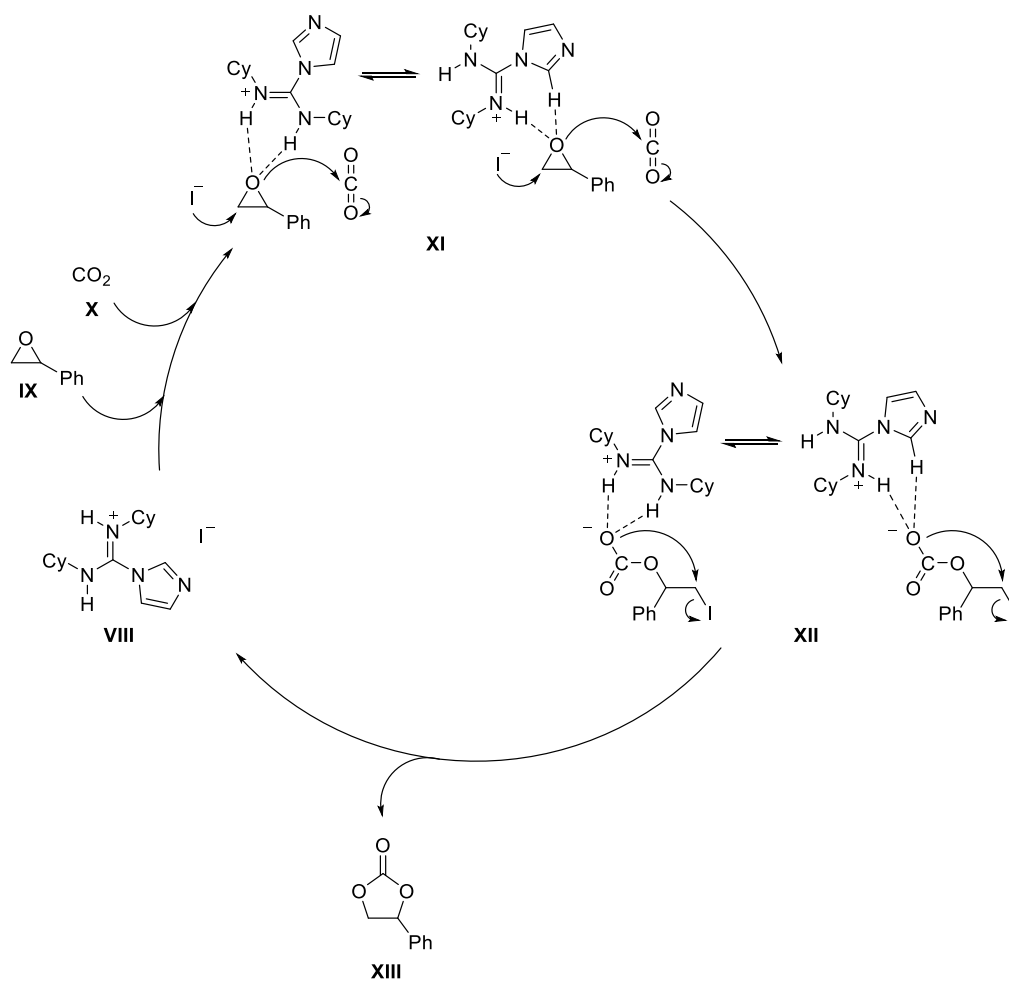


**Figure 3.5.** Possible geometrical conformations for catalyst **9**. In red, conformations with a low influence in the reaction mechanism, in blue, conformations with a moderate influence in the reaction mechanism, in green, conformations with a high influence in the reaction mechanism.

Inspired by the computational calculations depicted on chapter 2, which satisfactorily correlate the experimental results obtained, a mechanism is proposed when **9** was used as catalyst (Scheme 3.7). It was considered in the first step that, an interaction between guanidinium iodide salt **VIII**, styrene oxide **IX** and CO<sub>2</sub> **X** yield a complex **XI**, where a simultaneous ring opening of styrene oxide promoted by the iodide anion in the less substituted carbon due to its less steric hindrance with a subsequent CO<sub>2</sub> insertion takes place to yield a β-iodocarbonate **XII** which was stabilised by the guanidinium cation. Finally, a favourable entropic ring-closure occurs by nucleophilic attack of the oxygen atom of the carbonate functionality to the β position, rendering so, the desired styrene carbonate **XIII** and releasing the guanidinium iodide salt **VIII**. As observed and demonstrated with DFT calculations, iodide exhibited the best catalytic performance as a consequence of its unique nucleophilicity and leaving group ability.



**Scheme 3.7.** Proposed mechanism for the cycloaddition of CO<sub>2</sub> into styrene oxide catalysed by **9**.

### 3.3 Conclusions

In conclusion, preliminary studies for the cycloaddition of CO<sub>2</sub> into epoxides using protic guanidinium halide salts are reported. Guanidinium salts were prepared by simply protonation of the corresponding guanidine core using ammonium halides. The aforementioned guanidines were synthesised using DCC as building block, which was reacted with different secondary amines. Among the catalysts tested, **9**, with its imidazole ring, that has been reported as an efficient moiety for this reaction as a consequence of the hydrogen bond interaction between the proton in C2 and the oxygen atom of the epoxide, was the one which exhibited the highest activity under the preliminary reaction conditions tested. Further optimization was studied in terms of catalyst loading, temperature, time and anion influence using styrene oxide as model substrate. An efficient methodology that operates under mild conditions was developed for the synthesis of styrene carbonate.

### 3.4 References

1. T. Ishikawa, *Superbases for Organic Synthesis: Guanidines, Amidines, Phosphazenes and Related Organocatalysts*, Wiley, 2009.
2. C. Y. Kao, *Pharmacol. Rev.*, 1966, **18**, 997-1049.
3. A. Schatz and S. A. Waksman, *Exp. Biol. Med.*, 1944, **57**, 244-248.
4. K. Takada, N. Takemura, K. Cho, Y. Sohtome and K. Nagasawa, *Tetrahedron Lett.*, 2008, **49**, 1623-1626.
5. A. Martinez-Castaneda, K. Kedziora, I. Lavandera, H. Rodriguez-Solla, C. Concellon and V. del Amo, *Chem. Commun.*, 2014, **50**, 2598-2600.
6. E. J. Corey and M. J. Grogan, *Org. Lett.*, 1999, **1**, 157-160.
7. Z. Jiang, W. Ye, Y. Yang and C.-H. Tan, *Adv. Synth. Catal.*, 2008, **350**, 2345-2351.
8. J. Wang, J. Chen, C. W. Kee and C. H. Tan, *Angew. Chem. Int. Ed. Engl.*, 2012, **51**, 2382-2386.
9. Y. Sohtome, N. Horitsugi, R. Takagi and K. Nagasawa, *Adv. Synth. Catal.*, 2011, **353**, 2631-2636.
10. T. Ishikawa, S. Tokunou, W. Nakanishi, N. Kagawa and T. Kumamoto, *Heterocycles*, 2012, **84**.



11. J. Shen, T. T. Nguyen, Y.-P. Goh, W. Ye, X. Fu, J. Xu and C.-H. Tan, *J. Am. Chem. Soc.*, 2006, **128**, 13692-13693.
12. B. G. G. Lohmeijer, R. C. Pratt, F. Leibfarth, J. W. Logan, D. A. Long, A. P. Dove, F. Nederberg, J. Choi, C. Wade, R. M. Waymouth and J. L. Hedrick, *Macromolecules*, 2006, **39**, 8574-8583.
13. C. Uyeda and E. N. Jacobsen, *J. Am. Chem. Soc.*, 2008, **130**, 9228-9229.
14. B. Shin, S. Tanaka, T. Kita, Y. Hashimoto and K. Nagasawa, *Heterocycles*, 2008, **76**, 801-810.
15. S. Kobayashi, R. Yazaki, K. Seki and Y. Yamashita, *Angew. Chem. Int. Ed. Engl.*, 2008, **47**, 5613-5615.
16. A. R. Katritzky and B. V. Rogovoy, *ARKIVOC*, 2005, (iv), 49-87.
17. A. R. Ali, H. Ghosh and B. K. Patel, *Tetrahedron Lett.*, 2010, **51**, 1019-1021.
18. K. Ramadas and N. Srinivasan, *Tetrahedron Lett.*, 1995, **36**, 2841-2844.
19. J. Ma, X. Zhang, N. Zhao, A. S. N. Al-Arifi, T. Aouak, Z. A. Al-Othman, F. Xiao, W. Wei and Y. Sun, *J. Mol. Catal. A. Chem.*, 2010, **315**, 76-81.
20. F. S. Pereira, E. R. deAzevedo, E. F. da Silva, T. J. Bonagamba, D. L. da Silva Agostíni, A. Magalhães, A. E. Job and E. R. Pérez González, *Tetrahedron*, 2008, **64**, 10097-10106.
21. A. Barbarini, R. Maggi, A. Mazzacani, G. Mori, G. Sartori and R. Sartorio, *Tetrahedron Lett.*, 2003, **44**, 2931-2934.
22. H. F. Duan, S. H. Li, Y. J. Lin, H. B. Xie, S. B. Zhang and Z. M. Wang, *Chem. Res. Chin. Univ.*, 2004, **20**, 568-571.
23. H. Xie, S. Li and S. Zhang, *J. Mol. Catal. A. Chem.*, 2006, **250**, 30-34.
24. L.-N. He, X.-Y. Dou, J.-Q. Wang, Y. Du and E. Wang, *Synlett*, 2007, **2007**, 3058-3062.
25. Z.-Z. Yang, Y.-N. Zhao, L.-N. He, J. Gao and Z.-S. Yin, *Green Chem.*, 2012, **14**.
26. S. Foltran, J. Alsarraf, F. Robert, Y. Landais, E. Cloutet, H. Cramail and T. Tassaing, *Catal. Sci. Technol.*, 2013, **3**, 1046-1055.
27. D. Wei-Li, J. Bi, L. Sheng-Lian, L. Xu-Biao, T. Xin-Man and A. Chak-Tong, *J. Mol. Catal. A. Chem.*, 2013, **378**, 326-332.
28. B. Liu, M. Liu, L. Liang and J. Sun, *Catalysts*, 2015, **5**, 119-130.

29. S. Lim, Y. N. Lim and H.-Y. Jang, *Bull. Korean Chem. Soc.*, 2016, **37**, 608-611.
30. H. S. Seo and H. J. Kim, *Bull. Korean Chem. Soc.*, 2019, **40**, 169-172.
31. A.-L. Girard, N. Simon, M. Zanatta, S. Marmitt, P. Gonçalves and J. Dupont, *Green Chem.*, 2014, **16**, 2815-2825.
32. S. Foltran, R. Mereau and T. Tassaing, *Catal. Sci. Technol.*, 2014, **4**.
33. N. Fanjul-Mosteirín, C. Jehanno, F. Ruipérez, H. Sardon and A. P. Dove, *ACS Sustainable Chem. Eng.*, 2019, **7**, 10633-10640.
34. T. Werner, N. Tenhumberg and H. Büttner, *ChemCatChem*, 2014, **6**, 3493-3500.
35. F. Chen, D. Chen, L. Shi, N. Liu and B. Dai, *J. CO<sub>2</sub> Util.*, 2016, **16**, 391-398.
36. K. Gopi, B. Rathi and N. Thirupathi, *J. Chem. Sci.*, 2010, **122**, 157-167.

## **4. Synthesis of non-isocyanate poly(hydroxy urethane) (NIPU) from vanillin**

## 4.1 Introduction

Polyurethanes are the 6<sup>th</sup> most produced kind of polymers used worldwide. In industry they have been extensively prepared by the reaction between a diisocyanate and a diol catalysed by an organometallic species and in an organic toxic solvent.<sup>1, 2</sup> Although this strategy is highly efficient, this process has health and environmental drawbacks.<sup>3, 4</sup> The main one is the intrinsic use of toxic diisocyanate monomers. Therefore, non-isocyanate polyurethanes (NIPUs) have attracted lots of interest in both academia and industry as an alternative for the classical synthesis of polyurethanes.<sup>5-9</sup> One of the most promising strategies to bypass the use of toxic isocyanates for the synthesis of polyurethanes is the synthesis of poly(hydroxyurethanes) by reacting of a bis-cyclic carbonate with a bis-amine. At the same time, the most extensive synthetic route for the preparation of bis-cyclic carbonates is the cyclocarbonation of a bis-epoxide with CO<sub>2</sub>. This process has been widely studied<sup>10-13</sup> and represents an efficient revalorization of CO<sub>2</sub>. Nowadays, petroleum still represents the main source for the production of polymers and organic chemicals. This fact, along with the exhaustion of fossil fuels, represents a worrying challenge in terms of energy and sustainability. Herein, renewable biobased polymers have attracted lots of attention in the past few years.<sup>14-17</sup>

Among all the renewable resources available, lignin represents one of the most abundant biopolymers as it is present in all vascular plants along with cellulose and hemicellulose. These three biopolymers have different weight percentage distributions depending on the plant, in the case of lignin, this percentage range is from 25 to 35%.<sup>18</sup> Lignin is a cross-linked polymer formed by copolymerization of three different monolignols (*p*-coumaryl alcohol, coniferyl alcohol and sinapyl alcohol) (Figure 4.1), several industrial processes have been developed for the depolymerization of lignin.<sup>19</sup>

One of the compounds that can be isolated from lignin depolymerization in the so-called Kraft process is vanillin.<sup>20-24</sup> This aromatic compound has been extensively used in many applications such as food industry as a flavouring, fragrance industry, in perfumes and as intermediate in the production of fine chemicals.<sup>25, 26</sup>

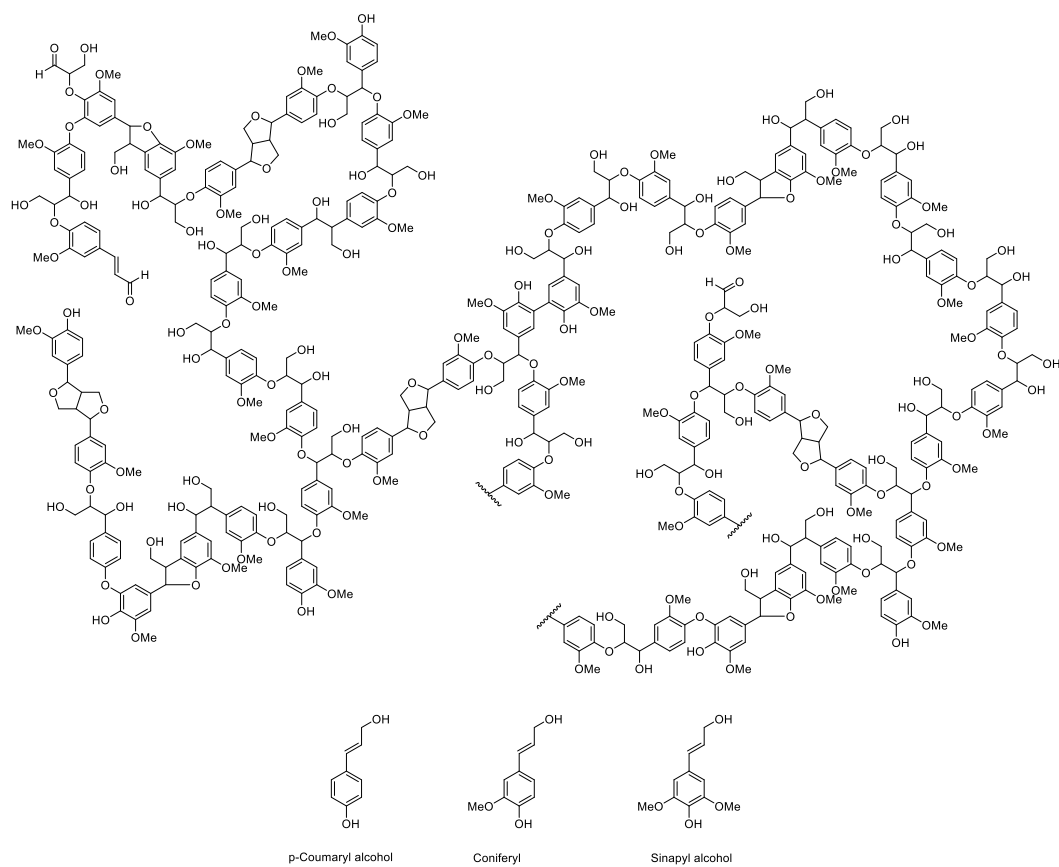
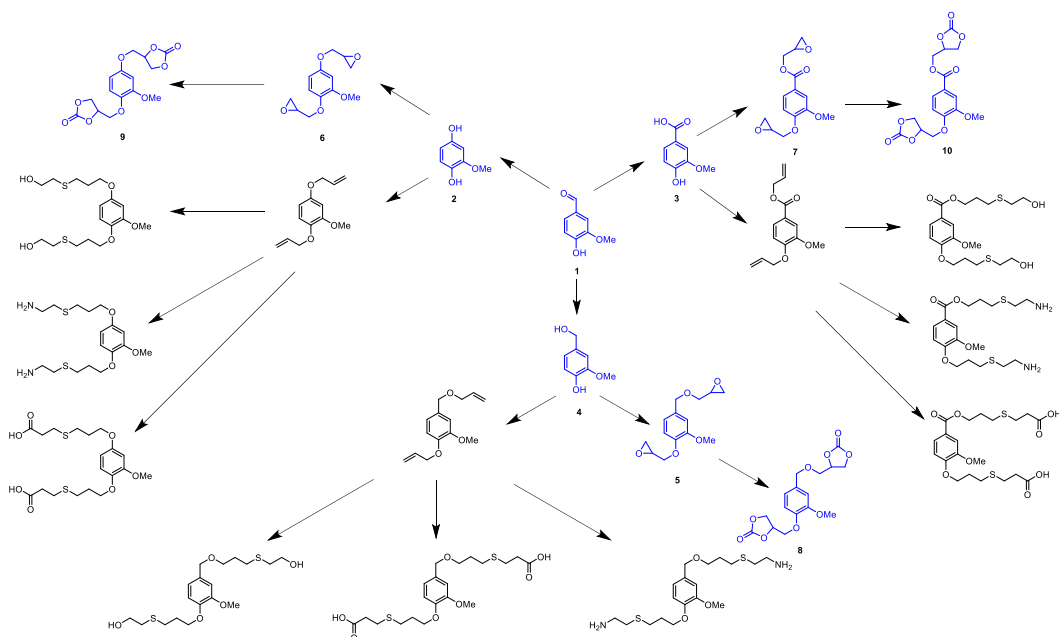


**Figure 4.1.** Monolignol precursors for the biosynthesis of lignin.

Vanillin, with its aldehyde and phenol functionality, represents a very versatile platform for the synthesis of a plethora of monomers for a broad kind of polymers.<sup>27</sup> When phenol is treated with a base renders a phenolate anion, this anion has a similar nucleophilicity as an amine, therefore it can react with different alkyl halides to render different alkyl phenyl ethers. Aldehyde functionalities can undergo both oxidation, to obtain an acid, and reduction, to render an alcohol. In addition, *ortho*- and *para*-hydroxylated phenyl aldehydes can be transformed into benzenediols through Dakin oxidation.<sup>28</sup> Moreover, those alcohols can undergo glycidylation reaction<sup>29, 30</sup> to render bis-epoxides compounds which in turn, can react with CO<sub>2</sub> yielding high-added value monomers for the synthesis of NIPUs if reacted with bis-amines (Scheme 4.1).



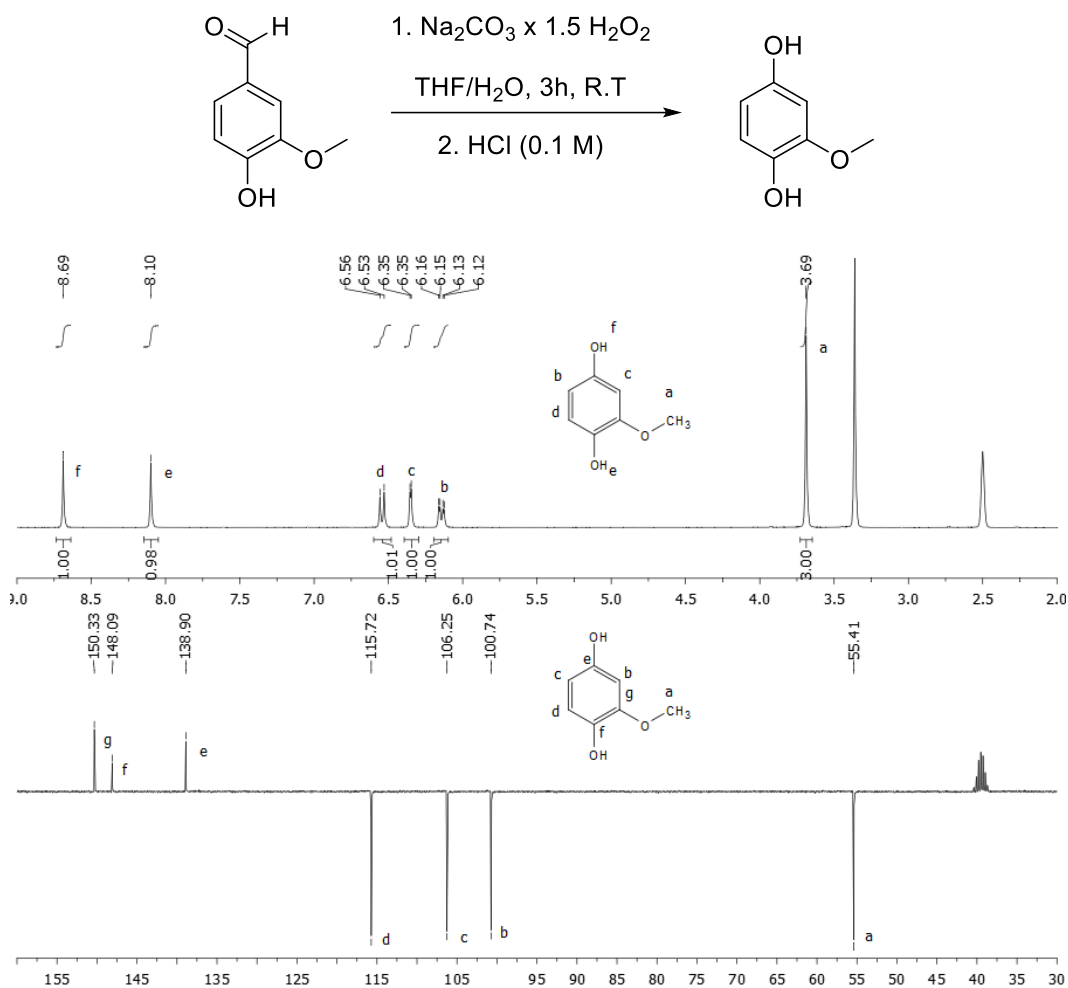
**Scheme 4.1.** Vanillin transformation for potential monomers (adapted from Ref 28).

Following the interest depicted in this thesis in CO<sub>2</sub> revalorization and inspired by the work of Boutevin and co-workers,<sup>27</sup> three different bis-carbonates based on vanillin were prepared and tested for the synthesis of novel non-isocyanate poly(hydroxyurethane)s (NIPUs) using 1,4-butanediamine and 1,6-hexamethylenediamine.

## 4.2 Results and discussion

### 4.2.1 Dakin oxidation of vanillin

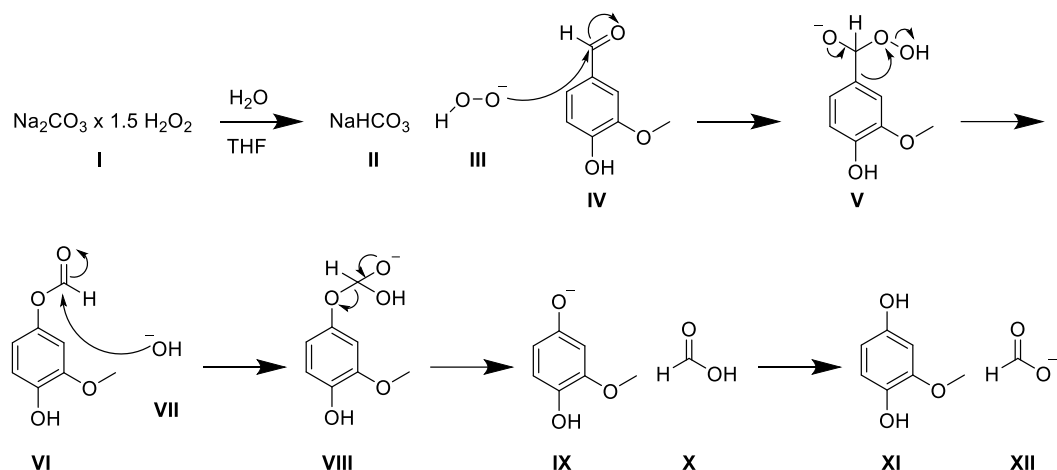
The aromatic aldehyde functional group of vanillin, **1**, can undergo different reduction and oxidation reactions to render three different platform functionalities, to wit, a) 2-methoxyhydroquinone, **2**, via a Dakin reaction, b) aldehyde reduction with NaBH<sub>4</sub> to render a vanillyl alcohol, **4**, c) aldehyde oxidation to obtain vanillic acid, **3**. The latter was used as is commercially available. Aromatic aldehydes substituted at the *ortho* and *para* positions with hydroxyl groups can react with an oxidiser species in a basic media to render a hydroquinone through the Dakin reaction (Scheme 4.2).



**Scheme 4.2.** Reaction scheme for the synthesis of **2** (top). <sup>1</sup>H and <sup>13</sup>C APT NMR spectrum of compound **2** in DMSO (bottom).

When sodium percarbonate, **I**, is dissolved in a mixture of water and THF dissociates into sodium bicarbonate, **II**, and hydrogen peroxide, the presence of the later one confers a basic media, therefore an hydroperoxide anion, **III**, is present, this hydroperoxide attacks as a nucleophile to the aldehyde, **IV**, obtaining so a tetrahedral intermediate, **V**, which suffers a [1,2]-aryl migration forming an phenyl ester, **VI**, which subsequently suffers a nucleophilic attack by a hydroxide, **VII**, obtaining an orthoester intermediate, **VIII**, which decomposes rendering a phenoxide, **IX**, and formic acid, **X**, final step of the mechanism involves an acid-base mechanism in which phenoxide reacts with formic acid and 2-methoxyhydroquinone, **XI**, and a formate anion, **XII**, is obtained. The reaction is quenched by acidification of the reaction media. Carbonates and hydroperoxide

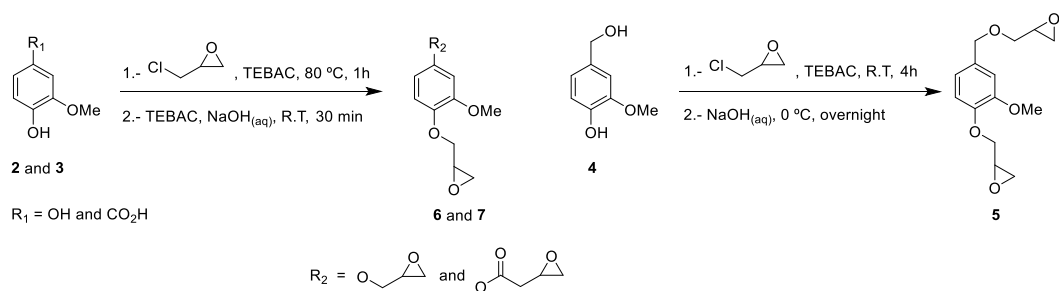
anions are quenched decomposing in CO<sub>2</sub> and water and O<sub>2</sub> and water respectively, moreover, in an acidic media it is ensured that 2-methoxyhydroquinone exists in the phenolic form, instead of phenolate, resulting in an effective extraction of the desired product (Scheme 4.3). The use of sodium percarbonate as oxidising agent turns out to be an effective (88% yield), inexpensive and a more sustainable reagent compared to other analogous *e.g* peroxyacetic acid, peroxybenzoic acid, mCPBA.



**Scheme 4.3.** Mechanism of vanillin oxidation *via* Dakin reaction.

#### 4.2.2 Glycidylation reactions

Glycidyl ether intermediates **5-7** were obtained with moderate to high yields (67-85%) following a previous reported procedure.<sup>27</sup> Glycidyl ethers were prepared in a one-pot two-step reaction (Scheme 4.4).



**Scheme 4.4.** Synthesis of glycidyl ethers **5-7**.

Compounds **6** and **7** were prepared using the same procedure inspired in a methodology developed by Aouf *et al.*<sup>30</sup>, in which, they studied the reactivity of



several natural phenolic compounds towards epichlorohydrin, for the preparation of sustainable substitutes of bisphenol A-based epoxy resins. However, the preparation of compound **5** was achieved with a modified protocol, since, a careful control of the temperature has to be taken in account in order to obtain the desired product, avoiding the formation of a crosslinked by-product. The formation of glycidyl ethers was successfully confirmed by both  $^1\text{H}$  and  $^{13}\text{C}$  NMR spectroscopy (Figure 4.2).

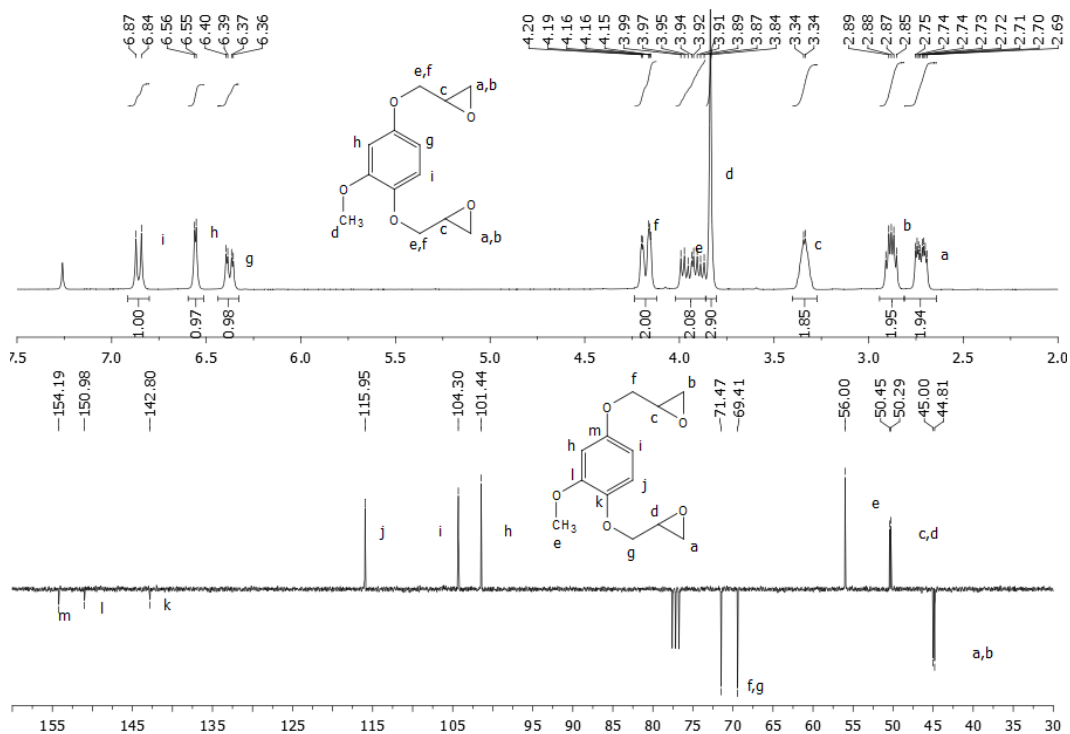
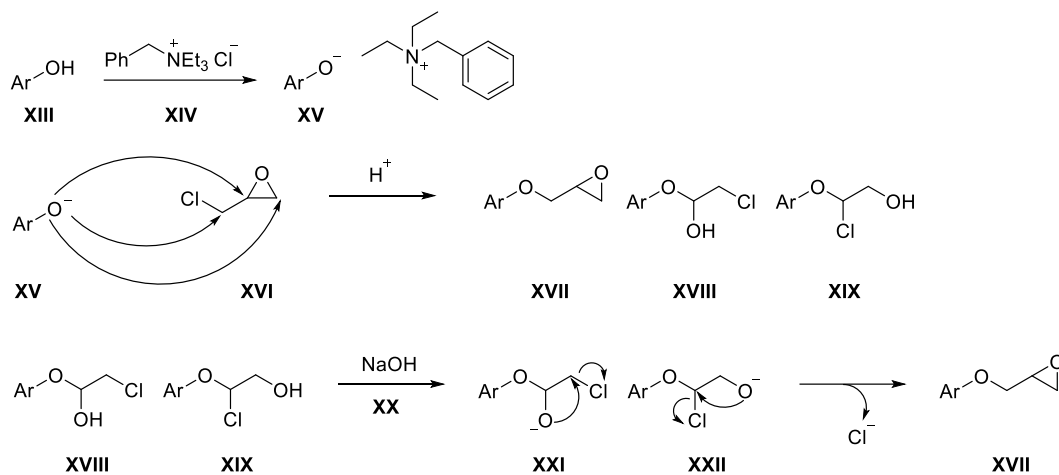


**Figure 4.2.**  $^1\text{H}$  NMR spectrum of compound **6** (300 MHz, 298 K,  $\text{CDCl}_3$ ) (top).  $^{13}\text{C}$  APT NMR spectrum of compound **6** (75 MHz, 298 K,  $\text{CDCl}_3$ ) (bottom).

Glycidation reactions proceed through a two-step mechanism, in the first step, precursors **2-4** were reacted with an excess of epichlorohydrin, which acts as solvent, in the presence of a phase transfer catalyst followed by the addition of an aqueous solution of NaOH in the second step. Phenol derivative, **XIII**, reacts with the phase transfer catalyst, **XIV** rendering a phenolate anion, **XV**, that can exist in the organic phase, then, phenolate **XV** reacts with epichlorohydrin **XVI** through two different mechanisms, nucleophilic attack to the methylene carbon adjacent to the chlorine atom, *i.e.*  $\text{S}_{\text{N}}2$  reaction rendering the desired bis-glycidyl ether intermediate **XVII**, the second one consists on the ring opening of the epoxide

leading to chlorohydrin ether isomers **XVIII** and **XIX** in the presence of NaOH **XX** deprotonation of the alcohol take place and the chloro-alkoxides **XXI** and **XXII** obtained suffer an intramolecular S<sub>N</sub>2 reaction obtaining so the desired bis-glycidyl ether intermediate **XVII** (Scheme 4.5).



**Scheme 4.5.** Aromatic glycidyl ether formation mechanism.

#### 4.2.3 Organocatalytic CO<sub>2</sub> insertion into bis-glycidyl intermediates

Bis-cyclic carbonates **8-10** derived from vanillin were efficiently prepared (81-82% yield) from bis-glycidyl intermediates using a metal-free methodology. As it was described in chapter 1, protic DBU salts, *i.e.* [HDBU]I, were demonstrated to catalyse the synthesis of cyclic carbonates from epoxides under solvent-free mild conditions. However, it was not possible to attach CO<sub>2</sub> under the conditions optimised in chapter 1, therefore reactions were performed under harsher conditions *i.e.* 10 mol% [HDBU]I, 3 MPa, 110°C, 48 h using DMF as solvent in a high pressure reactor. The formation of carbonate **9** functionalities was confirmed by <sup>1</sup>H NMR spectroscopy, on the one hand, the disappearance of the characteristic signals of the epoxide functionality of compound **6** at  $\delta = 3.37$ -3.30 ppm (m, 2H, CH<sub>3</sub>O-C=C-O-CH<sub>2</sub>-CH, CH<sub>3</sub>O-C-CH=C-O-CH<sub>2</sub>-CH), 2.91-2.85 ppm (m, 2H, CH<sub>3</sub>O-C=C-O-CH<sub>2</sub>-CH-CH<sub>b</sub>, CH<sub>3</sub>O-C-CH=C-O-CH<sub>2</sub>-CH-CH<sub>b</sub>) and 2.75-2.69 ppm (m, 2H, CH<sub>3</sub>O-C=C-O-CH<sub>2</sub>-CH-CH<sub>a</sub>, CH<sub>3</sub>O-C-CH=C-O-CH<sub>2</sub>-CH-CH<sub>a</sub>) was confirmed. On the other hand, three new different signals were arised and attributed to the formation of carbonate **9**. Indeed, those signals were observed at  $\delta = 5.14$ -5.07 ppm (m, 2H, CH<sub>3</sub>O-C-CH=C-O-CH<sub>2</sub>-CH, CH<sub>3</sub>O-C=C-O-CH<sub>2</sub>-CH), 4.65-4.58 ppm (m,

2H, CH<sub>3</sub>O-C=C-O-CH<sub>2</sub>-CH-CH<sub>b</sub>, CH<sub>3</sub>O-C-CH=C-O-CH<sub>2</sub>-CH-CH<sub>b</sub>) and 4.42-4.35 ppm (m, 2H, CH<sub>3</sub>O-C=C-O-CH<sub>2</sub>-CH-CH<sub>a</sub>, CH<sub>3</sub>O-C-CH=C-O-CH<sub>2</sub>-CH-CH<sub>a</sub>) (Figure 4.3).

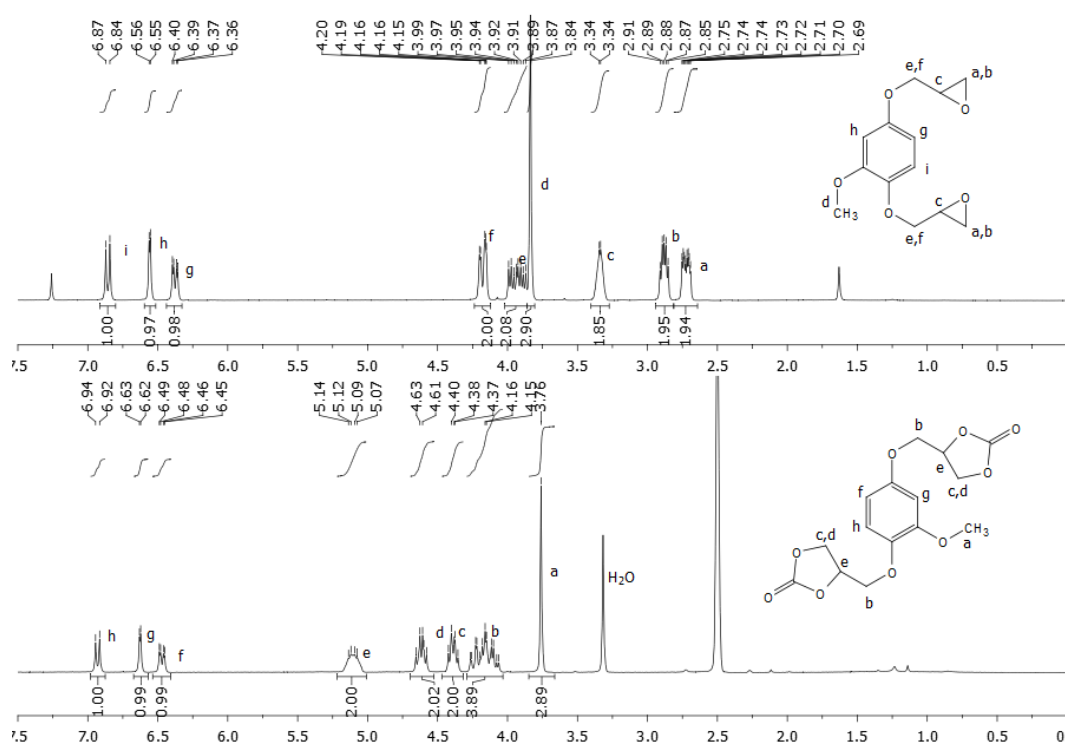
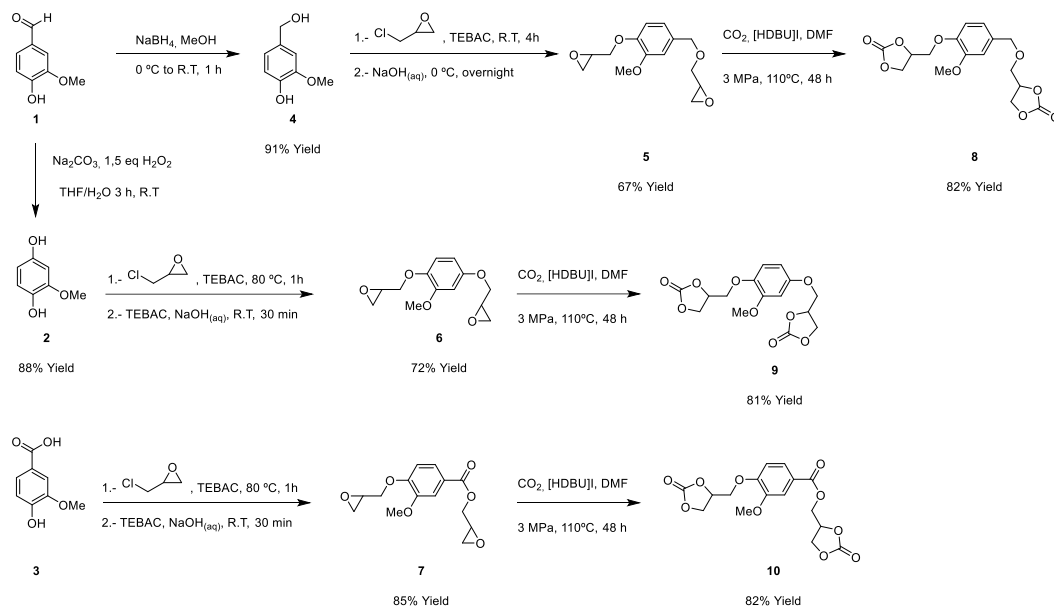


**Figure 4.3.** <sup>1</sup>H NMR spectrum of epoxide **6** (300 MHz, 298 K, CDCl<sub>3</sub>) (*top*) and the resultant carbonate **9** after cyclocarbonation reaction between **6** and CO<sub>2</sub> (300 MHz, 298 K, DMSO) (*bottom*).

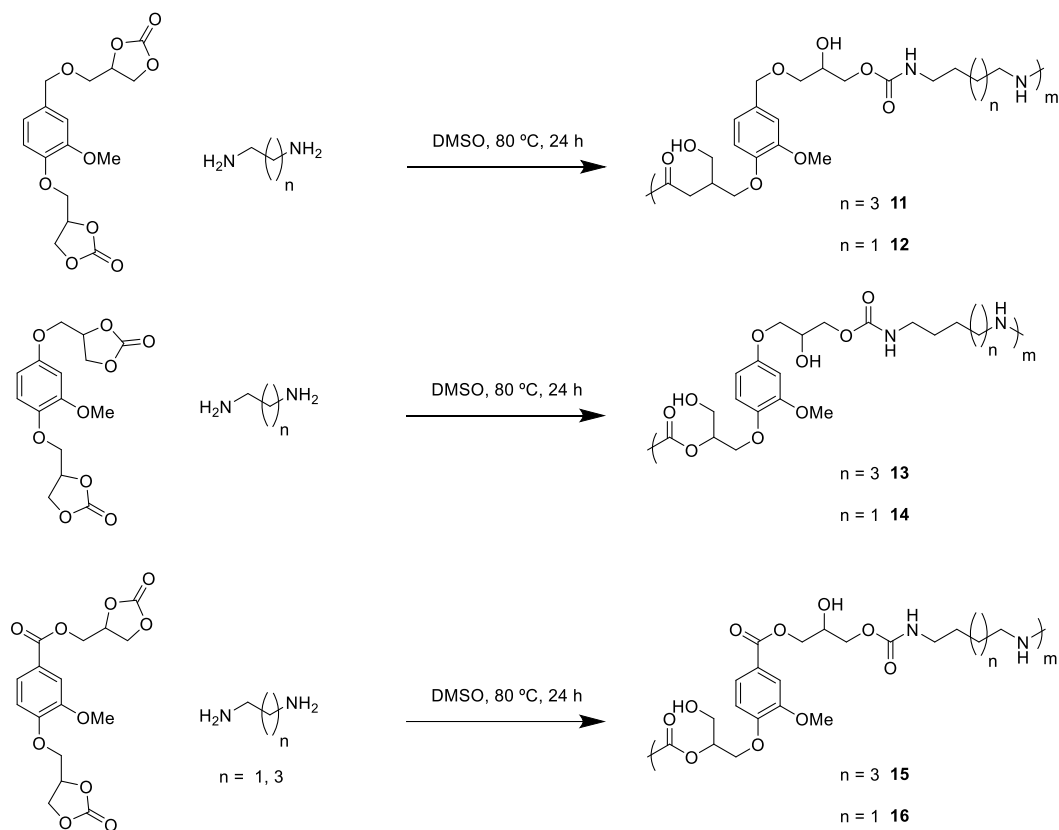
Compared with the methodology reported in the literature,<sup>27</sup> a metal-free procedure was used instead of the one reported in which LiBr was used as catalyst. However, the reported conditions are harsher than the ones described when LiBr was used as catalyst, *i.e.* 5 mol% LiBr, 1.2 MPa, 80 °C, 12 hours using acetone as solvent, compound **10** was obtained in a better yield than the one under the latter conditions, 82 vs 50% yield. Moreover, another benefit of the described methodology is the use of an organocatalyst instead of a metallic salt. Overall, bis-carbonate monomers derived from vanillin for the synthesis of NIPUs were prepared using a metal-free methodology with overall yields range between 50-70% (Scheme 4.6).



**Scheme 4.6.** Synthetic route for the synthesis of functional bis-carbonates derived from vanillin.

#### 4.2.4 Synthesis of NIPUs from bis-carbonate vanillin derivatives

After successful synthesis of three different bis-carbonate vanillin derivatives **8-10**, six different NIPUs formulations were subsequently prepared by reacting each bis-carbonate monomer with two different bis-amines, *i.e.* 1,4-butanediamine and 1,6-hexamethylenediamine (HMDA) respectively. Polymerizations were carried out using DMSO as solvent, at 80 °C, for 24 h. As compound **10** has an ester functionality, temperature control of the polymerization has to be taken in account since it has been reported that amines can react with esters leading to amide formations.<sup>31</sup> Therefore, all polymerizations were carried out at 80 °C, this way, chemoselectivity can be ensured and only reaction between bis amines and bis carbonates will occur leading to the satisfactory formation of NIPUs (Scheme 4.7).



**Scheme 4.7.** Synthesis of vanillin based non-isocyanate poly(hydroxyurethanes).

The so obtained NIPUs were characterised by FTIR spectroscopy along with  $^1\text{H}$  and  $^{13}\text{C}$  NMR spectroscopy and SEC, thermal properties were studied using DSC and TGA.  $^1\text{H}$  NMR spectroscopy confirmed the formation of the desired NIPUs (Figure 4.4), on the one hand, disappearance of  $\alpha$  protons ( $\delta = 5.12, 4.61$  and  $4.39$  ppm) with respect to carbonate functionalities was observed, on the other hand, three new characteristic signals arised. Between  $\delta = 7.20\text{-}7.10$  ppm a peak corresponding to the proton of new arising carbamate functionality was registered, in the range of  $\delta = 5.21\text{-}5.16$  ppm signals corresponding to the formation of primary and secondary alcohols were observed, last characteristic signal was registered around  $\delta = 2.95$  ppm, this signal was attributed to the methylene protons in  $\alpha$  position with respect to the  $\text{-NH-}$  moiety of the new formed urethane functionality.

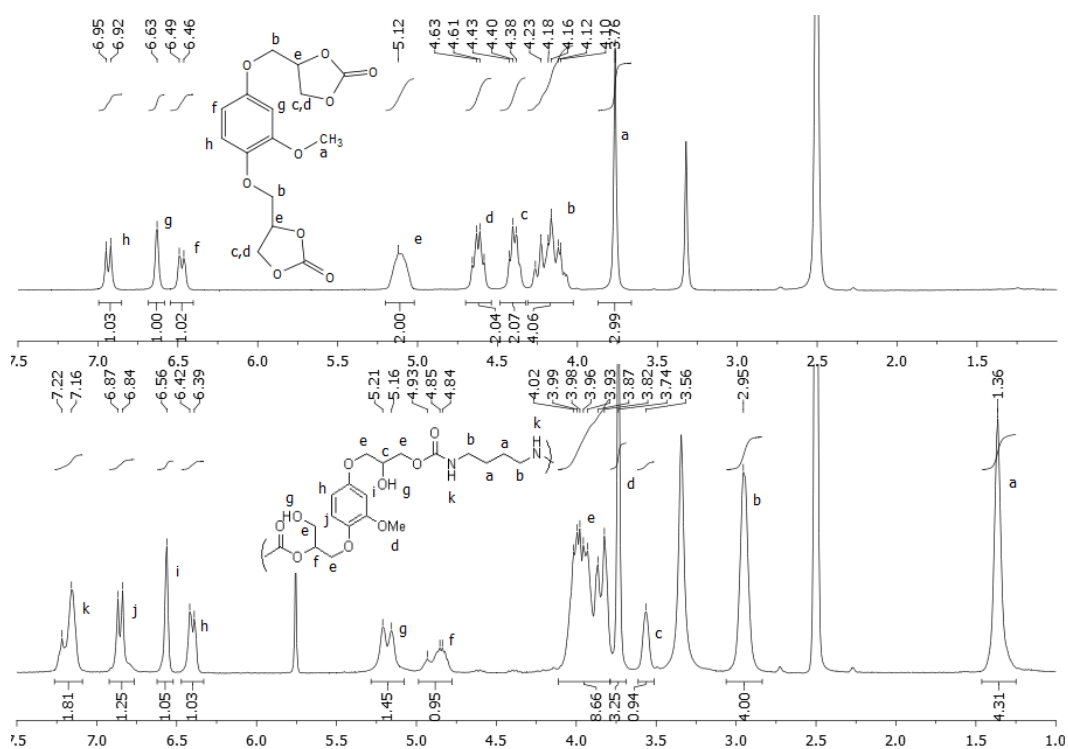


**Figure 4.4.** <sup>1</sup>H NMR spectrum of monomer **9** (top) and the resultant NIPU **13** (bottom) by reaction of **9** and hexamethylenediamine in DMSO at 80 °C for 24 h (300 MHz, 298 K, DMSO).

Further characterization was satisfactory confirmed by FTIR spectroscopy (Figure 4.5). In all examples same trend was observed, the corresponding peak to the carbonate functionality of each monomer *i.e.* vanillyl alcohol, 1779 cm<sup>-1</sup>, hydroquinone, 1783 cm<sup>-1</sup>, vanillic acid, 1791 and 1797 cm<sup>-1</sup>, disappeared and two new signals arised, broad signals around 3300 cm<sup>-1</sup> were observed, this signals were attributed to the new formed primary and secondary alcohol functionalities in the NIPU and the -NH- elongation vibration in the carbamate moiety, the second signal appeared around 1684-1689 cm<sup>-1</sup> depending on the starting material, this band corresponds to the -C=O deformation vibration in the formed carbamate moiety.

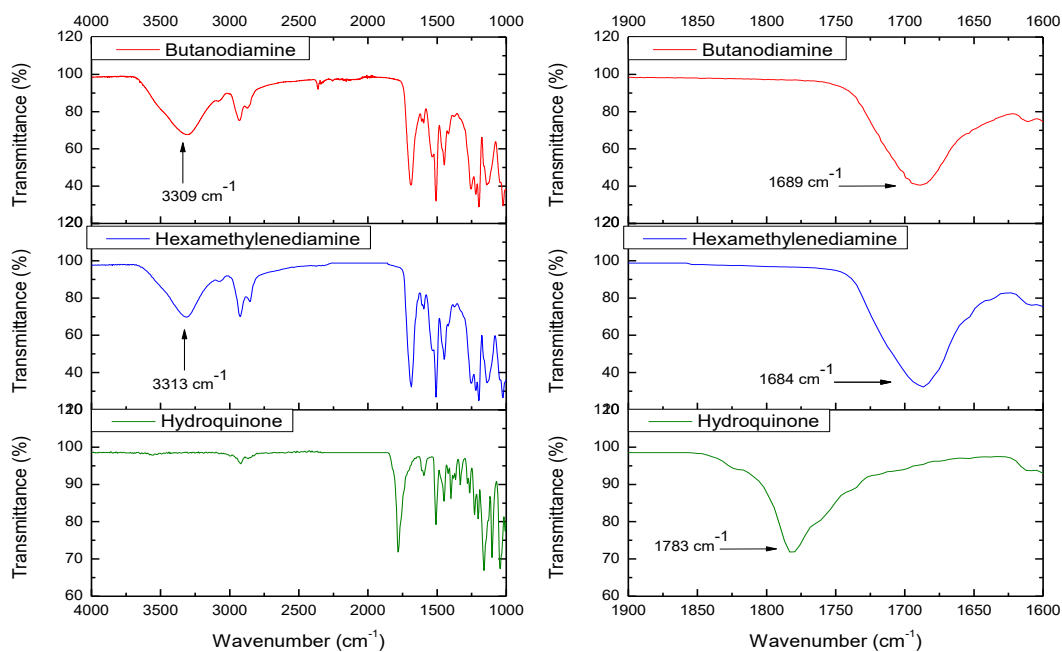


**Figure 4.5.** FTIR spectrum of NIPUs **14** and **13** prepared from monomer **9** (*left*), zoom in carbonyl stretching region of NIPUs **14** and **13** prepared from monomer **9** (*right*).

Molecular weight distribution was determined by SEC using DMF as solvent (Table 4.1). Molecular weight values obtained were between  $6.8\text{-}20.0 \text{ kg} \times \text{mol}^{-1}$  and dispersity ( $D_M$ ) were between 1.51-1.94, which are expected for this kind of polymerization. Thermal characterization performed by DSC showed a glass transition temperature ( $T_g$ ) in all formulations in a range between 41-66 °C (Table 4.1).

**Table 4.1.** Summary of molecular weight distributions and  $T_g$  registered from SEC and DSC calorimetry respectively of vanillin NIPUs.

Entry	NIPU	$M_w$ (g/mol) <sup>a</sup>	$M_n$ (g/mol) <sup>a</sup>	$D_M$ ( $M_w/M_n$ ) <sup>a</sup>	$T_g$ (°C) <sup>b</sup>
1	<b>11</b>	30.274	20.044	1.51	41
2	<b>12</b>	11.982	6.808	1.76	41
3	<b>13</b>	30.355	16.782	1.81	50
4	<b>14</b>	25.981	14.466	1.80	52
5	<b>15</b>	26.032	13.489	1.93	60
6	<b>16</b>	22.983	11.822	1.94	66

<sup>a</sup> Determined by SEC analysis in DMF against poly(styrene) (PS) standards. <sup>b</sup> Thermal transition calculated from the second heating run of the DSC analysis.

A relationship between structure and  $T_g$  was observed as the NIPUs derived from vanillic acid (Table 4.1, entries 1 and 4) exhibited the highest  $T_g$  *i.e.* 66 and 60 °C respectively when 1,4-butanediamine and HDMA were used. The NIPUs derived from hydroquinone showed a lower  $T_g$  compared with the ones derived from vanillic acid (Table 4.1, entries 2 and 5), finally, the NIPUs obtained when vanillyl alcohol bis-carbonate was used exhibited the lowest  $T_g$  (Table 4.1, entries 3 and 6). The presence of the ester functionality in the vanillic acid NIPUs confers a higher rigidity compared to the phenol of the hydroquinone NIPUs and so on to the ether of the vanillyl alcohol NIPUs, therefore higher  $T_g$  was observed in the first one compared to the later ones.

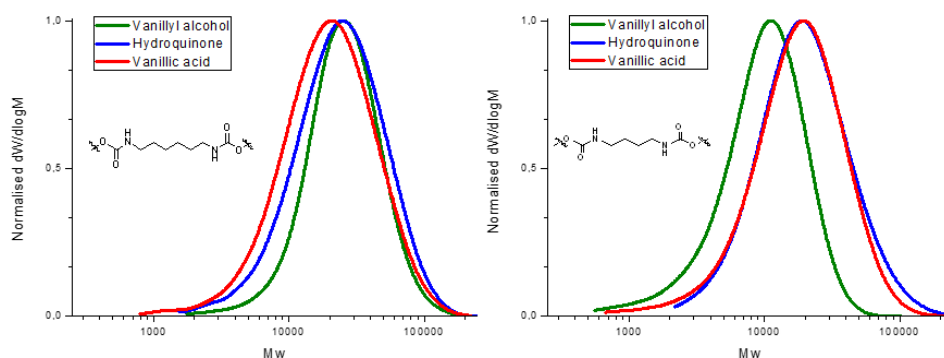


**Figure 4.6.** GPC traces of the different NIPUs obtained from functionalised vanillin bis-carbonates.



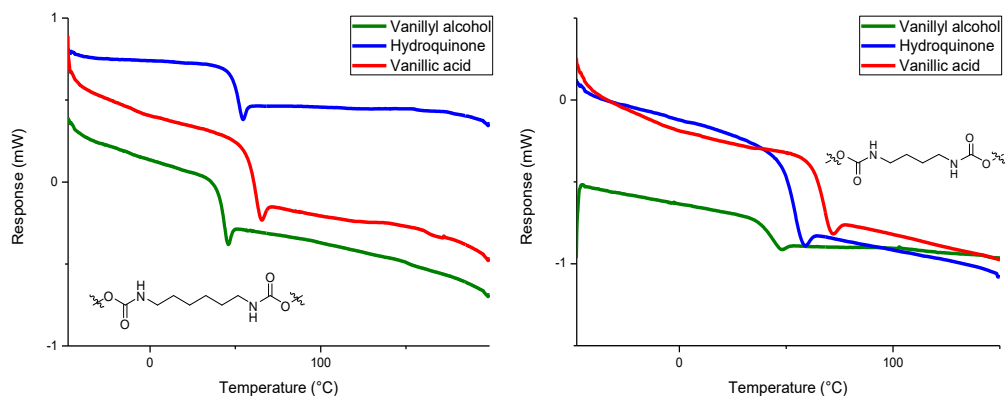


**Figure 4.7.** DSC curves of the different NIPUs obtained from functionalised vanillin bis-carbonates.

Thermal decomposition of obtained NIPUs was studied by TGA from room temperature to 600 °C under nitrogen atmosphere (Figure 4.8). On the one hand, the NIPUs obtained using HMDA showed higher thermal stability as those polymers start to show significant degradations around 300 °C. On the other hand, the NIPUs obtained using 1,4-butanediamine showed, firstly, a progressive thermal degradation around 125 °C followed by a sharp decay around 300 °C. Thermograms reveal that the NIPUs prepared around HMDA have indeed higher thermal stability compared with their homologous synthesised around 1,4-butanediamine.

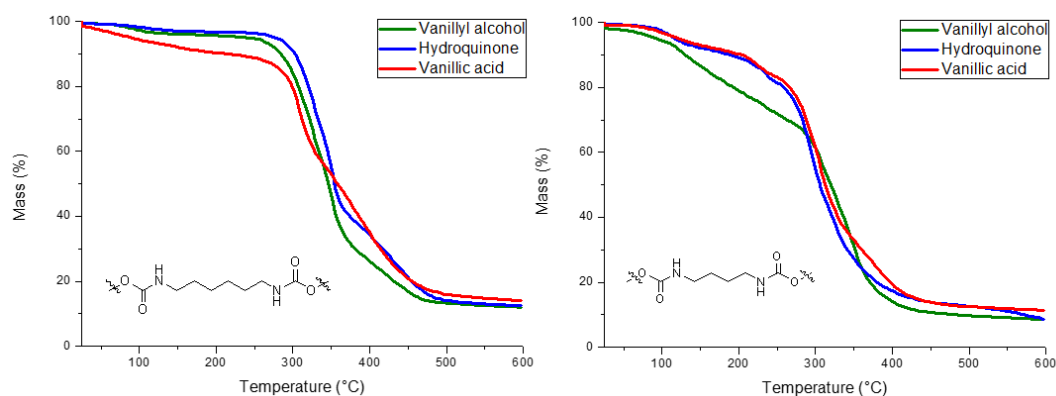


**Figure 4.8.** TGA curves of the different NIPUs obtained from functionalised vanillin bis-carbonates.

### 4.3 Conclusions

In conclusion, the first example of a vanillin-based bis-cyclic carbonate for the synthesis of bio-based non-isocyanate polyurethane (NIPU) is reported. Bis-cyclic epoxides were prepared following a methodology found in the literature, bis-cyclic carbonates were prepared using a metal-free methodology inspired by the protocol developed in chapter 2. NIPUs were successfully prepared using bio-based putrescine and hexamethylenediamine. The obtained NIPUs were fully characterised using  $^1\text{H}$  and  $^{13}\text{C}$  NMR spectroscopy along with FTIR, molecular weight distribution was determined by GPC and thermal characterisation was performed using DSC and TGA.

### 4.4 References

1. O. Bayer, *Angew. Chem*, 1947, **59**, 257-272.
2. J. O. Akindoyo, M. D. H. Beg, S. Ghazali, M. R. Islam, N. Jeyaratnam and A. R. Yuvaraj, *RSC Adv.*, 2016, **6**, 114453-114482.
3. V. R. Dhara and R. Dhara, *Arch. Environ. Health*, 2002, **57**, 391-404.
4. M. Carino, M. Aliani, C. Licitra, N. Sarno and F. Ioli, *Respiration*, 1997, **64**, 111-113.
5. L. Maisonneuve, O. Lamarzelle, E. Rix, E. Grau and H. Cramail, *Chem. Rev.*, 2015, **115**, 12407-12439.
6. M. S. Kathalewar, P. B. Joshi, A. S. Sabnis and V. C. Malshe, *RSC Adv.*, 2013, **3**.
7. G. Rokicki, P. G. Parzuchowski and M. Mazurek, *Polym. Adv. Technol.*, 2015, **26**, 707-761.
8. H. Blattmann, M. Fleischer, M. Bahr and R. Mulhaupt, *Macromol. Rapid Commun.*, 2014, **35**, 1238-1254.
9. A. Cornille, R. Auvergne, O. Figovsky, B. Boutevin and S. Caillol, *Eur. Polym. J.*, 2017, **87**, 535-552.
10. M. Alves, B. Grignard, R. Mereau, C. Jerome, T. Tassaing and C. Detrembleur, *Catal. Sci. Technol.*, 2017, **7**, 2651-2684.
11. R. R. Shaikh, S. Pornpraprom and V. D'Elia, *ACS Catal.*, 2017, **8**, 419-450.

12. D.-H. Lan, N. Fan, Y. Wang, X. Gao, P. Zhang, L. Chen, C.-T. Au and S.-F. Yin, *Chin. J. Catal.*, 2016, **37**, 826-845.
13. G. Fiorani, W. Guo and A. W. Kleij, *Green Chem.*, 2015, **17**, 1375-1389.
14. J. Zakzeski, P. C. Bruijninx, A. L. Jongerius and B. M. Weckhuysen, *Chem. Rev.*, 2010, **110**, 3552-3599.
15. C. Li, X. Zhao, A. Wang, G. W. Huber and T. Zhang, *Chem. Rev.*, 2015, **115**, 11559-11624.
16. R. Behling, S. Valange and G. Chatel, *Green Chem.*, 2016, **18**, 1839-1854.
17. A. J. Ragauskas, G. T. Beckham, M. J. Biddy, R. Chandra, F. Chen, M. F. Davis, B. H. Davison, R. A. Dixon, P. Gilna, M. Keller, P. Langan, A. K. Naskar, J. N. Saddler, T. J. Tschaplinski, G. A. Tuskan and C. E. Wyman, *Science*, 2014, **344**, 1246843.
18. S. Laurichesse and L. Avérous, *Prog. Polym. Sci.*, 2014, **39**, 1266-1290.
19. H. Lange, S. Decina and C. Crestini, *Eur. Polym. J.*, 2013, **49**, 1151-1173.
20. R. R. Gustafson, C. A. Sleicher, W. T. McKean and B. A. Finlayson, *Ind. Eng. Chem. Process Des. Dev.*, 1983, **22**, 87-96.
21. F. S. Chakar and A. J. Ragauskas, *Ind. Crop. Prod.*, 2004, **20**, 131-141.
22. E. A. B. d. Silva, M. Zabkova, J. D. Araújo, C. A. Cateto, M. F. Barreiro, M. N. Belgacem and A. E. Rodrigues, *Chem. Eng. Res. Des.*, 2009, **87**, 1276-1292.
23. A. Vishtal and A. Kraslawski, *BioResources*, 2011, **6**, 3547-3568.
24. J. Zakzeski, A. L. Jongerius, P. C. Bruijninx and B. M. Weckhuysen, *ChemSusChem*, 2012, **5**, 1602-1609.
25. R. S. Ramachandra and G. A. Ravishankar, *J. Sci. Food Agric.*, 2000, **80**, 289-304.
26. P. Kraft, J. A. Bajgrowicz, C. Denis and G. Fráter, *Angew. Chem. Int. Ed.*, 2000, **39**, 2981-3010.
27. M. Fache, E. Darroman, V. Besse, R. Auvergne, S. Caillol and B. Boutevin, *Green Chem.*, 2014, **16**, 1987-1998.
28. G. Kabalka, N. Reddy and C. Narayana, *Tetrahedron Lett.*, 1992, **33**, 865-866.
29. G. D. Yadav and S. V. Lande, *Appl. Catal., A*, 2005, **287**, 267-275.
30. C. Aouf, C. Le Guernevé, S. Caillol and H. Fulcrand, *Tetrahedron*, 2013, **69**, 1345-1353.

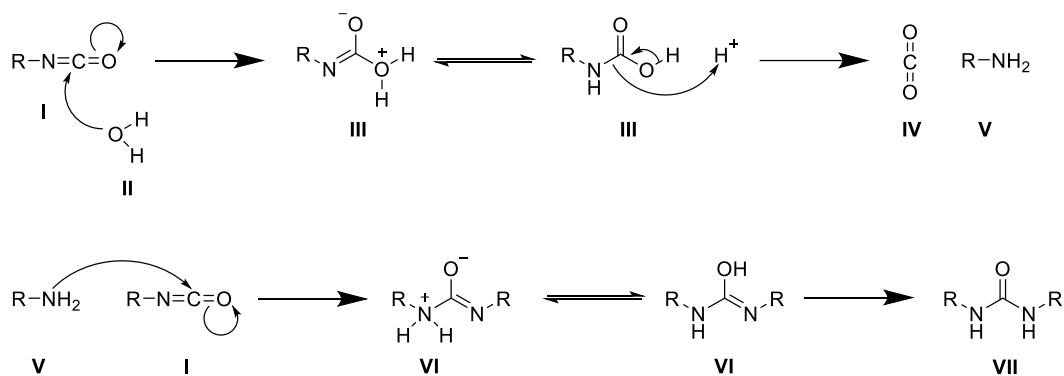
31. F. Camara, S. Benyahya, V. Besse, G. Boutevin, R. Auvergne, B. Boutevin and S. Caillol, *Eur. Polym. J.*, 2014, **55**, 17-26.

**5. Waterborne synthesis of non-  
isocyanate poly(hydroxy urethanes)  
thermo-responsive hydrogels**

## 5.1 Introduction

Hydrogels are three dimensional polymeric networks capable of holding large amounts of water.<sup>1, 2</sup> Aforesaid unique characteristic allows to use these materials to have many applications such as, in agriculture,<sup>3</sup> drug delivery systems,<sup>4, 5</sup> biomedical applications,<sup>6</sup> tissue engineering,<sup>7-9</sup> medical devices like soft contact lenses<sup>10</sup> and metal ion extraction.<sup>11</sup> Natural polymers can be exploited for the synthesis of hydrogels and they are indeed found in several different sources, such proteins *e.g* collagen,<sup>12</sup> or polysaccharides like chitosan,<sup>13</sup> hyaluronic acid,<sup>14</sup> starch,<sup>15</sup> alginate<sup>16</sup> or agarose.<sup>17</sup> However, despite being naturally derived, the main drawback of these materials is the batch to batch reproducibility. This issue can be overcome using synthetic hydrogels, allowing the mechanical and swelling properties to be controlled and tailored to specific applications by chemical transformations. 3D printing has recently arised as an excellent tool for the development of tissue engineering, particularly in the manufacturing of prefabricated scaffolds that are used as a support for the cells and growth factors.<sup>18</sup> As a consequence of their swelling ability and biocompatibility, hydrogels indeed, can be exploited for the development of prefabricated scaffolds in tissue engineering.

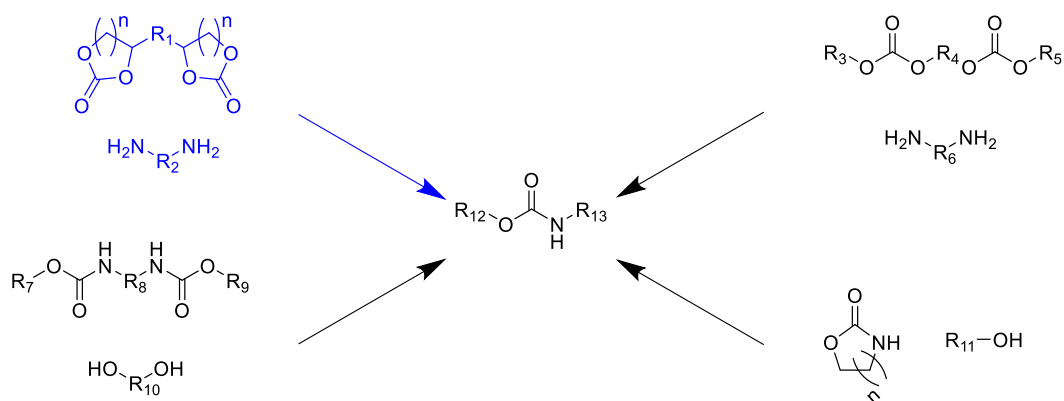
In industry, polyurethanes are prepared by the reaction of diisocyanates with diols catalysed by a metal-based catalyst in an organic solvent. Although methodologies are highly efficient and well established, the use of highly toxic isocyanates represents the main drawback for the synthesis of these materials.<sup>19, 20</sup> Along with its toxicity, another drawback for the synthesis of polyurethanes, is the impossibility of preparing these polymers in aqueous media. Isocyanate **I** reacts with water **II**, affording an unstable carbamic acid **III**. This carbamic acid **III** suffers a spontaneous decarboxylation releasing CO<sub>2</sub> **IV** and yielding a primary amine **V**. Isocyanate **I** is an electrophile, thus it reacts with the primary amine **V** present in the reaction media affording an intermediate **VI** which, after a tautomerization renders an urea **VII** instead of the desired urethane (Scheme 5.1).<sup>21</sup> Therefore, in the last years several new strategies for the synthesis of non-isocyanate polyurethanes (NIPUs) have been extensively studied.<sup>22</sup> There are four mainly different approaches for the synthesis of NIPUs; step-growth polyaddition of cyclic bis-carbonates and bis-amines, step-growth polycondensation of linear activated



**Scheme 5.1.** Formation of urea *via* reaction of isocyanate with water.

bis-carbonates and bis-amines, step-growth polycondensation of linear activated bis-carbamates and diols and ring-opening polymerization of cyclic carbonates (Scheme 5.2).<sup>23-25</sup> In this chapter, first approach was embraced. Cyclic carbonates can be prepared through a huge number of synthetic routes,<sup>26, 27</sup> indeed, in most of them the cycloaddition of CO<sub>2</sub> to epoxides is reported.<sup>28</sup> Therefore, not only the bypass of toxic isocyanates can be done by the development of NIPUs synthesis but also reducing the CO<sub>2</sub> footprint. The reactivity of cyclic carbonates *vs* amines has been studied and reported.

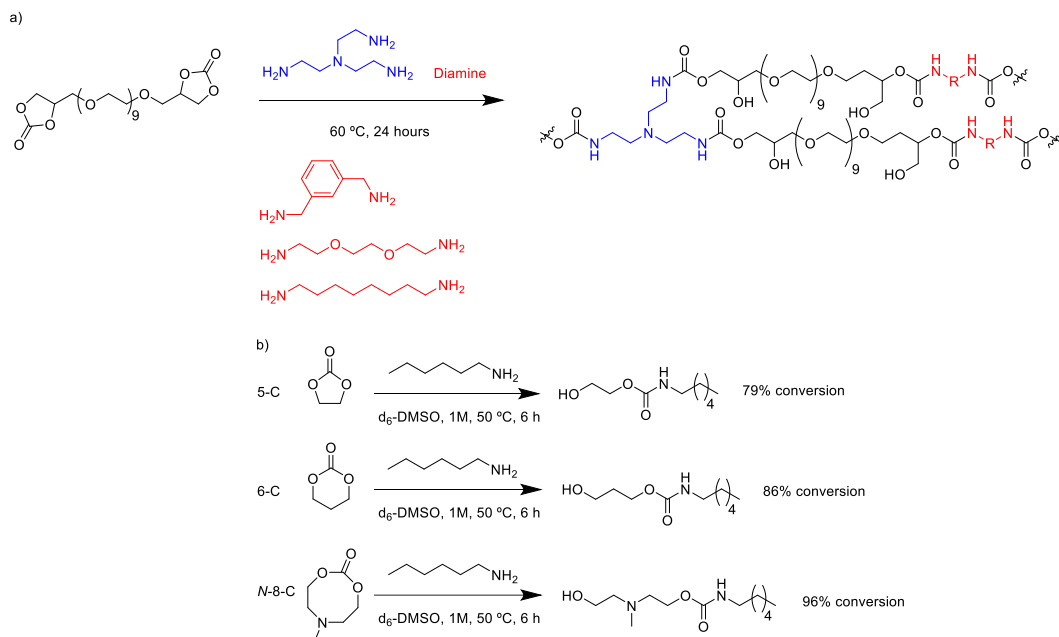
Yuen *et al.* demonstrated that eight-membered cyclic carbonates exhibited faster kinetics for aminolysis reaction compared to the five and six-membered analogous cyclic carbonates.<sup>29</sup> This higher reactivity is attributed to the higher ring strain in the eight-membered cyclic carbonate compared to the six and five-membered respectively. Gennen *et al.* reported the first example of NIPU hydrogels. Five-membered cyclic carbonates were prepared by organocatalytic cycloaddition of CO<sub>2</sub> of PEG diglycidyl ether and subsequently were reacted with different aliphatic and aromatic bis-amines and tris(2-aminoethyl)amine (TAEA) as cross-linker.<sup>30</sup> Indeed, NIPU hydrogels were obtained, however, reaction conditions were relatively harsh, as reaction was conducted at 60 °C during 24 hours. Polymerization was not quantitative, therefore unreacted monomers were extracted by immersing the formed gel in water for 4 days at room temperature.



**Scheme 5.2.** Different approaches for the synthesis of NIPUs.

Inspired by the studies of Yuen *et al.* and Gennen *et al.* (Scheme 5.3), first example of synthesis of poly(hydroxy urethane) in water is reported. The superior reactivity of eight-membered cyclic carbonates allows to conduct the step-growth polymerization under mild conditions *i.e* in aqueous media and at room temperature. The incorporation of TAEA as cross-linker along with the use of PEG-diamines as chain extender and hydrophilic moiety represents an ideal scenario for the synthesis of waterborne poly(hydroxy urethanes). Subsequently the influence of amount of water, cross-linker *vs* PEG-diamine ratios and temperature in the gelation process and the mechanical properties of the materials obtained was studied. To our delight, thermo-responsive materials were rendered since reversible moduli decay was observed when the materials were heated up and an increase when the materials were cooled down as a consequence of the interaction of the PEG moiety with water and its thermal transitions inherent to its crystallinity.<sup>31, 32</sup> This thermo-responsive behaviour was embraced by the design of 3D printing scaffolds.



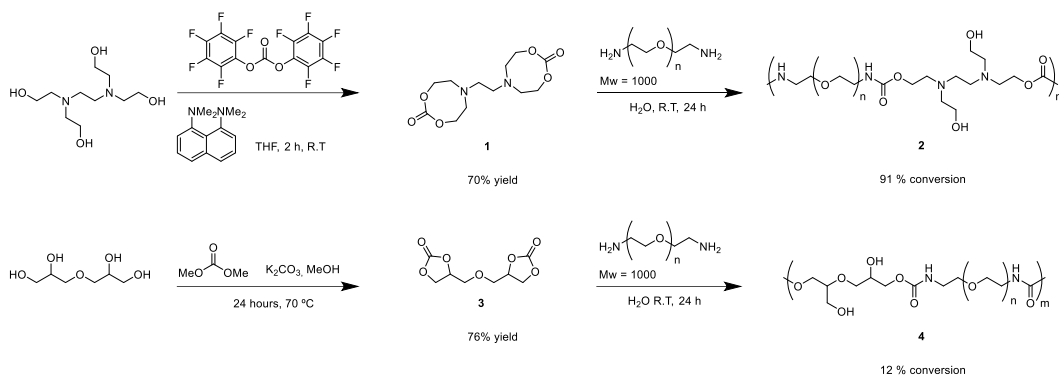


**Scheme 5.3.** a) Gennen *et al.* synthesis of five-membered poly(hydroxy urethanes), b) Yuen *et al.* aminolysis reaction study of five, six and eight-membered cyclic carbonates.

## 5.2 Results and discussion

### 5.2.1 Synthesis of five and eight-membered cyclic carbonate and kinetic study of their reactivity with PEG diamines in water

Five and eight-membered cyclic carbonates were prepared through a ring-closing reaction of diglycerol and *N,N,N',N'*-tetrakis(2-hydroxyethyl)ethylenediamine respectively (Scheme 5.4). Both methodologies were reproduced from procedures found in the literature.<sup>29, 33</sup> It is remarkably that in both synthesis, phosgene-free derivatives were used to prepare both bis-carbonates, stressing the fact of using sustainable methodologies. Yields obtained in both cases, were above 70%. After successful synthesis of **1** and **3**, the reactivity of those carbonates was tested against bis-amines in water at room temperature (Scheme 5.4). After 24 hours reaction, conversion was calculated by <sup>1</sup>H NMR spectroscopy analysis (Figure 5.1).



**Scheme 5.4.** Synthesis of precursors **1** and **3** for the preparation of hydrogels and subsequent synthesis of waterborne NIPUs **2** and **4** with PEG-1,000 diamine at room temperature.

Relative peak integration values from the reaction crude mixture, revealed a 91% conversion for compound **2** and 12% conversion in the case of compound **4**. Indeed, disappearance of the signals corresponding to methylene protons in  $\alpha$  and  $\beta$  position in **1** at  $\delta = 4.08$  and  $2.76$  respectively were observed. Three new different signals appeared and were attributed to the formation of **2**, those signals appeared at  $\delta = 7.07$  ppm ( $-\text{CH}_2\text{-OCO-NH-}$ ),  $3.95$  ppm ( $-\text{CH}_2\text{-OCO-NH-}$ ) and  $3.10$  ppm ( $-\text{CH}_2\text{-OCO-NH-CH}_2\text{-}$ ). Same trend was observed when monomer **3** was polymerised. Partial disappearance of the signals of **3** corresponding to methyne and methylene protons at  $\delta = 4.98\text{-}4.90$  and  $4.52^{\text{anti}}, 4.27\text{-}4.21^{\text{syn}}$  ppm were observed. New signals arising from formation of compound **4**. Indeed, at  $\delta = 7.12$  ppm ( $-\text{CH}_2\text{-OCO-NH-}$ ) and  $4.68$  ppm ( $\text{HO-CH}_2\text{-CH-CH}_2\text{-CO}_2\text{-NH-}$ ) were appeared.

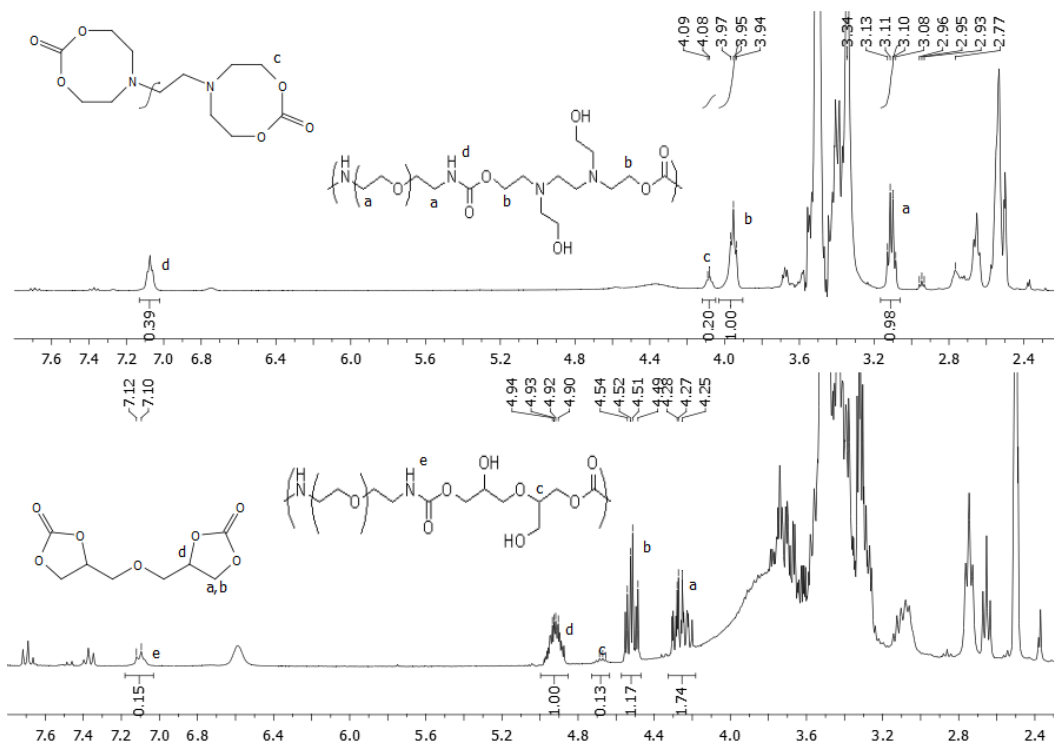
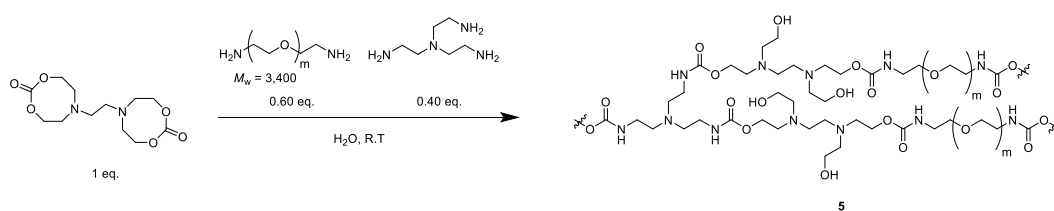


**Figure 5.1.** <sup>1</sup>H NMR spectrum of formation of **2** at R.T overnight. The conversion was calculated with the following equation:  $\% \text{ conversion} = \frac{b}{(b+c)}$ . Final conversion was 91% (*top*). <sup>1</sup>H NMR spectrum of formation of **4** at R.T overnight. The conversion was calculated with the following equation:  $\% \text{ conversion} = \frac{c}{(c+d)}$ . In this case, the final conversion was 12% (*bottom*). (300 MHz, 298 K, DMSO-*d*<sub>6</sub>).

## 5.2.2 Gelation process

Taking advantage of the higher reactivity of 8MCC compared to diglycerol carbonate in aqueous media under the conditions tested, the possibility of preparing hydrogel materials through a step-growth polymerization process was investigated (Scheme 5.5).



**Scheme 5.5.** Synthesis of waterborne hydrogels at room temperature.

Indeed, hydrogel **5** was obtained when 1 equivalent of 8MCC was reacted in water at room temperature with 0.60 equivalents of PEG diamine  $M_w = 3,400$  as chain extender, and 0.40 equivalents of tris(2-aminoethylene)amine (TAEA) as cross-linker. PEG diamines were used to bring hydrophilicity to the materials prepared. This approach, compared to the ones reported in the literature,<sup>30</sup> allows to perform the polymerization in milder conditions and in aqueous media, materials were obtained in shorter periods of time. In order to confirm the covalent nature of the hydrogels obtained, small amplitude oscillatory experiments (SAOS) were conducted in frequency sweeps. Formed gels showed no frequency dependence of the storage and loss moduli with a predominance of the elastic behaviour, as it corresponds to a chemically cross-linked network. In contrast linear PHU water solution showed a frequency dependence which correspond to the flow zone (Figure 5.2).

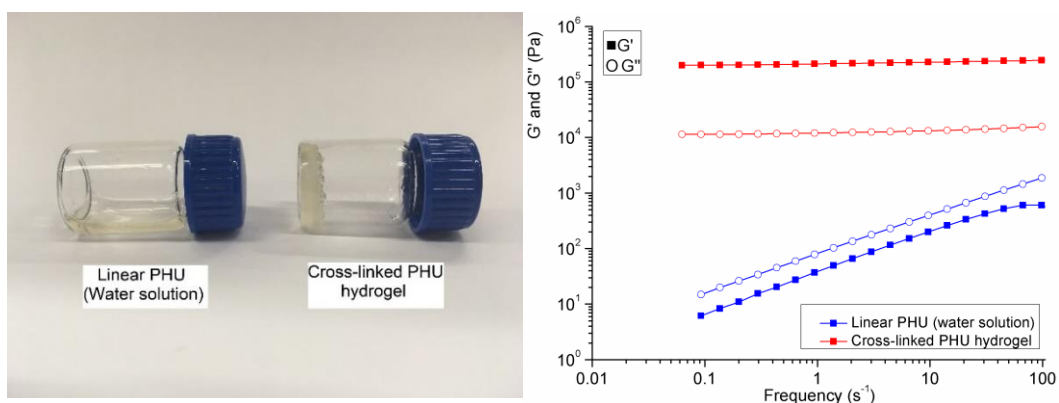


**Figure 5.2.** Synthesised water solution of **2** and cross-linked poly(hydroxyurethane) hydrogel **5** (*left*) and rheological characterization of both materials by frequency sweep experiments (*right*).

The crosslinking reaction was confirmed by FTIR. To our delight, the carbonyl stretching band at  $1726\text{ cm}^{-1}$  arising from **1** disappeared, while new absorption bands that are assigned to N-H deformation and carbonyl group appear at  $1696\text{ cm}^{-1}$  and  $1534\text{ cm}^{-1}$ , in addition, the formation of primary alcohols and the N-H elongation were identified as broad bands around  $3300\text{ cm}^{-1}$  (Figure 5.3).

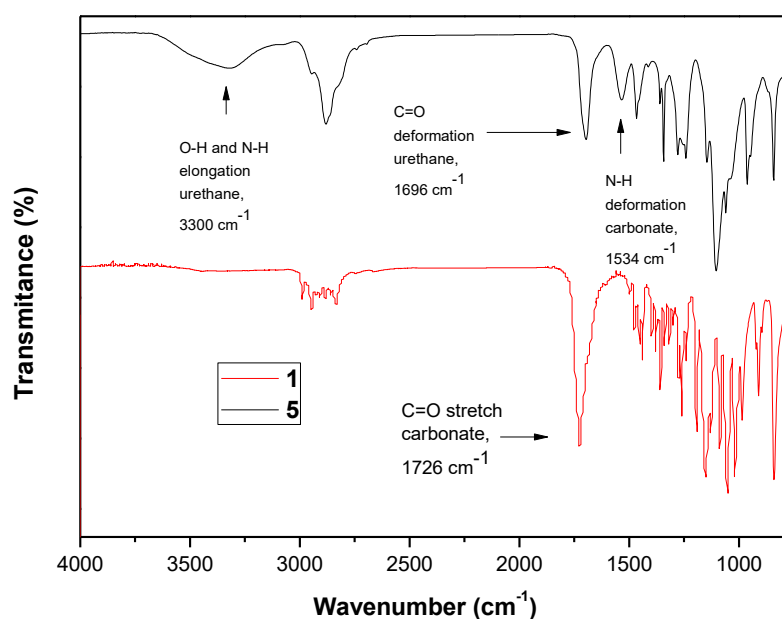
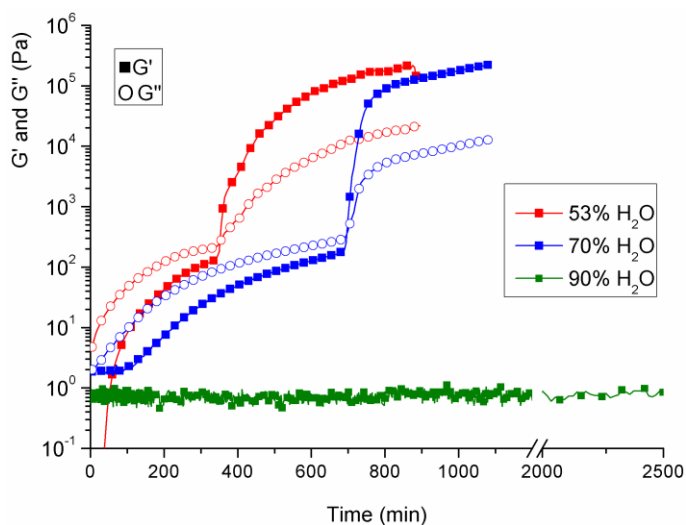


**Figure 5.3.** FTIR spectra of compound **1** (*bottom*) and a lyophilised hydrogel formulation of **5**.

### 5.2.3 Water influence in the gelation process

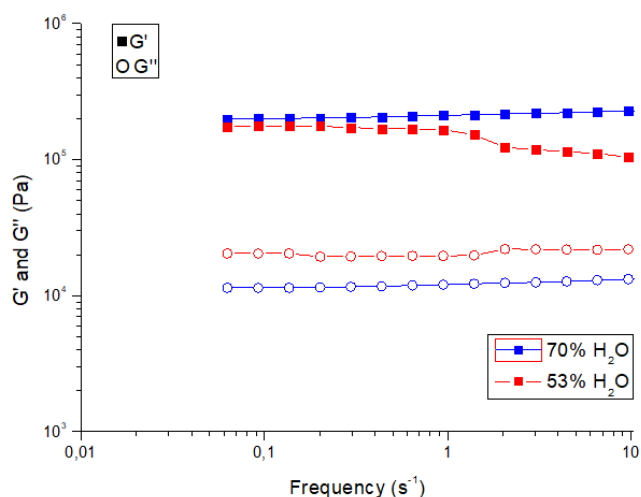
After satisfactory confirmation and characterization of waterborne poly(hydroxy urethane) hydrogels, the influence of water content in the gelation process was studied. Evolution of the storage ( $G'$ ) and loss moduli ( $G''$ ) with time at room temperature by SAOS was monitored for mixtures of hydrogel **5** with different amounts of water (Figure 5.4). Lower water contents lead to hydrogels with higher moduli, however, a minimal amount of water is needed to ensure the solubility of reagents, especially compound **1**, along with the homogeneity of the material obtained. The cross-over point of  $G'$  and  $G''$  was taken as indicative of the gelation time. Indeed, water had an impact on the gelation process as rheology shows that higher contents of water revealed longer reaction times. In the early stages of the reaction  $G''$  had a higher value than  $G'$  revealing the liquid nature of the mixture, as reaction proceeds, an increase on the moduli value was registered. Eventually, a sharp increment in both moduli with a cross-over point was observed. When  $G'$  exhibited a higher value than  $G''$ , this cross-over point was taken as indicative of the gelation time. Then moduli values reached a plateau confirming the obtention

of the desired hydrogel material. Finally, it was demonstrated that the water content can even jeopardise the formation of the hydrogel, since when 90% w/w was used, no hydrogel formation was recorded by the rheometer after 42 h reaction.



**Figure 5.4.** Evolution of the storage ( $G'$ ) and loss ( $G''$ ) moduli for a representative crosslinking formation of **5** at 25 °C using different amounts of water.

Moreover, frequency sweep tests were conducted at room temperature to determine the stability of the obtained hydrogel system (Figure 5.5). Over the entire range of frequencies tested, the value of the storage modulus ( $G'$ ) remained constant at approximately  $2.3 \times 10^5$  Pa and  $1.0 \times 10^5$  Pa for the hydrogels with a water content of 70 and 53% respectively. Therefore, it was proved that the obtained waterborne hydrogels are indeed viscoelastic materials and stable within the tested frequency range.

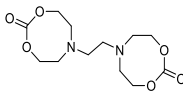
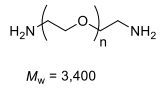
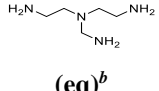


**Figure 5.5.** Frequency sweep test for hydrogel **5** using different amounts of water.

#### 5.2.4 Crosslinker-PEG diamine ratio influence

Subsequently the influence of the PEG diamine cross-linker ratio materials obtained by varying the ratios of PEG diamine and crosslinker was studied (Table 5.1).

**Table 5.1.** Synthesis of different PHU using different ratios of PEG diamine and TAEA.

Entry <sup>a</sup>	Compound	 (eq)	 (eq)	 (eq) <sup>b</sup>	Gel. time (min)
1	<b>6</b>	1	0.80	0.20	1780
2	<b>5</b>	1	0.60	0.40	690
3	<b>7</b>	1	0.40	0.60	200
4	<b>8</b>	1	0.20	0.80	Seconds

<sup>a</sup> Reaction conditions: 70% H<sub>2</sub>O w/w, room temperature. <sup>b</sup> 2/3 mmol of TAEA respect with eight-membered cyclic carbonate were used.

Unsurprisingly, faster gelation times were observed for samples with higher contents of cross-linker as the presence of a higher amount of TAEA units will statistically lead to the formation of a crosslinked material in a shorter period of time. In fact, gelation times range between 160 and 1750 min when the amount of

cross-linker decreases from 0.60 to 0.20 eq. (Figure 5.6). With regard to the moduli values registered, the sample with the highest amount of cross-linking measured *i.e* **7** (Table 5.1, entry 3), exhibited the lowest moduli value of all measured examples. This unexpected fact, can be attributed to the different reactivity ratios of the two different bis-amines present in the reaction media with respect to monomer **1**. According to the obtained data, it seems that, tris-amine has a higher reactivity compared to the PEG-diamine, therefore this higher reactivity leads to the vitrification of the material and avoids the reaction of the less reactive PEG-diamine, thus the material obtained is a non-homogeneous hydrogel. This same effect is expected for the case of **8** (Table 5.1, entry 4), which displays the higher amount of cross-linker (0.80 eq), gelation was observed within seconds, fact that avoid rheological characterization for this sample.

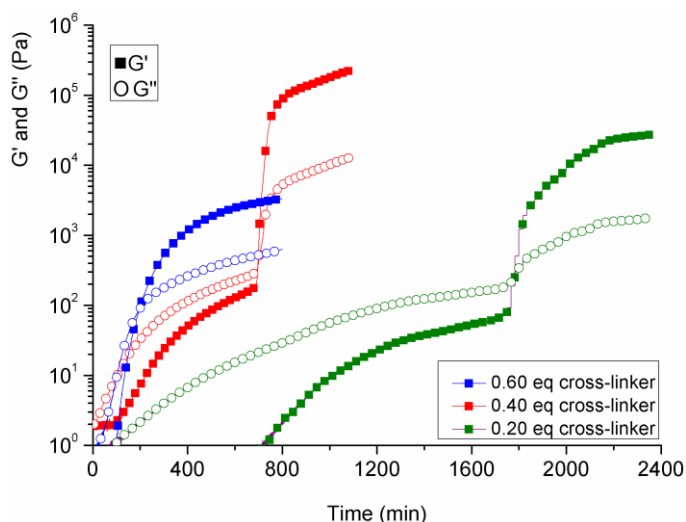


**Figure 5.6.** Evolution of the cross-linking reaction for hydrogel formulations **5**, **6** and **7**.

### 5.2.5 Temperature influence study

Temperature influence on the gelation process was studied for the formulation **5** which was prepared using 8MCC/PEG 3,400/TAEA (1.0/0.60/0.40 eq) with 70% w/w of H<sub>2</sub>O. The evolution of  $G'$  and  $G''$  with time was tracked at different temperatures. As expected, higher temperatures lead to shorter gelation time (780 min at 15 °C to 620 min at 37 °C). No gel formation was registered at 4 °C after 33 hours of reaction as no cross-over between  $G'$  and  $G''$  was observed. This



formulation was subsequently heated up to 37 °C and a gel was satisfactory obtained after 1200 min (Figure 5.7). Since hydrogels can be used for biomedical applications and poly(hydroxyurethanes) hydrogels are indeed biocompatible, the performed experiment illustrates the potential possibility of preparing these materials, store them in a fridge and whenever is required they can be injected and formed without jeopardising its formation and properties.

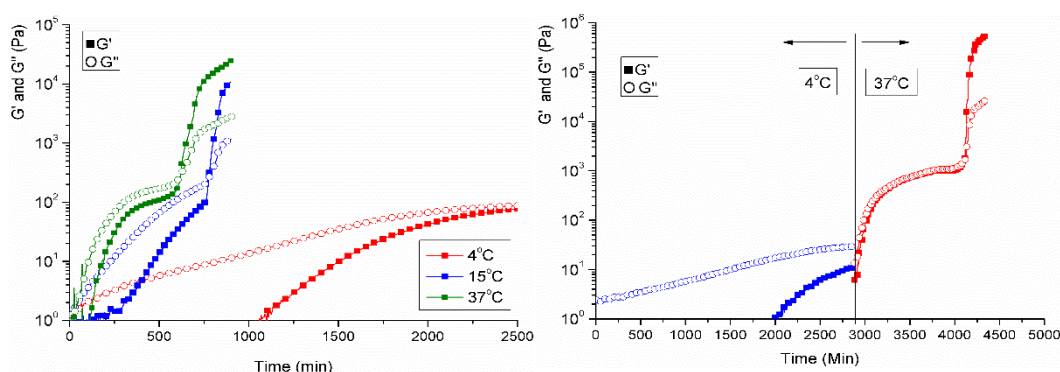


**Figure 5.7.** Modulus evolution at different temperatures for hydrogel **5** formulation.

### 5.2.6 Thermo responsive behaviour and 3D printing

Temperature sweep experiments were conducted to investigate the potential thermo-responsive behaviour of the materials previously prepared (Figure 5.8). Obtained hydrogels didn't showed any thermal response to temperature until several heating-cooling cycles on the rheometer plate were performed (*i.e.* 30 minutes at 60 °C). However, slightly increases, around one order of magnitude, were observed during the curing process.

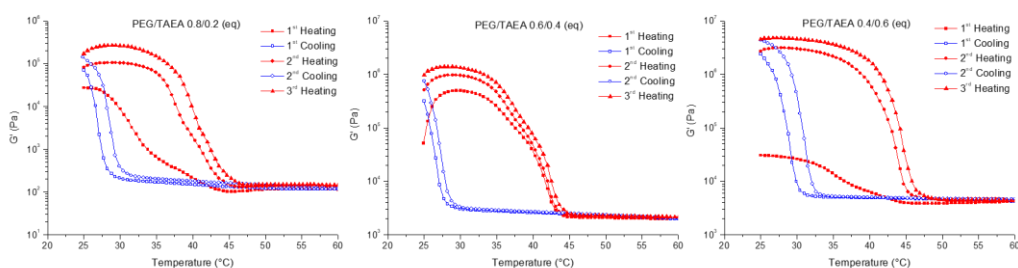


**Figure 5.8.** Temperature sweep-experiments for formulations **6**, **7** and **8**.

Those increases can be attributed to two main reasons; a) inevitable water evaporation from the inner hydrogel on the rheometer plate, b) unfinished polymerization as there are presumably have two different reactivity ratios for the two different amines present in our system, the curing process favours the completion of the reaction. The sequential increments of modulus when the temperature sweep experiments were performed reveal the importance of the water content in the hydrogel to observe the mentioned thermo-responsive behaviour. Since it is not possible to avoid, not quantify how much water is evaporated in the rheometer plate DSC experiments were conducted to study the effect of water in the thermo-responsive properties of the synthesised hydrogels (Figure 5.9). DSC experiment revealed that samples with a water content higher than 40% approximately didn't have any remarkable thermal transition in the rheometer tested range, *i.e* 25-60 °C. Nevertheless, while the water content decreased as a consequence of the heating-cooling cycles on the DSC experiment, both endothermic peaks appeared in the temperature ranges where the modulus decay and increase were observed in the rheological temperature sweep experiments. These thermal transitions are correlated to the melting (Figure 5.9 (a)) and the crystallization (Figure 5.9 (b)) of PEG domains present in the viscoelastic material. To the best of our knowledge, a certain amount of water is needed to solvate the hydrophilic PEG domains of the hydrogel. Below this critical amount, PEG domains are able to crystallise, and the registered melting and crystallization of these PEG domains are responsible of the thermo-responsive behaviour observed. Further to determine the critical amount of water for crystallization, the normalised melting enthalpy was plotted against the water % content (Figure 5.9 (c)) and it was determined that PEG domains start to crystallise in materials containing 15-20 wt% of H<sub>2</sub>O.

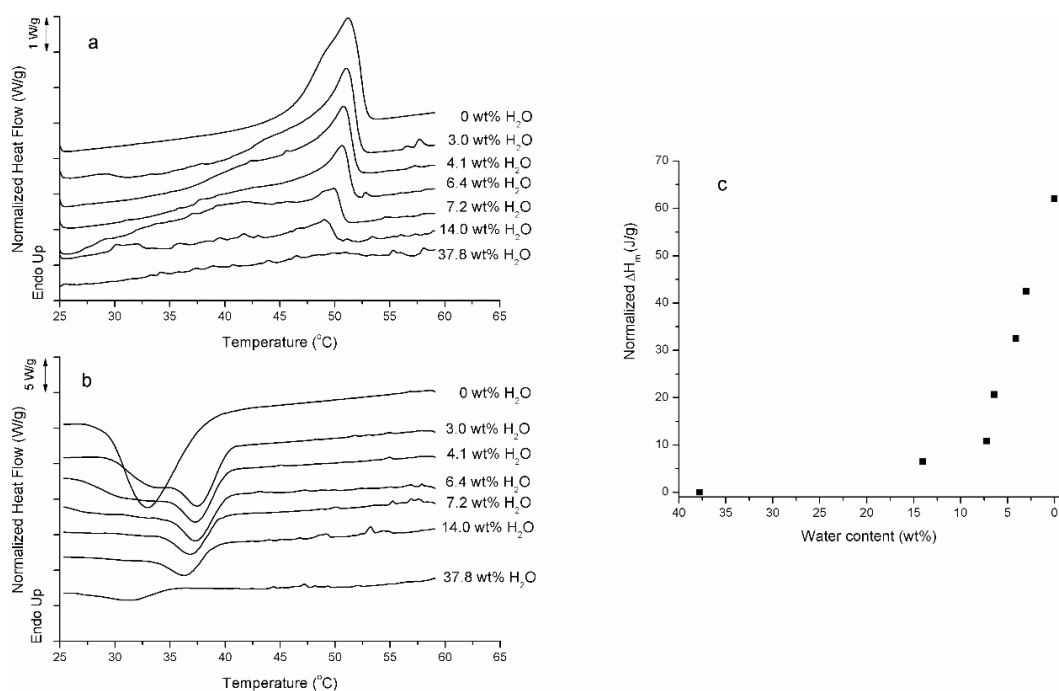


**Figure 5.9.** DSC heating (a) and cooling (b) scans for the hydrogel formulation **5** with different water contents. Evolution of the melting enthalpy as a function of the water content in the sample (c).

### 5.2.7 3D printing

As a consequence of the thermo-responsive behaviour of the poly(hydroxy urethanes) described before, the possibility of printing 3D scaffolds was investigated. Hydrogel formulation **5** was placed in a 3D printer cartridge after performing the same heating treatment that was depicted by the rheological studies. Then, the sample was passed through the printing needle and a printed hydrogel scaffold was successfully obtained (Figure 5.10). The modulus decay around 60 °C allows the material to flow through the printing needle, the subsequently cooling after the printing process provides robustness enough to the material to remain as a stable scaffold.

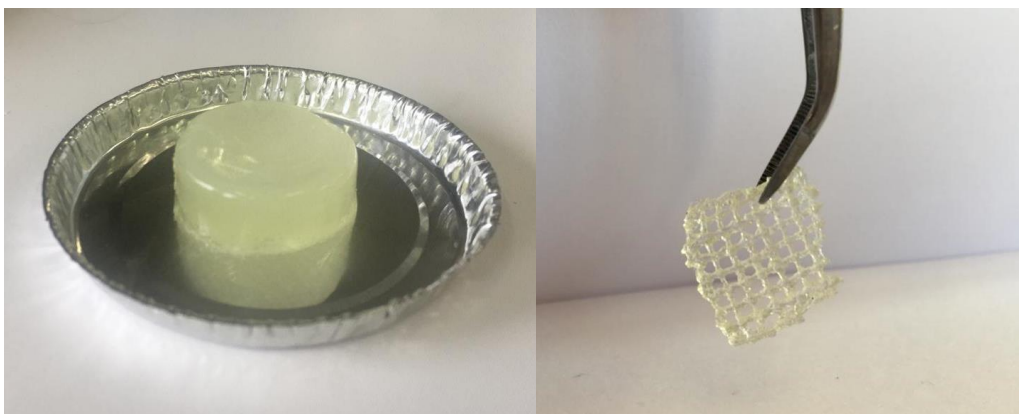


**Figure 5.10.** Freshly prepared hydrogel **5** (*left*) and 3D printed scaffolds after the heat treatment (*right*).

### 5.3 Conclusions

For the first time, waterborne non-isocyanate thermo-responsive poly(hydroxy urethanes) hydrogels were synthesised under mild conditions. Using an eight-membered cyclic carbonate, which was prepared throughout a free phosgene ring-closing procedure and subsequently polymerised through a step-growth polymerization process using a PEG diamine and a tris-amine as a cross-linker. Tuning the ratios of cross-linker and PEG diamine changed the mechanical properties of the materials obtained. The presence of PEG moieties along with the amount of water present on the hydrogel rendered thermo-responsive materials which were found to be printable as a consequence of the decay of the moduli when they were heated up and the increase of the moduli when they were cooled down.

### 5.4 References

1. E. A. Appel, J. del Barrio, X. J. Loh and O. A. Scherman, *Chem. Soc. Rev.*, 2012, **41**, 6195-6214.
2. A. S. Hoffmann, *Adv. Drug Deliv. Rev.*, 2002, **54**, 3-12.
3. H. Zhang, M. Yang, Q. Luan, H. Tang, F. Huang, X. Xiang, C. Yang and Y. Bao, *J. Agric. Food Chem.*, 2017, **65**, 3785-3791.
4. B. V. Slaughter, S. S. Khurshid, O. Z. Fisher, A. Khademhosseini and N. A. Peppas, *Adv. Mater.*, 2009, **21**, 3307-3329.

5. Q. Yong and K. Park, *Adv. Drug Deliv. Rev.*, 2001, **53**, 321-339.
6. V. X. Truong, M. P. Ablett, S. M. Richardson, J. A. Hoyland and A. P. Dove, *J. Am. Chem. Soc.*, 2015, **137**, 1618-1622.
7. J. L. Drury and D. J. Mooney, *Biomaterials*, 2003, **24**, 4337-4351.
8. J. Zhu, *Biomaterials*, 2010, **31**, 4639-4656.
9. S. Van Vlierberghe, P. Dubruel and E. Schacht, *Biomacromolecules*, 2011, **12**, 1387-1408.
10. P. C. Nicolson and J. Vogt, *Biomaterials*, 2001, **22**, 3273-3283.
11. M. Kawalec, A. P. Dove, L. Mespouille and P. Dubois, *Polym. Chem.*, 2013, **4**, 1260-1270.
12. T. Yuan, L. Zhang, K. Li, H. Fan, Y. Fan, J. Liang and X. Zhang, *J. Biomed. Mater. Res. B Appl. Biomater.*, 2014, **102**, 337-344.
13. V. X. Truong, M. P. Ablett, H. T. J. Gilbert, J. Bowen, S. M. Richardson, J. A. Hoyland and A. P. Dove, *Biomater. Sci.*, 2014, **2**, 167-175.
14. H. Tan, C. R. Chu, K. A. Payne and K. G. Marra, *Biomaterials*, 2009, **30**, 2499-2506.
15. A. G. Filatova, I. O. Volkov, N. I. Krikunova, T. A. Misharina and R. V. Golovnya, *Russ. Chem. Bull.*, 2000, **49**, 314-316.
16. A. D. Augst, H. J. Kong and D. J. Mooney, *Macromol. Biosci.*, 2006, **6**, 623-633.
17. Y. Ling, J. Rubin, Y. Deng, C. Huang, U. Demirci, J. M. Karp and A. Khademhosseini, *Lab Chip*, 2007, **7**, 756-762.
18. T. Jungst, W. Smolan, K. Schacht, T. Scheibel and J. Groll, *Chem. Rev.*, 2016, **116**, 1496-1539.
19. A. J. Bloodworth and A. G. Davies, *J. Chem. Soc.*, 1965, **0**, 5238-5244.
20. E. Delebecq, J. P. Pascault, B. Boutevin and F. Ganachaud, *Chem Rev*, 2013, **113**, 80-118.
21. J. H. Saunders and R. J. Slocombe, *Chem. Rev.*, 1948, **43**, 203-218.
22. M. S. Kathalewar, P. B. Joshi, A. S. Sabnis and V. C. Malshe, *RSC Adv.*, 2013, **3**.
23. H. Sardon, A. Pascual, D. Mecerreyes, D. Taton, H. Cramail and J. L. Hedrick, *Macromolecules*, 2015, **48**, 3153-3165.
24. O. Kreye, H. Mutlu and M. A. R. Meier, *Green Chem.*, 2013, **15**.

25. L. Maisonneuve, O. Lamarzelle, E. Rix, E. Grau and H. Cramail, *Chem. Rev.*, 2015, **115**, 12407-12439.
26. M. Yoshida and M. Ihara, *Chem. Eur. J.*, 2004, **10**, 2887-2893.
27. C. Martín, G. Fiorani and A. W. Kleij, *ACS Catal.*, 2015, **5**, 1353-1370.
28. M. Alves, B. Grignard, R. Mereau, C. Jerome, T. Tassaing and C. Detrembleur, *Catal. Sci. Technol.*, 2017, **7**, 2651-2684.
29. A. Yuen, A. Bossion, E. Gómez-Bengoa, F. Ruipérez, M. Isik, J. L. Hedrick, D. Mecerreyes, Y. Y. Yang and H. Sardon, *Polym. Chem.*, 2016, **7**, 2105-2111.
30. S. Gennen, B. Grignard, J. M. Thomassin, B. Gilbert, B. Vertruyen, C. Jerome and C. Detrembleur, *Eur. Polym. J.*, 2016, **84**, 849-862.
31. N. B. Graham, M. Zulfiqar, N. E. Nwachukut and A. Rashi, *Polymer*, 1989, **30**, 528-533.
32. Y. Yuan, H. Zhang, N. Zhang, Q. Sun and X. Cao, *J. Therm. Anal. Calorim.*, 2016, **126**, 699-708.
33. M. Tryznowski, A. Świdarska, Z. Żółek-Tryznowska, T. Gołofit and P. G. Parzuchowski, *Polymer*, 2015, **80**, 228-236.

## **6. Experimental**

## 6.1 Materials

All commercially available materials were purchased from Sigma-Aldrich, Alfa Aesar or Acros Organics and used as received unless otherwise indicated. CO<sub>2</sub> was purchased from Air Liquide (99.995%). DBU was dried over CaH<sub>2</sub>, distilled under reduced pressure and stored under an inert atmosphere of N<sub>2</sub>. Acetonitrile was dried over 3 Å molecular sieves and stored under an inert atmosphere of N<sub>2</sub>. Pyrrolidine and piperidine were dried over CaH<sub>2</sub>, distilled under reduced pressure and stored under an inert atmosphere of N<sub>2</sub>. Tris(2-aminoethyl)amine was stored in a glovebox as is moisture and CO<sub>2</sub> sensitive. 1,4-butanodiamine and 1,6-hexamethylenediamine were purified *via* sublimation and stored under N<sub>2</sub>.

## 6.2 Instrumentation

NMR spectra were recorded on a Bruker Avance 300 MHz spectrometer or Bruker Avance III HD 300 or 400 MHz spectrometer. Chemical shifts are reported in parts per million (ppm) and referenced to the residual solvent signal (CDCl<sub>3</sub>: <sup>1</sup>H,  $\delta$  = 7.26 ppm, <sup>13</sup>C,  $\delta$  = 77.2 ppm, DMSO: <sup>1</sup>H,  $\delta$  = 2.50 ppm, <sup>13</sup>C,  $\delta$  = 39.5 ppm, TMS: <sup>1</sup>H,  $\delta$  = 0.00 ppm). Multiplicities are reported as s = singlet, brs = broad singlet, d = doublet, dd = doublet of doublets, dt = doublet of triplets, ddd = doublet of doublet of doublets, ddt = doublet of doublet of triplets, t = triplet, tt = triplet of triplets q = quartet, quint = quintet, m = multiplet. Multiplicity is followed by coupling constant (*J*) in Hz and integration. CO<sub>2</sub> cycloaddition reactions were performed in a Paar Series 5500 HP Compact Reactor. Mass spectra were recorded on a Bruker HCT + ESI spectrometer. Infrared spectra were recorded (neat) on a Perkin Elmer Spectrum 100 FT-IR Spectrometer. Elemental analysis was performed in duplicate by Warwick Analytical Services. Size exclusion chromatography (SEC) was conducted on systems composed of a Varian 390-LC-Multi detector suite fitted with differential refractive index (RI), light scattering, and ultraviolet detectors, equipped with a guard column (Varian Polymer Laboratories PLGel 5  $\mu$ M, 50  $\times$  7.5 mm) and two mixed D columns (Varian Polymer Laboratories PLGel 5  $\mu$ M, 300  $\times$  7.5 mm). The mobile phase dimethylformamide (DMF), with a flow rate of 1.0 mL min<sup>-1</sup>. SEC samples were calibrated against either Varian Polymer Laboratories Easi-Vials linear poly(styrene) standards (162 – 2.4  $\times$  10<sup>5</sup> g mol<sup>-1</sup>) (DMF SEC).



Rheological testing was carried out using an Anton Parr MCR 302 rheometer equipped with a parallel plate configuration with a diameter of 25 mm. A peltier system was used to control the temperature at throughout the study. Data was analysed using RheoCompass software. The crystallization process of the thermo-responsive hydrogel samples was measured by differential scanning calorimetry (DSC) in a Pyris 1 DSC (Perkin Elmer) equipped with an intracooler at a heating and cooling rate of 10 °C/min. Samples were prepared using standard aluminium capsules. The printing process was carried out in a 3D-Bioplotter (Developer Series, EnvisionTEC) and the printing geometries were originally designed in Solidworks 2016 x 64 Editor.

## 6.3 Experimental protocols for Chapter 2

### 6.3.1 General procedure for the synthesis of [HDBU]X X = Halide salts

Ammonium halide (6.69 mmol) was dissolved in MeOH (6.7 mL), then DBU (6.69 mmol) was added. A reflux condenser was attached to the flask and the mixture was heated up to reflux overnight. Solvent was evaporated and the crude was recrystallized from CH<sub>2</sub>Cl<sub>2</sub>/Hexane. A solid was obtained.

**2,3,4,6,7,8,9,10-octahydropyrimido[1,2-*a*]azepin-1-ium chloride [HDBU]Cl (1).** A white solid was obtained [HDBU]Cl (1.199 g, 6.36 mmol, 95%). Characterization data was in agreement with those reported previously.<sup>1</sup> **<sup>1</sup>H NMR** (300 MHz, CDCl<sub>3</sub>)  $\delta$  11.62 (bs, 1H, N-*H*), 3.53-3.46 (m, 6H, NH-CH<sub>2</sub>-CH<sub>2</sub>-CH<sub>2</sub>-N, C-(CH<sub>2</sub>)<sub>5</sub>-CH<sub>2</sub>-N, CH<sub>2</sub>-NH), 3.01 (m, 2H, CH<sub>2</sub>-C), 2.05-2.01 (quint, 2H, <sup>3</sup>*J*<sub>H-H</sub> = 5.6 Hz, CH<sub>2</sub>-CH<sub>2</sub>-NH), 1.77-1.70 (m, 6H, CH<sub>2</sub>-CH<sub>2</sub>-CH<sub>2</sub>). **<sup>13</sup>C APT NMR** (75 MHz, CDCl<sub>3</sub>)  $\delta$  166.2 (C=N), 54.5 (C-(CH<sub>2</sub>)<sub>5</sub>-CH<sub>2</sub>-N), 48.8 (NH-CH<sub>2</sub>-CH<sub>2</sub>-CH<sub>2</sub>-N), 37.9 (CH<sub>2</sub>-NH), 32.2 (CH<sub>2</sub>-C), 29.0 (C-(CH<sub>2</sub>)<sub>3</sub>-CH<sub>2</sub>-CH<sub>2</sub>-N), 26.8 (CH<sub>2</sub>-CH<sub>2</sub>-C), 24.0 (C-(CH<sub>2</sub>)<sub>2</sub>-CH<sub>2</sub>-CH<sub>2</sub>-CH<sub>2</sub>-N), 19.5 (CH<sub>2</sub>-CH<sub>2</sub>-NH).

**2,3,4,6,7,8,9,10-octahydropyrimido[1,2-*a*]azepin-1-ium bromide [HDBU]Br (2).** A white solid was obtained [HDBU]Br (1.325 g, 5.55 mmol, 83%). Characterization data was in agreement with those reported previously.<sup>2</sup> **<sup>1</sup>H NMR** (300 MHz, CDCl<sub>3</sub>)  $\delta$  11.34 (bs, 1H, N-*H*), 3.54-3.42 (m, 6H, NH-CH<sub>2</sub>-CH<sub>2</sub>-CH<sub>2</sub>-N, C-(CH<sub>2</sub>)<sub>5</sub>-CH<sub>2</sub>-N, CH<sub>2</sub>-NH) 3.00 (m, 2H, CH<sub>2</sub>-C), 2.07-1.99 (quint, 2H, <sup>3</sup>*J*<sub>H-H</sub> = 5.9 Hz, CH<sub>2</sub>-CH<sub>2</sub>-NH), 1.77-1.69 (m, 6H, CH<sub>2</sub>-CH<sub>2</sub>-CH<sub>2</sub>). **<sup>13</sup>C APT NMR** (75

MHz, CDCl<sub>3</sub>)  $\delta$  166.4 (C=N), 54.6 (C-(CH<sub>2</sub>)<sub>5</sub>-CH<sub>2</sub>-N), 48.9 (NH-CH<sub>2</sub>-CH<sub>2</sub>-CH<sub>2</sub>-N), 38.0 (CH<sub>2</sub>-NH), 32.3 (CH<sub>2</sub>-C), 29.1 (C-(CH<sub>2</sub>)<sub>3</sub>-CH<sub>2</sub>-CH<sub>2</sub>-N), 27.0 (CH<sub>2</sub>-CH<sub>2</sub>-C), 24.2 (C-(CH<sub>2</sub>)<sub>2</sub>-CH<sub>2</sub>-CH<sub>2</sub>-CH<sub>2</sub>-N), 19.7 (CH<sub>2</sub>-CH<sub>2</sub>-NH).

**2,3,4,6,7,8,9,10-octahydropyrimido[1,2-*a*]azepin-1-ium iodide [HDBU]I (3).** A yellow solid was obtained [HDBU]I (1.818 g, 6.49 mmol, 97%). Characterization data was in agreement with those reported previously.<sup>3</sup> **<sup>1</sup>H NMR** (300 MHz, CDCl<sub>3</sub>)  $\delta$  8.46 (bs, 1H, N-*H*), 3.57-3.53 (m, 4H, NH-CH<sub>2</sub>-CH<sub>2</sub>-CH<sub>2</sub>-N, C-(CH<sub>2</sub>)<sub>5</sub>-CH<sub>2</sub>-N), 3.40-3.35 (broad quint, 2H, CH<sub>2</sub>-NH), 2.93-2.90 (m, 2H, CH<sub>2</sub>-C), 2.06-1.99 (quint, 2H, <sup>3</sup>*J*<sub>H-H</sub> = 5.9 Hz, CH<sub>2</sub>-CH<sub>2</sub>-NH), 1.79-1.73 (m, 6H, CH<sub>2</sub>-CH<sub>2</sub>-CH<sub>2</sub>). **<sup>13</sup>C APT NMR** (75 MHz, CDCl<sub>3</sub>)  $\delta$  166.0 (C=N), 54.8 (C-(CH<sub>2</sub>)<sub>5</sub>-CH<sub>2</sub>-N), 48.9 (NH-CH<sub>2</sub>-CH<sub>2</sub>-CH<sub>2</sub>-N), 37.7 (CH<sub>2</sub>-NH), 32.7 (CH<sub>2</sub>-C), 28.7 (C-(CH<sub>2</sub>)<sub>3</sub>-CH<sub>2</sub>-CH<sub>2</sub>-N), 26.5 (CH<sub>2</sub>-CH<sub>2</sub>-C), 23.7 (C-(CH<sub>2</sub>)<sub>2</sub>-CH<sub>2</sub>-CH<sub>2</sub>-CH<sub>2</sub>-N), 19.2 (CH<sub>2</sub>-CH<sub>2</sub>-NH).

### 6.3.2 General procedure for the synthesis of [HDBU]X (X = BF<sub>4</sub>, PhCO<sub>2</sub>, MsO, TfO, TsO) salts

In a round bottom flask, DBU (6.69 mmol) was dissolved in MeCN (6.7 mL). Stoichiometric amount of H-X (6.69 mmol) was added dropwise to the DBU solution at 0 °C. Once addition was finished the mixture was stirred overnight at room temperature. Liquors were evaporated under vacuum to afford a solid which was recrystallised from CH<sub>2</sub>Cl<sub>2</sub>/Hexane. In some examples a colourless oil was obtained and used without further purification.

**2,3,4,6,7,8,9,10-octahydropyrimido[1,2-*a*]azepin-1-ium tetrafluoroborate [HDBU]BF<sub>4</sub> (4).** A pale brown solid was obtained [HDBU]BF<sub>4</sub> (1.606 g, 6.69 mmol, 100%). Characterization data was in agreement with those reported previously.<sup>4</sup> **<sup>1</sup>H NMR** (300 MHz, CDCl<sub>3</sub>)  $\delta$  8.18 (bs, 1H, N-*H*), 3.57-3.51 (m, 4H, NH-CH<sub>2</sub>-CH<sub>2</sub>-CH<sub>2</sub>-N, C-(CH<sub>2</sub>)<sub>5</sub>-CH<sub>2</sub>-N), 3.45 (bs, 2H, CH<sub>2</sub>-NH), 2.71 (bs, 2H, CH<sub>2</sub>-C), 2.07 (m, 2H, CH<sub>2</sub>-CH<sub>2</sub>-NH), 1.77 (m, 6H, CH<sub>2</sub>-CH<sub>2</sub>-CH<sub>2</sub>). **<sup>13</sup>C APT NMR** (75 MHz, CDCl<sub>3</sub>)  $\delta$  166.4 (C=N), 54.8 (C-(CH<sub>2</sub>)<sub>5</sub>-CH<sub>2</sub>-N), 48.7 (NH-CH<sub>2</sub>-CH<sub>2</sub>-CH<sub>2</sub>-N), 38.6 (CH<sub>2</sub>-NH), 33.2 (CH<sub>2</sub>-C), 28.9 (C-(CH<sub>2</sub>)<sub>3</sub>-CH<sub>2</sub>-CH<sub>2</sub>-N), 26.4 (CH<sub>2</sub>-CH<sub>2</sub>-C), 23.7 (C-(CH<sub>2</sub>)<sub>2</sub>-CH<sub>2</sub>-CH<sub>2</sub>-CH<sub>2</sub>-N), 19.3 (CH<sub>2</sub>-CH<sub>2</sub>-NH).

**2,3,4,6,7,8,9,10-octahydropyrimido[1,2-*a*]azepin-1-ium benzoate [HDBU]PhCO<sub>2</sub> (5).** A white solid was obtained [HDBU]PhCO<sub>2</sub> (1.450 g, 5.28

mmol, 79%). Characterization data was in agreement with those reported previously.<sup>5</sup> **<sup>1</sup>H NMR** (300 MHz, CDCl<sub>3</sub>)  $\delta$  8.09-8.06 (m, 2H, H<sup>Ar</sup>), 7.34-7.26 (m, 3H, H<sup>Ar</sup>), 3.52 (t, 2H, <sup>3</sup>J<sub>H-H</sub> = 5.8 Hz, CH<sub>2</sub>-NH), 3.44-3.38 (m, 4H, NH-CH<sub>2</sub>-CH<sub>2</sub>-CH<sub>2</sub>-N, C-(CH<sub>2</sub>)<sub>5</sub>-CH<sub>2</sub>-N), 2.97-2.94 (m, 2H, CH<sub>2</sub>-C), 2.01 (quintet, 2H, <sup>3</sup>J<sub>H-H</sub> = 5.9 Hz, CH<sub>2</sub>-CH<sub>2</sub>-NH), 1.78-1.66 (m, 6H, CH<sub>2</sub>-CH<sub>2</sub>-CH<sub>2</sub>). **<sup>13</sup>C APT NMR** (75 MHz, CDCl<sub>3</sub>)  $\delta$  166.2 (C=N), 162.4 (Ph-COO), 138.7 (C<sup>ipso</sup>), 129.6 (C<sup>Ar</sup>), 129.5 (C<sup>Ar</sup>), 127.6 (C<sup>Ar</sup>), 54.2 (C-(CH<sub>2</sub>)<sub>5</sub>-CH<sub>2</sub>-N), 48.8 (NH-CH<sub>2</sub>-CH<sub>2</sub>-CH<sub>2</sub>-N), 38.2 (CH<sub>2</sub>-NH), 33.2 (CH<sub>2</sub>-C), 29.3 (C-(CH<sub>2</sub>)<sub>3</sub>-CH<sub>2</sub>-CH<sub>2</sub>-N), 27.2 (CH<sub>2</sub>-CH<sub>2</sub>-C), 24.4 (C-(CH<sub>2</sub>)<sub>2</sub>-CH<sub>2</sub>-CH<sub>2</sub>-N), 19.9 (CH<sub>2</sub>-CH<sub>2</sub>-NH).

**2,3,4,6,7,8,9,10-octahydropyrimido[1,2-*a*]azepin-1-ium methanesulfonate [HDBU]MsO (6).** A colourless oil was obtained [HDBU]MsO (1.113 g, 4.48 mmol, 67%). Characterization data was in agreement with those reported previously.<sup>6</sup> **<sup>1</sup>H NMR** (300 MHz, CDCl<sub>3</sub>)  $\delta$  10.34 (bs, 1H, N-*H*), 3.53-3.43 (m, 6H, NH-CH<sub>2</sub>-CH<sub>2</sub>-CH<sub>2</sub>-N, C-(CH<sub>2</sub>)<sub>5</sub>-CH<sub>2</sub>-N, CH<sub>2</sub>-NH), 2.82 (bs, 2H, CH<sub>2</sub>-C), 2.75 (s, 3H, CH<sub>3</sub>-SO<sub>3</sub>), 2.06-1.99 (quint, 2H, <sup>3</sup>J<sub>H-H</sub> = 5.9 Hz, CH<sub>2</sub>-CH<sub>2</sub>-NH), 1.76-1.68 (m, 6H, CH<sub>2</sub>-CH<sub>2</sub>-CH<sub>2</sub>). **<sup>13</sup>C APT NMR** (75 MHz, CDCl<sub>3</sub>)  $\delta$  166.5 (C=N), 54.6 (C-(CH<sub>2</sub>)<sub>5</sub>-CH<sub>2</sub>-N), 48.8 (NH-CH<sub>2</sub>-CH<sub>2</sub>-CH<sub>2</sub>-N), 39.5 (CH<sub>3</sub>), 38.3 (CH<sub>2</sub>-NH), 32.7 (CH<sub>2</sub>-C), 29.1 (C-(CH<sub>2</sub>)<sub>3</sub>-CH<sub>2</sub>-CH<sub>2</sub>-N), 26.9 (CH<sub>2</sub>-CH<sub>2</sub>-C), 24.1 (C-(CH<sub>2</sub>)<sub>2</sub>-CH<sub>2</sub>-CH<sub>2</sub>-N), 19.6 (CH<sub>2</sub>-CH<sub>2</sub>-NH).

**2,3,4,6,7,8,9,10-octahydropyrimido[1,2-*a*]azepin-1-ium trifluoromethanesulfonate [HDBU]TfO (7).** A colourless oil was obtained [HDBU]TfO (1.537 g, 5.08 mmol, 76 %). Characterization data was in agreement with those reported previously.<sup>7</sup> **<sup>1</sup>H NMR** (300 MHz, CDCl<sub>3</sub>)  $\delta$  11.29 (bs, 1H, N-*H*), 3.52-3.39 (m, 6H, NH-CH<sub>2</sub>-CH<sub>2</sub>-CH<sub>2</sub>-N, C-(CH<sub>2</sub>)<sub>5</sub>-CH<sub>2</sub>-N, CH<sub>2</sub>-NH), 2.81-2.77 (m, 2H, CH<sub>2</sub>-C), 2.06-1.98 (quint, 2H, <sup>3</sup>J<sub>H-H</sub> = 5.9 Hz, CH<sub>2</sub>-CH<sub>2</sub>-NH), 1.75-1.67 (m, 6H, CH<sub>2</sub>-CH<sub>2</sub>-CH<sub>2</sub>). **<sup>13</sup>C APT NMR** (75 MHz, CDCl<sub>3</sub>)  $\delta$  162.5 (C=N), 149.0 (CF<sub>3</sub>), 54.5 (C-(CH<sub>2</sub>)<sub>5</sub>-CH<sub>2</sub>-N), 48.8 (NH-CH<sub>2</sub>-CH<sub>2</sub>-CH<sub>2</sub>-N), 38.2 (CH<sub>2</sub>-NH), 32.5 (CH<sub>2</sub>-C), 29.1 (C-(CH<sub>2</sub>)<sub>3</sub>-CH<sub>2</sub>-CH<sub>2</sub>-N), 26.9 (CH<sub>2</sub>-CH<sub>2</sub>-C), 24.1 (C-(CH<sub>2</sub>)<sub>2</sub>-CH<sub>2</sub>-CH<sub>2</sub>-N), 19.6 (CH<sub>2</sub>-CH<sub>2</sub>-NH).

**2,3,4,6,7,8,9,10-octahydropyrimido[1,2-*a*]azepin-1-ium 4-methylbenzenesulfonate [HDBU]TsO (8).** A colourless oil was obtained [HDBU]TsO (1.606 g, 4.95 mmol, 74%). Characterization data was in agreement with those reported previously.<sup>5</sup> **<sup>1</sup>H NMR** (300 MHz, CDCl<sub>3</sub>)  $\delta$  7.77 (d, 2H, <sup>3</sup>J<sub>H-H</sub>

= 8.0 Hz, H<sup>Ar</sup>), 7.14 (d, 2H, <sup>3</sup>J<sub>H-H</sub> = 8.0 Hz, H<sup>Ar</sup>), 3.50-3.41 (m, 6H, NH-CH<sub>2</sub>-CH<sub>2</sub>-CH<sub>2</sub>-N, C-(CH<sub>2</sub>)<sub>5</sub>-CH<sub>2</sub>-N, CH<sub>2</sub>-NH), 2.82-2.80 (m, 2H, CH<sub>2</sub>-C), 2.33 (s, 3H, CH<sub>3</sub>-C<sup>ipso</sup>), 2.01 (quintet, 2H, <sup>3</sup>J<sub>H-H</sub> = 5.9 Hz, CH<sub>2</sub>-CH<sub>2</sub>-NH), 1.72-1.64 (m, 6H, CH<sub>2</sub>-CH<sub>2</sub>-CH<sub>2</sub>). <sup>13</sup>C APT NMR (75 MHz, CDCl<sub>3</sub>) δ 166.4 (C=N), 143.4 (C<sup>ipso</sup>-SO<sub>3</sub>), 139.5 (C<sup>ipso</sup>-CH<sub>3</sub>), 128.7 (C<sup>Ar</sup>), 126.0 (C<sup>Ar</sup>), 54.5 (C-(CH<sub>2</sub>)<sub>5</sub>-CH<sub>2</sub>-N), 48.7 (NH-CH<sub>2</sub>-CH<sub>2</sub>-CH<sub>2</sub>-N), 38.4 (CH<sub>2</sub>-NH), 32.7 (CH<sub>2</sub>-C), 29.0 (C-(CH<sub>2</sub>)<sub>3</sub>-CH<sub>2</sub>-CH<sub>2</sub>-N), 26.8 (CH<sub>2</sub>-CH<sub>2</sub>-C), 24.1 (C-(CH<sub>2</sub>)<sub>2</sub>-CH<sub>2</sub>-CH<sub>2</sub>-CH<sub>2</sub>-N), 21.4 (C<sup>ipso</sup>-CH<sub>3</sub>), 19.6 (CH<sub>2</sub>-CH<sub>2</sub>-NH).

### 6.3.3 General procedure for the synthesis of [R-DBU]X salts

Under inert atmosphere, a solution of alkyl or aryl halide (6.69 mmol) dissolved in dry MeCN (6.7 mL) was added by cannula transfer to DBU (6.69 mmol) dissolved in dry MeCN (6.7 mL) at 0 °C. Once addition was finished the mixture was stirred overnight at room temperature. Progression of the reaction was tracked by TLC. Upon completion, the solvent was removed under vacuum to afford a solid which was recrystallised from CH<sub>2</sub>Cl<sub>2</sub>/Hexane. In some examples, further purification was obtained by flash column chromatography.

**1-methyl-2,3,4,6,7,8,9,10-octahydropyrimido[1,2-*a*]azepin-1-ium iodide [Me-DBU]I (9).** A slightly yellow solid was obtained (1.102 g, 3.75 mmol, 56%). Characterization data was in agreement with those reported previously.<sup>8</sup> <sup>1</sup>H NMR (300 MHz, CDCl<sub>3</sub>) δ 3.69-3.61 (m, 6H, C=N-CH<sub>2</sub>-CH<sub>2</sub>-CH<sub>2</sub>-N, C-(CH<sub>2</sub>)<sub>5</sub>-CH<sub>2</sub>-N, CH<sub>2</sub>-N=C), 3.33 (s, 3H, CH<sub>3</sub>-N=C), 2.92-2.89 (m, 2H, CH<sub>2</sub>-C), 2.19 (quintet, 2H, <sup>3</sup>J<sub>H-H</sub> = 5.9 Hz, CH<sub>2</sub>-CH<sub>2</sub>-N), 1.85-1.75 (m, 6H, CH<sub>2</sub>-CH<sub>2</sub>-CH<sub>2</sub>). <sup>13</sup>C APT NMR (75 MHz, CDCl<sub>3</sub>) δ 167.0 (C=N), 55.8 (C-(CH<sub>2</sub>)<sub>5</sub>-CH<sub>2</sub>-N), 49.4 (C=N-CH<sub>2</sub>-CH<sub>2</sub>-CH<sub>2</sub>-N), 49.3 (CH<sub>2</sub>-N=C), 42.2 (CH<sub>3</sub>-N) 29.7 (CH<sub>2</sub>-C), 28.6 (C-(CH<sub>2</sub>)<sub>3</sub>-CH<sub>2</sub>-CH<sub>2</sub>-N), 26.3 (CH<sub>2</sub>-CH<sub>2</sub>-C), 22.4 (C-(CH<sub>2</sub>)<sub>2</sub>-CH<sub>2</sub>-CH<sub>2</sub>-CH<sub>2</sub>-N), 20.2 (CH<sub>2</sub>-CH<sub>2</sub>-N=C).

**1-ethyl-2,3,4,6,7,8,9,10-octahydropyrimido[1,2-*a*]azepin-1-ium iodide [Et-DBU]I (10).** Flash column chromatography (CH<sub>2</sub>Cl<sub>2</sub>:MeOH 19:1). A yellow solid was obtained (1.196 g, 3.88 mmol, 58%). <sup>1</sup>H NMR (400 MHz, CDCl<sub>3</sub>) δ 3.71-3.57 (m, 8H, C=N-CH<sub>2</sub>-CH<sub>2</sub>-CH<sub>2</sub>-N, C-(CH<sub>2</sub>)<sub>5</sub>-CH<sub>2</sub>-N, CH<sub>2</sub>-N=C, CH<sub>3</sub>-CH<sub>2</sub>-N), 2.90-2.88 (m, 2H, CH<sub>2</sub>-C), 2.19 (quintet, 2H, <sup>3</sup>J<sub>H-H</sub> = 6.0 Hz, CH<sub>2</sub>-CH<sub>2</sub>-N), 1.86-1.78 (m, 6H, CH<sub>2</sub>-CH<sub>2</sub>-CH<sub>2</sub>), 1.30 (t, 3H, <sup>3</sup>J<sub>H-H</sub> = 7.3 Hz, CH<sub>3</sub>). <sup>13</sup>C NMR (100 MHz, CDCl<sub>3</sub>)

$\delta$  166.4 (C=N), 55.8 (C-(CH<sub>2</sub>)<sub>5</sub>-CH<sub>2</sub>-N), 49.7 (C=N-CH<sub>2</sub>-CH<sub>2</sub>-CH<sub>2</sub>-N), 49.5 (CH<sub>2</sub>-N=C), 46.8 (CH<sub>3</sub>-CH<sub>2</sub>), 29.0 (CH<sub>2</sub>-C), 28.5 (CH<sub>2</sub>-CH<sub>2</sub>-N), 26.2 (CH<sub>2</sub>-CH<sub>2</sub>-C), 23.2 (C-(CH<sub>2</sub>)<sub>2</sub>-CH<sub>2</sub>-CH<sub>2</sub>-CH<sub>2</sub>-N), 20.3 (CH<sub>2</sub>-CH<sub>2</sub>-N=C), 14.1 (CH<sub>3</sub>). IR (max/cm<sup>-1</sup>) 2929 (CH<sub>2</sub>, m), 2848 (CH<sub>2</sub>, m), 1619 (C=N, s), 1328 (C-H, m), 1194 (C-N, m). HRMS (ESI-TOF) (m/z): [M]<sup>+</sup> calculated for C<sub>11</sub>H<sub>21</sub>N<sub>2</sub><sup>+</sup>, 181.1705; found 181.1703. Elemental analysis: Calculated for C<sub>11</sub>H<sub>21</sub>IN<sub>2</sub>, C, 42.87 %; H, 6.87 %; N, 9.09 %; found C, 42.71 %; H, 6.82 %; N, 9.02 %.

**1-hexyl-2,3,4,6,7,8,9,10-octahydropyrimido[1,2-a]azepin-1-ium bromide [CH<sub>3</sub>-(CH<sub>2</sub>)<sub>5</sub>-DBU]Br (11).** Flash column chromatography (CH<sub>2</sub>Cl<sub>2</sub>:MeOH 19:1). A white solid was obtained (1.210 g, 3.81 mmol, 57%). Characterization data was in agreement with those reported previously.<sup>9</sup> <sup>1</sup>H NMR (300 MHz, CDCl<sub>3</sub>)  $\delta$  3.76-3.62 (m, 6H, C=N-CH<sub>2</sub>-CH<sub>2</sub>-CH<sub>2</sub>-N, C-(CH<sub>2</sub>)<sub>5</sub>-CH<sub>2</sub>-N, CH<sub>2</sub>-N=C), 3.51 (t, 2H, <sup>3</sup>J<sub>H-H</sub> = 8.0 Hz, CH<sub>3</sub>-(CH<sub>2</sub>)<sub>4</sub>-CH<sub>2</sub>-N=C), 2.94-2.86 (m, 2H, CH<sub>2</sub>-C), 2.16 (quintet, 2H, <sup>3</sup>J<sub>H-H</sub> = 5.9 Hz, CH<sub>2</sub>-CH<sub>2</sub>-N) 1.84-1.74 (m, 6H, CH<sub>2</sub>-CH<sub>2</sub>-CH<sub>2</sub>), 1.67-1.54 (m, 2H, CH<sub>3</sub>-(CH<sub>2</sub>)<sub>3</sub>-CH<sub>2</sub>-CH<sub>2</sub>-N=C), 1.33-1.23, (m, 6H, CH<sub>2</sub>-CH<sub>2</sub>-CH<sub>2</sub>-CH<sub>3</sub>) 0.85 (t, 3H, <sup>3</sup>J<sub>H-H</sub> = 6.5 Hz, CH<sub>3</sub>). <sup>13</sup>C APT NMR (75 MHz, CDCl<sub>3</sub>)  $\delta$  166.6 (C=N), 55.7 (C-(CH<sub>2</sub>)<sub>5</sub>-CH<sub>2</sub>-N), 54.5 (C-(CH<sub>2</sub>)<sub>5</sub>-CH<sub>2</sub>-N), 49.6 (CH<sub>2</sub>-N=C), 47.5 (CH<sub>3</sub>-(CH<sub>2</sub>)<sub>4</sub>-CH<sub>2</sub>-N), 31.4 (CH<sub>2</sub>-C), 28.9 (CH<sub>3</sub>-(CH<sub>2</sub>)<sub>3</sub>-CH<sub>2</sub>-CH<sub>2</sub>-N), 28.8 (CH<sub>3</sub>-(CH<sub>2</sub>)<sub>2</sub>-CH<sub>2</sub>-(CH<sub>2</sub>)<sub>2</sub>-CH<sub>3</sub>), 28.6 (CH<sub>2</sub>-CH<sub>2</sub>-CH<sub>3</sub>), 26.3 (CH<sub>2</sub>-CH<sub>2</sub>-N), 26.2 (CH<sub>2</sub>-CH<sub>2</sub>-C), 23.3 (C-(CH<sub>2</sub>)<sub>2</sub>-CH<sub>2</sub>-CH<sub>2</sub>-CH<sub>2</sub>-N), 22.6 (CH<sub>2</sub>-CH<sub>3</sub>), 20.4 (CH<sub>2</sub>-CH<sub>2</sub>-N=C), 14.0 (CH<sub>3</sub>).

**1-benzyl-2,3,4,6,7,8,9,10-octahydropyrimido[1,2-a]azepin-1-ium iodide [Bn-DBU]I (12).** In a two-neck round bottom flask previously flame dried under high vacuum and refilled with N<sub>2</sub> three times, NaI (1.003 g, 6.69 mmol) was dissolved in 30 mL of acetone, then DBU (1 mL, 6.69 mmol) was added and finally benzyl bromide (0.80 mL, 6.69 mmol) dropwise. Just after benzyl bromide was added a white fine powder was precipitated. The mixture was stirred for 48 h at room temperature. The mixture was filtered in Buchner and the liquors were concentrated under vacuum to afford a yellow solid which was recrystallized from CH<sub>2</sub>Cl<sub>2</sub>/Hexane (841 mg, 1.34 mmol, 20%). Characterization data was in agreement with those reported previously.<sup>10</sup> <sup>1</sup>H NMR (300 MHz, CDCl<sub>3</sub>)  $\delta$  7.43-7.34 (m, 3H, H<sup>Ar</sup>), 7.21 (d, 2H, <sup>3</sup>J<sub>H-H</sub> = 7.2 Hz, H<sup>Ar</sup>), 4.84 (s, 2H, C<sup>ipso</sup>-CH<sub>2</sub>-N), 3.81-3.73 (m, 6H, C=N-CH<sub>2</sub>-CH<sub>2</sub>-CH<sub>2</sub>-N, C-(CH<sub>2</sub>)<sub>5</sub>-CH<sub>2</sub>-N, CH<sub>2</sub>-N=C), 2.94-2.91 (m, 2H, CH<sub>2</sub>-C), 2.25 (quintet, 2H, <sup>3</sup>J<sub>H-H</sub> = 5.9 Hz, CH<sub>2</sub>-CH<sub>2</sub>-N), 1.87-1.78 (m, 6H, CH<sub>2</sub>-CH<sub>2</sub>-CH<sub>2</sub>). <sup>13</sup>C APT NMR (75 MHz, CDCl<sub>3</sub>)  $\delta$  167.3 (C=N), 133.9 (C<sup>ipso</sup>),

129.3 (C<sup>Ar</sup>), 128.3 (C<sup>Ar</sup>), 126.3 (C<sup>Ar</sup>), 57.2 (C<sup>ipso</sup>-CH<sub>2</sub>), 56.0 (C-(CH<sub>2</sub>)<sub>5</sub>-CH<sub>2</sub>-N), 49.7 (C=N-CH<sub>2</sub>-CH<sub>2</sub>-CH<sub>2</sub>-N), 47.7 (CH<sub>2</sub>-N=C), 29.6 (CH<sub>2</sub>-C), 28.3 (CH<sub>2</sub>-CH<sub>2</sub>-N), 25.9 (CH<sub>2</sub>-CH<sub>2</sub>-C), 22.5 (C-(CH<sub>2</sub>)<sub>2</sub>-CH<sub>2</sub>-CH<sub>2</sub>-CH<sub>2</sub>-N), 20.2 (CH<sub>2</sub>-CH<sub>2</sub>-N=C).

**1-(6-hydroxyhexyl)-2,3,4,6,7,8,9,10-octahydropyrimido[1,2-*a*]azepin-1-ium**

**bromide [HO-(CH<sub>2</sub>)<sub>6</sub>-DBU]Br (13).** Flash column chromatography (CH<sub>2</sub>Cl<sub>2</sub>:MeOH 9:1). A white solid which was obtained (1.560 g, 4.68 mmol, 70%). <sup>1</sup>H NMR (400 MHz, CDCl<sub>3</sub>) δ 3.71-3.52 (m, 10H, HO-(CH<sub>2</sub>)<sub>5</sub>-CH<sub>2</sub>-N=C, C=N-CH<sub>2</sub>-CH<sub>2</sub>-CH<sub>2</sub>-N, C-(CH<sub>2</sub>)<sub>5</sub>-CH<sub>2</sub>-N, CH<sub>2</sub>-N=C, CH<sub>2</sub>-OH), 2.95-2.85 (m, 3H, CH<sub>2</sub>-C, CH<sub>2</sub>-OH), 2.16 (quintet, 2H, <sup>3</sup>J<sub>H-H</sub> = 5.7 Hz, CH<sub>2</sub>-CH<sub>2</sub>-N), 1.82-1.73 (s, 6H, CH<sub>2</sub>-CH<sub>2</sub>-CH<sub>2</sub>), 1.68-1.62 (m, 2H, CH<sub>2</sub>-CH<sub>2</sub>-OH), 1.57-1.50 (m, 2H, HO-(CH<sub>2</sub>)<sub>3</sub>-CH<sub>2</sub>-CH<sub>2</sub>-CH<sub>2</sub>-N), 1.45-1.32 (m, 4H, CH<sub>2</sub>-CH<sub>2</sub>-CH<sub>2</sub>-CH<sub>2</sub>-OH). <sup>13</sup>C APT NMR (100 MHz, CDCl<sub>3</sub>) δ 166.7 (C=N), 61.8 (CH<sub>2</sub>-OH), 55.7 (HO-(CH<sub>2</sub>)<sub>5</sub>-CH<sub>2</sub>-N=C), 54.5 (C-(CH<sub>2</sub>)<sub>5</sub>-CH<sub>2</sub>-N), 49.6 (C=N-CH<sub>2</sub>-CH<sub>2</sub>-CH<sub>2</sub>-N), 47.5 (CH<sub>2</sub>-N=C), 32.2 (HO-(CH<sub>2</sub>)<sub>4</sub>-CH<sub>2</sub>-CH<sub>2</sub>-N=C), 28.9 (CH<sub>2</sub>-CH<sub>2</sub>-CH<sub>2</sub>-OH), 28.7 (CH<sub>2</sub>-C), 28.6 (CH<sub>2</sub>-CH<sub>2</sub>-CH<sub>2</sub>-CH<sub>2</sub>-OH), 26.2 (CH<sub>2</sub>-CH<sub>2</sub>-N), 26.1 (CH<sub>2</sub>-CH<sub>2</sub>-C), 25.4 (C-(CH<sub>2</sub>)<sub>2</sub>-CH<sub>2</sub>-CH<sub>2</sub>-CH<sub>2</sub>-N), 23.3 (CH<sub>2</sub>-CH<sub>2</sub>-OH), 20.4 (CH<sub>2</sub>-CH<sub>2</sub>-N=C). IR (max/cm<sup>-1</sup>) 3304 (OH, s, br), 2930 (CH<sub>2</sub>, m), 2856 (CH<sub>2</sub>, m), 1617 (C=N, s), 1330 (C-H, m), 1057 (C-N, m). HRMS (ESI-TOF) (m/z): [M]<sup>+</sup> calculated for C<sub>15</sub>H<sub>29</sub>N<sub>2</sub>O<sup>+</sup>, 253.2274; found 253.2274. Elemental analysis: Calculated for C<sub>15</sub>H<sub>29</sub>BrN<sub>2</sub>O, C, 54.05 %; H, 8.77 %; N, 8.40 %; found C, 53.91 %; H, 8.51 %; N, 8.33 %.

**1-decyl-2,3,4,6,7,8,9,10-octahydropyrimido[1,2-*a*]azepin-1-ium iodide [CH<sub>3</sub>-(CH<sub>2</sub>)<sub>9</sub>-DBU]I (14).** Flash column chromatography (CH<sub>2</sub>Cl<sub>2</sub>:MeOH 19:1). A yellow solid was obtained (2.025 g, 4.81 mmol, 72%). <sup>1</sup>H NMR (400 MHz, CDCl<sub>3</sub>) δ 3.71-3.61 (m, 6H, C=N-CH<sub>2</sub>-CH<sub>2</sub>-CH<sub>2</sub>-N, C-(CH<sub>2</sub>)<sub>5</sub>-CH<sub>2</sub>-N, CH<sub>2</sub>-N=C), 3.48 (t, 2H, <sup>3</sup>J<sub>H-H</sub> = 8.0 Hz, CH<sub>3</sub>-(CH<sub>2</sub>)<sub>8</sub>-CH<sub>2</sub>-N), 2.88 (m, 2H, CH<sub>2</sub>-C), 2.19-2.11 (quintet, 2H, <sup>3</sup>J<sub>H-H</sub> = 5.7 Hz, CH<sub>2</sub>-CH<sub>2</sub>-N), 1.81 (s, 6H, CH<sub>2</sub>-CH<sub>2</sub>-CH<sub>2</sub>), 1.61 (s, 2H, CH<sub>3</sub>-(CH<sub>2</sub>)<sub>7</sub>-CH<sub>2</sub>-CH<sub>2</sub>-N=C), 1.27-1.23 (m, 14H, CH<sub>2</sub>-CH<sub>2</sub>-CH<sub>2</sub>-CH<sub>2</sub>-CH<sub>2</sub>-CH<sub>2</sub>-CH<sub>2</sub>-CH<sub>3</sub>), 0.85 (t, 3H, <sup>3</sup>J<sub>H-H</sub> = 6.5 Hz, CH<sub>3</sub>). <sup>13</sup>C APT NMR (100 MHz, CDCl<sub>3</sub>) δ 166.6 (C=N), 55.9 (C-(CH<sub>2</sub>)<sub>5</sub>-CH<sub>2</sub>-N), 54.6 (C-(CH<sub>2</sub>)<sub>5</sub>-CH<sub>2</sub>-N), 49.7 (CH<sub>2</sub>-N=C), 47.5 (CH<sub>3</sub>-(CH<sub>2</sub>)<sub>8</sub>-CH<sub>2</sub>-N=C), 31.9 (CH<sub>2</sub>-C), 29.5 (CH<sub>2</sub>-(CH<sub>2</sub>)<sub>2</sub>-CH<sub>3</sub>), 29.3 (CH<sub>2</sub>-(CH<sub>2</sub>)<sub>3</sub>-CH<sub>3</sub>), 29.2 (CH<sub>2</sub>-(CH<sub>2</sub>)<sub>4</sub>-CH<sub>3</sub>), 29.1 (CH<sub>3</sub>-(CH<sub>2</sub>)<sub>5</sub>-CH<sub>2</sub>-CH<sub>2</sub>-CH<sub>2</sub>-CH<sub>2</sub>-N=C), 29.1 (CH<sub>3</sub>-(CH<sub>2</sub>)<sub>6</sub>-CH<sub>2</sub>-CH<sub>2</sub>-CH<sub>2</sub>-N=C), 28.8 (CH<sub>3</sub>-(CH<sub>2</sub>)<sub>7</sub>-CH<sub>2</sub>-CH<sub>2</sub>-N=C), 28.6 (CH<sub>2</sub>-CH<sub>2</sub>-CH<sub>3</sub>), 26.6 (CH<sub>2</sub>-CH<sub>2</sub>-N), 26.1 (CH<sub>2</sub>-CH<sub>2</sub>-C), 23.2 (C-(CH<sub>2</sub>)<sub>2</sub>-CH<sub>2</sub>-CH<sub>2</sub>-CH<sub>2</sub>-N), 22.7 (CH<sub>2</sub>-CH<sub>3</sub>), 20.4 (CH<sub>2</sub>-CH<sub>2</sub>-N=C), 14.2 (CH<sub>3</sub>). IR (max/cm<sup>-1</sup>)

2921 (CH<sub>2</sub>, m), 2851 (CH<sub>2</sub>, m), 1622 (C=N, s), 1321 (C-H, m), 1084 (C-N, m). HRMS (ESI-TOF) (m/z): [M]<sup>+</sup> calculated for C<sub>19</sub>H<sub>37</sub>N<sub>2</sub><sup>+</sup>, 253.2951; found 253.2951. Elemental analysis: Calculated for C<sub>19</sub>H<sub>37</sub>IN<sub>2</sub>, C, 54.28 %; H, 8.77 %; N, 6.66 %; found C, 54.22 %; H, 8.74 %; N, 6.67%.

#### 6.3.4 General method for the synthesis of five-membered cyclic carbonates

In a round bottom flask [RDBU]X (0.88 mmol) salt was dissolved in epoxide (8.77 mmol). A rubber septum was used to stopper the flask before a balloon filled with CO<sub>2</sub> was inserted using a needle and used to flush the flask for two or three minutes through a release needle. Upon removal of the release needle, the mixture was stirred and heated to 70 °C for 4 h before removal of the CO<sub>2</sub> atmosphere and cooling to room temperature. Monomer conversion was measured by integration of the signals that correspond to epoxide and carbonate in the <sup>1</sup>H NMR spectrum. The carbonate was isolated by flash column chromatography using a mixture of ethyl acetate/hexane.

**4-Phenyl-1,3-dioxolan-2-one (15).** Yellow solid (1.223 g, 7.45 mmol, 85%). Characterization data was in agreement with those reported previously.<sup>11</sup> <sup>1</sup>H NMR (300 MHz, CDCl<sub>3</sub>) δ 7.46-7.40 (m, 3H, H<sup>Ar</sup>), 7.38-7.35 (m, 2H, H<sup>Ar</sup>), 5.68 (t, 1H, <sup>3</sup>J<sub>H-H</sub> = 8.0 Hz, CH), 4.80 (t, 1H, <sup>3</sup>J<sub>H-H</sub> = 8.0 Hz, CH<sup>anti</sup>), 4.35 (t, 1H, <sup>3</sup>J<sub>H-H</sub> = 8.0 Hz, CH<sup>syn</sup>). <sup>13</sup>C APT NMR (75 MHz, CDCl<sub>3</sub>) δ 155.0 (C=O), 135.9 (C<sup>Ar</sup> ipso), 129.7 (C<sup>Ar</sup>), 129.2 (C<sup>Ar</sup>), 126.0 (C<sup>Ar</sup>), 78.0 (CH), 71.2 (CH<sub>2</sub>).

**4-(Chloromethyl)-1,3-dioxolan-2-one (16).** Colourless liquid (874 mg, 6.40 mmol, 73%). Characterization data was in agreement with those reported previously.<sup>11</sup> <sup>1</sup>H NMR (300 MHz, CDCl<sub>3</sub>) δ 5.02-4.94 (m, 1H, CH), 4.61 (t, 1H, <sup>3</sup>J<sub>H-H</sub> = 8.0 Hz, CH<sup>anti</sup>), 4.45-4.40 (m, 1H, CH<sup>syn</sup>), 3.83-3.72 (m, 2H, CH<sub>2</sub>). <sup>13</sup>C APT NMR (75 MHz, CDCl<sub>3</sub>) δ 154.4 (C=O), 74.4 (CH), 67.0 (CH<sub>2</sub>), 43.9 (Cl-CH<sub>2</sub>).

**4-Allyloxymethyl-1,3-dioxan-2-one (17).** Colourless oil (1.207 g, 7.63 mmol, 87%). Characterization data was in agreement with those reported previously.<sup>11</sup> <sup>1</sup>H NMR (300 MHz, CDCl<sub>3</sub>) δ 5.93-5.80 (m, 1H, CH<sub>2</sub>=CH), 5.31-5.24 (m, 2H, CH<sub>2</sub>=CH), 4.85-4.78 (m, 1H, CH-O-COO), 4.52-4.37 (m, 2H, CH<sub>2</sub>-O-COO), 4.07-4.03 (m, 2H, CH<sub>2</sub>-CH), 3.71-3.66 (dd, <sup>3</sup>J<sub>H-H</sub> = 11.1 and 3.5 Hz, 1H, CH<sup>anti</sup>-CH=CH<sub>2</sub>), 3.63-3.58 (dd, <sup>3</sup>J<sub>H-H</sub> = 11.1 and 3.7 Hz, 1H, CH<sup>syn</sup>-CH=CH<sub>2</sub>). <sup>13</sup>C APT NMR (75 MHz, CDCl<sub>3</sub>) δ 162.4 (C=O), 133.8 (CH=CH<sub>2</sub>), 118.1 (CH<sub>2</sub>=CH), 75.1 (CH-O-COO), 72.7 (CH<sub>2</sub>-O-COO), 69.0 (CH<sub>2</sub>-CH), 66.4 (CH-CH=CH<sub>2</sub>).

**4-((Benzyloxy)methyl)-1,3-dioxan-2-one (18).** Slightly yellow solid (1.497 g, 7.20 mmol, 82%). Characterization data was in agreement with those reported previously.<sup>11</sup>  $^1\text{H NMR}$  (300 MHz,  $\text{CDCl}_3$ )  $\delta$  7.41-7.28 (m, 5H,  $\text{H}^{\text{Ar}}$ ), 4.84-4.78 (m, 1H,  $\text{CH-O-COO}$ ), 4.65-4.55 (m, 2H,  $\text{Ph-CH}_2$ ), 4.48 (t, 1H,  $^3J_{\text{H-H}} = 8.4$  Hz,  $\text{O-COO-CH}^{\text{anti}}$ -CH), 4.41-4.36 (m, 1H,  $\text{O-COO-CH}^{\text{syn}}$ -CH), 3.74-3.69 (dd, 1H, dd,  $^3J_{\text{H-H}} = 10.9$  and 3.8 Hz,  $\text{O-CH}^{\text{anti}}$ -CH), 3.65-3.60 (dd, 1H, dd,  $^3J_{\text{H-H}} = 10.9$  and 3.8 Hz,  $\text{O-CH}^{\text{syn}}$ -CH).  $^{13}\text{C APT NMR}$  (75 MHz,  $\text{CDCl}_3$ )  $\delta$  155.1 (C=O), 137.2 ( $\text{C}^{\text{Ar ipso}}$ ), 128.6 ( $\text{C}^{\text{Ar}}$ ), 128.1 ( $\text{C}^{\text{Ar}}$ ), 127.8 ( $\text{C}^{\text{Ar}}$ ), 75.1 (CH), 73.7 ( $\text{CH}_2$ ), 68.9 ( $\text{Ph-CH}_2$ ), 66.4 ( $\text{O-CH}_2$ ).

**4-(Hydroxymethyl)-1,3-dioxolan-2-one (19).** Colourless oil (673 mg, 5.70 mmol, 65%). Characterization data was in agreement with those reported previously.<sup>12</sup>  $^1\text{H NMR}$  (300 MHz,  $\text{CDCl}_3$ )  $\delta$  4.85-4.78 (m, 1H, CH), 4.55-4.43 (m, 2H,  $\text{CH}_2$ ), 4.02-3.95 (m, 1H,  $\text{CH}^{\text{anti}}$ ), 3.74-3.67 (m, 1H,  $\text{CH}^{\text{syn}}$ ), 2.80 (s, 1H, OH).  $^{13}\text{C APT NMR}$  (75 MHz,  $\text{CDCl}_3$ )  $\delta$  162.5 (C=O), 76.8 (CH), 65.9 ( $\text{CH}_2$ ), 61.8 ( $\text{HO-CH}_2$ ).

**4-Hexyl-1,3-dioxan-2-one (20).** Slightly yellow oil (1.254 g, 7.28 mmol, 83%). Characterization data was in agreement with those reported previously.<sup>11</sup>  $^1\text{H NMR}$  (300 MHz,  $\text{CDCl}_3$ )  $\delta$  4.74-4.64 (m, 1H, CH), 4.51 (t, 1H,  $^3J_{\text{H-H}} = 8.1$  Hz,  $\text{CH}^{\text{anti}}$ ), 4.05 (t, 1H,  $^3J_{\text{H-H}} = 8.1$  Hz,  $\text{CH}^{\text{syn}}$ ), 1.76-1.67 (m, 2H,  $\text{CH}_2$ -CH), 1.50-1.22 (m, 8H,  $\text{CH}_2$ - $\text{CH}_2$ - $\text{CH}_2$ - $\text{CH}_2$ - $\text{CH}_3$ ), 0.87 (t, 3H,  $^3J_{\text{H-H}} = 6.5$  Hz,  $\text{CH}_3$ ).  $^{13}\text{C APT NMR}$  (75 MHz,  $\text{CDCl}_3$ )  $\delta$  155.2 (C=O), 77.2 (CH), 69.5 ( $\text{CH}_2$ -O), 34.0 ( $\text{CH}_2$ -CH), 31.6 ( $\text{CH}_2$ - $\text{CH}_2$ -CH), 28.9 ( $\text{CH}_2$ - $\text{CH}_2$ - $\text{CH}_2$ -CH), 24.4 ( $\text{CH}_2$ - $\text{CH}_2$ - $\text{CH}_3$ ), 22.5 ( $\text{CH}_2$ - $\text{CH}_3$ ), 14.1 ( $\text{CH}_3$ ).

**4-Butyl-1,3-dioxan-2-one (21).** Slightly yellow oil (1.100 g, 7.63 mmol, 87%). Characterization data was in agreement with those reported previously.<sup>11</sup>  $^1\text{H NMR}$  (300 MHz,  $\text{CDCl}_3$ )  $\delta$  4.73-4.64 (m, 1H, CH), 4.51 (t, 1H,  $^3J_{\text{H-H}} = 8.1$  Hz,  $\text{CH}^{\text{anti}}$ ), 4.05 (t, 1H,  $^3J_{\text{H-H}} = 8.1$  Hz,  $\text{CH}^{\text{syn}}$ ), 1.77-1.67 (m, 2H,  $\text{CH}_2$ -CH), 1.40-1.33 (m, 4H,  $\text{CH}_2$ - $\text{CH}_2$ - $\text{CH}_3$ ), 0.90 (t, 3H,  $^3J_{\text{H-H}} = 6.8$ ,  $\text{CH}_3$ ).  $^{13}\text{C APT NMR}$  (75 MHz,  $\text{CDCl}_3$ )  $\delta$  155.2 (C=O), 77.2 (CH), 69.5 ( $\text{CH}_2$ -O), 33.6 ( $\text{CH}_2$ -CH), 26.5 ( $\text{CH}_2$ - $\text{CH}_2$ -CH), 22.3 ( $\text{CH}_2$ - $\text{CH}_3$ ), 13.9 ( $\text{CH}_3$ ).

**Hexahydrobenzo[d][1,3]dioxol-2-one (22).** In a stainless steel autoclave, cyclohexene oxide (861 mg, 8.77 mmol) and [HDBU]I (246.5 mg, 0.88 mmol) were dissolved in DMF (1 mL), then the autoclave was sealed and pressurised to 3MPa and heated up to 140 °C for 48 h. Then the autoclave was allowed to cool down to R.T and  $\text{CO}_2$  was vented. DMF was evaporated under reduced pressure affording



an oily residue. White solid (985 mg, 6.93 mmol, 79%). Characterization data was in agreement with those reported previously.<sup>13</sup> **<sup>1</sup>H NMR** (300 MHz, CDCl<sub>3</sub>)  $\delta$  4.70-4.64 (m, 2H, CH), 1.91-1.86 (m, 4H, CH<sub>2</sub>-CH), 1.63-1.38 (m, 4H, CH<sub>2</sub>-CH<sub>2</sub>-CH). **<sup>13</sup>C APT NMR** (75 MHz, CDCl<sub>3</sub>)  $\delta$  155.5 (C=O), 75.8 (CH), 26.9 (CH<sub>2</sub>-CH), 19.2 (CH<sub>2</sub>-CH<sub>2</sub>-CH).

### 6.3.5 Computational details

All the calculations were done using the  $\omega$ B97XD functional. Geometry optimisations were carried out using the *6-31+G(d,p)* basis set for all atoms, except for I for which we use the *def2-svp* basis set. Vibrational frequencies were obtained to determine whether the structures are minima or transition states, and then used to evaluate the zero-point vibrational energy (ZPVE) and the thermal vibrational corrections to the enthalpy ( $H_{DZ}^{corr}$ ) at T=298 K. Single-point calculations using the *6-311++G(2df,2p)* basis set (*def2-TZVPP* for iodine) were performed on the optimised structures in order to refine the electronic energy ( $E_{TZ}$ ), and the previously calculated corrections to the enthalpy were used to calculate the H of each species, namely:  $H_{TZ}^{298} = E_{TZ} + H_{DZ}^{corr}$ .

## 6.4 Experimental protocols for Chapter 3

### 6.4.1 General procedure for the synthesis of guanidines

A solution of an equimolecular mixture of *N,N'*-dicyclohexylcarbodiimide (DCC) (1.0 g, 4.85 mmol) and secondary amine (4.85 mmol) in THF (16 mL) was heated to reflux and left overnight. THF was evaporated in a rotavap and an oily residue or a solid was obtained, dried under high vacuum and used without further purification.

***N,N'*-Dicyclohexylpirrolidine-1-carboxamidine (1)**. A colourless oil was obtained (1.305 g, 4.70 mmol, 97%). Characterization data was in agreement with those reported in the literature.<sup>14</sup> **<sup>1</sup>H NMR** (300 MHz, CDCl<sub>3</sub>)  $\delta$  3.26-3.22 (m, 4H, NH-C-N-CH<sub>2</sub>), 2.94 (bs, 2H, CH-NH-C=N-CH) 1.93-1.23 (m, 24H, CH<sub>2</sub>-CH<sub>2</sub>-CH<sub>2</sub>-CH-NH-C=N-CH-CH<sub>2</sub>-CH<sub>2</sub>-CH<sub>2</sub>, NH-C-N-CH<sub>2</sub>-CH<sub>2</sub>). **<sup>13</sup>C APT NMR** (75 MHz, CDCl<sub>3</sub>)  $\delta$  153.5 (NH-C), 55.9 (CH-NH-C=N-CH), 48.0 (NH-C-N-CH<sub>2</sub>), 35.1 (CH<sub>2</sub>-CH-NH-C=N-CH-CH<sub>2</sub>), 25.9 (CH<sub>2</sub>-CH-NH-C=N-CH-CH<sub>2</sub>, NH-C-N-CH<sub>2</sub>-

CH<sub>2</sub>) 25.7 (CH<sub>2</sub>-CH<sub>2</sub>-CH-NH-C=N-CH-CH<sub>2</sub>-CH<sub>2</sub>), 25.3 (CH<sub>2</sub>-CH<sub>2</sub>-CH<sub>2</sub>-CH-NH-C=N-CH-CH<sub>2</sub>-CH<sub>2</sub>-CH<sub>2</sub>).

***N,N'*-Dicyclohexylpiperidine-1-carboxamidine (2).** A colourless oil was obtained (1.357 g, 4.66 mmol, 96%). Characterization data was in agreement with those reported in the literature.<sup>14</sup> <sup>1</sup>H NMR (300 MHz, CDCl<sub>3</sub>) δ 3.19-3.17 (m, 2H, CH-NH-C=N-CH), 3.03 (bs, 4H, NH-C-N-CH<sub>2</sub>), 1.93-1.23 (m, 26H, CH<sub>2</sub>-CH<sub>2</sub>-CH<sub>2</sub>-CH-NH-C=N-CH-CH<sub>2</sub>-CH<sub>2</sub>-CH<sub>2</sub>, NH-C-N-CH<sub>2</sub>-CH<sub>2</sub>-CH<sub>2</sub>-CH<sub>2</sub>). <sup>13</sup>C APT NMR (75 MHz, CDCl<sub>3</sub>) δ 162.5 (NH-C), 55.9 (CH-NH-C=N-CH), 49.2 (NH-C-N-CH<sub>2</sub>), 35.1 (CH<sub>2</sub>-CH-NH-C=N-CH-CH<sub>2</sub>), 25.6 (CH<sub>2</sub>-CH<sub>2</sub>-CH-NH-C=N-CH-CH<sub>2</sub>-CH<sub>2</sub>, NH-C-N-CH<sub>2</sub>-CH<sub>2</sub>), 24.8 (CH<sub>2</sub>-CH<sub>2</sub>-CH<sub>2</sub>-CH-NH-C=N-CH-CH<sub>2</sub>-CH<sub>2</sub>-CH<sub>2</sub>, NH-C-N-CH<sub>2</sub>-CH<sub>2</sub>-CH<sub>2</sub>).

***N,N'*-Dicyclohexylmorpholine-1-carboxamidine (3).** A white solid was obtained (1.309 g, 4.46 mmol, 92%). Characterization data was in agreement with those reported in the literature.<sup>14</sup> <sup>1</sup>H NMR (300 MHz, CDCl<sub>3</sub>) δ 3.69-3.67 (m, 4H, NH-C-N-CH<sub>2</sub>-CH<sub>2</sub>), 3.10-3.07 (m, 4H, NH-C-N-CH<sub>2</sub>), 3.00-2.91 (m, 2H, CH-NH-C=N-CH), 1.93-1.60 (m, 10H, 1.93-1.04, CH<sub>2</sub>-CH<sub>2</sub>-CH<sub>2</sub>-CH-NH-C=N-CH-CH<sub>2</sub>-CH<sub>2</sub>-CH<sub>2</sub>). <sup>13</sup>C APT NMR (75 MHz, CDCl<sub>3</sub>) δ 155.0 (NH-C), 67.2 (O-CH<sub>2</sub>), 56.4 (N-CH) 53.7 (NH-CH), 48.8 (NH-C-NH-CH<sub>2</sub>), 35.3 (N-CH-CH<sub>2</sub>), 34.6 (NH-CH-CH<sub>2</sub>), 25.9 (N-CH-CH<sub>2</sub>-CH<sub>2</sub>), 25.7 (NH-CH-CH<sub>2</sub>-CH<sub>2</sub>) 25.5 (CH<sub>2</sub>-CH<sub>2</sub>-CH<sub>2</sub>-CH-NH-C=N-CH-CH<sub>2</sub>-CH<sub>2</sub>-CH<sub>2</sub>).

***N,N'*-Dicyclohexylimidazole-1-carboxamidine (4).** A solution of an equimolecular mixture of DCC (1.0 g, 4.85 mmol) and imidazole (330.2 mg, 4.85 mmol) in THF (16 mL) was heated to reflux and left overnight. THF was evaporated and the residue was recrystallised in EtOAc to afford colourless crystals (932 mg, 3.40 mmol, 70%) Characterization data was in agreement with those reported in the literature.<sup>15</sup> <sup>1</sup>H NMR (300 MHz, DMSO) δ 7.67 (s, 1H, NH-C-N-CH=N), 7.19 (s, 1H, NH-C-N-CH=CH), 6.98 (s, 1H, NH-C-N-CH=CH), 6.46 (d, 1H, <sup>3</sup>J<sub>H-H</sub> = 6.9 Hz, NH), 3.44-3.43 (m, 1H, NH-C=N-CH), 2.60-2.55 (m, 1H, NH-CH), 1.96-1.91 (m, 2H, NH-C=N-CH-CH<sub>a</sub>), 1.75-1.00 (m, 18H, NH-C=N-CH-CH<sub>b</sub>-CH<sub>2</sub>-CH<sub>2</sub>). <sup>13</sup>C NMR (75 MHz, DMSO) δ 139.4 (NH-C), 136.1 (NH-C-N-CH=N), 127.8 (NH-C-N-CH=CH), 118.9 (NH-C-N-CH=CH), 55.8 (NH-CH), 49.9 (NH-C=N-CH), 35.1

(NH-CH-CH<sub>2</sub>), 31.7 (NH-C=N-CH-CH<sub>2</sub>), 25.6 (NH-C=N-CH-CH<sub>2</sub>-CH<sub>2</sub>), 24.7 (NH-C=N-CH-CH<sub>2</sub>-CH<sub>2</sub>-CH<sub>2</sub>).

***N,N'*-Dicyclohexylbenzimidazole-1-carboxamide (5).** A solution of an equimolecular mixture of DCC (1.0 g, 4.85 mmol) and benzimidazole (330.2 mg, 4.85 mmol) in THF (16 mL) was heated to reflux and left overnight. THF was evaporated and the residue was purified by flash column chromatography using EtOAc as eluent (850 mg, 2.62 mmol, 54%). Characterization data was in agreement with those reported in the literature.<sup>15</sup> **<sup>1</sup>H NMR** (300 MHz, DMSO)  $\delta$  8.25 (s, 1H, NH-C-N-CH=N), 7.72 (d, 2H, <sup>3</sup>*J*<sub>H-H</sub> = 7.9 Hz, NH-C-N-CH), 7.39-7.26 (m, 2H, NH-C-N-CH=CH), 6.70 (d, 2H, <sup>3</sup>*J*<sub>H-H</sub> = 7.9 Hz, NH), 3.60 (bs, 1H, CH-NH), 2.02 (bs, 1H, NH-C=N-CH), 1.71-1.19 (m, 20H, CH<sub>2</sub>-CH<sub>2</sub>-CH<sub>2</sub>-CH-NH-C=N-CH-CH<sub>2</sub>-CH<sub>2</sub>-CH<sub>2</sub>). **<sup>13</sup>C NMR** (75 MHz, DMSO)  $\delta$  156.6 (NH-C), 142.2 (NH-C-N-CH=N), 138.5 (NH-C-N-CH=N-C), 133.2 (NH-C-N-C), 123.4 (NH-C-N-C-CH=CH), 122.2 (NH-C-N-CH=N-C-CH=CH), 119.6 (NH-C-N-C-CH), 110.7 (NH-C-N-CH=N-C-CH), 56.1 (NH-CH), 49.8 (NH-C=N-CH), 35.1 (NH-CH-CH<sub>2</sub>), 31.7 (NH-C=N-CH-CH<sub>2</sub>), 25.6 (NH-CH-CH<sub>2</sub>-CH<sub>2</sub>), 25.3 (NH-C-N-CH-CH<sub>2</sub>-CH<sub>2</sub>), 24.6 (NH-CH-CH<sub>2</sub>-CH<sub>2</sub>-CH<sub>2</sub>), 24.1 (NH-C=N-CH-CH<sub>2</sub>-CH<sub>2</sub>-CH<sub>2</sub>).

#### 6.4.2 General procedure for the synthesis of guanidinium salts

Guanidine (4 mmol) was dissolved in MeOH (4 mL), then ammonium iodide (580 mg, 4 mmol) was added. A reflux condenser was attached to the flask and the mixture was heated up to reflux overnight. Solvent was evaporated and the crude was recrystallized from CH<sub>2</sub>Cl<sub>2</sub>/Hexane. A solid was obtained.

**(Z)-N-((cyclohexylamino)(pyrrolidin-1-yl)methylene)cyclohexanaminium iodide (6).** A yellow solid was obtained (1.476 g, 3.64 mmol, 91%). **<sup>1</sup>H NMR** (400 MHz, CDCl<sub>3</sub>)  $\delta$  6.18 (d 2H, <sup>3</sup>*J*<sub>H-H</sub> = 8.0 Hz, NH-C=NH), 3.69-3.67 (t, 4H, <sup>3</sup>*J*<sub>H-H</sub> = 6.6 Hz, NH-C-N-CH<sub>2</sub>), 3.44-3.37 (m, 2H, CH-NH-C=NH-CH), 1.93-1.60 (m, 24H, 1.97-1.18 (CH<sub>2</sub>-CH<sub>2</sub>-N-C=NH-CH-CH<sub>2</sub>-CH<sub>2</sub>-CH<sub>2</sub>)). **<sup>13</sup>C APT NMR** (100 MHz, CDCl<sub>3</sub>)  $\delta$  155 (NH-C), 55.7 (CH-NH-C=NH-CH) 50.6 (N-CH<sub>2</sub>), 34.0 (NH-C=NH-CH-CH<sub>2</sub>), 25.9 (CH<sub>2</sub>-CH-NH-C-N-CH<sub>2</sub>-CH<sub>2</sub>), 25.7 (CH<sub>2</sub>-CH<sub>2</sub>-CH-NH-C=NH-CH-CH<sub>2</sub>-CH<sub>2</sub>), 25.5 (CH<sub>2</sub>-CH<sub>2</sub>-CH<sub>2</sub>-CH-NH-C=NH-CH-CH<sub>2</sub>-CH<sub>2</sub>-CH<sub>2</sub>). IR (max/cm<sup>-1</sup>) 3208.5 (C=NH<sup>+</sup>, s), 1607.4 (C=N, s). HRMS (ESI-TOF) (m/z): [M]<sup>+</sup>

calculated for  $C_{17}H_{32}N_3^+$ , 278.2596; found 278.2597. Elemental analysis: Calculated for  $C_{17}H_{32}IN_3$ , C, 50.37 %; H, 7.96 %; N, 10.37 %; found C, 50.30 %; H, 7.92 %; N, 10.29 %.

**(Z)-N-((cyclohexylamino)(piperidin-1-yl)methylene)cyclohexanaminium**

**iodide (7).** A yellow solid was obtained (1.493 g, 4.56 mmol, 89%).  $^1H$  NMR (400 MHz,  $CDCl_3$ )  $\delta$  3.41 (s, 6H,  $CH-NH-C=NH-CH$ ,  $NH-C-N-CH_2$ ), (m, 26H, 1.97-1.18 ( $CH_2-CH_2-CH_2-CH-NH-C=NH-CH-CH_2-CH_2-CH_2$ ,  $NH-C-N-CH_2-CH_2-CH_2$ ).  $^{13}C$  APT NMR (100 MHz,  $CDCl_3$ )  $\delta$  162.4 (NH-C), 55.6 ( $CH-NH-C=NH-CH$ ) 50.3 (N- $CH_2$ ), 33.4 ( $CH_2-CH-NH-C=NH-CH-CH_2$ ), 25.8 (NH-C-N- $CH_2-CH_2$ ), 25.3 ( $CH_2-CH_2-CH-NH-C=NH-CH-CH_2-CH_2$ ), 24.8 (NH-C-N- $CH_2-CH_2-CH_2$ ), 23.8 ( $CH_2-CH_2-CH_2-CH-NH-C=NH-CH-CH_2-CH_2-CH_2$ ). IR (max/ $cm^{-1}$ ) 3222.0 (C=NH<sup>+</sup>, s), 1606.9 (C=N, s). HRMS (ESI-TOF) (m/z): [M]<sup>+</sup> calculated for  $C_{18}H_{34}N_3^+$ , 292.2755; found 278.2753. Elemental analysis: Calculated for  $C_{18}H_{34}IN_3$ , C, 51.55 %; H, 8.17 %; N, 10.02 %; found C, 51.47 %; H, 8.05 %; N, 9.93 %.

**(Z)-N-((cyclohexylamino)(morpholino)methylene)cyclohexanaminium iodide**

**(8).** A yellow solid was obtained (1.601 g, 3.80 mmol, 95%).  $^1H$  NMR (400 MHz,  $CDCl_3$ )  $\delta$  6.91 (s, 1H,  $NH-C=NH$ ), 3.80 (s, 4H,  $NH-C-N-CH_2-CH_2$ ), 3.58 (s, 4H,  $NH-C-N-CH_2$ ), 3.49 (s, 1H,  $NH-C$ ), 3.39 (s, 2H,  $CH-NH-C=NH-CH$ ), 1.82-1.63 (m, 16H,  $CH_2-CH_2-CH-NH-C=NH-CH-CH_2-CH_2$ ), 1.30-1.25 (m, 4H,  $CH_2-CH_2-CH_2-CH-NH-C=NH-CH-CH_2-CH_2-CH_2$ ).  $^{13}C$  APT NMR (100 MHz,  $CDCl_3$ )  $\delta$  162.4 (NH-C), 66.6 (NH-C-N- $CH_2-CH_2$ ), 56.1 ( $CH-NH-C=NH-CH$ ), 49.3 (NH-C-N- $CH_2$ ), 35.6 ( $CH_2-CH-NH-C=NH-CH-CH_2$ ), 25.4 ( $CH_2-CH_2-CH-NH-C=NH-CH-CH_2-CH_2$ ), 24.8 ( $CH_2-CH_2-CH_2-CH-NH-C=NH-CH-CH_2-CH_2-CH_2$ ). IR (max/ $cm^{-1}$ ) 3142.9 (C=NH<sup>+</sup>, s), 1597.7 (C=N, s). HRMS (ESI-TOF) (m/z): [M]<sup>+</sup> calculated for  $C_{17}H_{32}N_3O^+$ , 294.2545; found 294.2547. Elemental analysis: Calculated for  $C_{17}H_{32}IN_3O$ , C, 48.46 %; H, 7.66 %; N, 9.97 %; found C, 48.39 %; H, 7.51 %; N, 9.90 %.

**(Z)-N-((cyclohexylamino)(1H-imidazol-1-yl)methylene)cyclohexanaminium**

**iodide (9).** A yellow solid was obtained (1.464 g, 3.64 mmol, 91%).  $^1H$  NMR (400 MHz, DMSO)  $\delta$  8.24 (s, 1H,  $NH-C-N-CH=N$ ), 7.31-7.29 (m, 2H,  $NH-C-N-CH=CH$ ), 6.93 (d, 1H,  $^3J_{H-H} = 8.3$  Hz,  $NH-C=NH$ ), 5.60 (d, 1H,  $^3J_{H-H} = 8.0$  Hz,  $NH-C=N-CH$ ), 3.45-3.37 (m, 2H,  $CH-NH-C=NH-CH$ ), 1.80-1.65 (m, 8H,  $CH_2-CH-NH-C=NH-CH-CH_2$ ), 1.30-1.14 (m, 12H,  $CH_2-CH_2-CH_2-CH-NH-C=NH-CH-$

CH<sub>2</sub>-CH<sub>2</sub>-CH<sub>2</sub>). <sup>13</sup>C NMR (100 MHz, DMSO) δ 153.7 (NH-C), 134.9 (NH-C-N-CH=N), 120.7 (NH-C-N-CH=CH), 49.5 (NH-CH), 32.2 (NH-CH-CH<sub>2</sub>), 24.8 (NH-CH-CH<sub>2</sub>-CH<sub>2</sub>), 24.1 (NH-CH-CH<sub>2</sub>-CH<sub>2</sub>-CH<sub>2</sub>). IR (max/cm<sup>-1</sup>) 3170.5 (C=NH<sup>+</sup>, s), 1620.6 (C=N, s). HRMS (ESI-TOF) (m/z): [M]<sup>+</sup> calculated for C<sub>16</sub>H<sub>27</sub>N<sub>4</sub><sup>+</sup>, 275.2230; found 275.2231. Elemental analysis: Calculated for C<sub>16</sub>H<sub>27</sub>IN<sub>4</sub>, C, 47.77 %; H, 6.76 %; N, 13.93 %; found C, 47.69 %; H, 6.74 %; N, 13.89 %.

**(Z)-N-((1H-benzo[d]imidazol-1-**

**yl)(cyclohexylamino)methylene)cyclohexanaminium iodide (10).** A yellow solid was obtained (1.683 g, 3.72 mmol, 93%). <sup>1</sup>H NMR (400 MHz, DMSO) δ 8.29 (s, 1H, NH-C-N-CH), 7.61-7.58 (m, 2H, NH-C-N-C-CH), 7.21-7.19 (m, 2H, NH-C-N-C-CH=CH), 6.93 (d, 1H, <sup>3</sup>J<sub>H-H</sub> = 8.3 Hz, NH-C=NH), 3.84 (s, 1H, NH-C), 3.59-3.56 (m, 1H, NH-C=NH-CH), 3.42-3.11 (m, 1H, CH-NH-C), 1.80-1.53 (8H, m, CH<sub>2</sub>-CH-NH-C=NH-CH-CH<sub>2</sub>), 1.30-1.14 (12 H, m, CH<sub>2</sub>-CH<sub>2</sub>-CH<sub>2</sub>-CH-NH-C=NH-CH-CH<sub>2</sub>-CH<sub>2</sub>-CH<sub>2</sub>). <sup>13</sup>C NMR (100 MHz, DMSO) δ 153.7 (NH-C), 141.9 (NH-C-N-CH=N), 137.6 (NH-C-N-C), 122.0 (NH-C-N-C-CH=CH), 115.3 (NH-C-N-C-CH), 57.4 (NH-CH), 49.5 (NH-C=N-CH), 32.2 (CH<sub>2</sub>-CH-NH-C=NH-CH-CH<sub>2</sub>), 24.7 (CH<sub>2</sub>-CH<sub>2</sub>-CH-NH-C=NH-CH-CH<sub>2</sub>-CH<sub>2</sub>), 24.1 (CH<sub>2</sub>-CH<sub>2</sub>-CH<sub>2</sub>-CH-NH-C=NH-CH-CH<sub>2</sub>-CH<sub>2</sub>-CH<sub>2</sub>). IR (max/cm<sup>-1</sup>) 3170.5 (C=NH<sup>+</sup>, s), 1620.6 (C=N, s), 1568.5 (N-H, s). HRMS (ESI-TOF) (m/z): [M]<sup>+</sup> calculated for C<sub>20</sub>H<sub>29</sub>N<sub>4</sub><sup>+</sup>, 325.2387; found 325.2385. Elemental analysis: Calculated for C<sub>20</sub>H<sub>29</sub>IN<sub>4</sub>, C, 53.10 %; H, 6.46 %; N, 12.39 %; found C, 53.04 %; H, 6.43 %; N, 12.36 %.

**mono((Z)-1-((cyclohexylamino)(cyclohexyliminio)methyl)-1H-imidazol-3-**

**ium) monoiodide (11).** Guanidine **4** (1.098 g, 4 mmol) was dissolved in MeOH (4 mL), then ammonium iodide (1.160 g, 8 mmol) was added. A reflux condenser was attached to the flask and the mixture was heated up to reflux overnight. Solvent was evaporated and the crude was recrystallized from CH<sub>2</sub>Cl<sub>2</sub>/Hexane. A yellow solid was obtained (1.994 g, 3.76 mmol, 94%). <sup>1</sup>H NMR (400 MHz, DMSO) δ 8.87 (s, 1H, NH-C-N-CH=NH), 7.60-7.59 (m, 2H, NH-C-N-CH=CH), 7.30 (s, 1H, NH-C-N-CH=NH), 6.92 (d, 1H, <sup>3</sup>J<sub>H-H</sub> = 8.3 Hz, NH-C=NH), 5.60 (d, 1H, <sup>3</sup>J<sub>H-H</sub> = 8.0 Hz, NH-C=NH-CH), 3.46-3.30 (m, 2H, CH-NH-C=NH-CH), 1.80-1.64 (m, 8H, CH<sub>2</sub>-CH-NH-C=NH-CH-CH<sub>2</sub>), 1.30-1.17 (m, 12H, CH<sub>2</sub>-CH<sub>2</sub>-CH<sub>2</sub>-CH-NH-C=NH-CH-CH<sub>2</sub>-CH<sub>2</sub>-CH<sub>2</sub>). <sup>13</sup>C NMR (100 MHz, DMSO) δ 153.7 (NH-C), 134.6 (NH-C-N-CH=N), 119.7 (NH-C-N-CH=CH), 49.5 (NH-CH), 32.2 (NH-CH-CH<sub>2</sub>), 24.7 (NH-CH-CH<sub>2</sub>-CH<sub>2</sub>), 24.1 (NH-CH-CH<sub>2</sub>-CH<sub>2</sub>-CH<sub>2</sub>). IR (max/cm<sup>-1</sup>) 3170.5 (C=NH<sup>+</sup>, s),

1620.6 (C=N, s), 1572.2 (N-H, s). HRMS (ESI-TOF) (m/z): [M]<sup>+</sup> calculated for C<sub>16</sub>H<sub>27</sub>N<sub>4</sub><sup>+</sup>, 275.2230; found 275.2232. Elemental analysis: Calculated for C<sub>16</sub>H<sub>28</sub>I<sub>2</sub>N<sub>4</sub>, C, 36.24 %; H, 5.32 %; N, 10.57 %; found C, 36.19 %; H, 5.29 %; N, 10.52 %.

**mono((Z)-1-((cyclohexylamino)(cyclohexyliminio)methyl)-1H-**

**benzo[d]imidazol-3-ium) monoiodide (12).** Guanidine **5** (1.298 g, 4 mmol) was dissolved in MeOH (4 mL), then ammonium iodide (1.160 g, 8 mmol) was added. A reflux condenser was attached to the flask and the mixture was heated up to reflux overnight. Solvent was evaporated and the crude was recrystallized from CH<sub>2</sub>Cl<sub>2</sub>/Hexane. A yellow solid was obtained (2.112 g, 3.64 mmol, 91%). <sup>1</sup>H NMR (400 MHz, DMSO) δ 8.68 (s, 1H, NH-C-N-CH), 7.69-7.66 (m, 2H, NH-C-N-C-CH), 7.33-7.31 (m, 2H, NH-C-N-C-CH=CH), 7.23-6.97 (m, 1H, NH-C-N-CH=NH), 6.93 (d, 1H, <sup>3</sup>J<sub>H-H</sub> = 8.3 Hz, NH-C=NH), 3.89 (s, 1H, NH-C), 3.58-3.55 (m, 1H, NH-C=NH-CH), 3.42-3.27 (m, 1H, CH-NH-C), 1.80-1.53 (8H, m, CH<sub>2</sub>-CH-NH-C=NH-CH-CH<sub>2</sub>), 1.27-1.02 (12 H, m, CH<sub>2</sub>-CH<sub>2</sub>-CH<sub>2</sub>-CH-NH-C=NH-CH-CH<sub>2</sub>-CH<sub>2</sub>-CH<sub>2</sub>). <sup>13</sup>C NMR (100 MHz, DMSO) δ 153.7 (NH-C), 141.5 (NH-C-N-CH=N), 135.4 (NH-C-N-C), 123.3 (NH-C-N-C-CH=CH), 115.0 (NH-C-N-C-CH), 57.4 (NH-CH), 49.5 (NH-C=N-CH), 32.2 (CH<sub>2</sub>-CH-NH-C=NH-CH-CH<sub>2</sub>), 24.8 (CH<sub>2</sub>-CH<sub>2</sub>-CH-NH-C=NH-CH-CH<sub>2</sub>-CH<sub>2</sub>), 24.1 (CH<sub>2</sub>-CH<sub>2</sub>-CH<sub>2</sub>-CH-NH-C=NH-CH-CH<sub>2</sub>-CH<sub>2</sub>-CH<sub>2</sub>). IR (max/cm<sup>-1</sup>) 3170.5 (C=NH<sup>+</sup>, s), 1620.6 (C=N, s), 1575.9 (N-H, s). HRMS (ESI-TOF) (m/z): [M]<sup>+</sup> calculated for C<sub>20</sub>H<sub>29</sub>N<sub>4</sub><sup>+</sup>, 325.2387; found 325.2389. Elemental analysis: Calculated for C<sub>20</sub>H<sub>30</sub>I<sub>2</sub>N<sub>4</sub>, C, 41.40 %; H, 5.21 %; N, 9.66 %; found C, 41.35 %; H, 5.20 %; N, 9.63 %.

**(Z)-N-((cyclohexylamino)(1H-imidazol-1-yl)methylene)cyclohexanaminium**

**chloride (14).** A white solid was obtained (1.132 g, 3.64 mmol, 91%). <sup>1</sup>H NMR (400 MHz, DMSO) δ 8.99 (s, 1H, NH-C-N-CH=N), 7.65-7.62 (m, 2H, NH-C-N-CH=CH), 7.49 (s, 1H, NH-C=NH), 5.71 (d, 1H, <sup>3</sup>J<sub>H-H</sub> = 6.9 Hz, NH-C=N-CH), 3.46-3.31 (m, 2H, CH-NH-C=NH-CH), 1.79-1.52 (m, 8H, CH<sub>2</sub>-CH-NH-C=NH-CH-CH<sub>2</sub>), 1.30-1.15 (m, 12H, CH<sub>2</sub>-CH<sub>2</sub>-CH<sub>2</sub>-CH-NH-C=NH-CH-CH<sub>2</sub>-CH<sub>2</sub>-CH<sub>2</sub>). <sup>13</sup>C NMR (100 MHz, DMSO) δ 154.1 (NH-C), 134.2 (NH-C-N-CH=N), 119.4 (NH-C-N-CH=CH), 49.2 (NH-CH), 32.2 (NH-CH-CH<sub>2</sub>), 24.9 (NH-CH-CH<sub>2</sub>-CH<sub>2</sub>), 24.0 (NH-CH-CH<sub>2</sub>-CH<sub>2</sub>-CH<sub>2</sub>). IR (max/cm<sup>-1</sup>) 3127.0 (C=NH<sup>+</sup>, s), 1622.3 (C=N, s). HRMS (ESI-TOF) (m/z): [M]<sup>+</sup> calculated for C<sub>16</sub>H<sub>27</sub>N<sub>4</sub><sup>+</sup>, 275.2230; found

275.2229. Elemental analysis: Calculated for C<sub>16</sub>H<sub>27</sub>ClN<sub>4</sub>, C, 61.82 %; H, 8.75 %; N, 18.02 %; found C, 61.79 %; H, 8.74 %; N, 17.98 %.

**(Z)-N-((cyclohexylamino)(1H-imidazol-1-yl)methylene)cyclohexanaminium**

**bromide (15).** A white solid was obtained (1.336 g, 3.76 mmol, 94%). <sup>1</sup>H NMR (400 MHz, DMSO) δ 9.09 (s, 1H, NH-C-N-CH=N), 7.69 (s, 2H, NH-C-N-CH=CH), 7.37 (s, 1H, NH-C=NH), 7.11 (d, 1H, <sup>3</sup>J<sub>H-H</sub> = 8.4 Hz, NH-C=NH), 5.63 (d, 1H, <sup>3</sup>J<sub>H-H</sub> = 8.0 Hz, NH-C=N-CH), 3.84 (s, 1H, NH-C=NH) 3.47-3.33 (m, 2H, CH-NH-C=NH-CH), 1.77-1.66 (m, 8H, CH<sub>2</sub>-CH-NH-C=NH-CH-CH<sub>2</sub>), 1.30-1.14 (m, 12H, CH<sub>2</sub>-CH<sub>2</sub>-CH<sub>2</sub>-CH-NH-C=NH-CH-CH<sub>2</sub>-CH<sub>2</sub>-CH<sub>2</sub>). <sup>13</sup>C NMR (100 MHz, DMSO) δ 153.8 (NH-C), 134.4 (NH-C-N-CH=N), 119.4 (NH-C-N-CH=CH), 49.4 (NH-CH), 32.2 (NH-CH-CH<sub>2</sub>), 24.8 (NH-CH-CH<sub>2</sub>-CH<sub>2</sub>), 24.1 (NH-CH-CH<sub>2</sub>-CH<sub>2</sub>-CH<sub>2</sub>). IR (max/cm<sup>-1</sup>) 3152.6 (C=NH<sup>+</sup>, s), 1653.7 (C=N, s). HRMS (ESI-TOF) (m/z): [M]<sup>+</sup> calculated for C<sub>16</sub>H<sub>27</sub>N<sub>4</sub><sup>+</sup>, 275.2230; found 275.2232. Elemental analysis: Calculated for C<sub>16</sub>H<sub>27</sub>BrN<sub>4</sub>, C, 54.08 %; H, 7.66 %; N, 15.77 %; found C, 54.01 %; H, 7.62 %; N, 15.71 %.

#### 6.4.3 General method for the synthesis of five-membered cyclic carbonates

In a round bottom flask guanidinium salt (0.88 mmol) was dissolved in epoxide (8.77 mmol). A rubber septum was used to stopper the flask before a balloon filled with CO<sub>2</sub> was inserted using a needle and used to flush the flask for two or three minutes through a release needle. Upon removal of the release needle, the mixture was stirred and heated to 70 °C for 4 h before removal of the CO<sub>2</sub> atmosphere and cooling to room temperature. Monomer conversion was measured by integration of the signals that correspond to epoxide and carbonate in the <sup>1</sup>H NMR spectrum. The carbonate was isolated by flash column chromatography using a mixture of ethyl acetate/hexane.

**4-Phenyl-1,3-dioxolan-2-one (13).** Yellow solid (1.267 g, 7.71 mmol, 88%). Characterization data was in agreement with those reported previously.<sup>11</sup> <sup>1</sup>H NMR (300 MHz, CDCl<sub>3</sub>) δ 7.46-7.40 (m, 3H, H<sup>Ar</sup>), 7.38-7.35 (m, 2H, H<sup>Ar</sup>), 5.68 (t, 1H, <sup>3</sup>J<sub>H-H</sub> = 8.0 Hz, CH), 4.80 (t, 1H, <sup>3</sup>J<sub>H-H</sub> = 8.0 Hz, CH<sup>anti</sup>), 4.35 (t, 1H, <sup>3</sup>J<sub>H-H</sub> = 8.0 Hz, CH<sup>syn</sup>). <sup>13</sup>C APT NMR (75 MHz, CDCl<sub>3</sub>) δ 155.0 (C=O), 135.9 (C<sup>Ar ipso</sup>), 129.7 (C<sup>Ar</sup>), 129.2 (C<sup>Ar</sup>), 126.0 (C<sup>Ar</sup>), 78.0 (CH), 71.2 (CH<sub>2</sub>).

## 6.5 Experimental protocols for Chapter 4

### 6.5.1 Synthesis of methoxyhydroquinone (2)

A two-necked RBF was charged with a solution of vanillin (15.00 g, 98.59 mmol) in THF (395 mL). Deionized water (158 mL) was then added. The mixture was degassed with N<sub>2</sub>. Sodium percarbonate (Na<sub>2</sub>CO<sub>3</sub>·1.5H<sub>2</sub>O<sub>2</sub>, 17.03 g, 108.4 mmol) was then added in portions under N<sub>2</sub> and agitation. The reaction was stirred for 3 h at room temperature. Portions of a HCl solution (0.1 mol L<sup>-1</sup>) were added to the mixture under vigorous stirring until pH = 3 was reached to quench the reaction. The volatiles were evaporated and the aqueous phase was extracted with EtOAc. The organic phases were collected, washed with brine, dried over anhydrous Na<sub>2</sub>SO<sub>4</sub> before the EtOAc was removed under reduced pressure. A white solid was obtained (12.16 g, 86.77 mmol, 88%). Characterization data was in agreement with those reported in the literature.<sup>16</sup> **<sup>1</sup>H NMR** (300 MHz, DMSO) δ 8.69 (s, 1H, CH<sub>3</sub>O-C=C-OH), 8.10 (s, 1H, CH<sub>3</sub>O-C-CH=C-OH), 6.54 (d, 1H, <sup>3</sup>J<sub>H-H</sub> = 8.4 Hz, CH<sub>3</sub>O-C=C-CH), 6.35 (d, 1H, <sup>4</sup>J<sub>H-H</sub> = 2.5 Hz, CH<sub>3</sub>O-C-CH), 6.14 (dd, 1H, <sup>4</sup>J<sub>H-H</sub> = 2.5 Hz, <sup>3</sup>J<sub>H-H</sub> = 8.4 Hz, CH<sub>3</sub>O-C=C-CH=CH), 3.69 (s, 3H, OCH<sub>3</sub>). **<sup>13</sup>C APT NMR** (75 MHz, DMSO) δ 150.3 (CH<sub>3</sub>O-C-CH=C-OH), 148.1 (CH<sub>3</sub>O-C), 138.7 (CH<sub>3</sub>O-C=C-OH), 115.7 (CH<sub>3</sub>O-C=C-CH), 106.2 (CH<sub>3</sub>O-C=C-CH=CH), 100.7 (CH<sub>3</sub>O-C-CH), 55.4 (CH<sub>3</sub>).

### 6.5.2 Synthesis of vanillyl alcohol (4)

Vanillin (15.00 g, 98.6 mmol) was dissolved in MeOH (300 mL) and the mixture was cooled down with an ice-bath. NaBH<sub>4</sub> (7.46 g, 197.15 mmol) were added to the previous mixture in small portions. Once addition was finished, the mixture was allowed to warm to room temperature. After 1 h, the mixture was diluted with EtOAc and extracted 3 times before the organic layers were combined and washed with NH<sub>4</sub>Cl, brine, and dried over Na<sub>2</sub>SO<sub>4</sub>. The EtOAc was removed by evaporation and the solid afforded was dried under high vacuum. A white solid was obtained (13.83 g, 89.73 mmol, 91%). Characterization data was in agreement with those reported in the literature.<sup>17</sup> **<sup>1</sup>H NMR** (300 MHz, DMSO) δ 8.78 (s, 1H, CH<sub>3</sub>O-C=C-OH), 6.88 (s, 1H, CH<sub>3</sub>O-C=C-CH=CH), 6.71-6.70 (m, 2H, CH<sub>3</sub>O-C=C-CH, CH<sub>3</sub>O-C-CH) 5.00 (t, 1H, <sup>3</sup>J<sub>H-H</sub> = 5.7 Hz, CH<sub>2</sub>-OH), 4.38 (d, 2H, <sup>3</sup>J<sub>H-H</sub> = 5.7 Hz, HO-CH<sub>2</sub>), 3.75 (s, 3H, OCH<sub>3</sub>). **<sup>13</sup>C NMR** (75 MHz, DMSO) δ 147.4 (CH<sub>3</sub>O-C), 145.3 (CH<sub>3</sub>O-



C=C-OH), 133.5 (CH<sub>3</sub>O-C-CH=C-CH<sub>2</sub>OH), 119.1 (HO-CH<sub>2</sub>-C-CH=CH), 115.1 (HO-CH<sub>2</sub>-C-CH=CH), 111.0 (CH<sub>3</sub>O-C-CH), 63.0 (HO-CH<sub>2</sub>), 55.4 (CH<sub>3</sub>).

### 6.5.3 General method for synthesis of bis epoxides

**2-((3-methoxy-4-((oxiran-2-ylmethoxy)methyl)phenoxy)methyl)oxirane (5).** A RBF was charged with vanillyl alcohol (5 g, 32.43 mmol) and TEBAC (739 mg, 3.24 mmol). Epichlorohydrin (25.6 mL, 324.32 mmol) was added and the mixture was stirred for 4 h until a slightly pink solution was obtained. This solution was cooled down to 0 °C with an ice bath. A NaOH solution (19.5 g, 486.5 mmol) in deionised water (39 mL) was poured into the cold mixture under vigorous stirring. The reaction was conducted overnight at room temperature (ice bath was left to melt over time). Deionised water was added to the mixture to dilute 4 times the NaOH solution. An equal volume of EtOAc was added. The mixture was stirred and the aqueous phase was extracted 2 more times with EtOAc. The organic phases were combined, rinsed with brine and dried over anhydrous Na<sub>2</sub>SO<sub>4</sub>. EtOAc and excess epichlorohydrin were removed under high vacuum. Further purification was achieved by recrystallization in EtOAc. A white solid was obtained (5.82 g, 21.73 mmol, 67%). Characterization data was in agreement with those reported in the literature.<sup>16</sup> **<sup>1</sup>H NMR** (300 MHz, CDCl<sub>3</sub>) δ 6.91-6.83 (m, 3H, CH<sub>3</sub>O-C-CH, CH<sub>3</sub>O-C=C-CH, CH<sub>3</sub>O-C=C-CH=CH), 4.51 (q, 2H, <sup>3</sup>J<sub>H-H</sub> = 11.6 Hz, CH<sub>3</sub>O-C-CH=C-CH<sub>2</sub>), 4.25-4.20 (m, 1H, CH<sub>3</sub>O-C=C-O-CH<sub>b</sub>) 4.05-4.00 (m, 1H, CH<sub>3</sub>O-C-CH=C-CH<sub>2</sub>-O-CH<sub>b</sub>), 3.87 (s, 3H, CH<sub>3</sub>), 3.78-3.73 (m, 1H, CH<sub>3</sub>O-C=C-O-CH<sub>a</sub>), 3.41-3.37 (m, 2H, CH<sub>3</sub>O-C-CH=C-CH<sub>2</sub>-O-CH<sub>2</sub>-CH, CH<sub>3</sub>O-C=C-O-CH<sub>2</sub>-CH) 3.18-3.16 (m, 1H, CH<sub>3</sub>O-C-CH=C-CH<sub>2</sub>-O-CH<sub>a</sub>), 2.90-2.78 (m, 2H, CH<sub>3</sub>O-C=C-O-CH<sub>2</sub>-CH-CH<sub>b</sub>, CH<sub>3</sub>O-C-CH=C-CH<sub>2</sub>-O-CH<sub>2</sub>-CH-CH<sub>b</sub>), 2.74-2.59 (m, 2H, CH<sub>3</sub>O-C=C-O-CH<sub>2</sub>-CH-CH<sub>a</sub>, CH<sub>3</sub>O-C-CH=C-CH<sub>2</sub>-O-CH<sub>2</sub>-CH-CH<sub>a</sub>). **<sup>13</sup>C APT NMR** (75 MHz, CDCl<sub>3</sub>) δ 149.8 (CH<sub>3</sub>O-C), 147.8 (CH<sub>3</sub>O-C=C), 131.7 (CH<sub>3</sub>O-C-CH=C), 120.5 (CH<sub>3</sub>O-C=C-CH=CH), 114.1 (CH<sub>3</sub>O-C-CH), 111.8 (CH<sub>3</sub>O-C=C-CH), 73.3 (CH<sub>3</sub>O-C-CH=C-CH<sub>2</sub>), 70.8 (CH<sub>3</sub>O-C=C-O-CH<sub>2</sub>), 70.4 (CH<sub>3</sub>O-C-CH=C-CH<sub>2</sub>-O-CH<sub>2</sub>) 56.0 (CH<sub>3</sub>), 51.0 (CH<sub>3</sub>O-C=C-O-CH<sub>2</sub>-CH), 50.3 (CH<sub>3</sub>O-C-CH=C-CH<sub>2</sub>-O-CH<sub>2</sub>-CH), 45.1 (CH<sub>3</sub>O-C=C-O-CH<sub>2</sub>-CH-CH<sub>2</sub>), 44.4 (CH<sub>3</sub>O-C-CH=C-CH<sub>2</sub>-O-CH<sub>2</sub>-CH-CH<sub>2</sub>).

**2,2'-(((3-methoxy-1,4-phenylene)bis(oxy))bis(methylene))bis(oxirane) (6).**

2,2'-(((3-Methoxy-1,4-phenylene)bis(oxy))bis(methylene))bis(oxirane) was prepared according a procedure found in the literature.<sup>16</sup> A RBF was charged with methoxyhydroquinone (8.33 g, 59.47 mmol) and TEBAC (1.355 g, 5.95 mmol). Epichlorohydrin (46.5 mL, 594.7 mmol) was added and the mixture was heated to 80 °C and stirred for 1 h. The solution was then cooled down to room temperature. An aqueous solution of TEBAC (1.355 g, 5.95 mmol) and NaOH (9.50 g, 237.9 mmol) in deionised water (48 mL) was added before the mixture was stirred for 30 minutes at room temperature. EtOAc (50 mL) and deionised water (50 mL) were then added. The mixture was stirred and the aqueous phase was extracted with EtOAc. The organic phases were combined, rinsed with brine and dried on anhydrous Na<sub>2</sub>SO<sub>4</sub>. Ethyl acetate and epichlorohydrin excess were removed under high vacuum. Further purification was achieved by recrystallization from EtOAc. A white solid was obtained (10.80 g, 42.82 mmol, 72%). Characterization data was in agreement with those reported in the literature.<sup>16</sup> **<sup>1</sup>H NMR** (300 MHz, CDCl<sub>3</sub>) δ 6.86 (d, 1H, <sup>3</sup>J<sub>H-H</sub> = 8.7 Hz, CH<sub>3</sub>O-C=C-CH), 6.56 (d, 1H, <sup>4</sup>J<sub>H-H</sub> = 2.6 Hz, CH<sub>3</sub>O-C-CH), 6.38 (dd, 1H, <sup>4</sup>J<sub>H-H</sub> = 2.7 Hz, <sup>3</sup>J<sub>H-H</sub> = 8.7 Hz, CH<sub>3</sub>O-C=C-CH=CH), 4.20-4.15 (m, 2H, CH<sub>3</sub>O-C=C-O-CH<sub>b</sub>, CH<sub>3</sub>O-C-CH=C-O-CH<sub>b</sub>), 3.99-3.91 (m, 2H, CH<sub>3</sub>O-C=C-O-CH<sub>a</sub>, CH<sub>3</sub>O-C-CH=C-O-CH<sub>a</sub>), 3.84 (s, 3H, CH<sub>3</sub>), 3.33 (m, 2H, CH<sub>3</sub>O-C=C-O-CH<sub>2</sub>-CH, CH<sub>3</sub>O-C-CH=C-O-CH<sub>2</sub>-CH), 2.91-2.85 (m, 2H, CH<sub>3</sub>O-C=C-O-CH<sub>2</sub>-CH-CH<sub>b</sub>, CH<sub>3</sub>O-C-CH=C-O-CH<sub>2</sub>-CH-CH<sub>b</sub>), 2.75-2.70 (m, 2H, CH<sub>3</sub>O-C=C-O-CH<sub>2</sub>-CH-CH<sub>a</sub>, CH<sub>3</sub>O-C-CH=C-O-CH<sub>2</sub>-CH-CH<sub>a</sub>). **<sup>13</sup>C APT NMR** (75 MHz, CDCl<sub>3</sub>) δ 154.2 (CH<sub>3</sub>O-C-CH=C), 151.0 (CH<sub>3</sub>O-C), 142.8 (CH<sub>3</sub>O-C=C), 116.0 (C<sup>5</sup> CH<sub>3</sub>O-C=C-CH), 104.3 (CH<sub>3</sub>O-C=C-CH=CH), 101.4 (CH<sub>3</sub>O-C-CH), 71.5 (CH<sub>3</sub>O-C=C-O-CH<sub>2</sub>), 69.4 (CH<sub>3</sub>O-C-CH=C-O-CH<sub>2</sub>), 56.0 (CH<sub>3</sub>), 50.5 (CH<sub>3</sub>O-C=C-O-CH<sub>2</sub>-CH), 50.3 (CH<sub>3</sub>O-C-CH=C-O-CH<sub>2</sub>-CH), 45.0 (CH<sub>3</sub>O-C=C-O-CH<sub>2</sub>-CH-CH<sub>2</sub>), 44.8 (CH<sub>3</sub>O-C-CH=C-O-CH<sub>2</sub>-CH-CH<sub>2</sub>).

**Oxiran-2-ylmethyl 3-methoxy-4-(oxiran-2-ylmethoxy)-benzoate (7).** Prepared following the same procedure as compound **4**. A white solid was obtained (12.22 g, 50.55 mmol, 85%). Characterization data was in agreement with those reported in the literature.<sup>16</sup> **<sup>1</sup>H NMR** (300 MHz, CDCl<sub>3</sub>) δ 7.69 (dd, 1H, <sup>4</sup>J<sub>H-H</sub> = 1.8 Hz, <sup>3</sup>J<sub>H-H</sub> = 8.4 Hz, CH<sub>3</sub>O-C=C-CH=CH), 7.57 (d, 1H, <sup>4</sup>J<sub>H-H</sub> = 1.7 Hz, CH<sub>3</sub>O-C-CH), 6.94 (d, 1H, <sup>3</sup>J<sub>H-H</sub> = 8.5 Hz, CH<sub>3</sub>O-C=C-CH), 4.64 (m, 1H, CH<sub>3</sub>O-C-CH=C-CO<sub>2</sub>-CH<sub>b</sub>),

4.34 (m, 1H, CH<sub>3</sub>O-C=C-O-CH<sub>b</sub>), 4.17-4.05 (m, 2H, CH<sub>3</sub>O-C=C-O-CH<sub>a</sub>, CH<sub>3</sub>O-C-CH=C-CO<sub>2</sub>-CH<sub>a</sub>), 3.92 (s, 3H, CH<sub>3</sub>), 3.41-3.33 (m, 2H, CH<sub>3</sub>O-C=C-O-CH<sub>2</sub>-CH, CH<sub>3</sub>O-C-CH=C-CO<sub>2</sub>-CH<sub>2</sub>-CH), 2.94-2.88 (m, 2H, CH<sub>3</sub>O-C=C-O-CH<sub>2</sub>-CH-CH<sub>b</sub>, CH<sub>3</sub>O-C-CH=C-CO<sub>2</sub>-CH<sub>2</sub>-CH-CH<sub>b</sub>), 2.78-2.71 (m, 2H, CH<sub>3</sub>O-C=C-O-CH<sub>2</sub>-CH-CH<sub>a</sub>, CH<sub>3</sub>O-C-CH=C-CO<sub>2</sub>-CH<sub>2</sub>-CH-CH<sub>a</sub>). <sup>13</sup>C APT NMR (75 MHz, CDCl<sub>3</sub>) δ 164.5 (CH<sub>3</sub>O-C-CH=C-CO<sub>2</sub>), 153.2 (CH<sub>3</sub>O-C=C), 149.2 (CH<sub>3</sub>O-C), 123.8 (CH<sub>3</sub>O-C=C-CH=CH), 123.0 (CH<sub>3</sub>O-C-CH=C), 112.8 (CH<sub>3</sub>O-C-CH), 112.4 (CH<sub>3</sub>O-C=C-CH), 70.0 (CH<sub>3</sub>O-C=C-O-CH<sub>2</sub>), 65.6 (CH<sub>3</sub>O-C-CH=C-CO<sub>2</sub>-CH<sub>2</sub>), 56.2 (CH<sub>3</sub>), 50.1 (CH<sub>3</sub>O-C=C-O-CH<sub>2</sub>-CH), 49.7 (CH<sub>3</sub>O-C-CH=C-CO<sub>2</sub>-CH<sub>2</sub>-CH), 45.0 (CH<sub>3</sub>O-C=C-O-CH<sub>2</sub>-CH-CH<sub>2</sub>), 44.9 (CH<sub>3</sub>O-C-CH=C-CO<sub>2</sub>-CH<sub>2</sub>-CH-CH<sub>2</sub>).

#### 6.5.4 General method for the synthesis of bis carbonates

The corresponding bis-epoxide (24.97 mmol) was dissolved in DMF (25 mL) in a cylindrical glass vessel. To this mixture [HDBU]I (699 mg, 2.50 mmol) was added before it was placed in a stainless steel autoclave. The autoclave was subsequently sealed and filled to a pressure of 3 MPa of CO<sub>2</sub>. The autoclave was heated to 110 °C using an oil bath for 48 h to ensure full conversion of the bis-epoxide. After 48 h the autoclave was allowed to cool down in an ice bath and the CO<sub>2</sub> was vented. The reaction crude was diluted in EtOAc (150 mL) and transferred to a separation funnel. Distilled water (150 mL) was added and aqueous phase was extracted three times. The organic layers were combined and washed with brine, then dried over Na<sub>2</sub>SO<sub>4</sub>, filtered and concentrated under vacuum. The obtained crude was further purified by recrystallization in EtOAc.

**4-((2-methoxy-4-(((2-oxo-1,3-dioxolan-4-yl)methoxy)methyl)phenoxy)methyl)-1,3-dioxolan-2-one (8)**. A slightly yellow oil was obtained and further purified by flash column chromatography (6.97 g, 20.48 mmol, 82%). Characterization data was in agreement with those reported in the literature.<sup>16</sup> <sup>1</sup>H NMR (300 MHz, DMSO) δ 6.98 (d, 2H, <sup>3</sup>J<sub>H-H</sub> = 8.2 Hz, CH<sub>3</sub>O-C-CH, CH<sub>3</sub>O-C=C-CH), 6.85 (d, 1H, <sup>3</sup>J<sub>H-H</sub> = 8.1 Hz, CH<sub>3</sub>O-C=C-CH=CH), 5.13-5.12 (m, 1H, CH<sub>3</sub>O-C=C-O-CH<sub>2</sub>-CH), 4.96-4.94 (m, 1H, CH<sub>3</sub>O-C-CH=C-CH<sub>2</sub>-O-CH<sub>2</sub>-CH), 4.62 (t, 1H, <sup>3</sup>J<sub>H-H</sub> = 8.5 Hz, CH<sub>3</sub>O-C-CH=C-O-CH<sub>2</sub>-CH-CH<sub>b</sub>), 4.55-4.48 (m, 3H, CH<sub>3</sub>O-C-CH=C-CH<sub>2</sub>, CH<sub>3</sub>O-C-CH=C-O-CH<sub>2</sub>-CH-CH<sub>a</sub>), 4.42-4.37 (m,

1H, CH<sub>3</sub>O-C-CH=C-CH<sub>2</sub>-O-CH<sub>2</sub>-CH-CH<sub>b</sub>), 4.31-4.14 (m, 3H, CH<sub>3</sub>O-C=C-O-CH<sub>2</sub>, CH<sub>3</sub>O-C-CH=C-CH<sub>2</sub>-O-CH<sub>2</sub>-CH-CH<sub>a</sub>), 3.87 (s, 3H, CH<sub>3</sub>), 3.70-3.56 (m, 2H, CH<sub>3</sub>O-C-CH=C-CH<sub>2</sub>-O-CH<sub>2</sub>). <sup>13</sup>C APT NMR (75 MHz, DMSO) δ 155.0 (CH<sub>3</sub>O-C-CH=C-O-CH<sub>2</sub>-CH-OCO<sub>2</sub>, CH<sub>3</sub>O-C=C-CH<sub>2</sub>-O-CH<sub>2</sub>-CH-OCO<sub>2</sub>), 149.2 (CH<sub>3</sub>O-C), 147.0 (CH<sub>3</sub>O-C-CH=C-CH<sub>2</sub>), 131.7 (CH<sub>3</sub>O-C-CH=C), 120.0 (CH<sub>3</sub>O-C=C-CH=CH), 114.4 (CH<sub>3</sub>O-C=C-CH), 112.0 (CH<sub>3</sub>O-C-CH), 75.5 (CH<sub>3</sub>O-C-CH=C-CH<sub>2</sub>-O-CH<sub>2</sub>-CH), 75.0 (CH<sub>3</sub>O-C=C-O-CH<sub>2</sub>-CH), 72.1 (CH<sub>3</sub>O-C-CH=C-CH<sub>2</sub>), 68.9 (CH<sub>3</sub>O-C=C-O-CH<sub>2</sub>), 68.8 (CH<sub>3</sub>O-C-CH=C-CH<sub>2</sub>-O-CH<sub>2</sub>), 66.2 (CH<sub>3</sub>O-C-CH=C-CH<sub>2</sub>-O-CH<sub>2</sub>-CH-CH<sub>2</sub>), 66.0 (CH<sub>3</sub>O-C=C-O-CH<sub>2</sub>-CH-CH<sub>2</sub>), 55.6 (CH<sub>3</sub>).

**4,4'-(((3-methoxy-1,4-phenylene)bis(oxy))bis(methylene))bis(1,3-dioxolan-2-one) (9).** A white solid was obtained (6.60 g, 20.23 mmol, 81%). Characterization data was in agreement with those reported in the literature.<sup>16</sup> <sup>1</sup>H NMR (300 MHz, DMSO) δ 6.93 (d, 1H, <sup>3</sup>J<sub>H-H</sub> = 8.8 Hz, CH<sub>3</sub>O-C=C-CH), 6.63 (d, 1H, <sup>4</sup>J<sub>H-H</sub> = 2.6 Hz, CH<sub>3</sub>O-C-CH), 6.47 (dd, 1H, <sup>4</sup>J<sub>H-H</sub> = 2.7 Hz, <sup>3</sup>J<sub>H-H</sub> = 8.7 Hz, CH<sub>3</sub>O-C=C-CH=CH), 5.14-5.07 (m, 2H, CH<sub>3</sub>O-C-CH=C-O-CH<sub>2</sub>-CH, CH<sub>3</sub>O-C=C-O-CH<sub>2</sub>-CH), 4.65-4.58 (m, 2H, CH<sub>3</sub>O-C=C-O-CH<sub>2</sub>-CH-CH<sub>b</sub>, CH<sub>3</sub>O-C-CH=C-O-CH<sub>2</sub>-CH-CH<sub>b</sub>), 4.42-4.35 (m, 2H, CH<sub>3</sub>O-C=C-O-CH<sub>2</sub>-CH-CH<sub>a</sub>, CH<sub>3</sub>O-C-CH=C-O-CH<sub>2</sub>-CH-CH<sub>a</sub>), 4.27-4.06 (m, 4H, CH<sub>3</sub>O-C=C-O-CH<sub>2</sub>, CH<sub>3</sub>O-C-CH=C-O-CH<sub>2</sub>) 3.76 (s, 3H, CH<sub>3</sub>). <sup>13</sup>C APT NMR (75 MHz, DMSO) δ 161.9 (CH<sub>3</sub>O-C-CH=C-O-CH<sub>2</sub>-CH-OCO<sub>2</sub>, CH<sub>3</sub>O-C=C-O-CH<sub>2</sub>-CH-OCO<sub>2</sub>), 153.6 (CH<sub>3</sub>O-C-CH=C), 150.5 (CH<sub>3</sub>O-C), 142.1 (CH<sub>3</sub>O-C-CH=C-CH<sub>2</sub>), 116.3 (CH<sub>3</sub>O-C=C-CH), 104.8 (CH<sub>3</sub>O-C=C-CH=CH), 101.3 (CH<sub>3</sub>O-C-CH), 75.1 (CH<sub>3</sub>O-C=C-O-CH<sub>2</sub>-CH), 74.9 (CH<sub>3</sub>O-C-CH=C-O-CH<sub>2</sub>-CH), 69.7 (CH<sub>3</sub>O-C=C-O-CH<sub>2</sub>), 67.9 (CH<sub>3</sub>O-C-CH=C-O-CH<sub>2</sub>), 66.0 (CH<sub>3</sub>O-C=C-O-CH<sub>2</sub>-CH-CH<sub>2</sub>), 65.9 (CH<sub>3</sub>O-C-CH=C-O-CH<sub>2</sub>-CH-CH<sub>2</sub>), 55.7 (CH<sub>3</sub>).

**(2-oxo-1,3-dioxolan-4-yl)methyl 3-methoxy-4-((2-oxo-1,3-dioxolan-4-yl)methoxy)benzoate (10).** A white solid was obtained (7.61 g, 20.48 mmol, 82%). Characterization data was in agreement with those reported in the literature.<sup>16</sup> <sup>1</sup>H NMR (300 MHz, DMSO) δ 7.57 (dd, 1H, <sup>4</sup>J<sub>H-H</sub> = 1.7 Hz, <sup>3</sup>J<sub>H-H</sub> = 8.4 Hz, CH<sub>3</sub>O-C=C-CH=CH), 7.47 (d, 1H, <sup>4</sup>J<sub>H-H</sub> = 1.7 Hz, CH<sub>3</sub>O-C-CH), 7.15 (d, 1H, <sup>3</sup>J<sub>H-H</sub> = 8.5 Hz, CH<sub>3</sub>O-C=C-CH), 5.19-5.17 (m, 2H, CH<sub>3</sub>O-C=C-O-CH<sub>2</sub>-CH, CH<sub>3</sub>O-C-CH=C-CO<sub>2</sub>-CH<sub>2</sub>-CH), 4.67-4.61 (m, 2H, CH<sub>3</sub>O-C-CH=C-O-CH<sub>2</sub>-CH-CH<sub>b</sub>, CH<sub>3</sub>O-C-CH=C-CO<sub>2</sub>-CH<sub>2</sub>-CH-CH<sub>b</sub>), 4.52-4.32 (m, 6H, CH<sub>3</sub>O-C-CH=C-O-CH<sub>2</sub>-CH-CH<sub>a</sub>,

CH<sub>3</sub>O-C=C-O-CH<sub>2</sub>, CH<sub>3</sub>O-C=C-O-CH<sub>2</sub>, CH<sub>3</sub>O-C-CH=C-CO<sub>2</sub>-CH<sub>2</sub>-CH-CH<sub>a</sub>), 3.82 (s, 3H, CH<sub>3</sub>). <sup>13</sup>C APT NMR (75 MHz, DMSO) δ 164.4 (CH<sub>3</sub>O-C-CH=C-CO<sub>2</sub>), 154.9 (CH<sub>3</sub>O-C-CH=C-O-CH<sub>2</sub>-CH-OCO<sub>2</sub>), 154.7 (CH<sub>3</sub>O-C=C-CO<sub>2</sub>-CH<sub>2</sub>-CH-OCO<sub>2</sub>), 151.9 (CH<sub>3</sub>O-C-CH=C-CH<sub>2</sub>), 148.8 (CH<sub>3</sub>O-C), 123.1 (CH<sub>3</sub>O-C=C-CH=CH), 122.1 (CH<sub>3</sub>O-C-CH=C), 113.0 (CH<sub>3</sub>O-C-CH), 112.4 (CH<sub>3</sub>O-C=C-CH), 74.7 (CH<sub>3</sub>O-C=C-O-CH<sub>2</sub>-CH), 74.4 (CH<sub>3</sub>O-C-CH=C-CO<sub>2</sub>-CH<sub>2</sub>-CH), 68.4 (CH<sub>3</sub>O-C=C-O-CH<sub>2</sub>), 66.4 (CH<sub>3</sub>O-C=C-O-CH<sub>2</sub>-CH-CH<sub>2</sub>), 65.9 (CH<sub>3</sub>O-C-CH=C-CO<sub>2</sub>-CH<sub>2</sub>-CH-CH<sub>2</sub>), 64.3 (CH<sub>3</sub>O-C-CH=C-CO<sub>2</sub>-CH<sub>2</sub>), 55.7 (CH<sub>3</sub>).

### 6.5.5 General method for the synthesis of NIPUs

In a vial, equimolecular amounts of bis-amine and bis-carbonate were dissolved in DMSO (1 mL). The mixture was heated up to 80 °C for 24 hours in an oil bath. Then mixture was allowed to cool down before being precipitated into CH<sub>2</sub>Cl<sub>2</sub> in a falcon tube. The suspension was centrifuged and CH<sub>2</sub>Cl<sub>2</sub> was decanted. The polymer obtained was dried under high vacuum affording a solid foam.

**NIPU 11.** <sup>1</sup>H NMR (300 MHz, DMSO) δ 7.20-7.08 (m, 2H, NH-CO<sub>2</sub>), 6.93-6.90 (m, 2H, CH<sub>3</sub>O-C-CH=C-CH=CH), 6.83-6.80 (s, 1H, CH<sub>3</sub>O-C=C-CH=CH), 5.19 (s, 1H, CH<sub>3</sub>O-C-CH=C-CH<sub>2</sub>-O-CH<sub>2</sub>-CH-OH), 4.96 (s, 1H, CH<sub>3</sub>O-C=C-O-CH<sub>2</sub>-CH-CH<sub>2</sub>-OH), 4.89-4.71 (m, 1H, CH<sub>3</sub>O-C=C-O-CH<sub>2</sub>-CH), 4.39 (m, 2H, CH<sub>3</sub>O-C=C-CH<sub>2</sub>), 4.00-3.89 (m, 7H, CH<sub>3</sub>O-C-CH=C-CH<sub>2</sub>-O-CH<sub>2</sub>-CH-CH<sub>anti</sub>-O-CONH, CH<sub>3</sub>O-C=C-O-CH<sub>2</sub>-CH-CH<sub>2</sub>-OH), 3.74 (m, 3H, CH<sub>3</sub>O), 3.57, (s, 1H, CH<sub>3</sub>O-C-CH=C-CH<sub>2</sub>-O-CH<sub>2</sub>-CH-OH), 2.95-2.93 (m, 4H), 1.36-1.22 (m, 8H, CH<sub>2</sub>-CH<sub>2</sub>-NH-CO<sub>2</sub>). <sup>13</sup>C APT NMR (75 MHz, DMSO) δ 156.2 (CH<sub>3</sub>O-C=C-O-CH<sub>2</sub>-CH-O-CONH), 149.0 (CH<sub>3</sub>O-C=C), 147.4 (CH<sub>3</sub>O-C), 131.3 (CH<sub>3</sub>O-C-CH=C), 120.0 (CH<sub>3</sub>O-C=C-CH=CH), 113.3 (CH<sub>3</sub>O-C=C-CH), 111.9 (CH<sub>3</sub>O-C-CH), 72.2 (CH<sub>3</sub>O-C=C-O-CH<sub>2</sub>), 71.3 (CH<sub>3</sub>O-C-CH=C-CH<sub>2</sub>), 70.3 (CH<sub>3</sub>O-C-CH=C-CH<sub>2</sub>-O-CH<sub>2</sub>-CH-CH<sub>2</sub>), 67.8 (CH<sub>3</sub>O-C=C-O-CH<sub>2</sub>-CH<sub>2</sub>), 67.3 (CH<sub>3</sub>O-C-CH=C-CH<sub>2</sub>-O-CH<sub>2</sub>-CH), 65.5 (CH<sub>3</sub>O-C=C-O-CH<sub>2</sub>-CH<sub>2</sub>-CH-CH<sub>2</sub>), 65.1 (CH<sub>3</sub>O-C-CH=C-CH<sub>2</sub>-O-CH<sub>2</sub>), 55.5 (CH<sub>3</sub>O), 40.2 (CH<sub>2</sub>-NH-CO<sub>2</sub>), 29.4 (CH<sub>2</sub>-CH<sub>2</sub>-NH-CO<sub>2</sub>), 26.0 (CH<sub>2</sub>-CH<sub>2</sub>-CH<sub>2</sub>-NH-CO<sub>2</sub>). M<sub>n</sub> = 20.044 g/mol, Đ<sub>M</sub> = 1.51 (Determined by SEC analysis in DMF against poly(styrene) (PS) standards using RI detection).

**NIPU 12.**  $^1\text{H NMR}$  (300 MHz, DMSO)  $\delta$  7.15-7.13 (m, 2H,  $\text{NH-CO}_2$ ), 6.92-6.90 (m, 2H,  $\text{CH}_3\text{O-C-CH=C-CH=CH}$ ), 6.83-6.81 (s, 1H,  $\text{CH}_3\text{O-C=C-CH=CH}$ ), 5.20 (s, 1H,  $\text{CH}_3\text{O-C-CH=C-CH}_2\text{-O-CH}_2\text{-CH-OH}$ ), 4.96 (s, 1H,  $\text{CH}_3\text{O-C=C-O-CH}_2\text{-CH-CH}_2\text{-OH}$ ), 4.85-4.73 (m, 1H,  $\text{CH}_3\text{O-C-CH=C-CH}_2\text{-O-CH}_2\text{-CH-CH}_{\text{syn}}\text{-O-CONH}$ ), 4.39 (m, 2H,  $\text{CH}_3\text{O-C=C-CH}_2$ ) 4.00-3.89 (m, 7H,  $\text{CH}_3\text{O-C-CH=C-CH}_2\text{-O-CH}_2\text{-CH-CH}_{\text{anti}}\text{-O-CONH}$ ,  $\text{CH}_3\text{O-C=C-O-CH}_2\text{-CH-CH}_2\text{-OH}$ ), 3.75 (m, 3H,  $\text{CH}_3\text{O}$ ), 3.57, (s, 1H,  $\text{CH}_3\text{O-C-CH=C-CH}_2\text{-O-CH}_2\text{-CH-OH}$ ), 2.94 (m, 4H), 1.36 (m, 4H,  $\text{CH}_2\text{-CH}_2\text{-NH-CO}_2$ ).  $^{13}\text{C APT NMR}$  (75 MHz, DMSO)  $\delta$  156.2 ( $\text{CH}_3\text{O-C=C-O-CH}_2\text{-CH-O-CONH}$ ), 149.0 ( $\text{CH}_3\text{O-C=C}$ ), 147.4 ( $\text{CH}_3\text{O-C}$ ), 131.3 ( $\text{CH}_3\text{O-C-CH=C}$ ), 120.0 ( $\text{CH}_3\text{O-C=C-CH=CH}$ ), 113.2 ( $\text{CH}_3\text{O-C=C-CH}$ ), 111.8 ( $\text{CH}_3\text{O-C-CH}$ ), 72.2 ( $\text{CH}_3\text{O-C=C-O-CH}_2$ ), 71.3 ( $\text{CH}_3\text{O-C-CH=C-CH}_2$ ), 70.3 ( $\text{CH}_3\text{O-C-CH=C-CH}_2\text{-O-CH}_2\text{-CH-CH}_2$ ), 67.9 ( $\text{CH}_3\text{O-C=C-O-CH}_2\text{-CH}_2$ ), 67.3 ( $\text{CH}_3\text{O-C-CH=C-CH}_2\text{-O-CH}_2\text{-CH}$ ), 65.5 ( $\text{CH}_3\text{O-C=C-O-CH}_2\text{-CH}_2\text{-CH-CH}_2$ ), 65.2 ( $\text{CH}_3\text{O-C-CH=C-CH}_2\text{-O-CH}_2$ ), 55.5 ( $\text{CH}_3\text{O}$ ), 40.2 ( $\text{CH}_2\text{-NH-CO}_2$ ), 28.7 ( $\text{CH}_2\text{-CH}_2\text{-NH-CO}_2$ ).  $M_n = 6.808$  g/mol,  $D_M = 1.76$  (Determined by SEC analysis in DMF against poly(styrene) (PS) standards using RI detection).

**NIPU 13.**  $^1\text{H NMR}$  (300 MHz, DMSO)  $\delta$  7.20-7.10 (m, 2H,  $\text{NH-CO}_2$ ), 6.85 (d, 1H,  $^3J_{\text{H-H}} = 8.8$  Hz,  $\text{CH}_3\text{O-C=C-CH}$ ), 6.56 (s, 1H,  $\text{CH}_3\text{O-C-CH}$ ), 6.42-6.38 (m, 1H,  $\text{CH}_3\text{O-C=C-CH=CH}$ ), 5.19 (s, 1H,  $\text{CH}_3\text{O-C=C-O-CH}_2\text{-CH-CH}_2\text{-OH}$ ), 5.13 (s, 1H,  $\text{CH}_3\text{O-C-CH=C-O-CH}_2\text{-CH-OH}$ ), 4.91-4.81 (m, 1H,  $\text{CH}_3\text{O-C=C-O-CH}_2\text{-CH-CH}_2\text{-OH}$ ), 4.06-3.78 (m, 8H,  $\text{CH}_3\text{O-C-CH=C-O-CH}_2\text{-CH-CH}_2\text{-O-CONH}$ ,  $\text{CH}_3\text{O-C=C-O-CH}_2\text{-CH-CH}_2\text{-OH}$ ), 3.74 (m, 3H,  $\text{CH}_3\text{O}$ ), 3.57, (s, 1H,  $\text{CH}_3\text{O-C-CH=C-O-CH}_2\text{-CH-OH}$ ), 2.94 (d, 4H,  $^3J_{\text{H-H}} = 6.4$  Hz,  $\text{CH}_2\text{-NH-CO}_2$ ), 1.36-1.22 (m, 8H,  $\text{CH}_2\text{-CH}_2\text{-NH-CO}_2$ ).  $^{13}\text{C APT NMR}$  (75 MHz, DMSO)  $\delta$  156.2 ( $\text{CH}_3\text{O-C=C-O-CH}_2\text{-CH-O-CONH}$ ), 153.6 ( $\text{CH}_3\text{O-C-CH=C}$ ), 150.2 ( $\text{CH}_3\text{O-C}$ ), 142.3 ( $\text{CH}_3\text{O-C=C}$ ), 115.2 ( $\text{CH}_3\text{O-C=C-CH}$ ), 104.3 ( $\text{CH}_3\text{O-C=C-CH=CH}$ ), 101.1 ( $\text{CH}_3\text{O-C-CH}$ ), 71.2 ( $\text{CH}_3\text{O-C-CH=C-O-CH}_2\text{-CH-CH}_2$ ), 69.7 ( $\text{CH}_3\text{O-C=C-O-CH}_2$ ), 67.4 ( $\text{CH}_3\text{O-C-CH=C-O-CH}_2\text{-CH}$ ), 65.1 ( $\text{CH}_3\text{O-C=C-O-CH}_2\text{-CH}$ ), 55.6 ( $\text{CH}_3\text{O}$ ), 40.2 ( $\text{CH}_2\text{-NH-CO}_2$ ), 29.4 ( $\text{CH}_2\text{-CH}_2\text{-NH-CO}_2$ ), 26.0 ( $\text{CH}_2\text{-CH}_2\text{-CH}_2\text{-NH-CO}_2$ ).  $M_n = 16.782$  g/mol,  $D_M = 1.81$  (Determined by SEC analysis in DMF against poly(styrene) (PS) standards using RI detection).

**NIPU 14.**  $^1\text{H NMR}$  (300 MHz, DMSO)  $\delta$  7.22-7.16 (m, 2H,  $\text{NH-CO}_2$ ), 6.85 (d, 1H,  $^3J_{\text{H-H}} = 8.7$  Hz,  $\text{CH}_3\text{O-C=C-CH}$ ), 6.56 (s, 1H,  $\text{CH}_3\text{O-C-CH}$ ), 6.42-6.39 (m, 1H,

CH<sub>3</sub>O-C=C-CH=CH), 5.21 (s, 1H, CH<sub>3</sub>O-C=C-O-CH<sub>2</sub>-CH-CH<sub>2</sub>-OH), 5.16 (s, 1H, CH<sub>3</sub>O-C-CH=C-O-CH<sub>2</sub>-CH-OH), 4.93-4.84 (m, 1H, CH<sub>3</sub>O-C=C-O-CH<sub>2</sub>-CH-CH<sub>2</sub>-OH), 4.02-3.82 (m, 8H, CH<sub>3</sub>O-C-CH=C-O-CH<sub>2</sub>-CH-CH<sub>2</sub>-O-CONH, CH<sub>3</sub>O-C=C-O-CH<sub>2</sub>-CH-CH<sub>2</sub>-OH), 3.74 (m, 3H, CH<sub>3</sub>O), 3.56, (s, 1H, CH<sub>3</sub>O-C-CH=C-O-CH<sub>2</sub>-CH-OH), 2.95 (d, 4H, <sup>3</sup>J<sub>H-H</sub> = 6.4 Hz, CH<sub>2</sub>-NH-CO<sub>2</sub>), 1.36 (m, 4H, CH<sub>2</sub>-CH<sub>2</sub>-NH-CO<sub>2</sub>). <sup>13</sup>C APT NMR (75 MHz, DMSO) δ 156.2 (CH<sub>3</sub>O-C=C-O-CH<sub>2</sub>-CH-O-CONH), 153.6 (CH<sub>3</sub>O-C-CH=C), 150.2 (CH<sub>3</sub>O-C), 142.3 (CH<sub>3</sub>O-C=C), 115.2 (CH<sub>3</sub>O-C=C-CH), 104.3 (CH<sub>3</sub>O-C=C-CH=CH), 101.1 (CH<sub>3</sub>O-C-CH), 71.2 (CH<sub>3</sub>O-C-CH=C-O-CH<sub>2</sub>-CH-CH<sub>2</sub>), 69.7 (CH<sub>3</sub>O-C=C-O-CH<sub>2</sub>), 67.4 (CH<sub>3</sub>O-C-CH=C-O-CH<sub>2</sub>-CH), 65.2 (CH<sub>3</sub>O-C=C-O-CH<sub>2</sub>-CH), 55.6 (CH<sub>3</sub>O), 40.0 (CH<sub>2</sub>-NH-CO<sub>2</sub>), 26.8 (CH<sub>2</sub>-CH<sub>2</sub>-NH-CO<sub>2</sub>). M<sub>n</sub> = 14.466 g/mol, Đ<sub>M</sub> = 1.80 (Determined by SEC analysis in DMF against poly(styrene) (PS) standards using RI detection).

**NIPU 15.** <sup>1</sup>H NMR (300 MHz, DMSO) δ 7.61-7.49 (m, 2H, CH<sub>3</sub>O-C-CH=C-CH=CH), 7.13-7.06 (m, 3H, CH<sub>3</sub>O-C-CH=C-CH, NH-CO<sub>2</sub>), 5.30 (s, 1H, CH<sub>3</sub>O-C-CH=C-CO<sub>2</sub>-CH<sub>2</sub>-CH-OH), 4.94 (s, 1H, CH<sub>3</sub>O-C=C-O-CH<sub>2</sub>-CH-CH<sub>2</sub>-OH), 4.19 (s, 2H, CH<sub>3</sub>O-C-CH=C-CO<sub>2</sub>-CH<sub>2</sub>), 4.00 (s, 6H, CH<sub>3</sub>O-C-CH=C-CO<sub>2</sub>-CH<sub>2</sub>-CH-CH<sub>2</sub>, CH<sub>3</sub>O-C=C-O-CH<sub>2</sub>-CH-CH<sub>2</sub>), 3.82 (m, 3H, CH<sub>3</sub>O), 3.59, (s, 1H, CH<sub>3</sub>O-C-CH=C-CO<sub>2</sub>-CH<sub>2</sub>-CH), 2.93 (s, 4H, CH<sub>2</sub>-NH-CO<sub>2</sub>), 1.35-1.21 (m, 8H, CH<sub>2</sub>-CH<sub>2</sub>-CH<sub>2</sub>-NH-CO<sub>2</sub>). <sup>13</sup>C APT NMR (75 MHz, DMSO) δ 165.4 (CH<sub>3</sub>O-C-CH=C-CO<sub>2</sub>), 156.1 (CH<sub>3</sub>O-C=C-O-CH<sub>2</sub>-CH-O-CONH), 152.3 (CH<sub>3</sub>O-C=C), 148.6 (CH<sub>3</sub>O-C), 122.0 (CH<sub>3</sub>O-C-CH=C), 112.2 (CH<sub>3</sub>O-C-CH, CH<sub>3</sub>O-C-CH=C-CH=CH), 70.1 (CH<sub>3</sub>O-C-CH=C-CO<sub>2</sub>-CH<sub>2</sub>-CH-CH<sub>2</sub>), 70.0 (CH<sub>3</sub>O-C=C-O-CH<sub>2</sub>), 67.1 (CH<sub>3</sub>O-C-CH=C-O-CH<sub>2</sub>-CH), 66.7 (CH<sub>3</sub>O-C-CH=C-CO<sub>2</sub>-CH<sub>2</sub>-CH), 65.0 (CH<sub>3</sub>O-C-CH=C-CO<sub>2</sub>-CH<sub>2</sub>-CH-CH<sub>2</sub>), 64.9 (CH<sub>3</sub>O-C=C-O-CH<sub>2</sub>-CH-CH<sub>2</sub>), 55.7 (CH<sub>3</sub>O), 40.2 (CH<sub>2</sub>-NH-CO<sub>2</sub>), 29.4 (CH<sub>2</sub>-CH<sub>2</sub>-NH-CO<sub>2</sub>), 26.0 (CH<sub>2</sub>-CH<sub>2</sub>-CH<sub>2</sub>-NH-CO<sub>2</sub>). M<sub>n</sub> = 13.489 g/mol, Đ<sub>M</sub> = 1.93 (Determined by SEC analysis in DMF against poly(styrene) (PS) standards using RI detection).

**NIPU 16.** <sup>1</sup>H NMR (300 MHz, DMSO) δ 7.61-7.44 (m, 2H, CH<sub>3</sub>O-C-CH=C-CH=CH), 7.25-7.06 (m, 3H, CH<sub>3</sub>O-C-CH=C-CH, NH-CO<sub>2</sub>), 5.33-5.29 (m, 1H, CH<sub>3</sub>O-C-CH=C-CO<sub>2</sub>-CH<sub>2</sub>-CH-OH), 4.99-4.94 (s, 1H, CH<sub>3</sub>O-C=C-O-CH<sub>2</sub>-CH-CH<sub>2</sub>-OH), 4.21-4.17 (s, 2H, CH<sub>3</sub>O-C-CH=C-CO<sub>2</sub>-CH<sub>2</sub>), 4.00 (s, 6H, CH<sub>3</sub>O-C-CH=C-CO<sub>2</sub>-CH<sub>2</sub>-CH-CH<sub>2</sub>, CH<sub>3</sub>O-C=C-O-CH<sub>2</sub>-CH-CH<sub>2</sub>), 3.82 (m, 3H, CH<sub>3</sub>O), 3.59, (s, 1H, CH<sub>3</sub>O-C-CH=C-CO<sub>2</sub>-CH<sub>2</sub>-CH), 2.93 (s, 4H, CH<sub>2</sub>-NH-CO<sub>2</sub>), 1.36 (s,

4H, CH<sub>2</sub>-CH<sub>2</sub>-NH-CO<sub>2</sub>). <sup>13</sup>C APT NMR (75 MHz, DMSO) δ 165.4 (CH<sub>3</sub>O-C-CH=C-CO<sub>2</sub>), 156.2 (CH<sub>3</sub>O-C=C-O-CH<sub>2</sub>-CH-O-CONH), 152.3 (CH<sub>3</sub>O-C=C), 148.5 (CH<sub>3</sub>O-C), 123.3 (CH<sub>3</sub>O-C-CH=C-CH), 122.0 (CH<sub>3</sub>O-C-CH=C), 112.1 (CH<sub>3</sub>O-C-CH=C-CH=CH), 70.2 (CH<sub>3</sub>O-C-CH=C-CO<sub>2</sub>-CH<sub>2</sub>-CH-CH<sub>2</sub>), 70.1 (CH<sub>3</sub>O-C=C-O-CH<sub>2</sub>), 67.1 (CH<sub>3</sub>O-C-CH=C-CO<sub>2</sub>-CH<sub>2</sub>-CH), 66.7 (CH<sub>3</sub>O-C-CH=C-O-CH<sub>2</sub>-CH), 65.7 (CH<sub>3</sub>O-C-CH=C-CO<sub>2</sub>-CH<sub>2</sub>-CH-CH<sub>2</sub>), 65.0 (CH<sub>3</sub>O-C=C-O-CH<sub>2</sub>-CH-CH<sub>2</sub>), 55.6 (CH<sub>3</sub>O), 40.0 (CH<sub>2</sub>-NH-CO<sub>2</sub>), 26.7 (CH<sub>2</sub>-CH<sub>2</sub>-NH-CO<sub>2</sub>). M<sub>n</sub> = 11.822 g/mol, Đ<sub>M</sub> = 1.94 (Determined by SEC analysis in DMF against poly(styrene) (PS) standards using RI detection).

## 6.6 General protocols for Chapter 5

### 6.6.1 Synthesis of bis cyclic carbonates

#### 6.6.1.1 Synthesis of 6,6'-(ethane-1,2-diyl)bis(1,3,6-dioxazocan-2-one) (1)

A 1 L single neck RBF was charged with a stir bar, *N, N, N', N'*-tetrakis(2-hydroxyethyl)ethylenediamine (5.00 g, 21.16 mmol), 1,8-bis(dimethylamino)naphthalene (2.25 g, 10.48 mmol), and anhydrous THF (400 mL). An additional funnel was affixed to the round bottom flask and charged with bis(pentafluorophenyl)carbonate (18.4 g, 46.69 mmol) and anhydrous THF (50 mL). The bis(pentafluorophenyl)carbonate and THF mixture were then dripped into the round bottom flask and stirred at room temperature for 2 h. The reaction mixture was then concentrated under reduced pressure and then treated with excess ether. This mixture was then placed in the refrigerator overnight. The precipitated material was collected and dried to give compound **1** (4.33 g, 14.81 mmol, 70%) as a white solid. Characterization data was in agreement with those reported in literature.<sup>18</sup> <sup>1</sup>H NMR (300 MHz, DMSO) δ 4.08 (t, 8H, <sup>3</sup>J<sub>H-H</sub> = 5.2 Hz, CH<sub>2</sub>-OCOO), 2.76 (t, 8H, <sup>3</sup>J<sub>H-H</sub> = 5.2 Hz, CH<sub>2</sub>-CH<sub>2</sub>-OCOO), 2.62 (bs, 4H, CH<sub>2</sub>-N). <sup>13</sup>C NMR (75 MHz, DMSO) δ 155.5 (OCOO), 69.1 (CH<sub>2</sub>-OCOO), 53.6 (CH<sub>2</sub>-CH<sub>2</sub>-OCOO), 53.5 (CH<sub>2</sub>-N).



### 6.6.1.2 Synthesis of 4,4'-(oxybis(methylene))bis(1,3-dioxolan-2-one) (2)

A 50 mL RBF was charged with a stirring bar, diglycerol (mixture of isomers) (1.00 g, 6.02 mmol), dimethyl carbonate (3.210 g, 35.6 mmol) and K<sub>2</sub>CO<sub>3</sub> (0.005 g, 0.04 mmol). A reflux condenser was equipped and the reaction mixture was heated at 70 °C for 24 h. Then a mixture of dimethyl carbonate and methanol (1.8 mL) was distilled off at atmospheric pressure at 65 °C over a period of 6 h. Subsequently, the reaction mixture was cooled down to room temperature. The precipitated catalyst was filtered off and washed with dimethyl carbonate. The combined organic phases were evaporated to dryness and crystallised from ethyl acetate. Compound **2** (876 mg, 4.39 mmol, 73%) was obtained as a white solid. Characterization data was in agreement with those reported in literature.<sup>19</sup> <sup>1</sup>H NMR (300 MHz, DMSO) δ 4.98-4.90 (m, 2H, CH<sub>2</sub>-CH-OCOO), 4.52 (t, 2H, <sup>3</sup>J<sub>H-H</sub> = 8.5 Hz, CH<sup>anti</sup>-OCOO), 4.27-4.21 (m, 2H, CH<sup>syn</sup>-OCOO) 3.78-3.65 (m, 4H, O-CH<sub>2</sub>). <sup>13</sup>C NMR (75 MHz, DMSO) δ 154.9 (OCOO), 75.4 (CH), 70.4 (CH<sub>2</sub>-OCOO), 65.9 (CH<sub>2</sub>-O).

### 6.6.2 Synthesis of linear poly(hydroxy urethane)

In a 5 mL vial, PEG-diamine M<sub>w</sub> = 1,000 (100 mg, 0.1 mmol) and bis-cyclic carbonate (0.1 mmol) were dissolved in distilled water (1 mL). Mixture was stirred overnight and the water was evaporated in a rotary evaporator, the remaining water was removed in a freeze-drier affording a white powder. Conversion was calculated by <sup>1</sup>H NMR spectroscopic analysis using relative peak integration values from the reaction crude mixture.

### 6.6.3 Synthesis of poly(hydroxy urethane) hydrogels

In a 5 mL vial a stock solution of TAEA 0.2 M was added, then water was added to obtain a final volume of 400 μL. Then PEG diamine was added to the previous mixture and the vial was stirred in a vortex until total dissolution of the PEG diamine. Subsequently 8MCC was added to the mixture and stirred in a vortex until was dissolved. Mixture was left overnight at room temperature without further stirring and a gel was obtained.

### 6.6.4 3D printing of hydrogels

Extrusions were conducted at 25 °C and the needle diameter used was 0.25 mm. In addition to this, a preflow of 0.3 s and a postflow of 0.1 s were necessary.

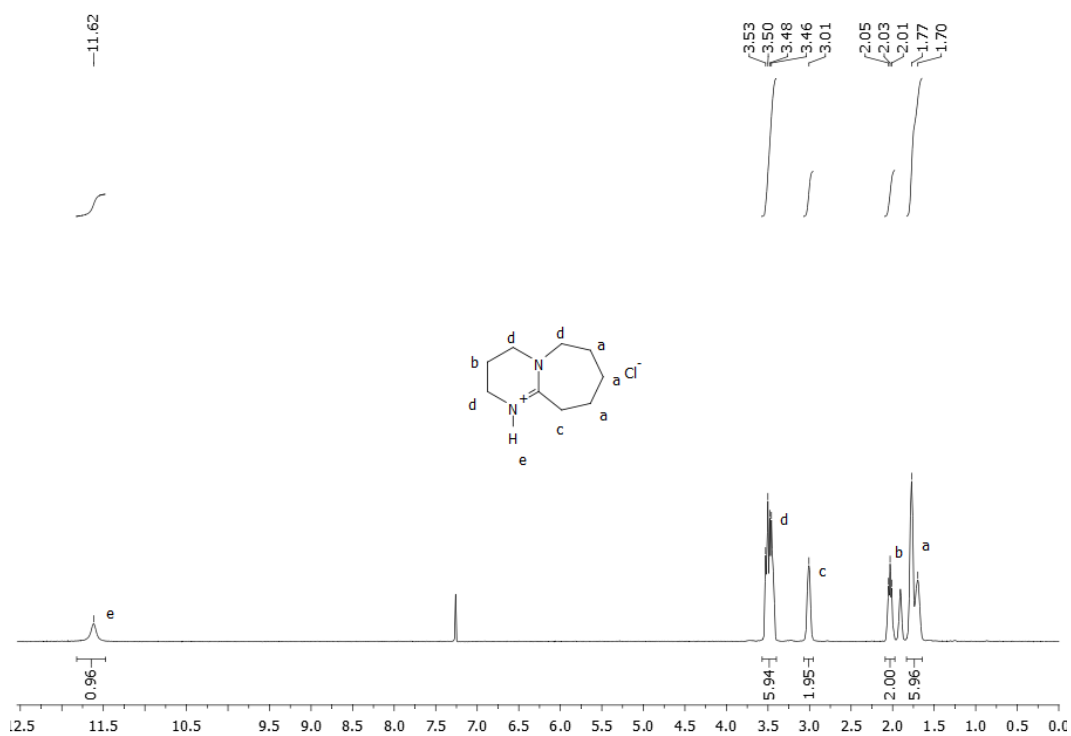
### 6.7 References

1. Z.-Z. Yang, L.-N. He, C.-X. Miao and S. Chanfreau, *Adv. Synth. Catal.*, 2010, **352**, 2233-2240.
2. Z. Zhang, F. Fan, H. Xing, Q. Yang, Z. Bao and Q. Ren, *ACS Sustainable Chem. Eng.*, 2017, **5**, 2841-2846.
3. N. Aoyagi, Y. Furusho and T. Endo, *J. Polym. Sci. Part A*, 2018, **56**, 986-993.
4. H. W. Cheung, J. Li, W. Zheng, Z. Zhou, Y. H. Chiu, Z. Lin and C. P. Lau, *Dalton Trans.*, 2010, **39**, 265-274.
5. D. J. Coady, K. Fukushima, H. W. Horn, J. E. Rice and J. L. Hedrick, *Chem. Commun.*, 2011, **47**, 3105-3107.
6. M. S. Miran, H. Kinoshita, T. Yasuda, M. A. Susan and M. Watanabe, *Phys. Chem. Chem. Phys.*, 2012, **14**, 5178-5186.
7. L. Fan and O. V. Ozerov, *Chem. Commun.*, 2005, 4450-4452.
8. C. Thomas, A. Milet, F. Peruch and B. Bibal, *Polym. Chem.*, 2013, **4**, 3491-3498.
9. J. Nowicki, M. Muszyński and S. Gryglewicz, *J. Chem. Technol. Biotechnol.*, 2014, **89**, 48-55.
10. JP Pat., H05100490 (A), 1993.
11. X. Liu, S. Zhang, Q.-W. Song, X.-F. Liu, R. Ma and L.-N. He, *Green Chem.*, 2016, **18**, 2871-2876.
12. Y. Ren, O. Jiang, H. Zeng, Q. Mao and H. Jiang, *RSC Adv.*, 2016, **6**, 3243-3249.
13. L. Wang, K. Kodama and T. Hirose, *Catal. Sci. Technol.*, 2016, **6**, 3872-3877.
14. A. Baishya, M. K. Barman, T. Peddarao and S. Nembenna, *J. Organomet. Chem.*, 2014, **769**, 112-118.

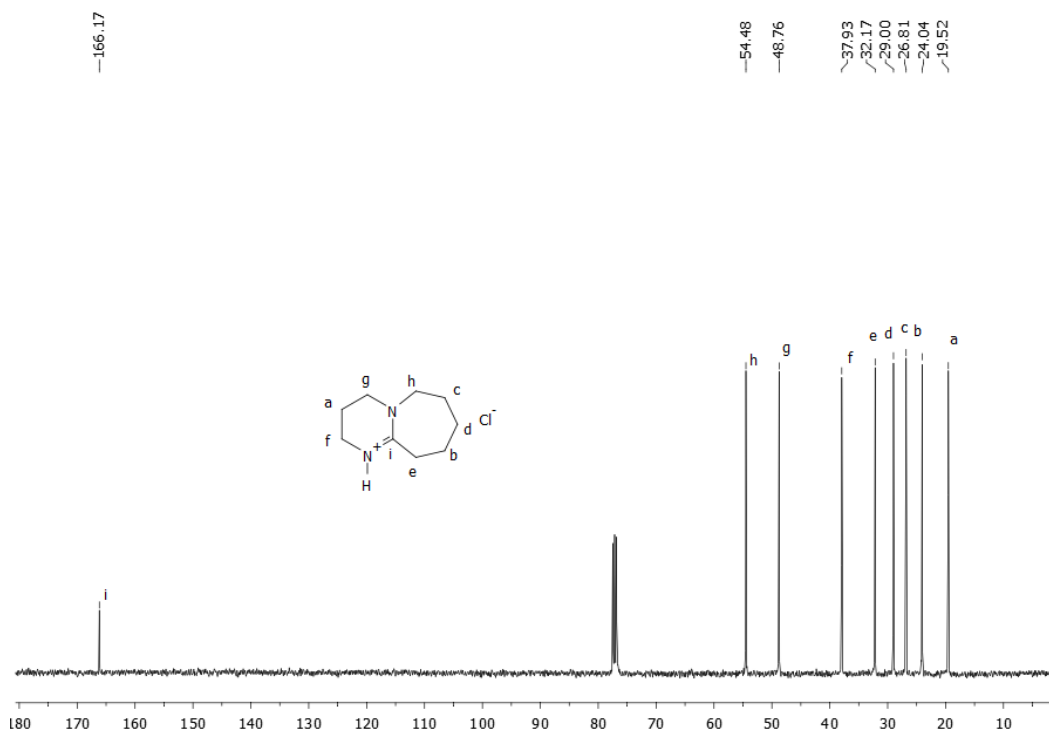
15. S. Long, V. Muthusamy, P. G. Willis, S. Parkin and A. Cammers, *Beilstein J. Org. Chem.*, 2008, **4**, 23.
16. M. Fache, E. Darroman, V. Besse, R. Auvergne, S. Caillol and B. Boutevin, *Green Chem.*, 2014, **16**, 1987-1998.
17. Z. Lu, C. Hu, J. Guo, J. Li, Y. Cui and Y. Jia, *Org. Lett.*, 2010, **12**, 480-483.
18. A. Yuen, A. Bossion, E. Gómez-Bengoa, F. Ruipérez, M. Isik, J. L. Hedrick, D. Mecerreyes, Y. Y. Yang and H. Sardon, *Polym. Chem.*, 2016, **7**, 2105-2111.
19. M. Tryznowski, A. Świdarska, Z. Żółek-Tryznowska, T. Gołofit and P. G. Parzuchowski, *Polymer*, 2015, **80**, 228-236.

# **A. Appendix: Supplementary Information**

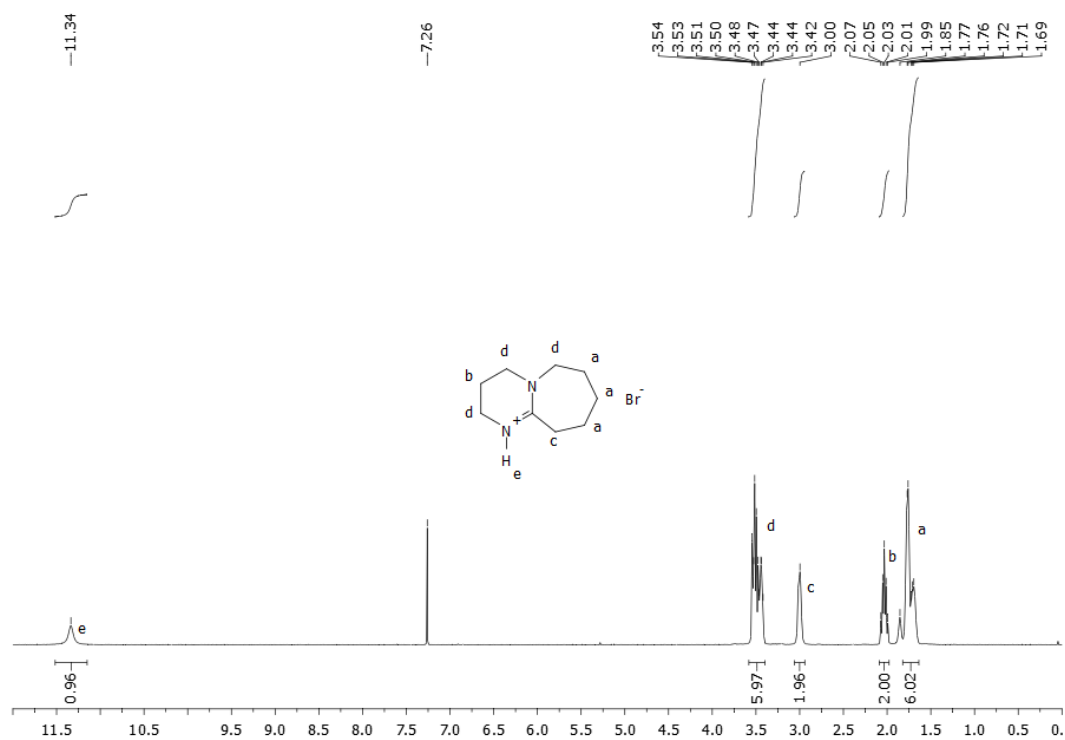
## A.1 Supplementary NMR spectra for Chapter 2



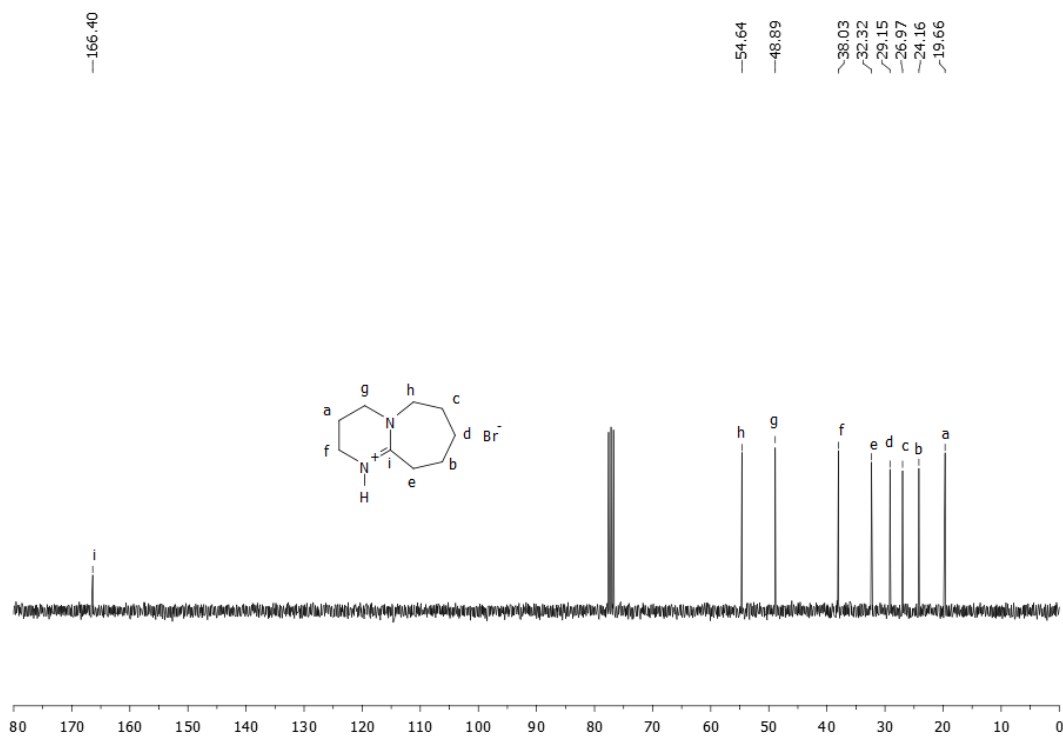
**Figure A.1.1.**  $^1\text{H}$  NMR spectrum of **1** (300 MHz, 298 K,  $\text{CDCl}_3$ ).



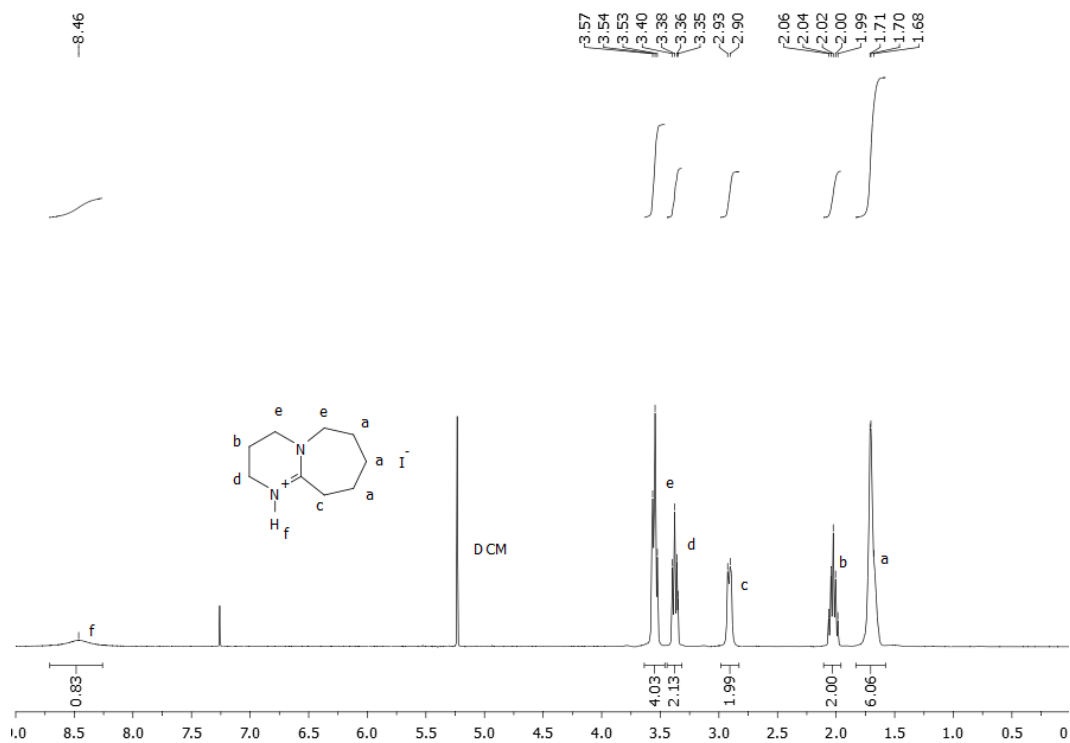
**Figure A.1.2.**  $^{13}\text{C}$  APT NMR spectrum of **1** (75 MHz, 298 K,  $\text{CDCl}_3$ ).



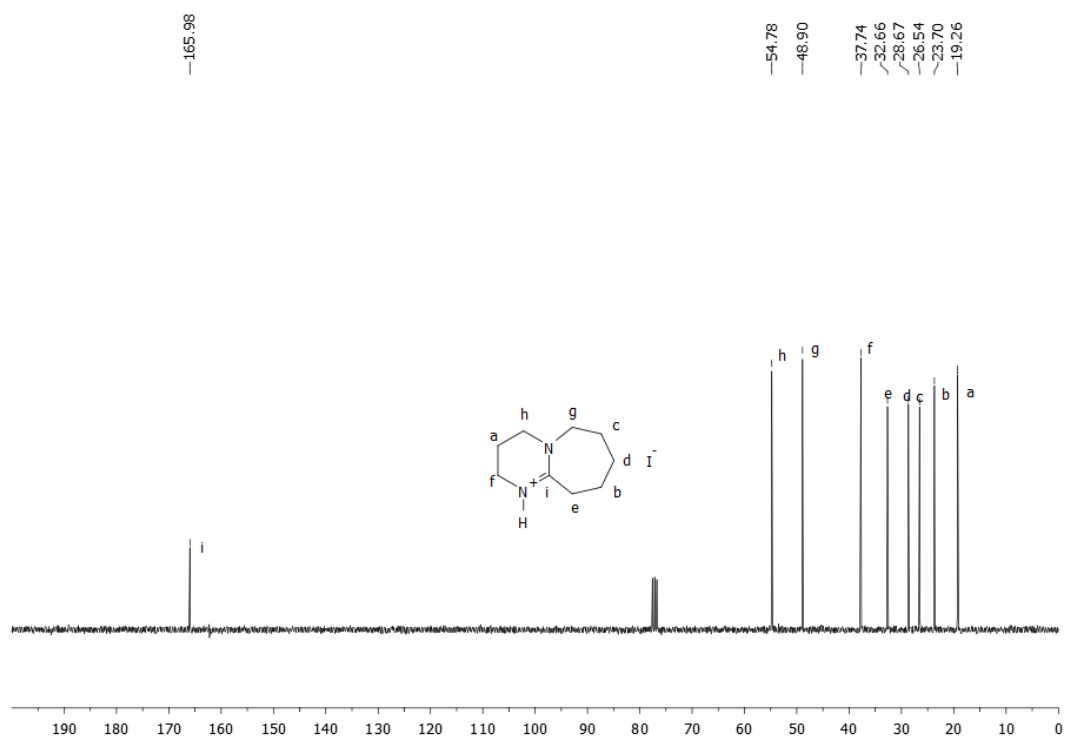
**Figure A.1.3.**  $^1\text{H}$  NMR spectrum of **2** (300 MHz, 298 K,  $\text{CDCl}_3$ ).



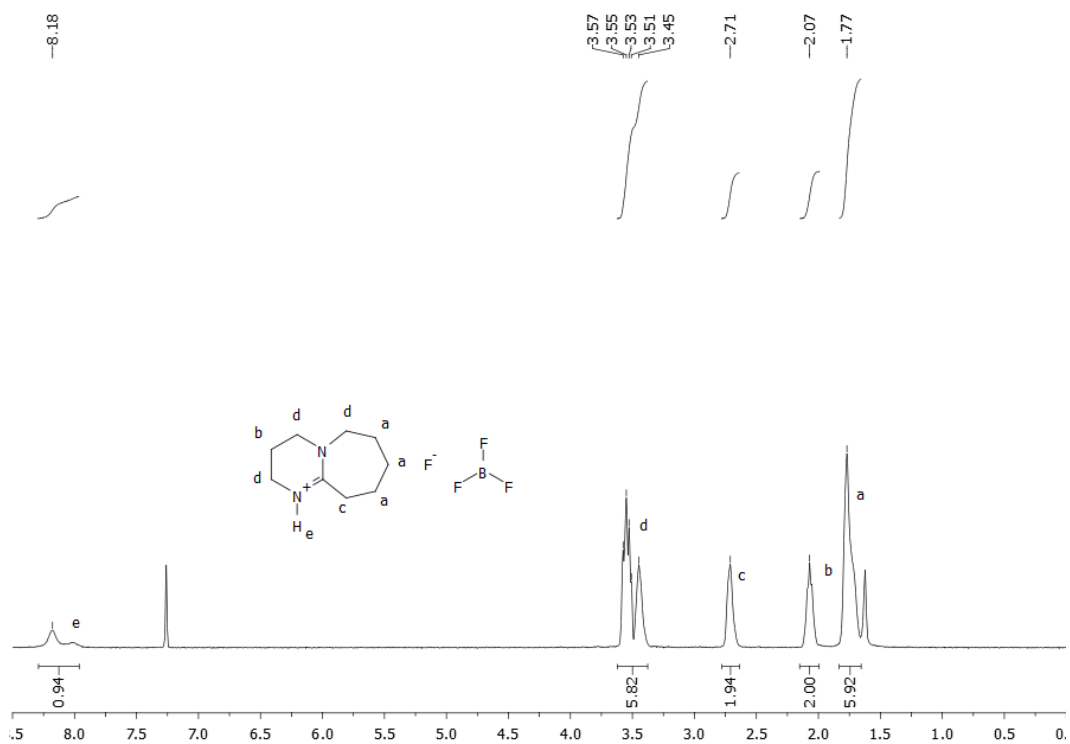
**Figure A.1.4.**  $^{13}\text{C}$  APT NMR spectrum of **2** (75 MHz, 298 K,  $\text{CDCl}_3$ ).



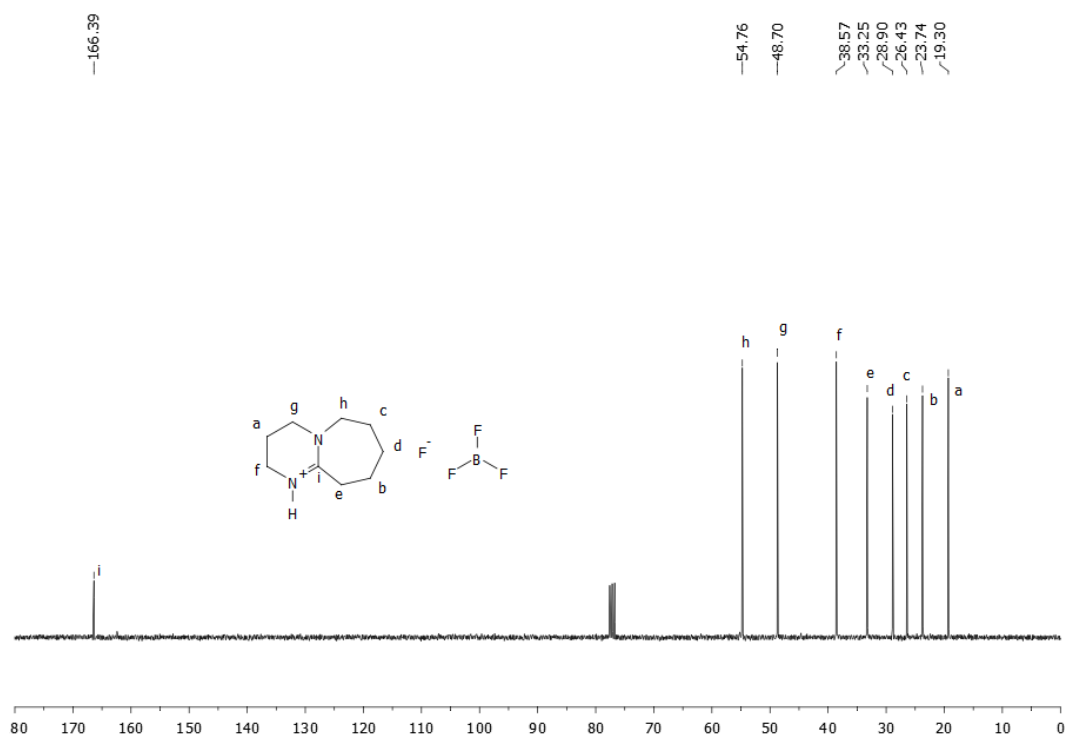
**Figure A.1.5.**  $^1\text{H}$  NMR spectrum of **3** (300 MHz, 298 K,  $\text{CDCl}_3$ ).



**Figure A.1.6.**  $^{13}\text{C}$  APT NMR spectrum of **3** (75 MHz, 298 K,  $\text{CDCl}_3$ ).

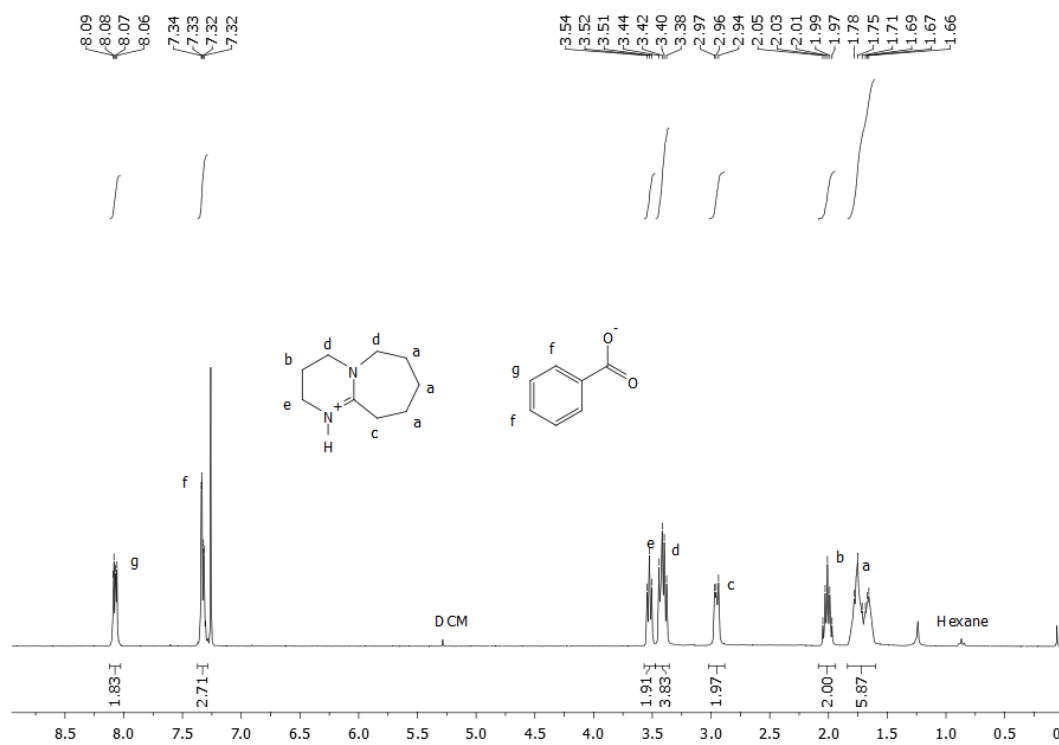


**Figure A.1.7.** <sup>1</sup>H NMR spectrum of **4** (300 MHz, 298 K, CDCl<sub>3</sub>).

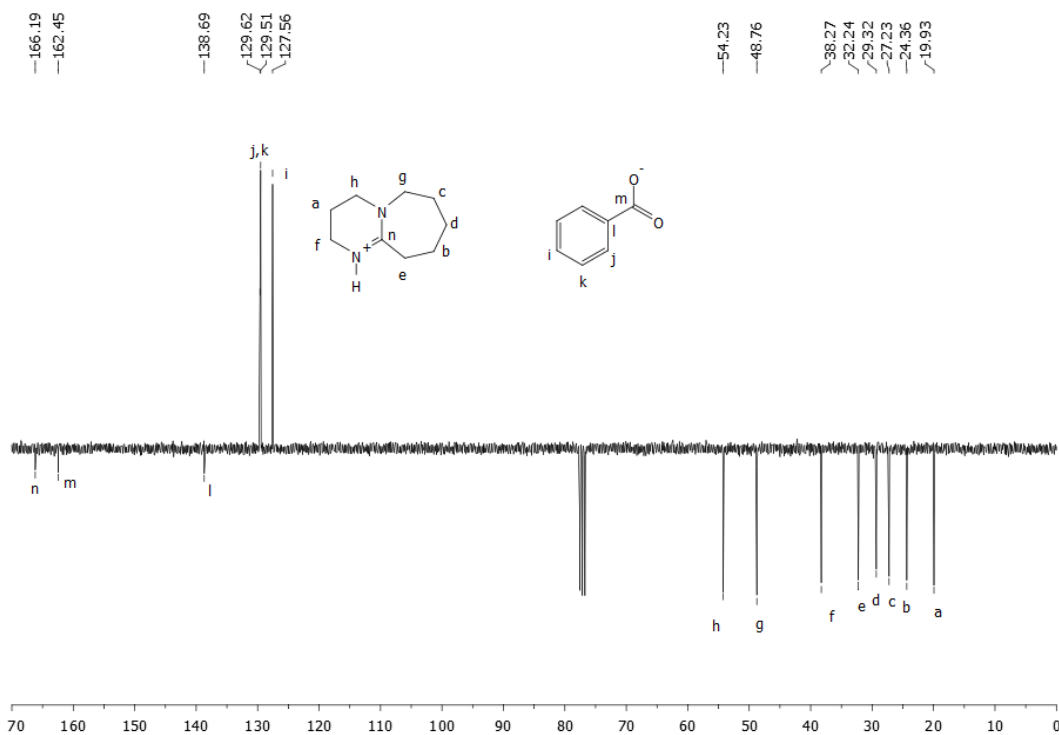


**Figure A.1.8.** <sup>13</sup>C APT NMR spectrum of **4** (75 MHz, 298 K, CDCl<sub>3</sub>).

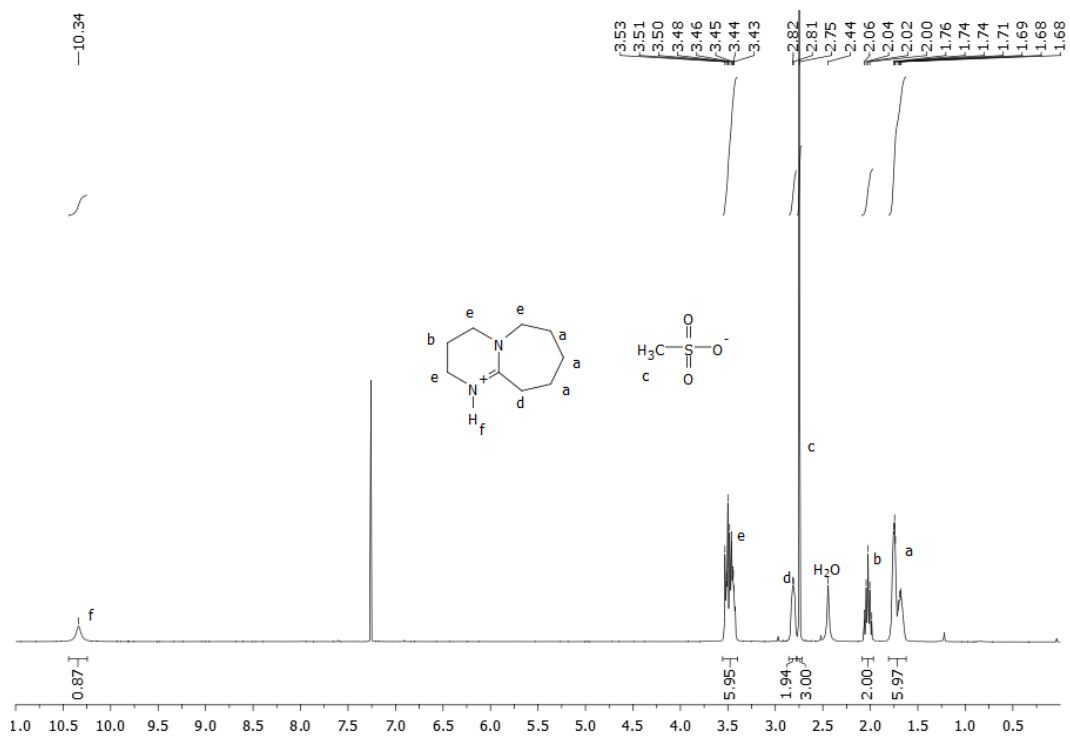




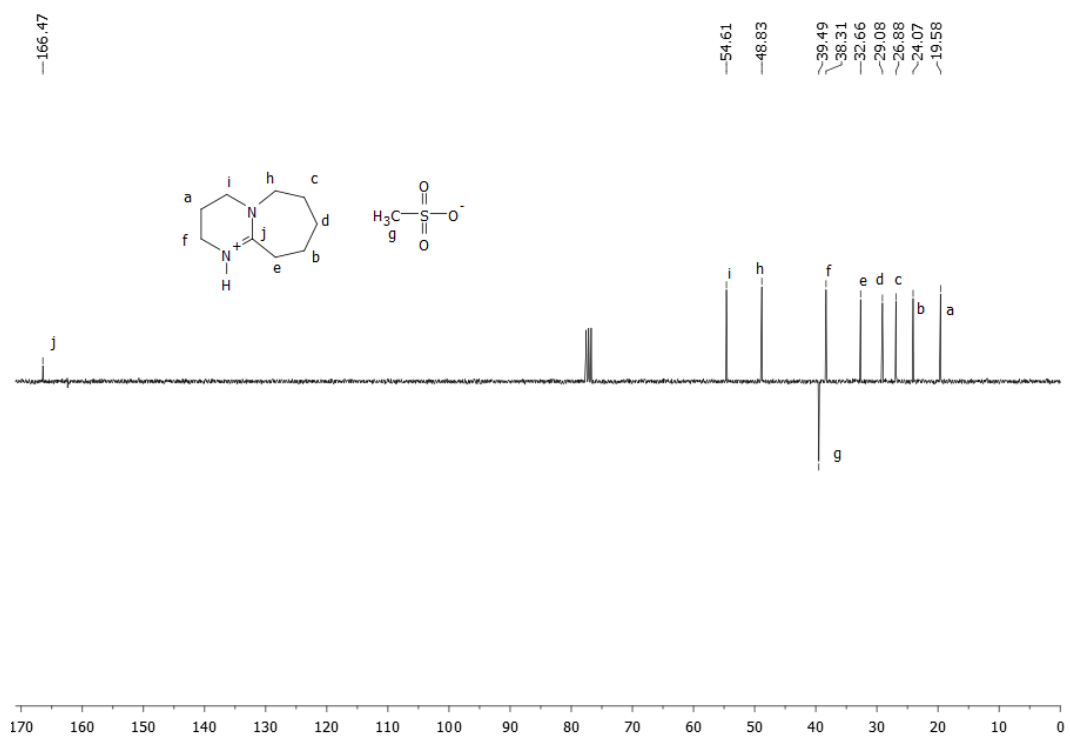
**Figure A.1.9.**  $^1\text{H}$  NMR spectrum of **5** (300 MHz, 298 K,  $\text{CDCl}_3$ ).



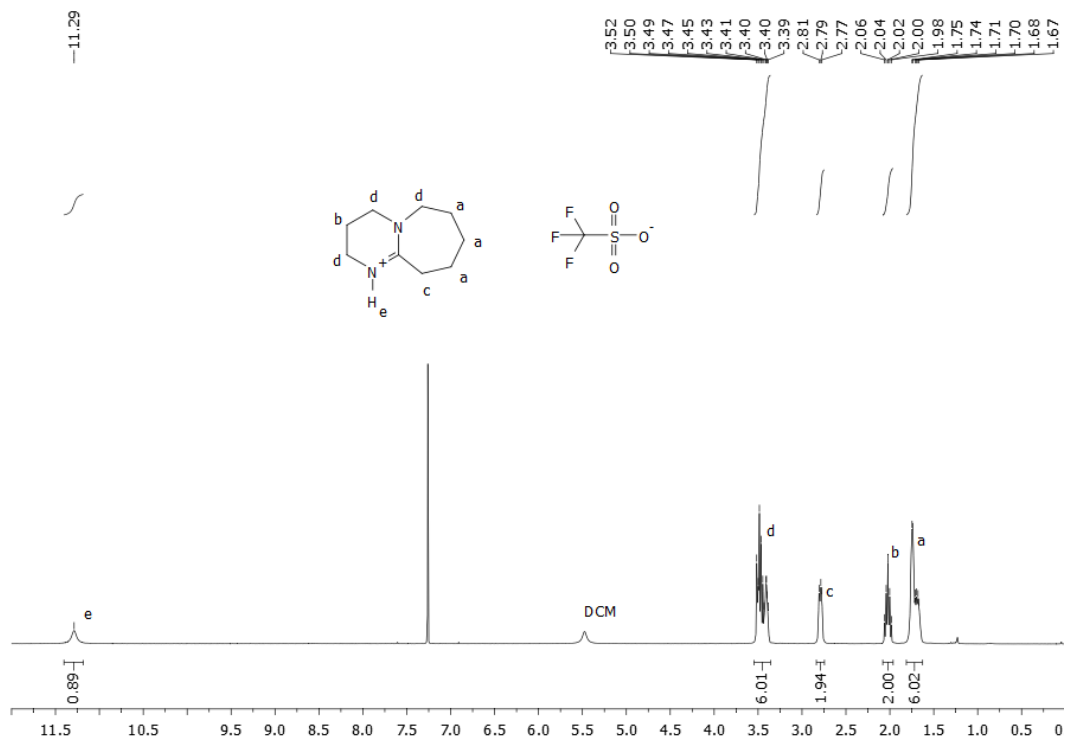
**Figure A.1.10.**  $^{13}\text{C}$  APT NMR spectrum of **5** (75 MHz, 298 K,  $\text{CDCl}_3$ ).



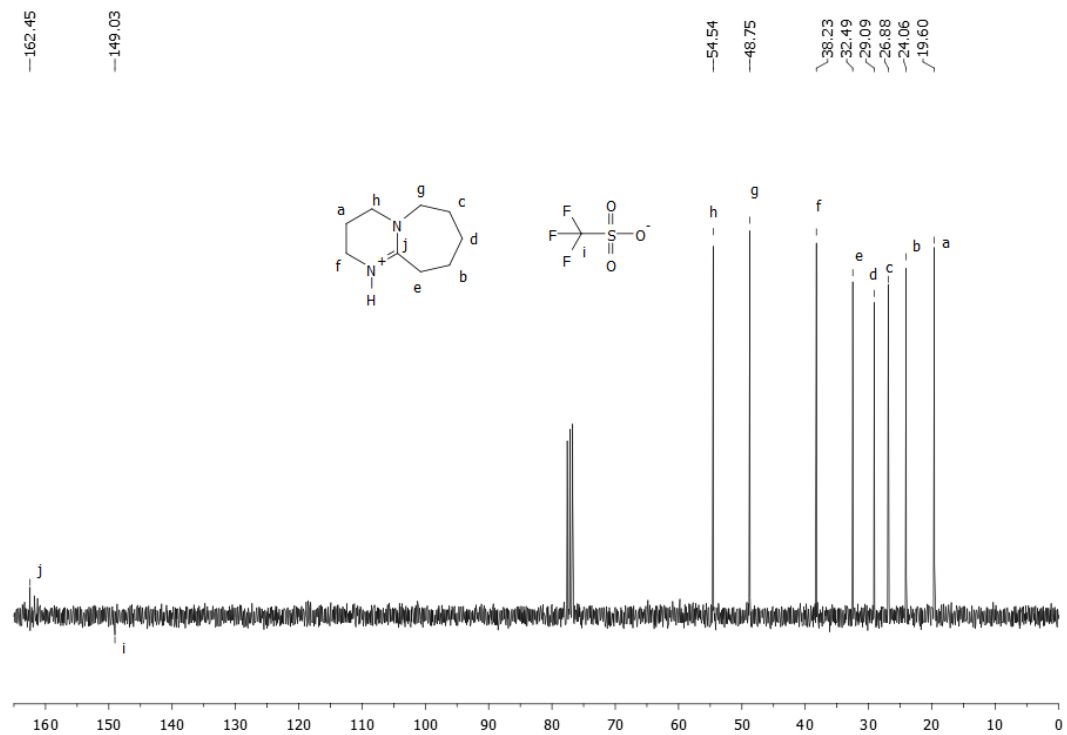
**Figure A.1.11.**  $^1\text{H}$  NMR spectrum of **6** (300 MHz, 298 K,  $\text{CDCl}_3$ ).



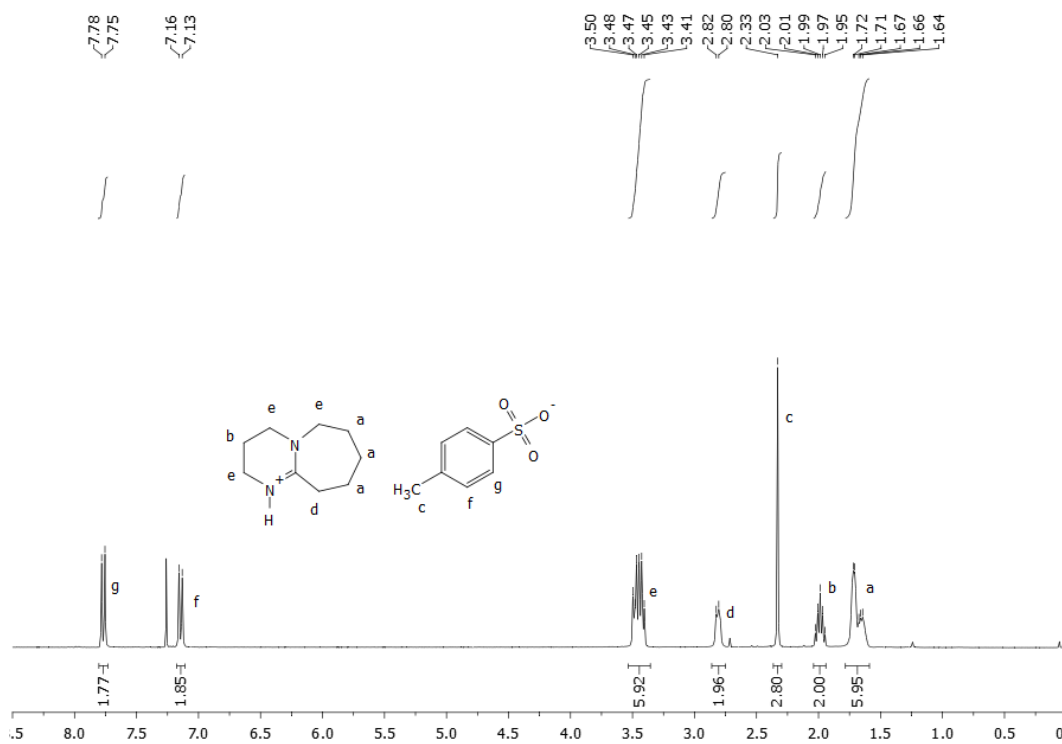
**Figure A.1.12.**  $^{13}\text{C}$  APT NMR spectrum of **6** (75 MHz, 298 K,  $\text{CDCl}_3$ ).



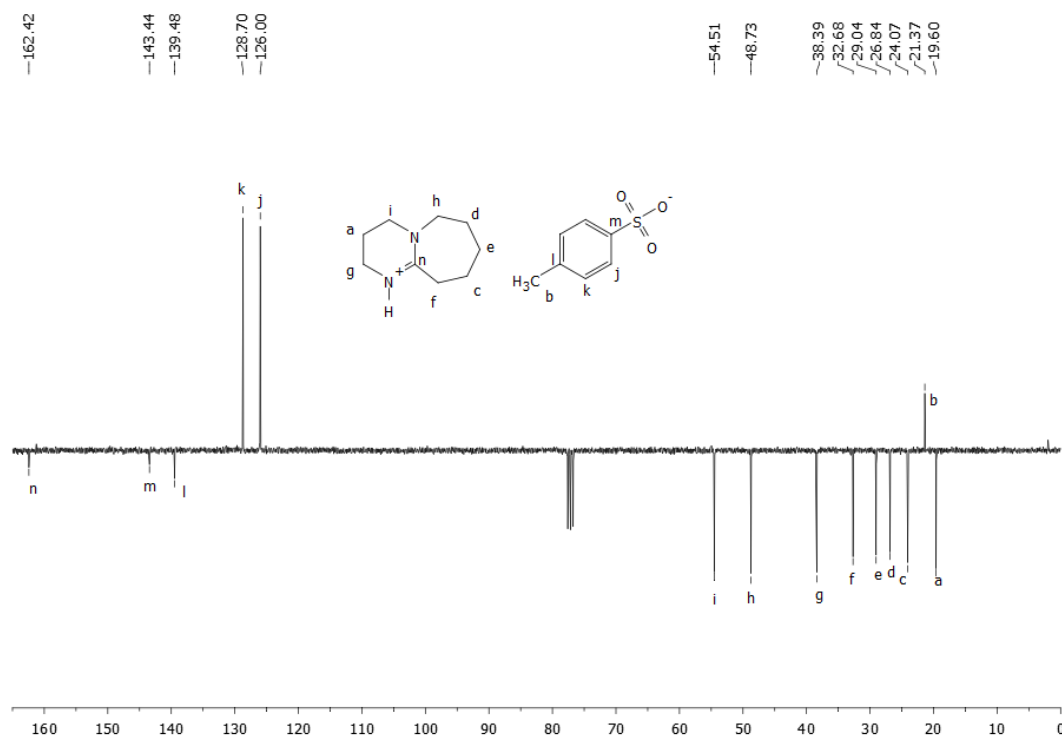
**Figure A.1.13.**  $^1\text{H}$  NMR spectrum of **7** (300 MHz, 298 K,  $\text{CDCl}_3$ ).



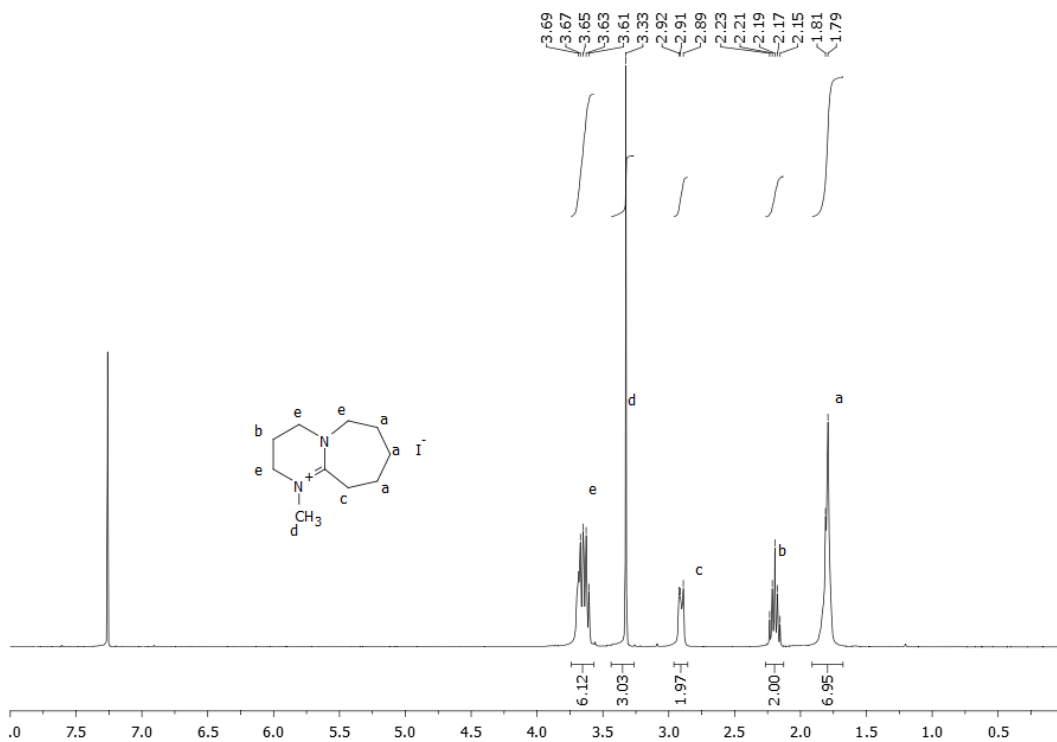
**Figure A.1.14.**  $^{13}\text{C}$  APT NMR spectrum of **7** (75 MHz, 298 K,  $\text{CDCl}_3$ ).



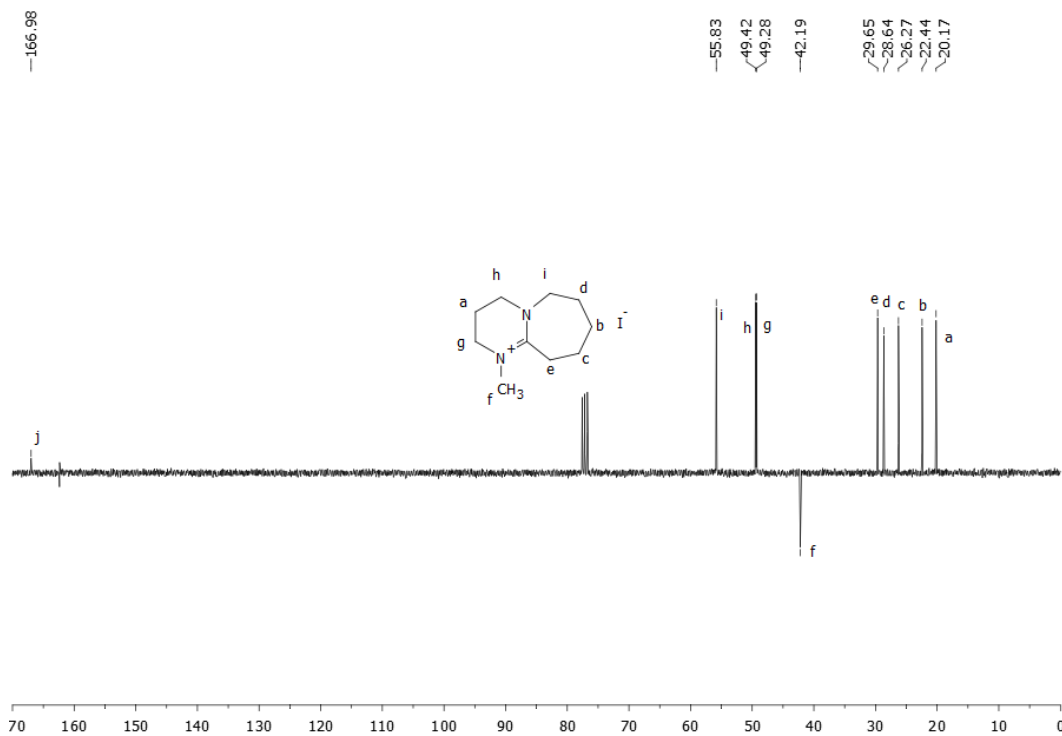
**Figure A.1.15.**  $^1\text{H}$  NMR spectrum of **8** (300 MHz, 298 K,  $\text{CDCl}_3$ ).



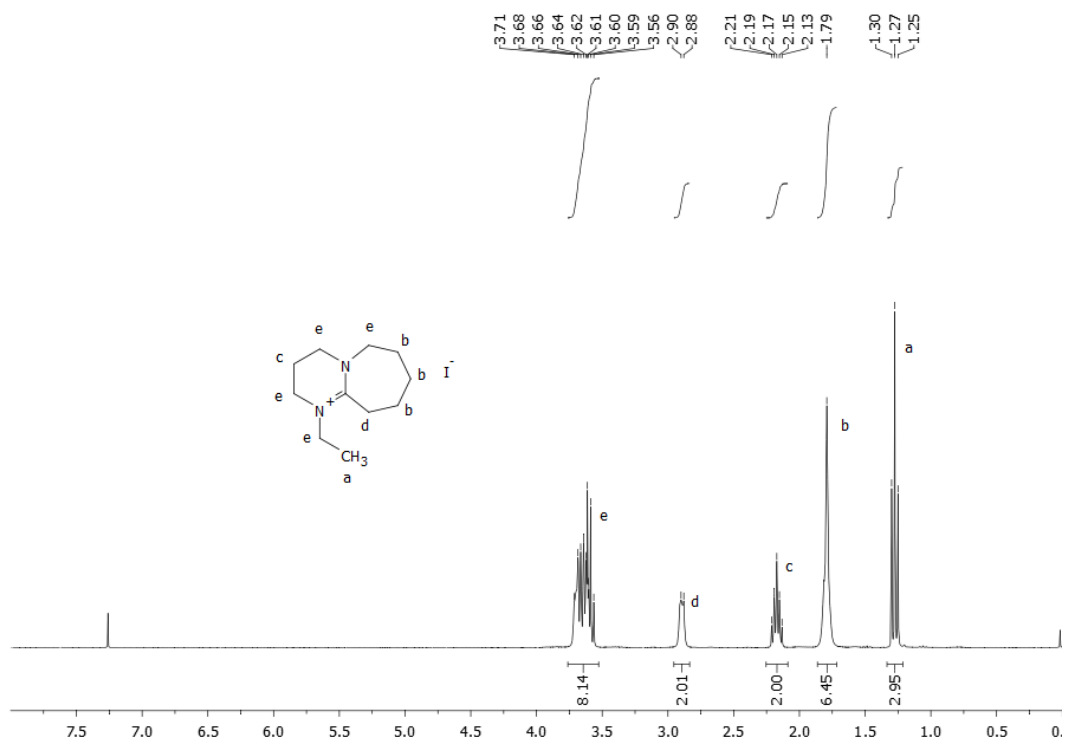
**Figure A.1.16.**  $^{13}\text{C}$  APT NMR spectrum of **8** (75 MHz, 298 K,  $\text{CDCl}_3$ ).



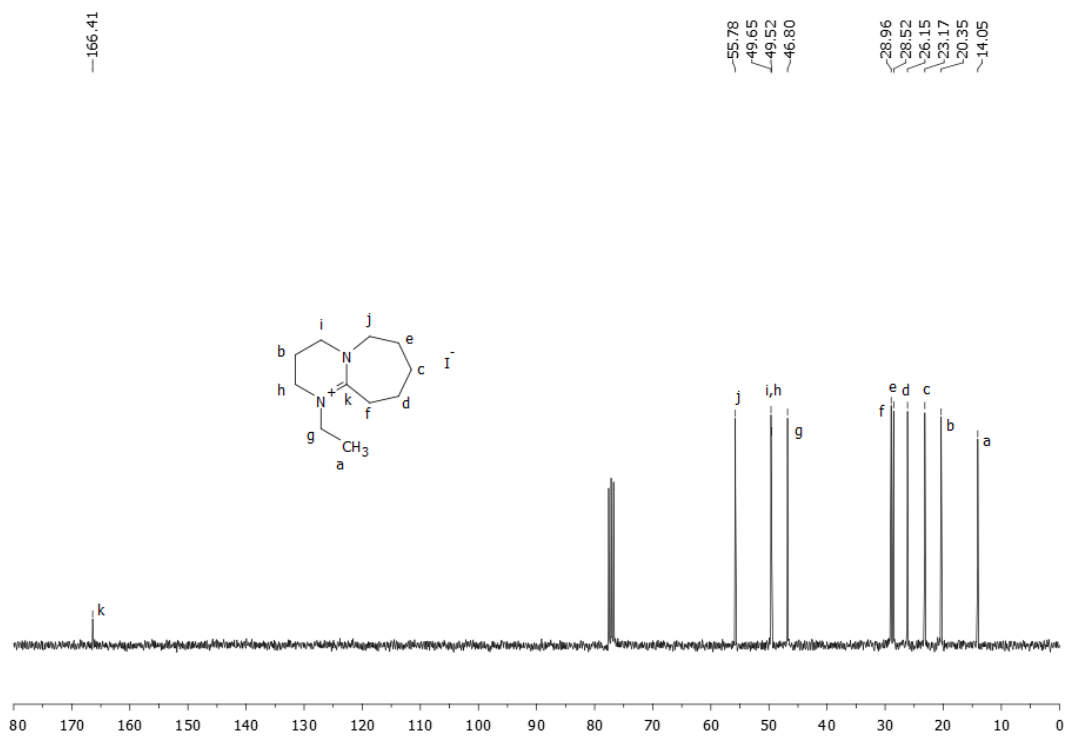
**Figure A.1.17.**  $^1\text{H}$  NMR spectrum of **9** (300 MHz, 298 K,  $\text{CDCl}_3$ ).



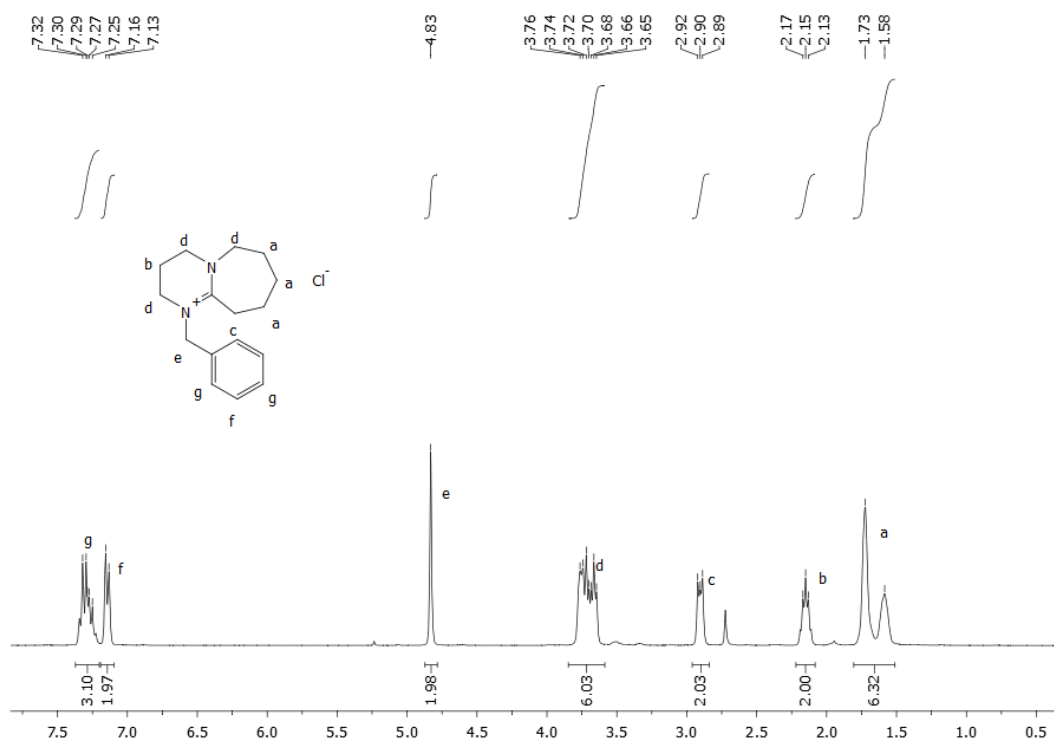
**Figure A.1.18.**  $^{13}\text{C}$  APT NMR spectrum of **9** (75 MHz, 298 K,  $\text{CDCl}_3$ ).



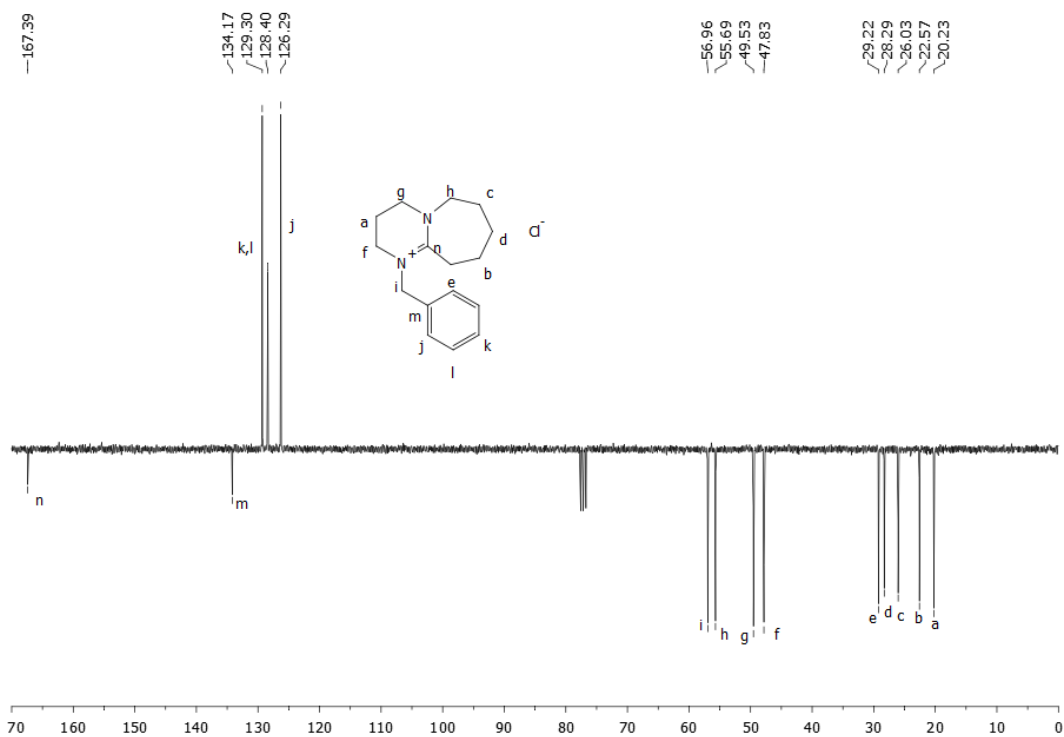
**Figure A.1.19.** <sup>1</sup>H NMR spectrum of **10** (400 MHz, 298 K, CDCl<sub>3</sub>).



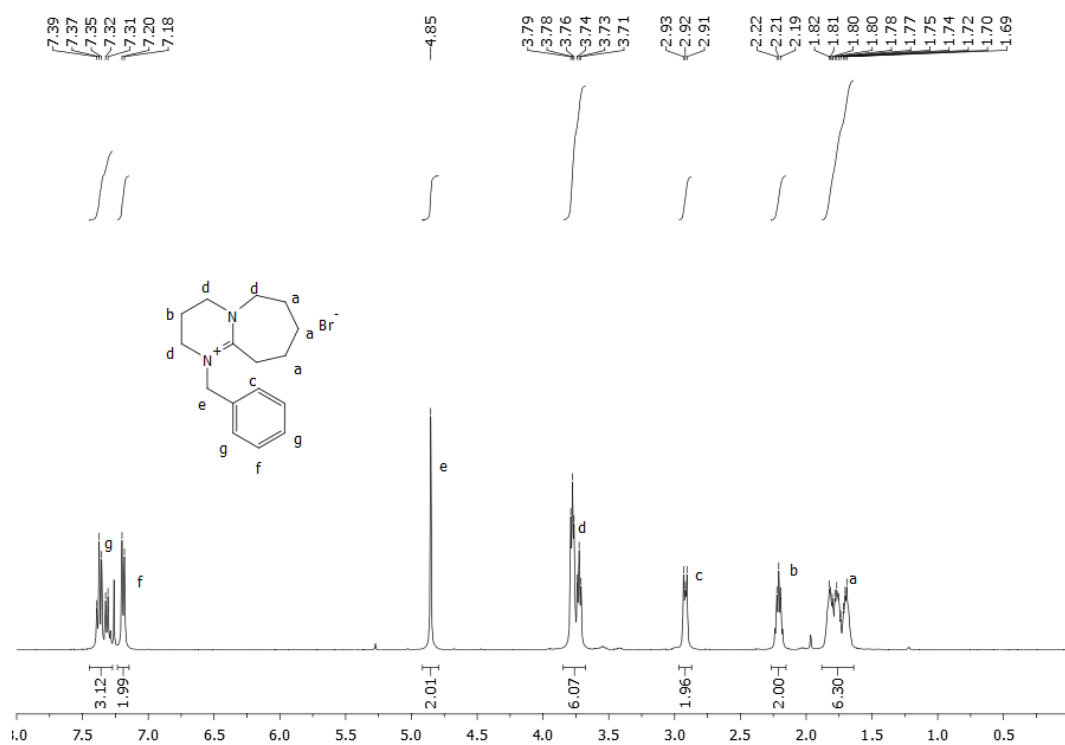
**Figure A.1.20.** <sup>13</sup>C NMR spectrum of **10** (100 MHz, 298 K, CDCl<sub>3</sub>).



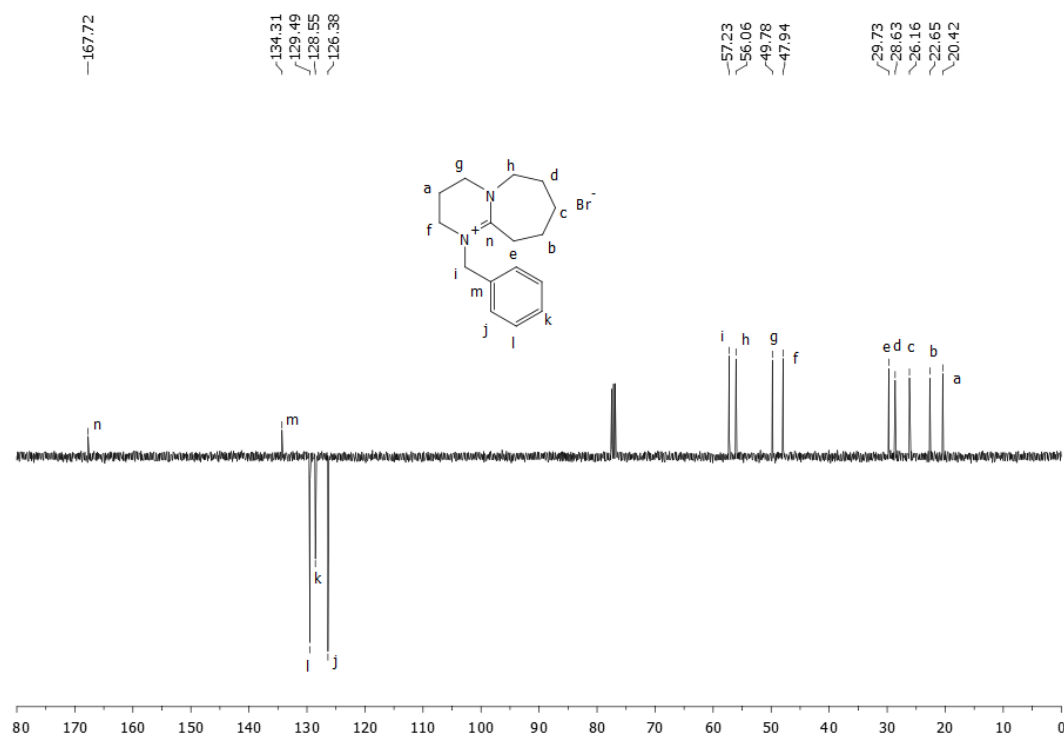
**Figure A.1.21.** <sup>1</sup>H NMR spectrum of **11** (300 MHz, 298 K, CDCl<sub>3</sub>).



**Figure A.1.22.** <sup>13</sup>C APT NMR spectrum of **11** (75 MHz, 298 K, CDCl<sub>3</sub>).

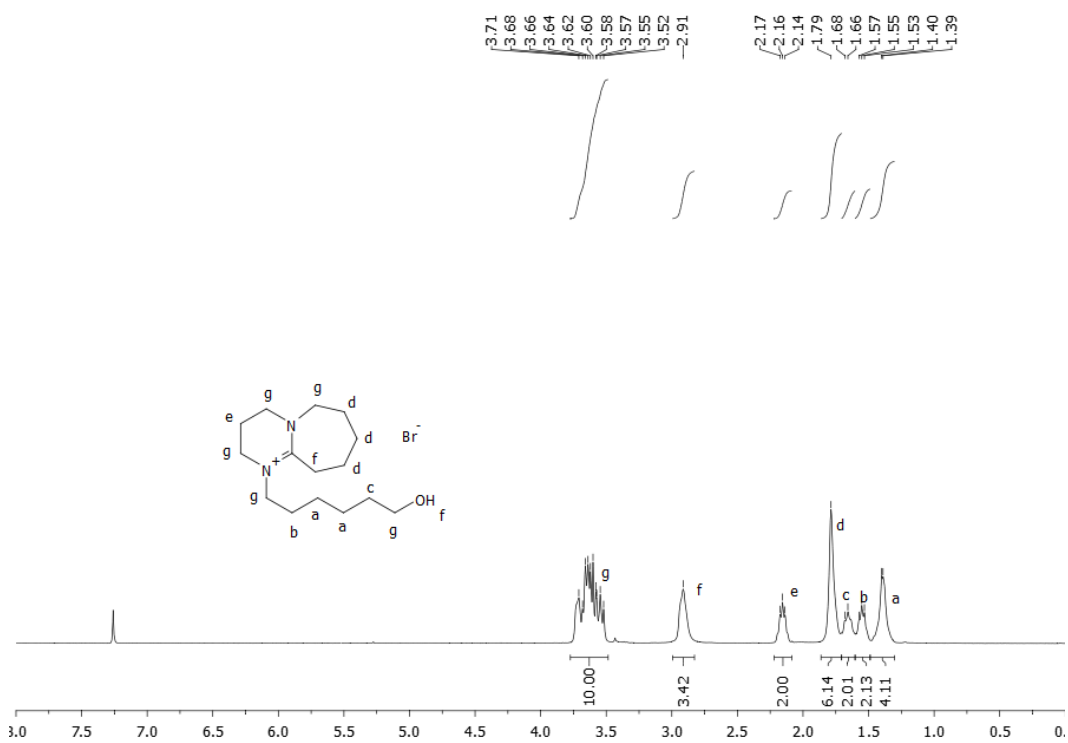


**Figure A.1.23.**  $^1\text{H}$  NMR spectrum of **12** (300 MHz, 298 K,  $\text{CDCl}_3$ ).

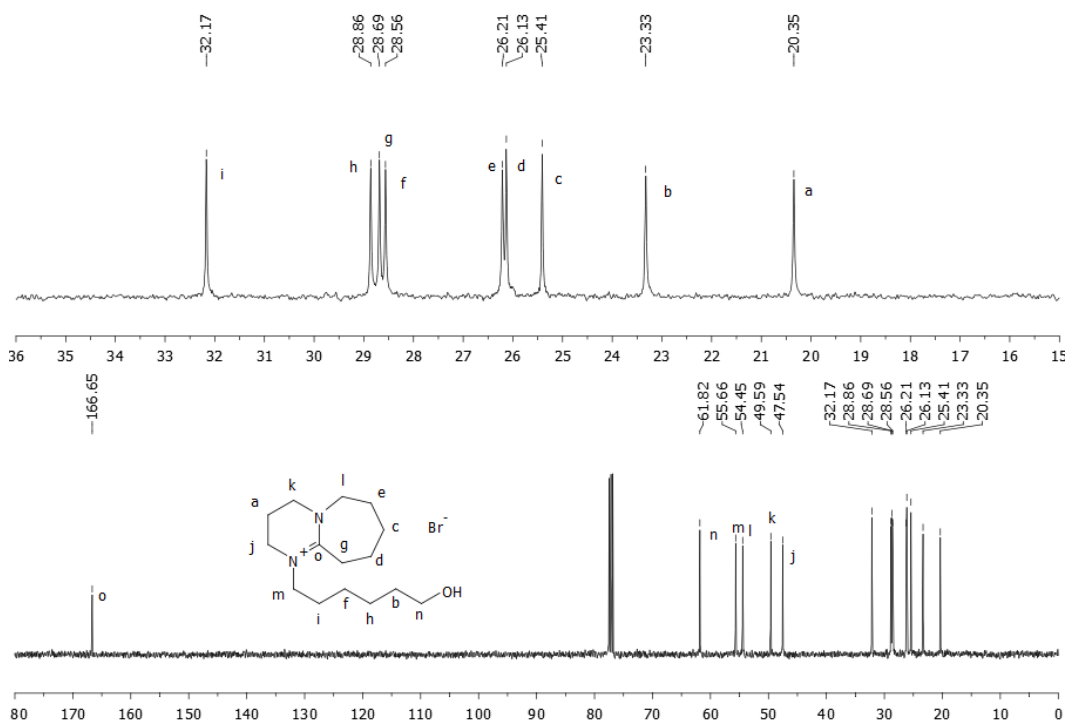


**Figure A.1.24.**  $^{13}\text{C}$  APT NMR spectrum of **12** (75 MHz, 298 K,  $\text{CDCl}_3$ ).

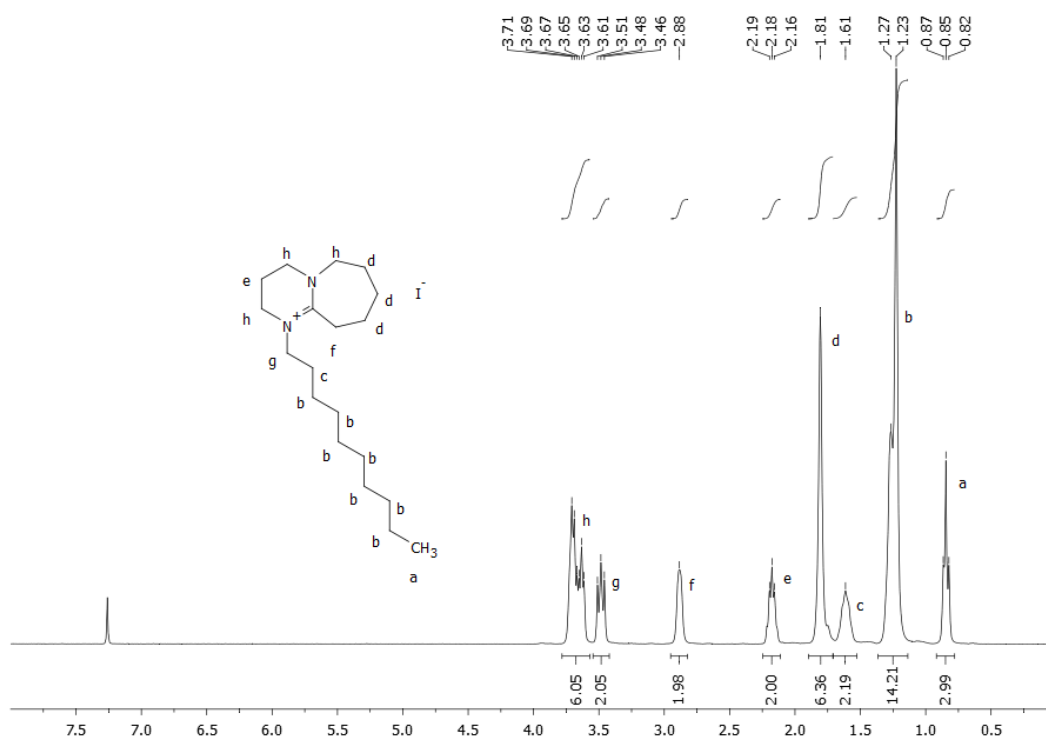




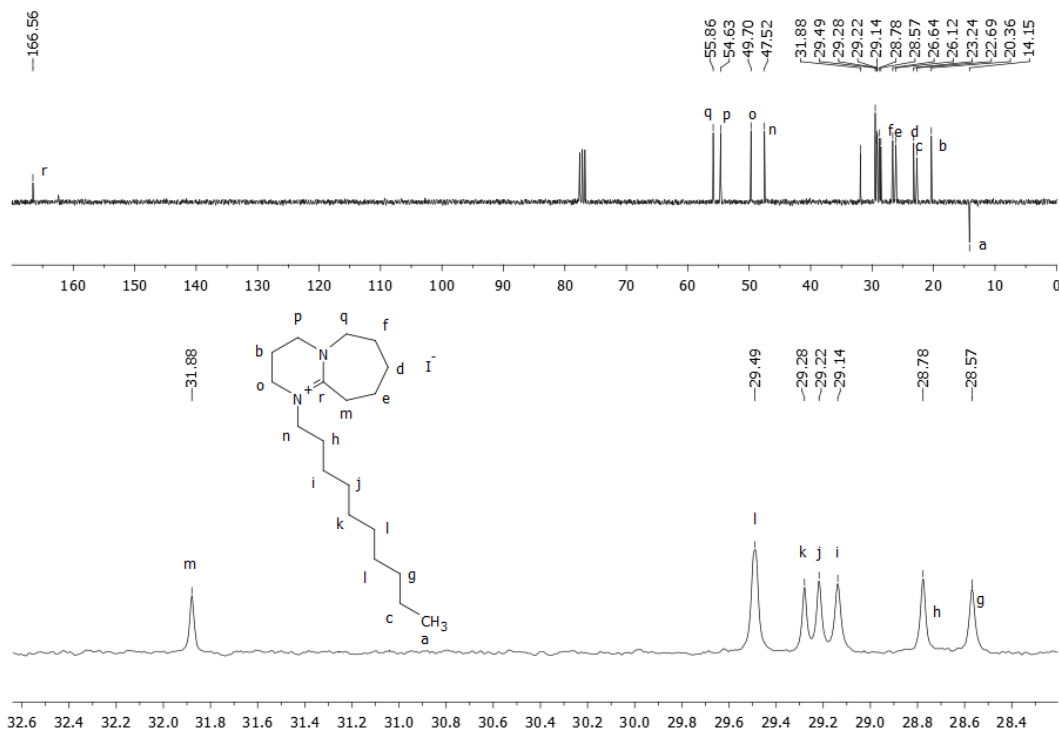
**Figure A.1.25.** <sup>1</sup>H NMR spectrum of **13** (400 MHz, 298 K, CDCl<sub>3</sub>).



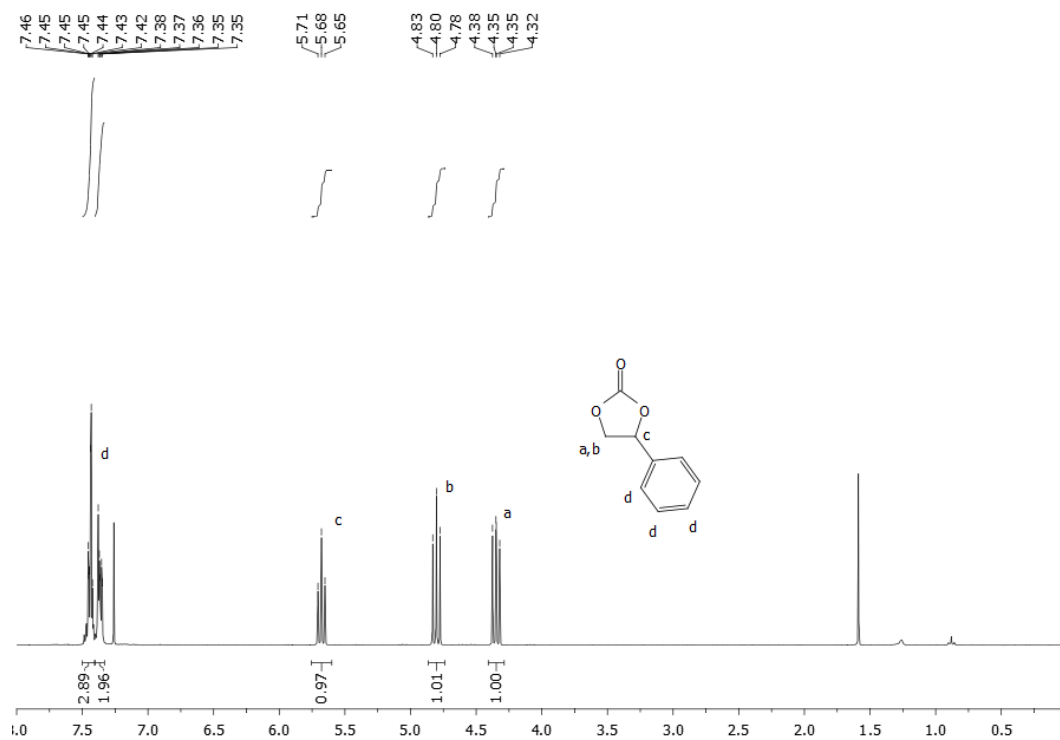
**Figure A.1.26.** <sup>13</sup>C APT NMR spectrum of **13** (100 MHz, 298 K, CDCl<sub>3</sub>).



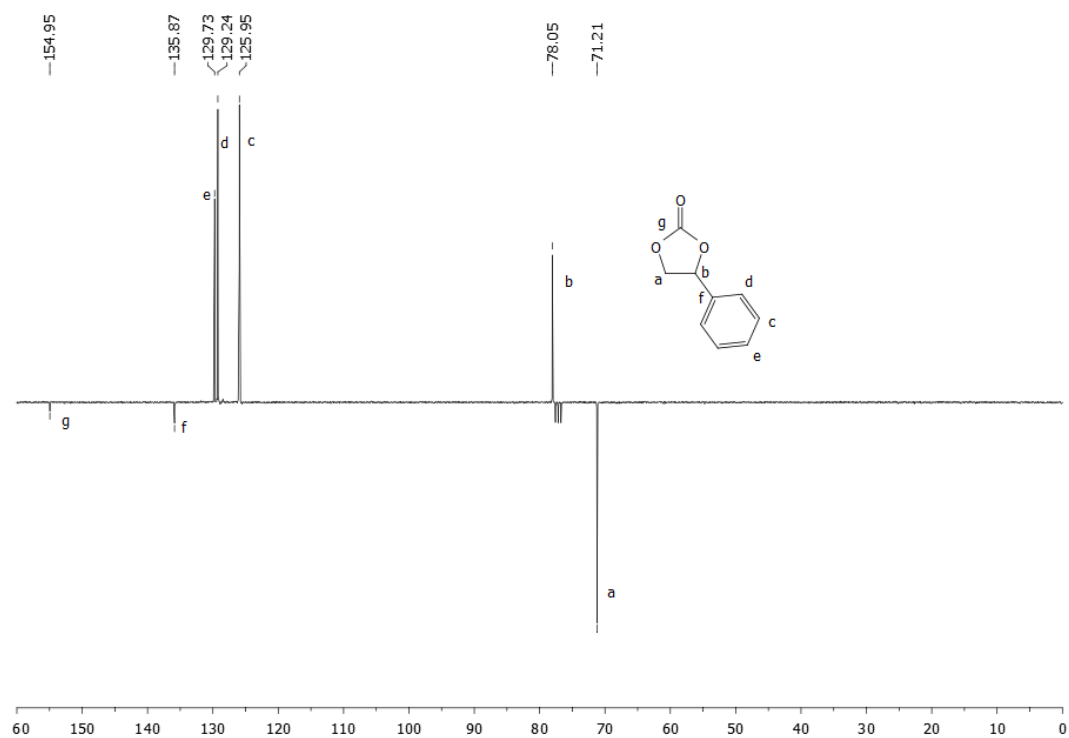
**Figure A.1.27.**  $^1\text{H}$  NMR spectrum of **14** (400 MHz, 298 K,  $\text{CDCl}_3$ ).



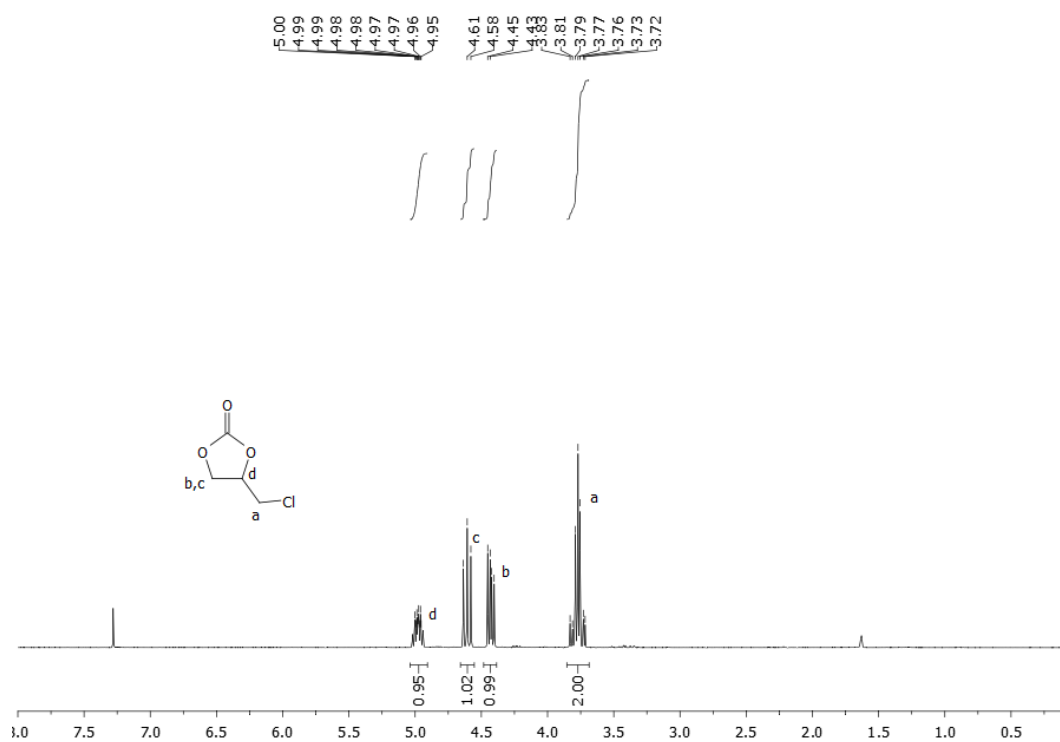
**Figure A.1.28.**  $^{13}\text{C}$  APT NMR spectrum of **14** (100 MHz, 298 K,  $\text{CDCl}_3$ ).



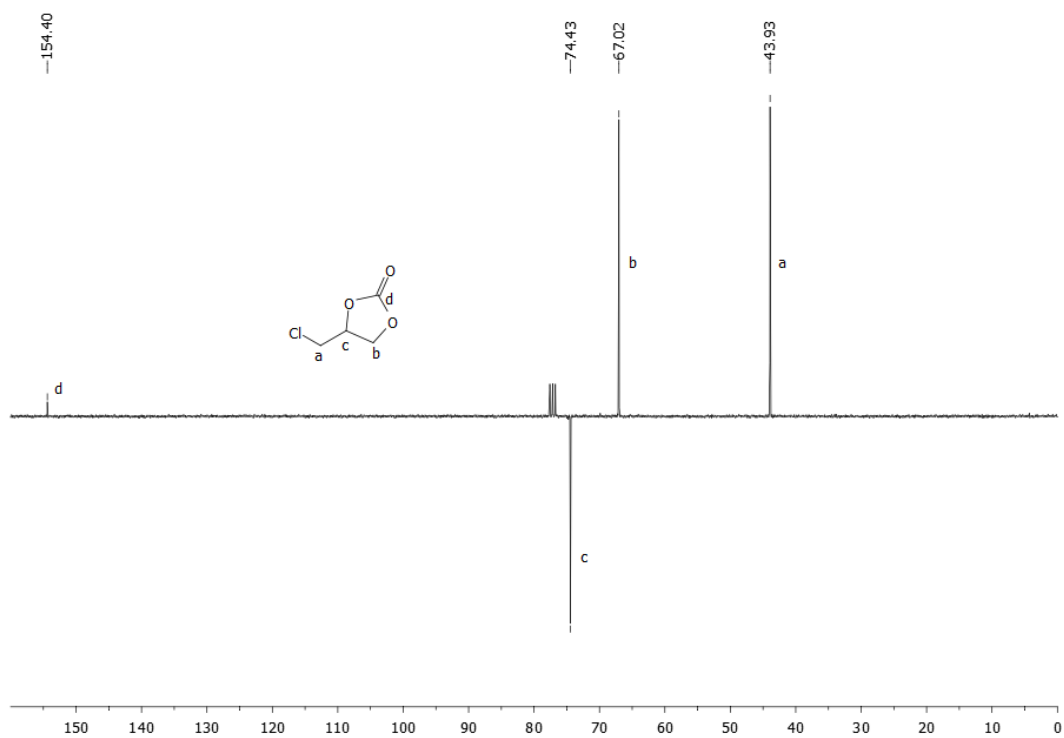
**Figure A.1.29.** <sup>1</sup>H NMR spectrum of **15** (300 MHz, 298 K, CDCl<sub>3</sub>).



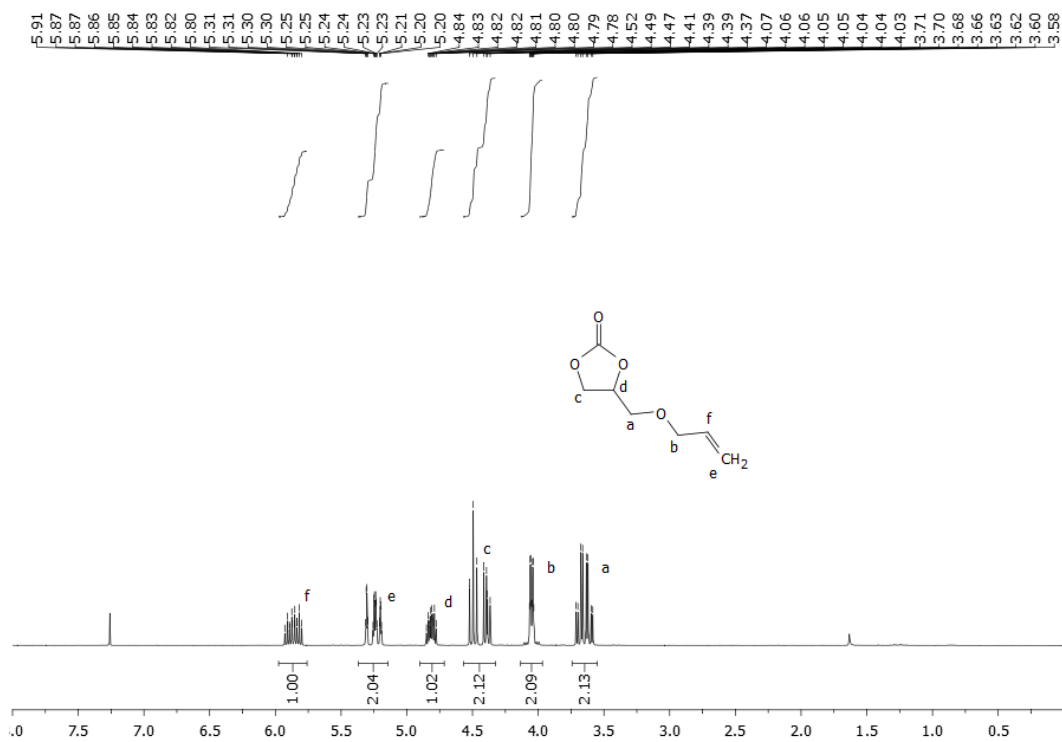
**Figure A.1.30.** <sup>13</sup>C APT NMR spectrum of **15** (75 MHz, 298 K, CDCl<sub>3</sub>).



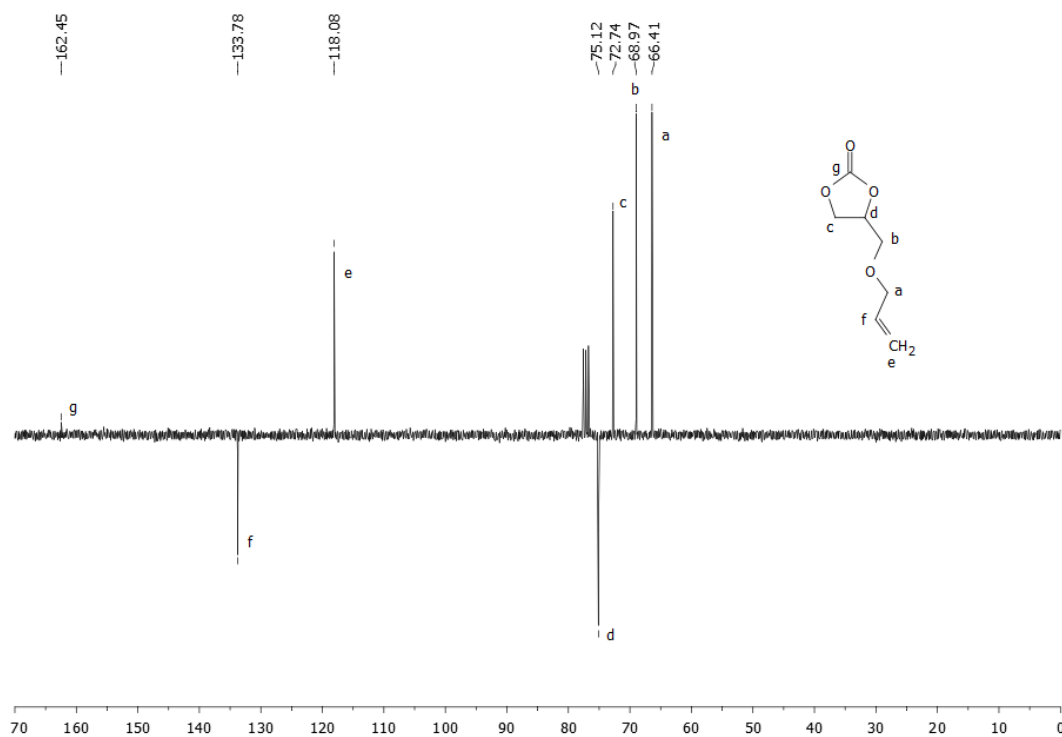
**Figure A.1.31.**  $^1\text{H}$  NMR spectrum of **16** (300 MHz, 298 K,  $\text{CDCl}_3$ ).



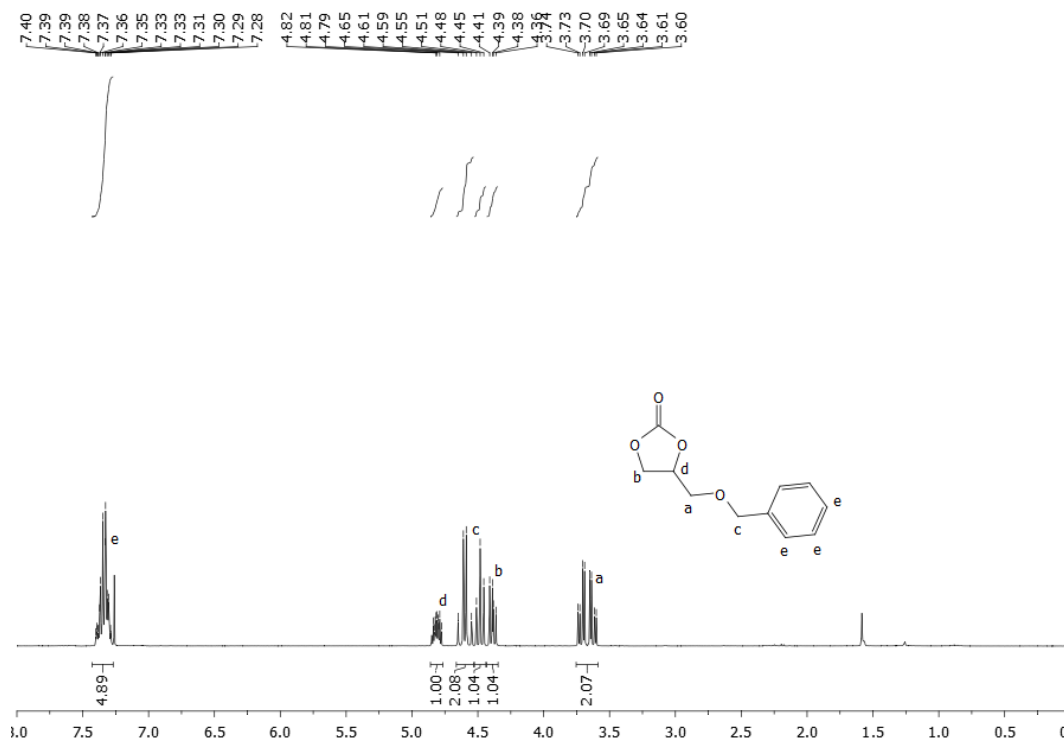
**Figure A.1.32.**  $^{13}\text{C}$  APT NMR spectrum of **16** (75 MHz, 298 K,  $\text{CDCl}_3$ ).



**Figure A.1.33.** <sup>1</sup>H NMR spectrum of **17** (300 MHz, 298 K, CDCl<sub>3</sub>).



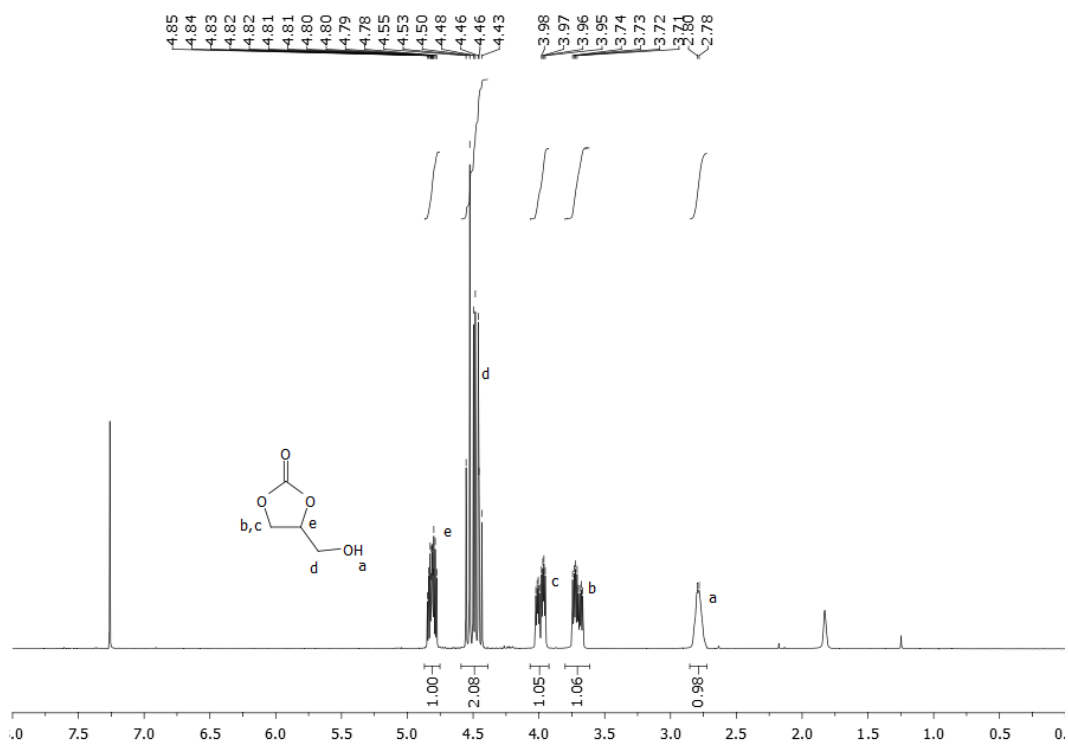
**Figure A.1.34.** <sup>13</sup>C APT NMR spectrum of **17** (75 MHz, 298 K, CDCl<sub>3</sub>).



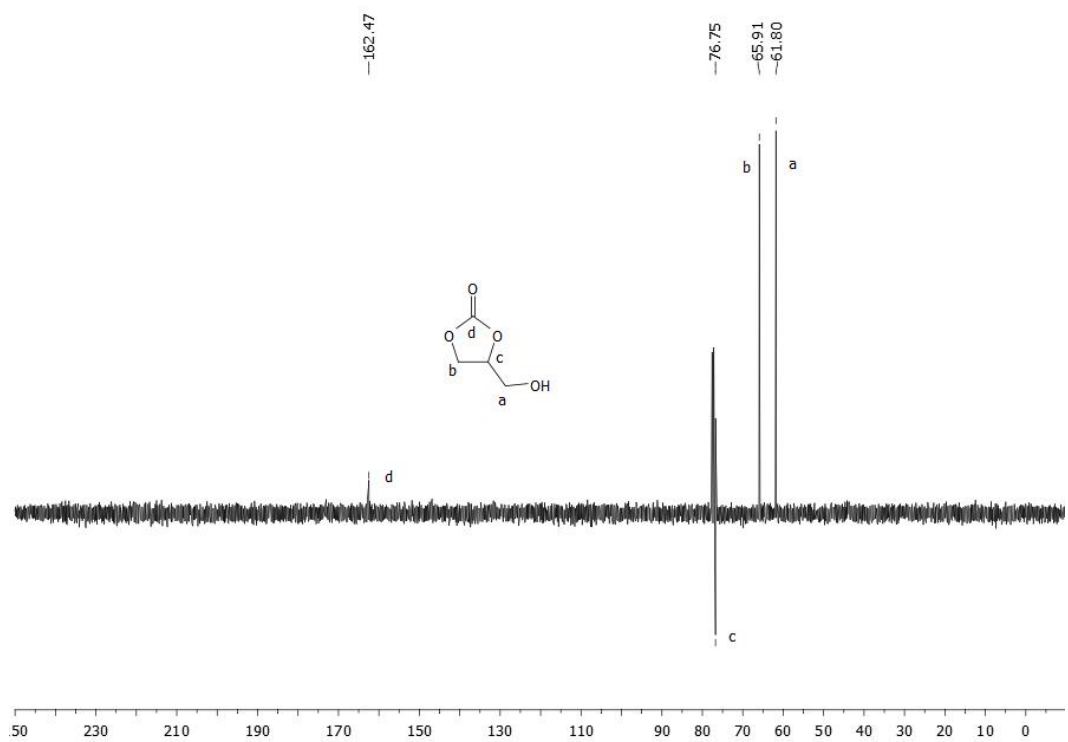
**Figure A.1.35.**  $^1\text{H}$  NMR spectrum of **18** (300 MHz, 298 K,  $\text{CDCl}_3$ ).



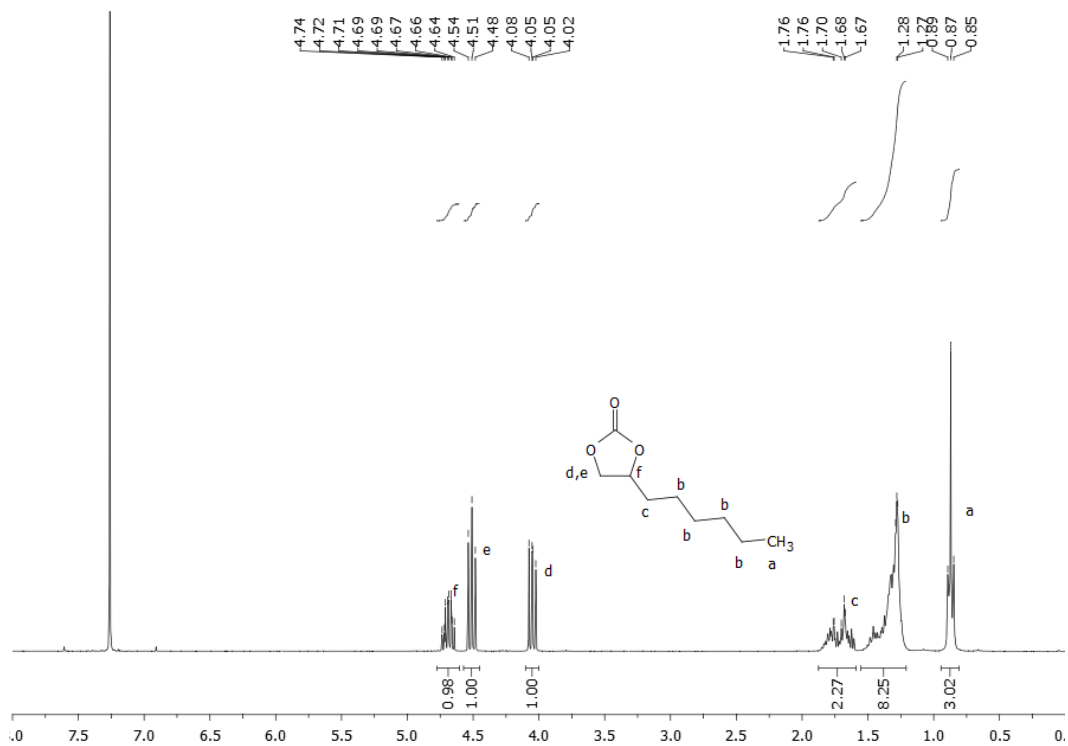
**Figure A.1.36.**  $^{13}\text{C}$  APT NMR spectrum of **18** (75 MHz, 298 K,  $\text{CDCl}_3$ ).



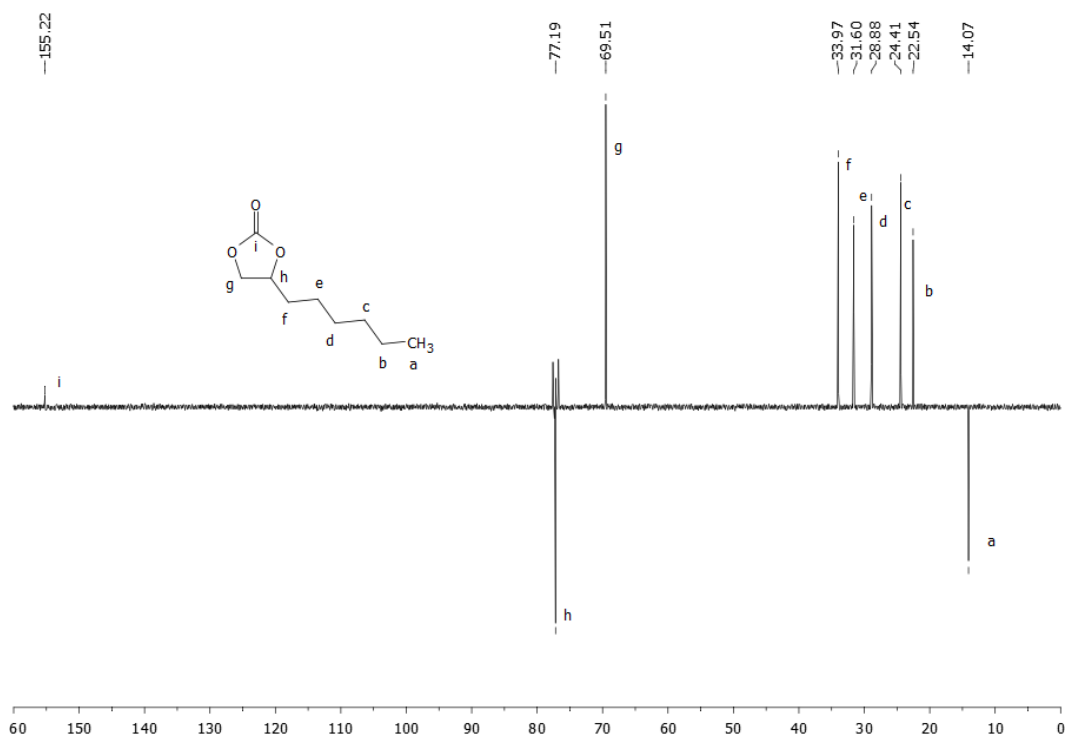
**Figure A.1.37.** <sup>1</sup>H NMR spectrum of **19** (300 MHz, 298 K, CDCl<sub>3</sub>).



**Figure A.1.38.** <sup>13</sup>C APT NMR spectrum of **19** (75 MHz, 298 K, CDCl<sub>3</sub>).

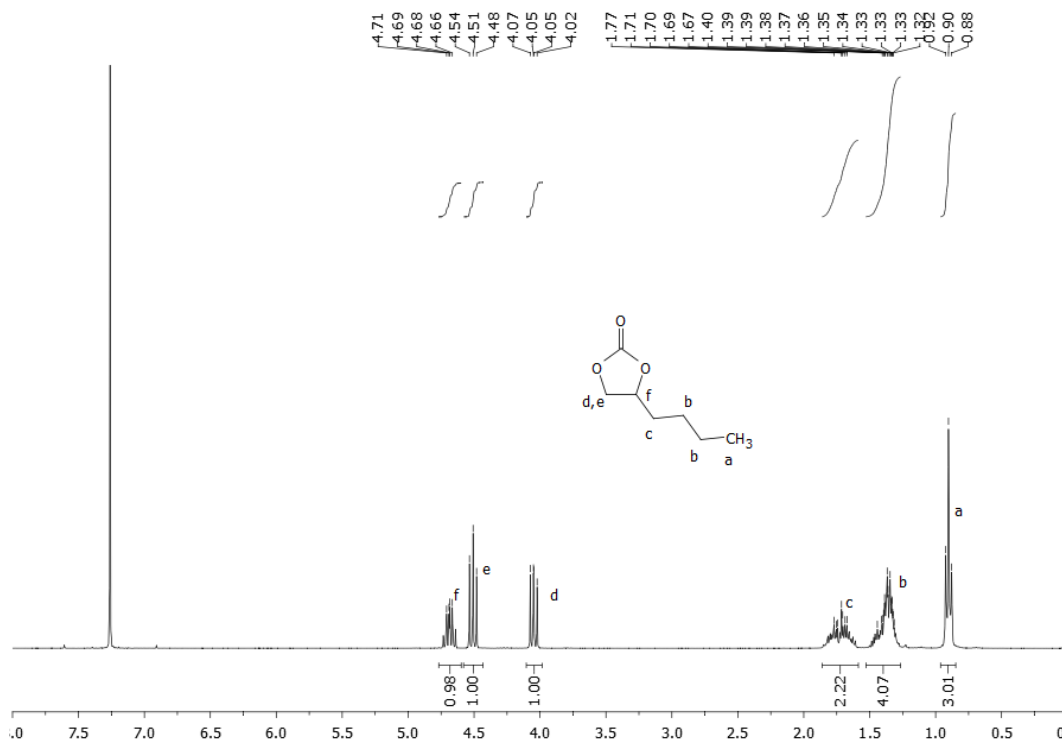


**Figure A.1.39.**  $^1\text{H}$  NMR spectrum of **20** (300 MHz, 298 K,  $\text{CDCl}_3$ ).

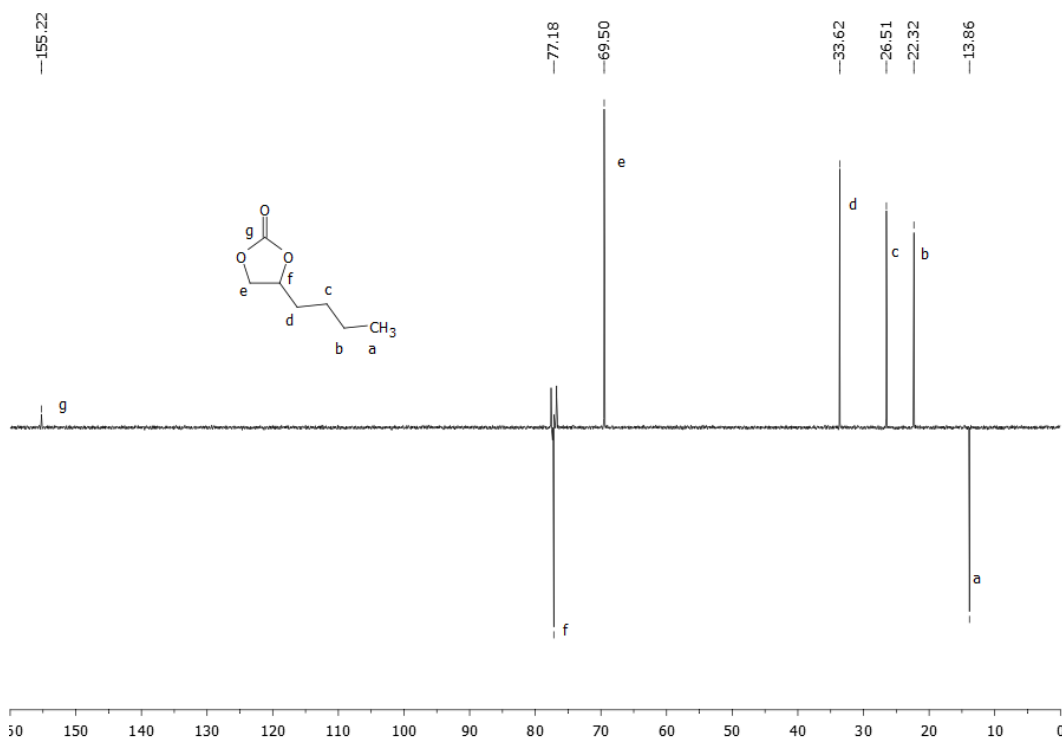


**Figure A.1.40.**  $^{13}\text{C}$  APT NMR spectrum of **20** (75 MHz, 298 K,  $\text{CDCl}_3$ ).

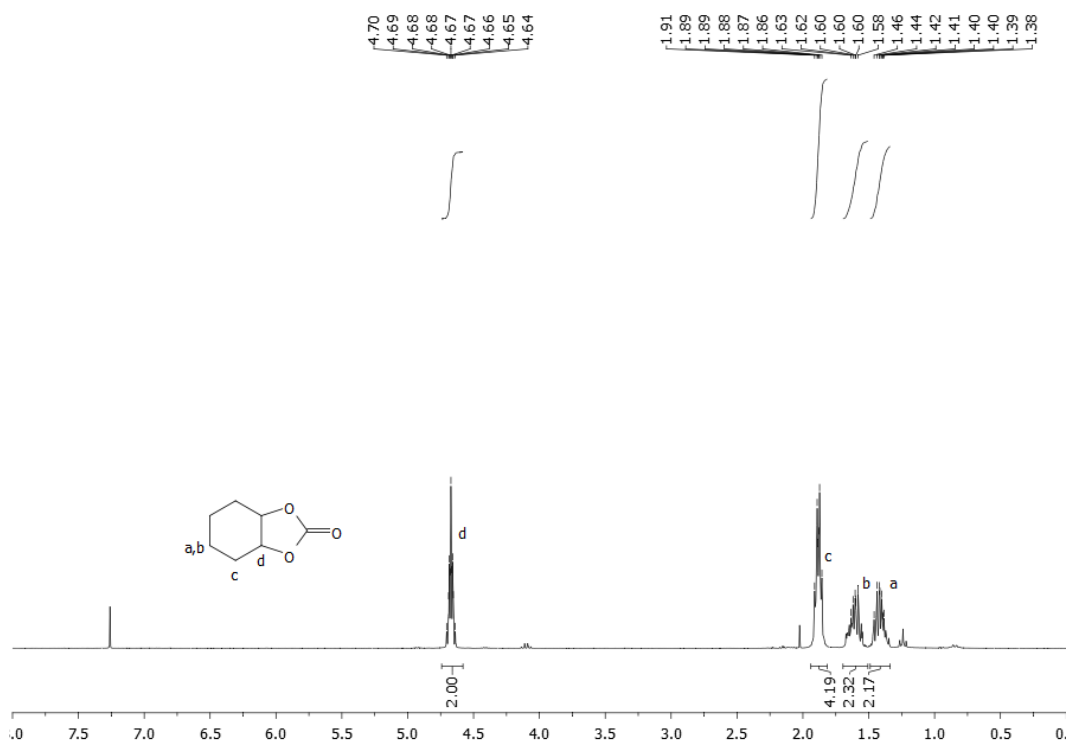




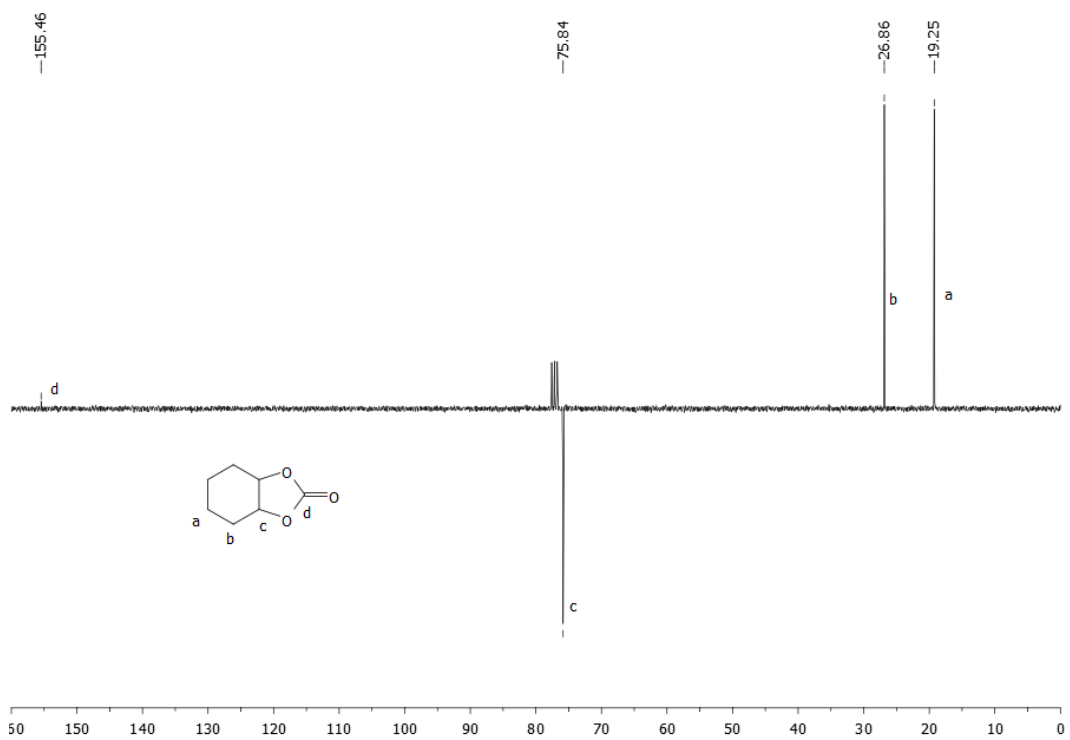
**Figure A.1.41.**  $^1\text{H}$  NMR spectrum of **21** (300 MHz, 298 K,  $\text{CDCl}_3$ ).



**Figure A.1.42.**  $^{13}\text{C}$  APT NMR spectrum of **21** (75 MHz, 298 K,  $\text{CDCl}_3$ ).

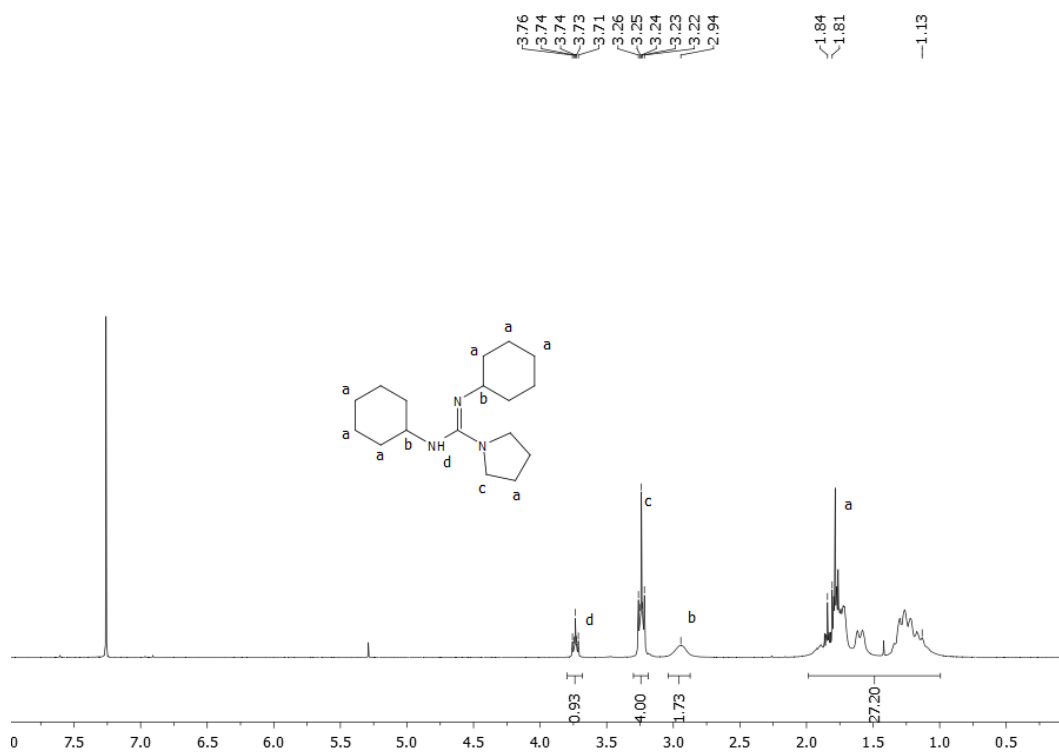


**Figure A.1.43.** <sup>1</sup>H NMR spectrum of **22** (300 MHz, 298 K, CDCl<sub>3</sub>).

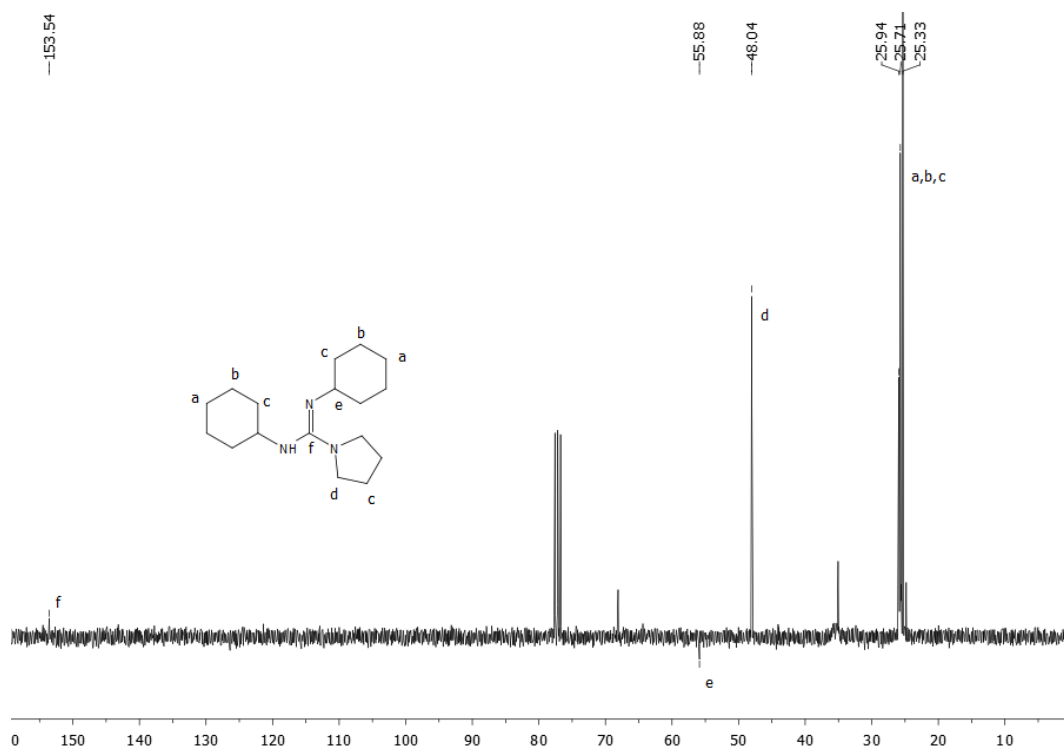


**Figure A.1.44.** <sup>13</sup>C APT NMR spectrum of **22** (75 MHz, 298 K, CDCl<sub>3</sub>).

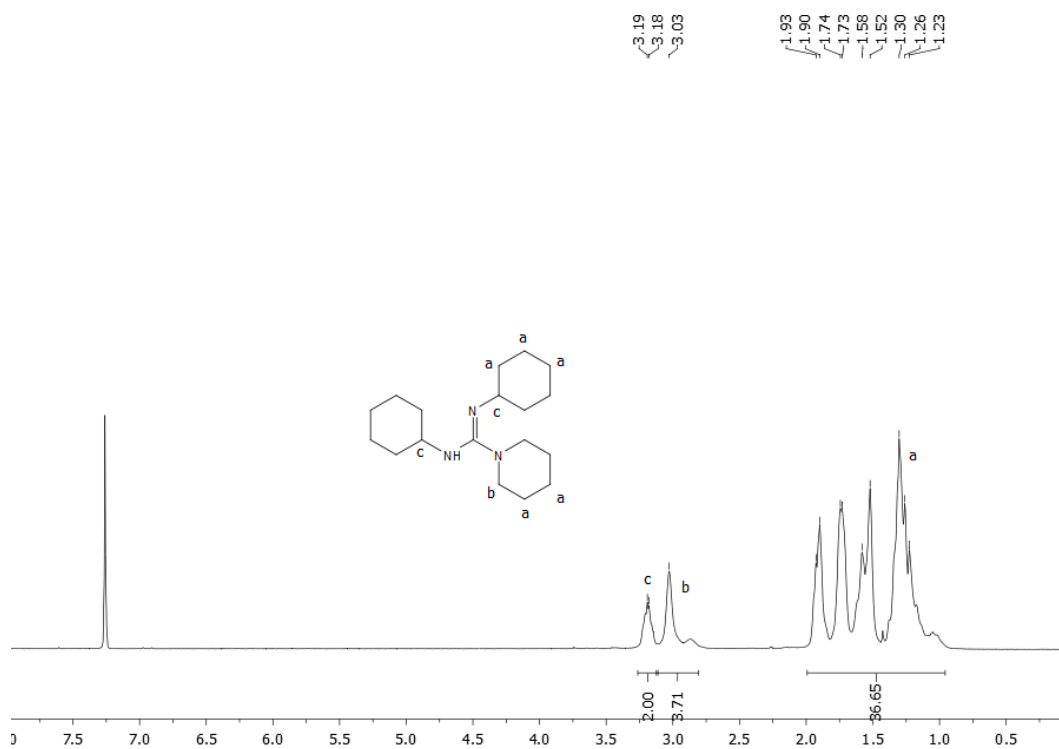
## A.2 Supplementary NMR spectra for Chapter 3



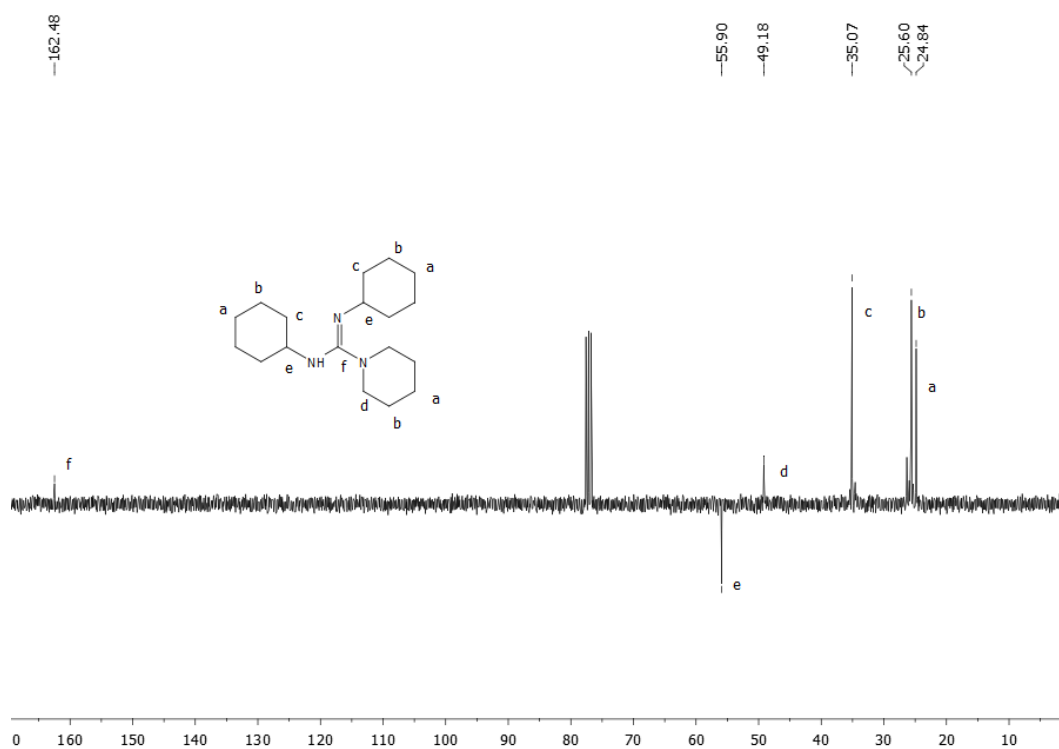
**Figure A.2.1.**  $^1\text{H}$  NMR spectrum of **1** (300 MHz, 298 K,  $\text{CDCl}_3$ ).



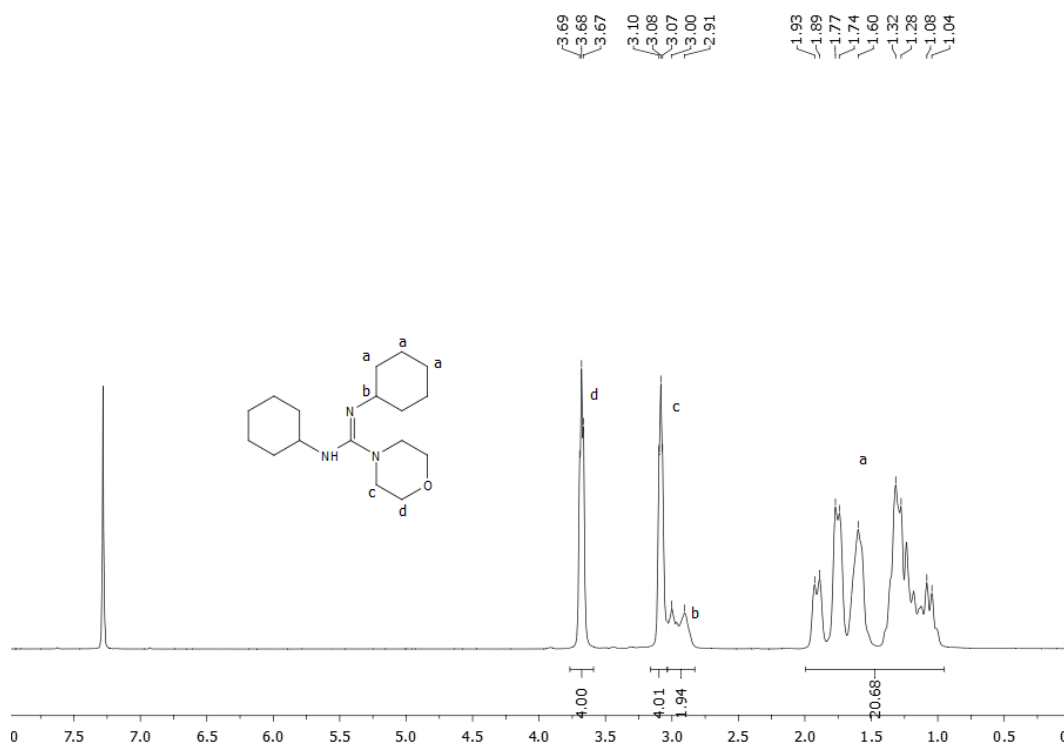
**Figure A.2.2.**  $^{13}\text{C}$  APT NMR spectrum of **1** (75 MHz, 298 K,  $\text{CDCl}_3$ ).



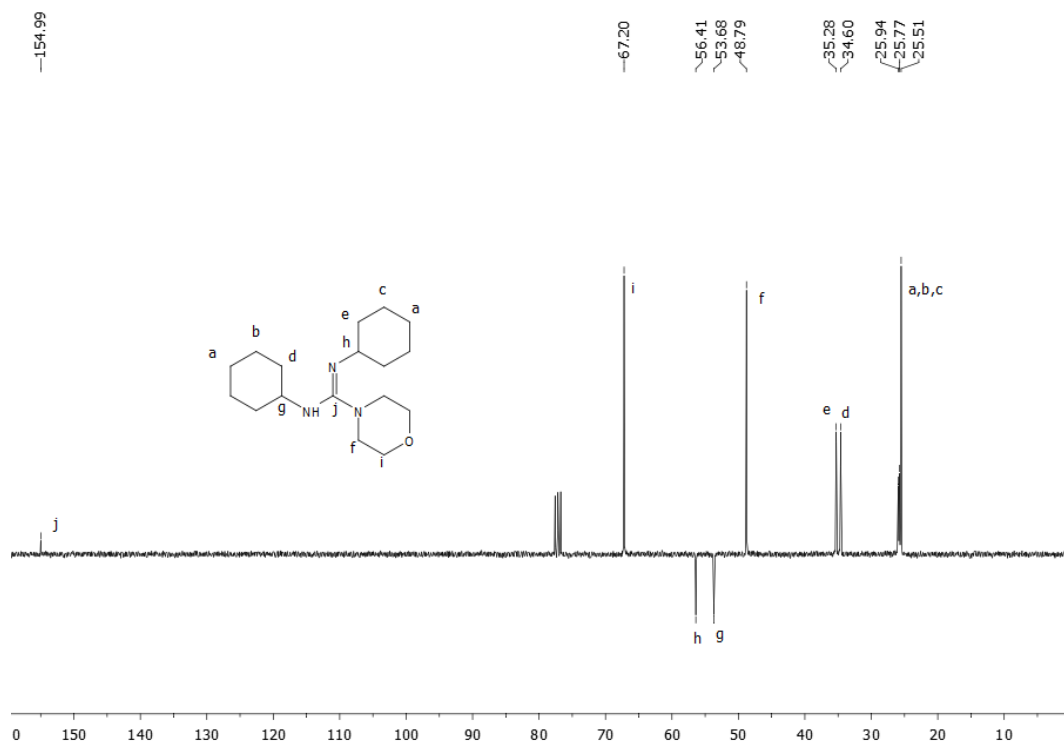
**Figure A.2.3.**  $^1\text{H}$  NMR spectrum of **2** (300 MHz, 298 K,  $\text{CDCl}_3$ ).



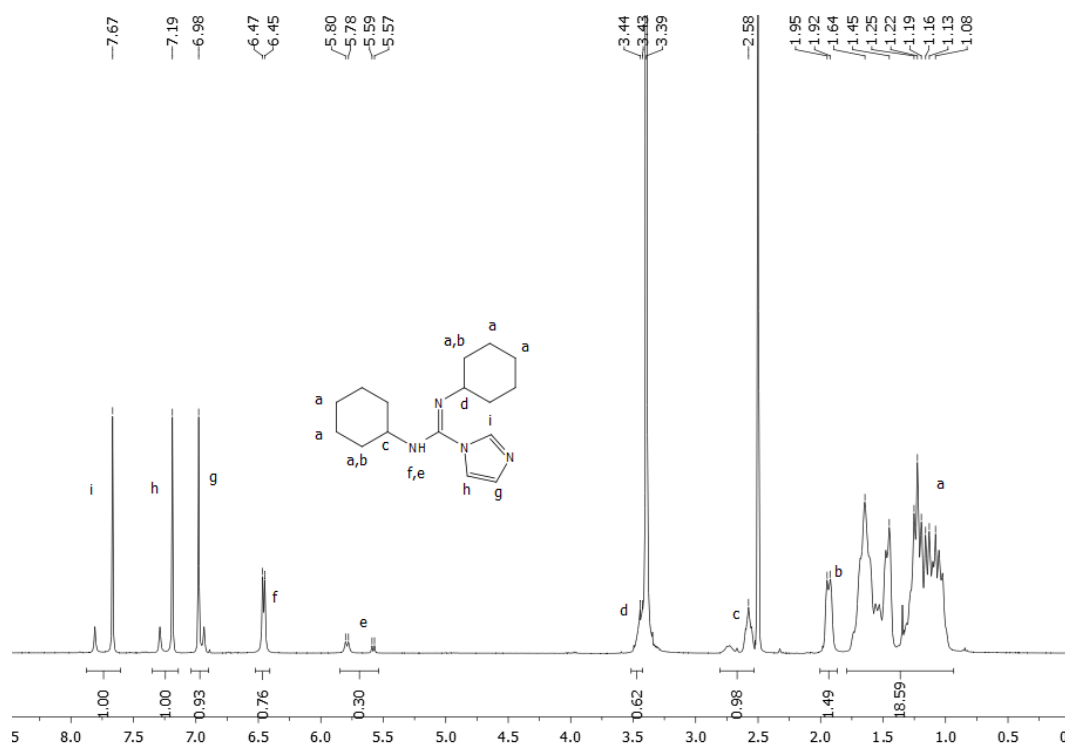
**Figure A.2.4.**  $^{13}\text{C}$  APT NMR spectrum of **2** (75 MHz, 298 K,  $\text{CDCl}_3$ ).



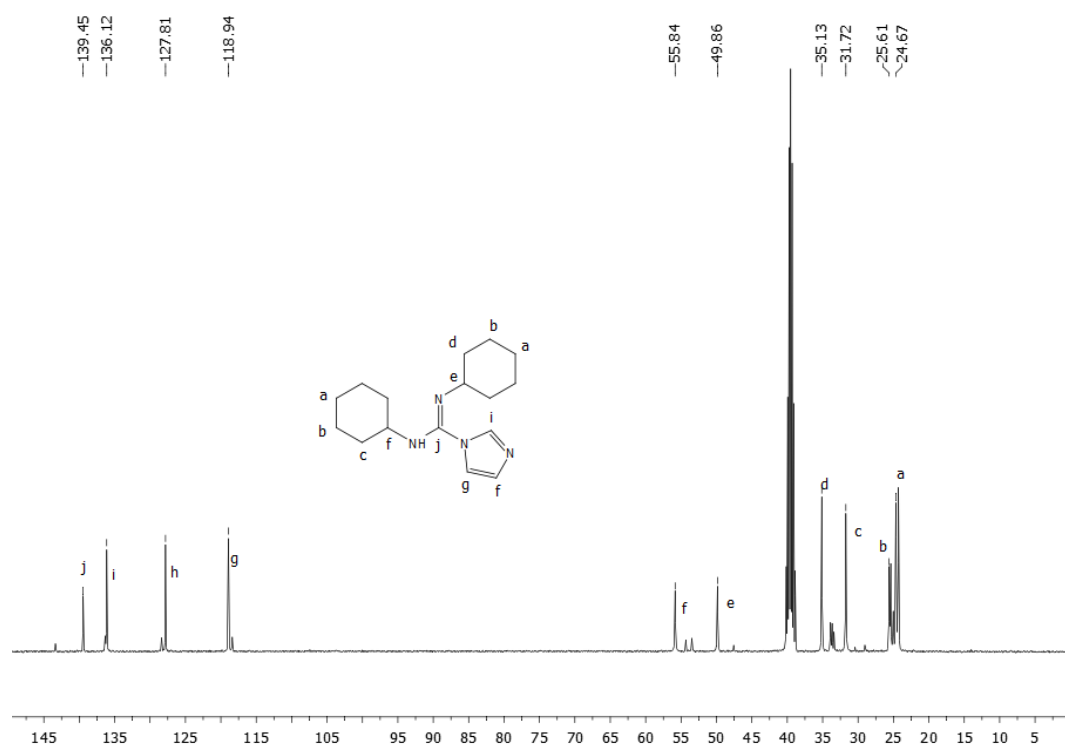
**Figure A.2.5.**  $^1\text{H}$  NMR spectrum of **3** (300 MHz, 298 K,  $\text{CDCl}_3$ ).



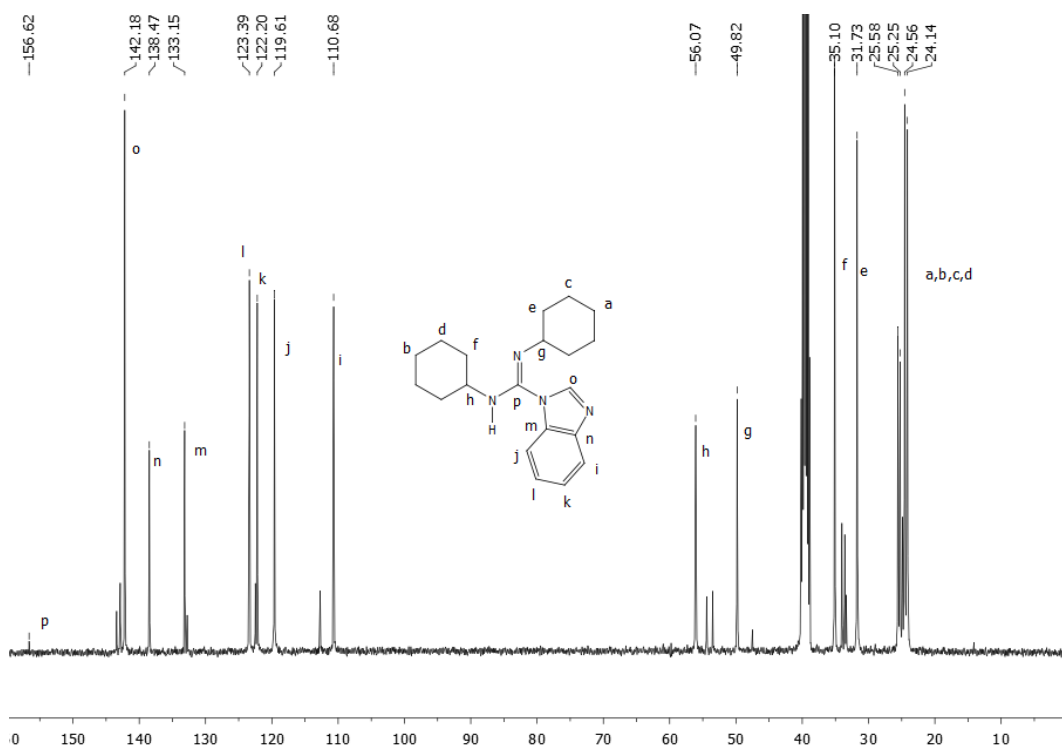
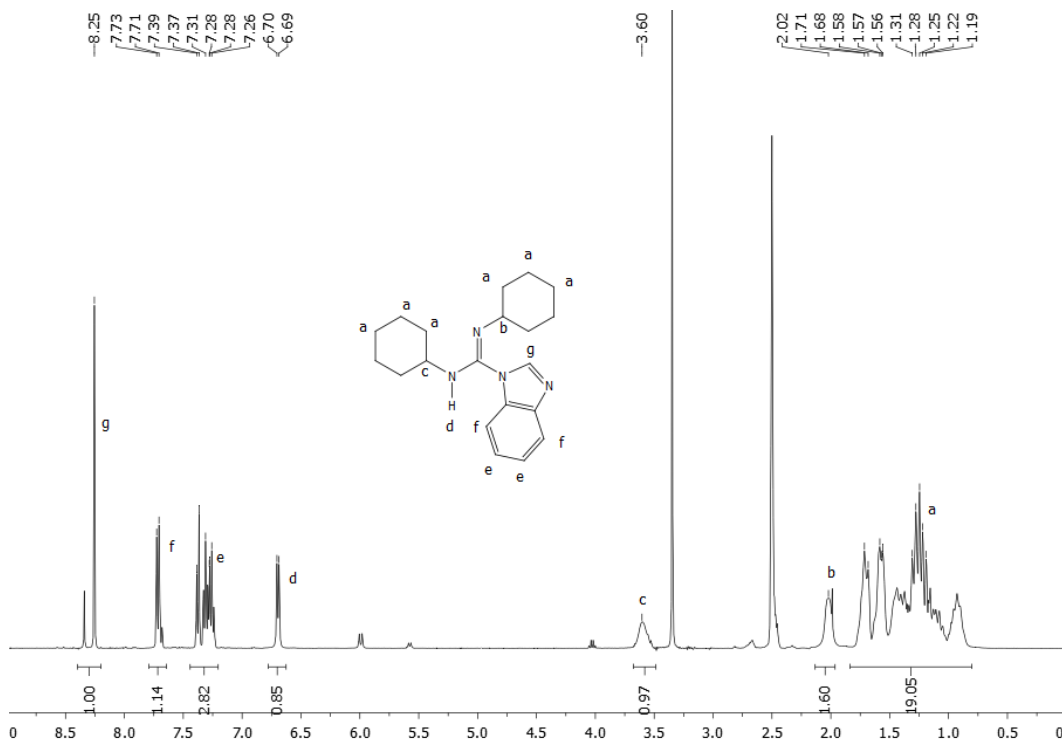
**Figure A.2.6.**  $^{13}\text{C}$  APT NMR spectrum of **3** (75 MHz, 298 K,  $\text{CDCl}_3$ ).

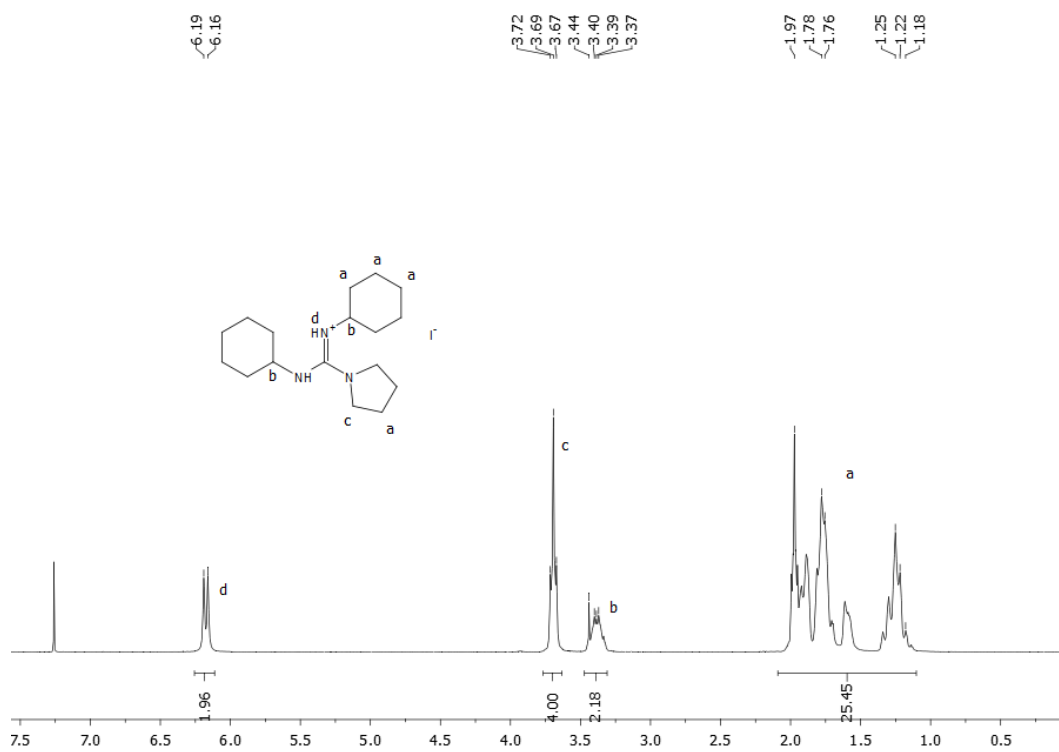


**Figure A.2.7.**  $^1\text{H}$  NMR spectrum of **4** (400 MHz, 298 K,  $\text{CDCl}_3$ ).

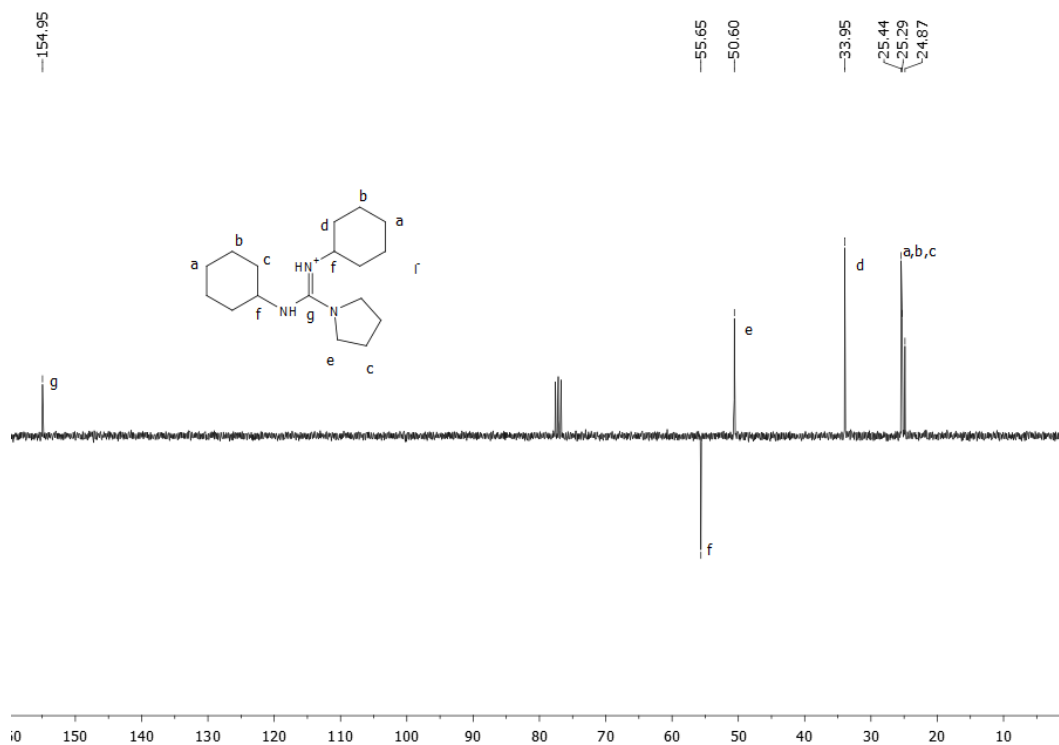


**Figure A.2.8.**  $^{13}\text{C}$  NMR spectrum of **4** (100 MHz, 298 K,  $\text{CDCl}_3$ ).



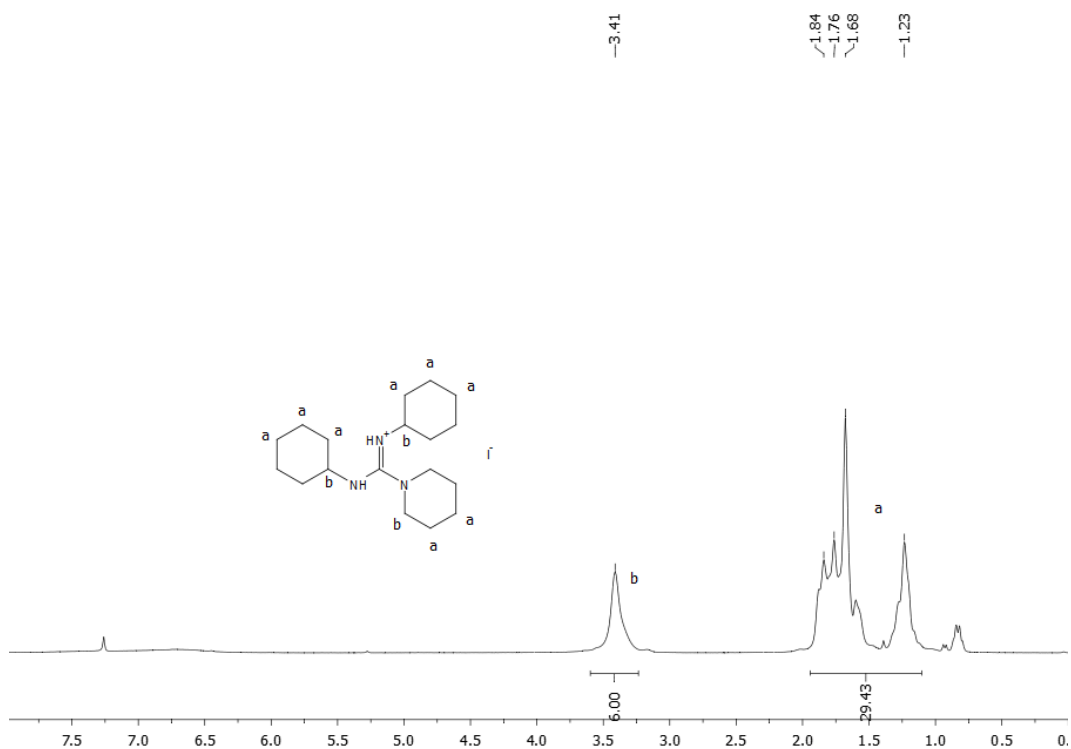


**Figure A.2.11.** <sup>1</sup>H NMR spectrum of **6** (400 MHz, 298 K, CDCl<sub>3</sub>).

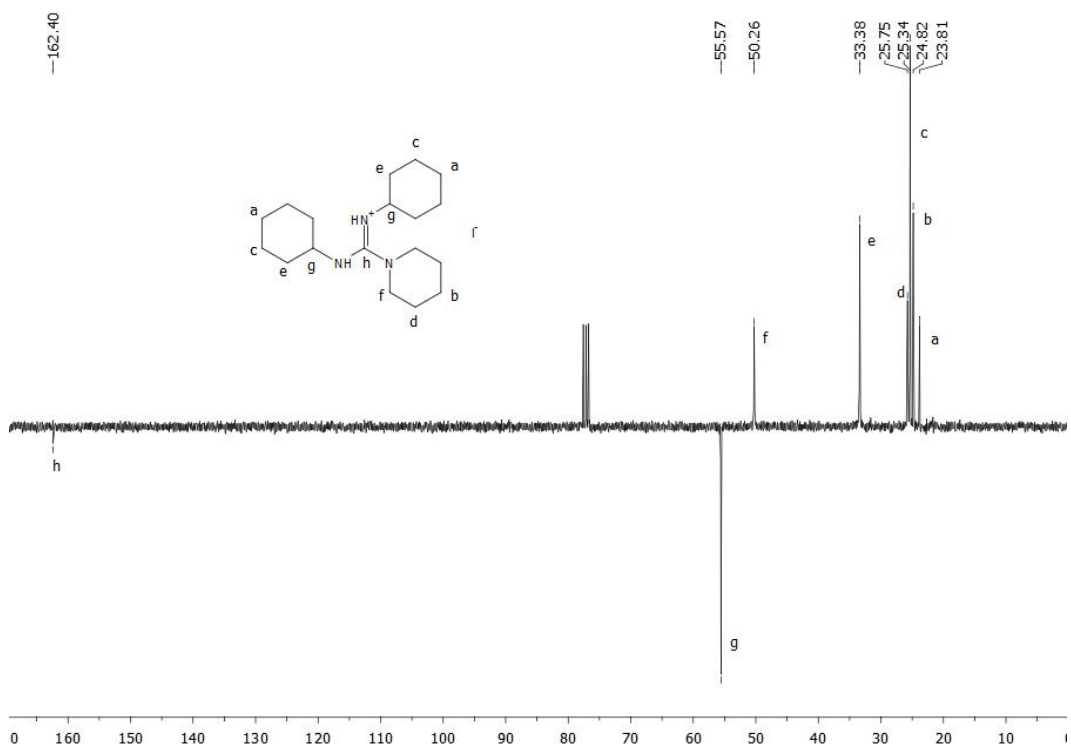


**Figure A.2.12.** <sup>13</sup>C APT NMR spectrum of **6** (100 MHz, 298 K, CDCl<sub>3</sub>).

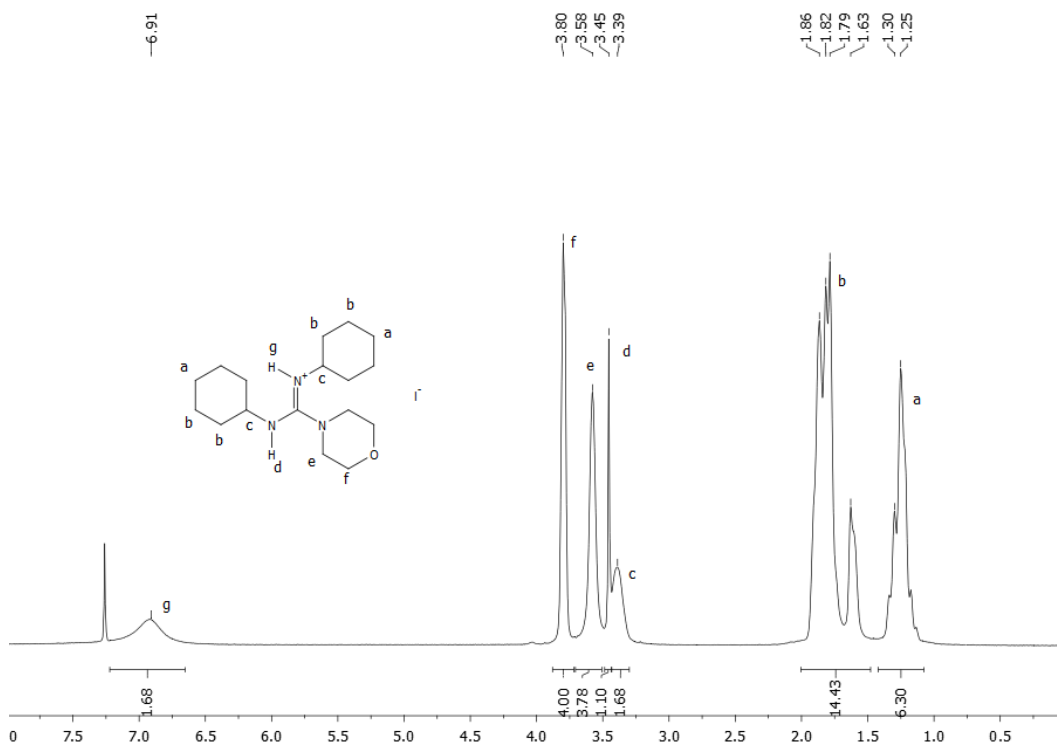




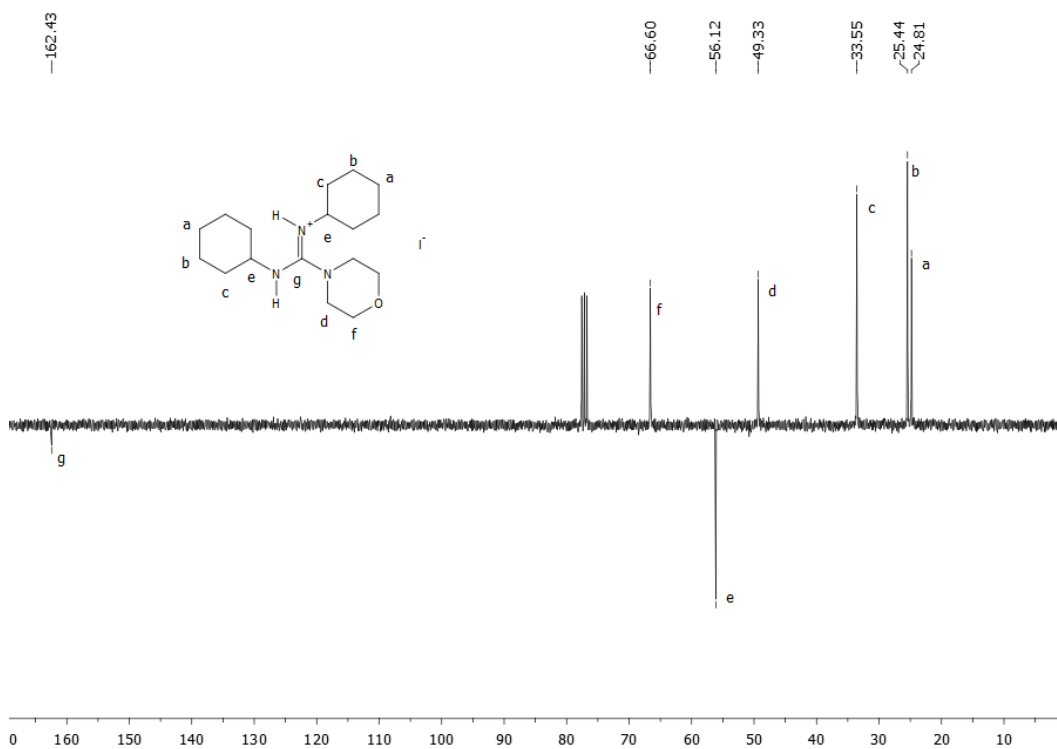
**Figure A.2.13.**  $^1\text{H}$  NMR spectrum of **7** (400 MHz, 298 K,  $\text{CDCl}_3$ ).



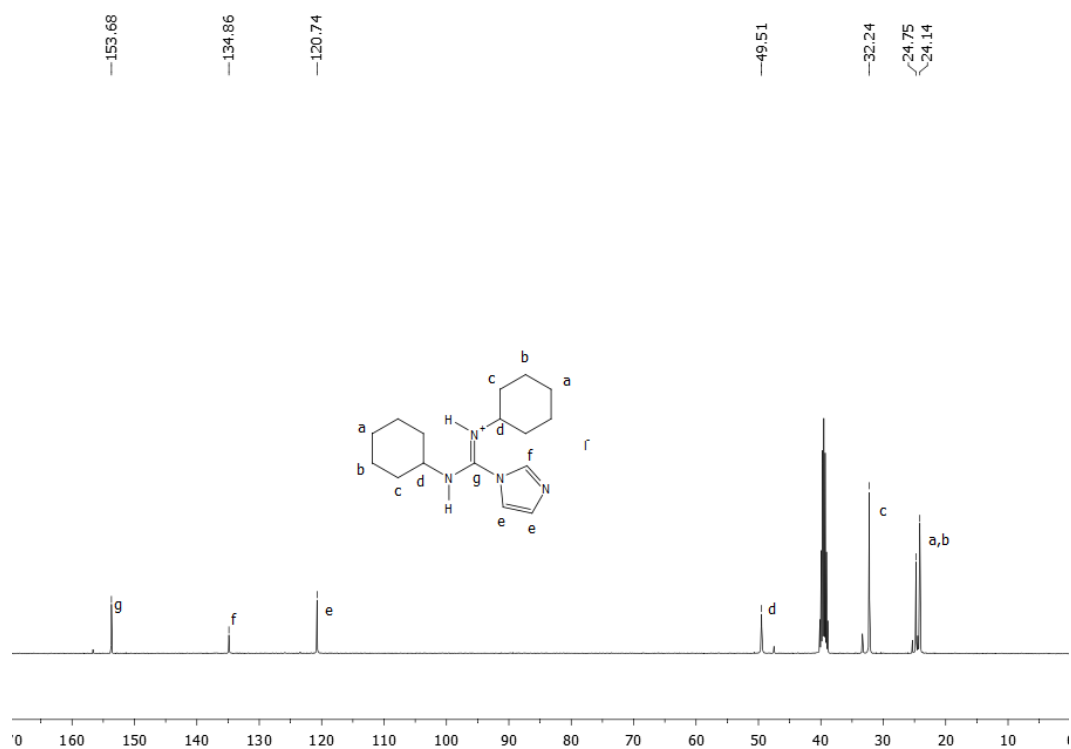
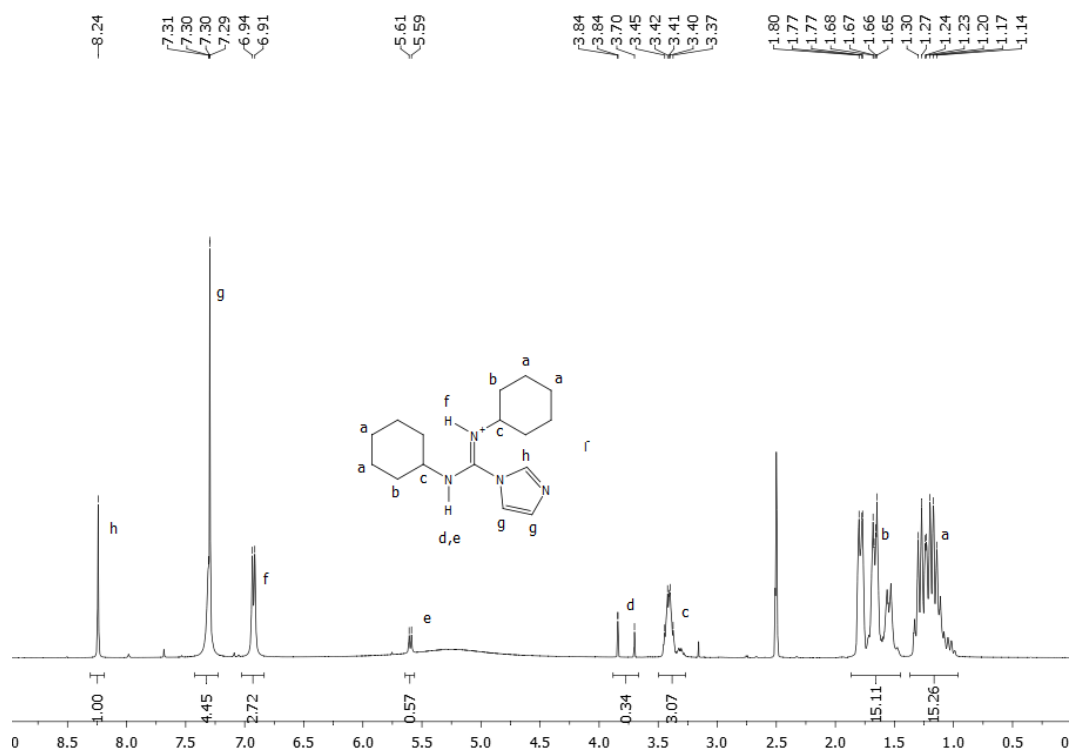
**Figure A.2.14.**  $^{13}\text{C}$  APT NMR spectrum of **7** (100 MHz, 298 K,  $\text{CDCl}_3$ ).



**Figure A.2.15.**  $^1\text{H}$  NMR spectrum of **8** (400 MHz, 298 K,  $\text{CDCl}_3$ ).



**Figure A.2.16.**  $^{13}\text{C}$  APT NMR spectrum of **8** (100 MHz, 298 K,  $\text{CDCl}_3$ ).



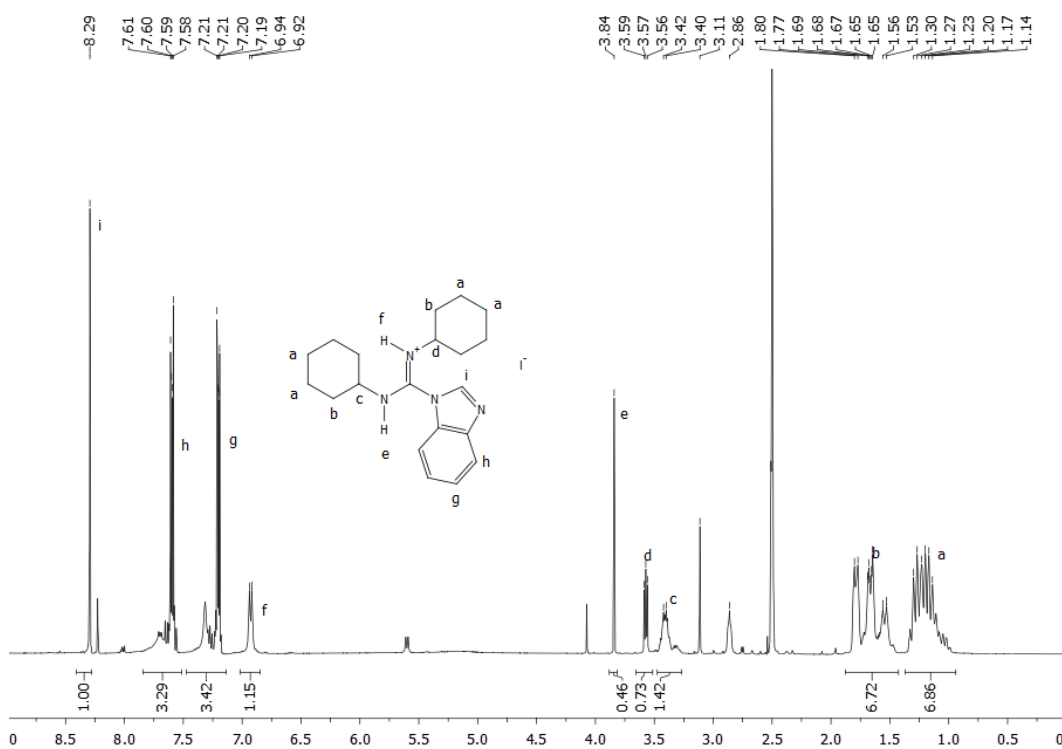


**Figure A.2.19.**  $^1\text{H}$  NMR spectrum of **10** (400 MHz, 298 K, DMSO).

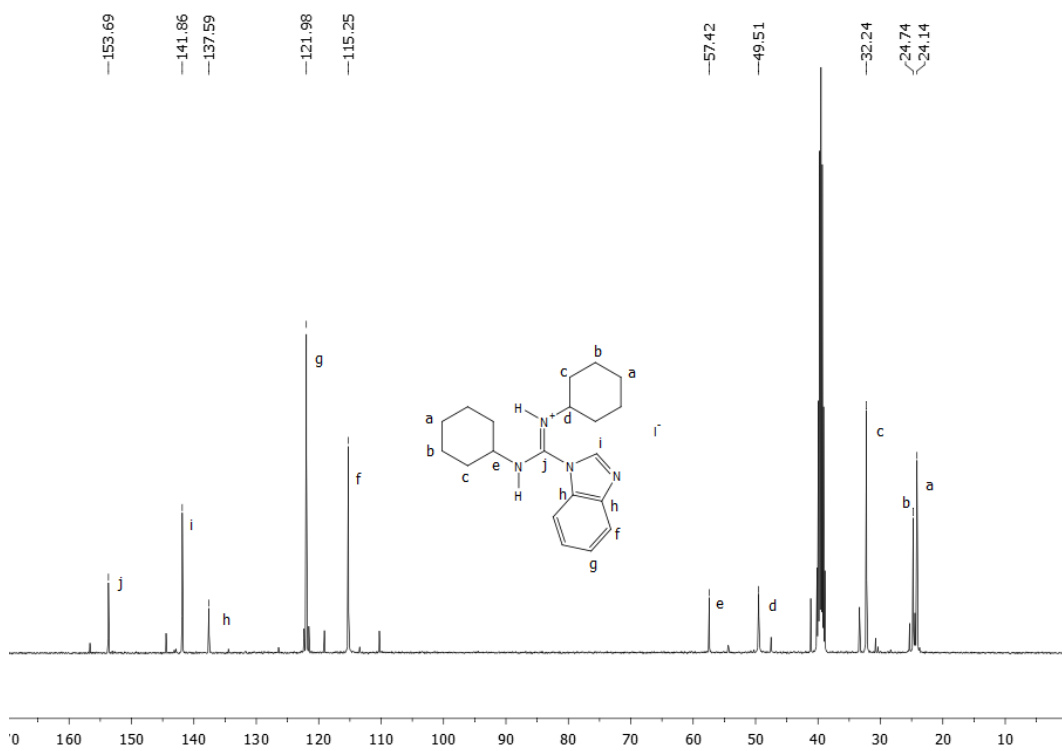


**Figure A.2.20.**  $^{13}\text{C}$  NMR spectrum of **10** (100 MHz, 298 K, DMSO).

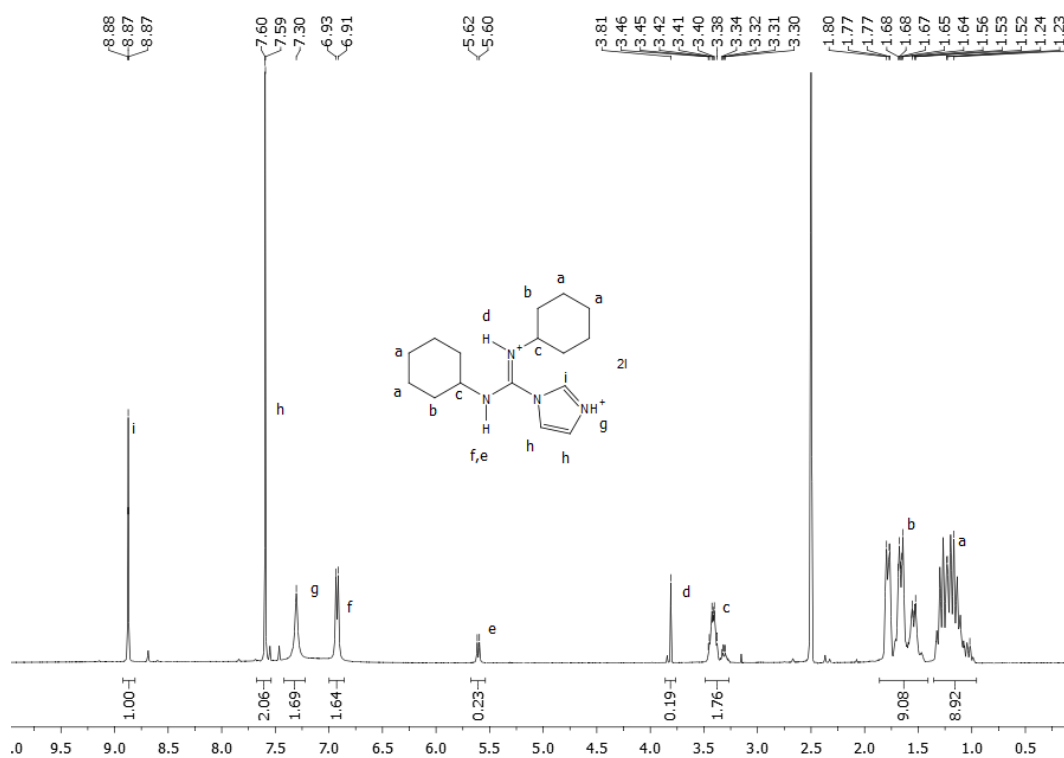


**Figure A.2.21.**  $^1\text{H}$  NMR spectrum of **11** (400 MHz, 298 K, DMSO).

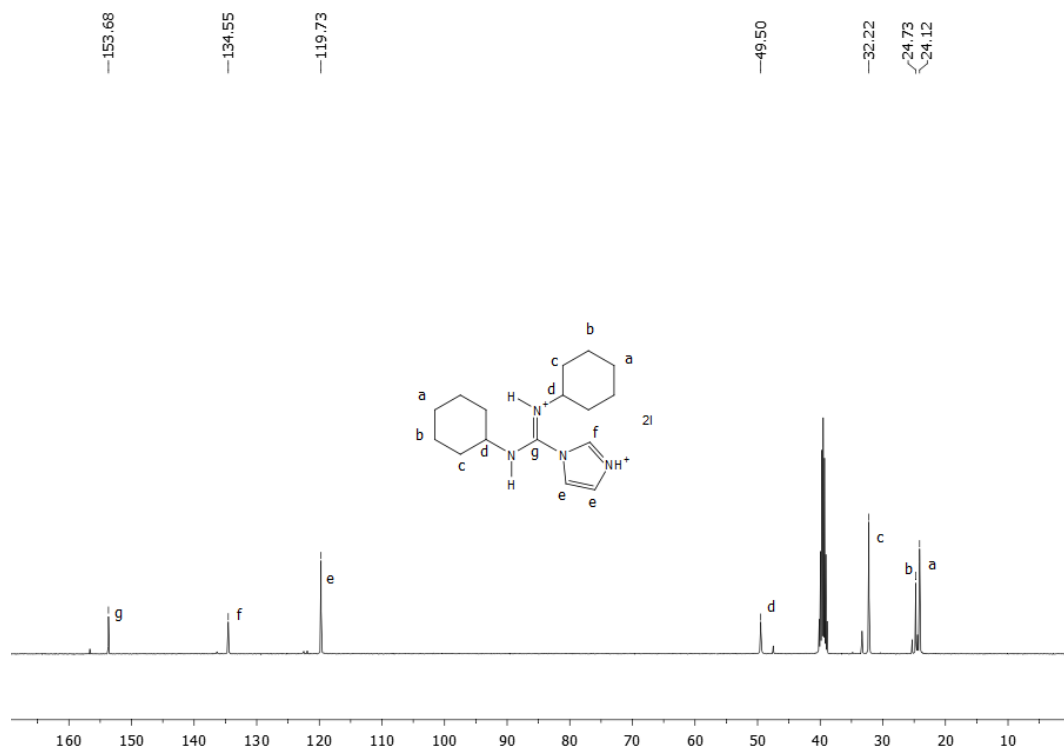


**Figure A.2.22.**  $^{13}\text{C}$  NMR spectrum of **11** (100 MHz, 298 K, DMSO).

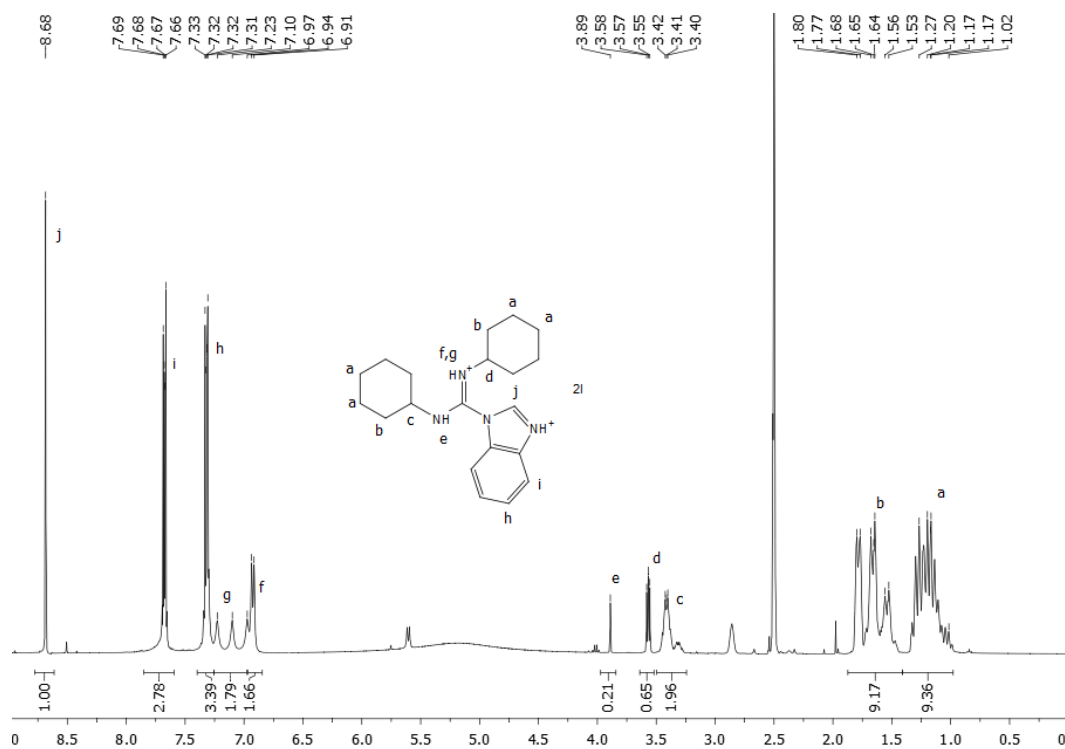


**Figure A.2.23.**  $^1\text{H}$  NMR spectrum of **12** (400 MHz, 298 K, DMSO).

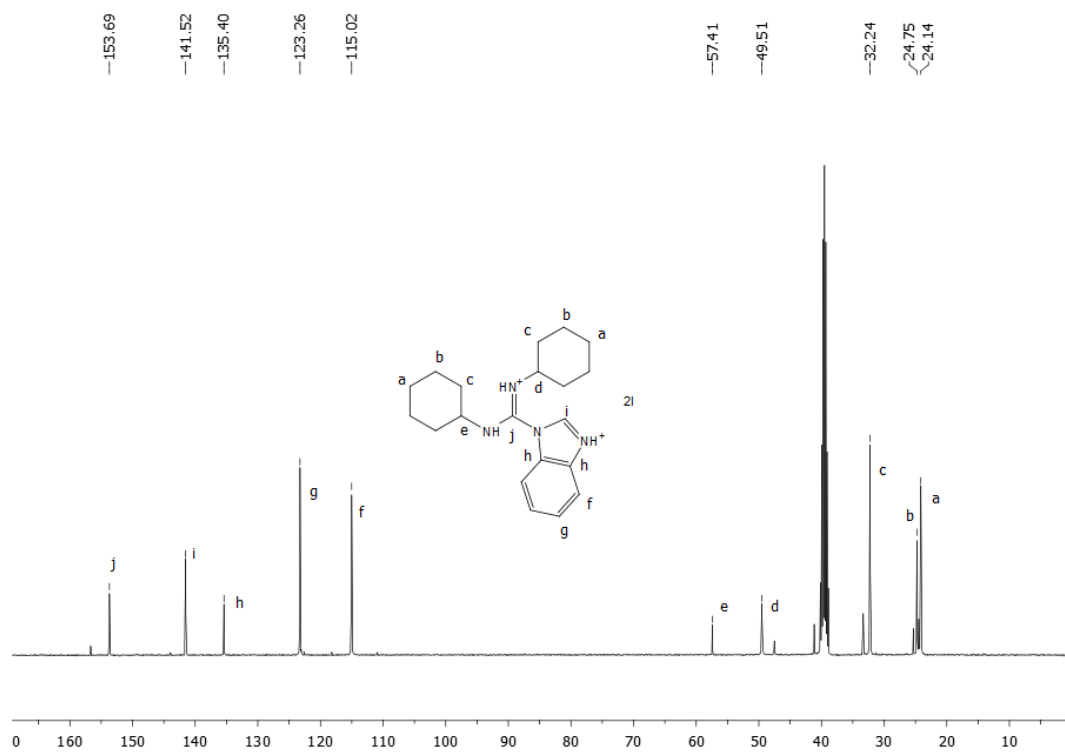


**Figure A.2.24.**  $^{13}\text{C}$  NMR spectrum of **12** (100 MHz, 298 K, DMSO).

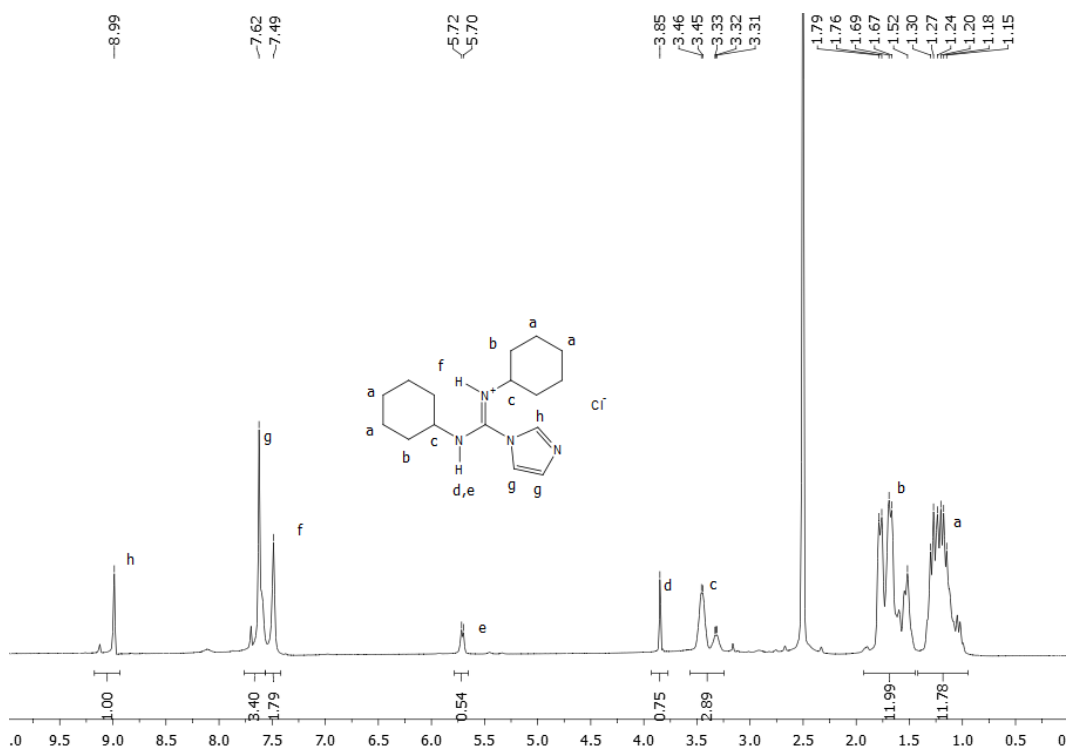


**Figure A.2.25.**  $^1\text{H}$  NMR spectrum of **13** (400 MHz, 298 K, DMSO).

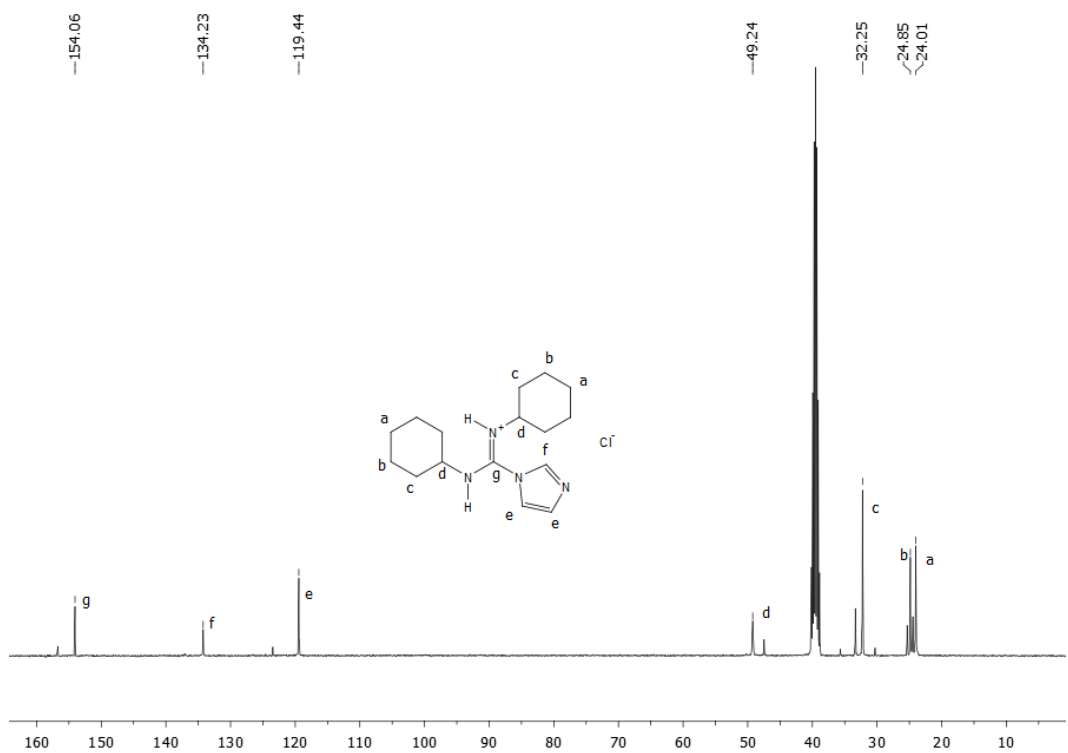


**Figure A.2.26.**  $^{13}\text{C}$  NMR spectrum of **13** (100 MHz, 298 K, DMSO).

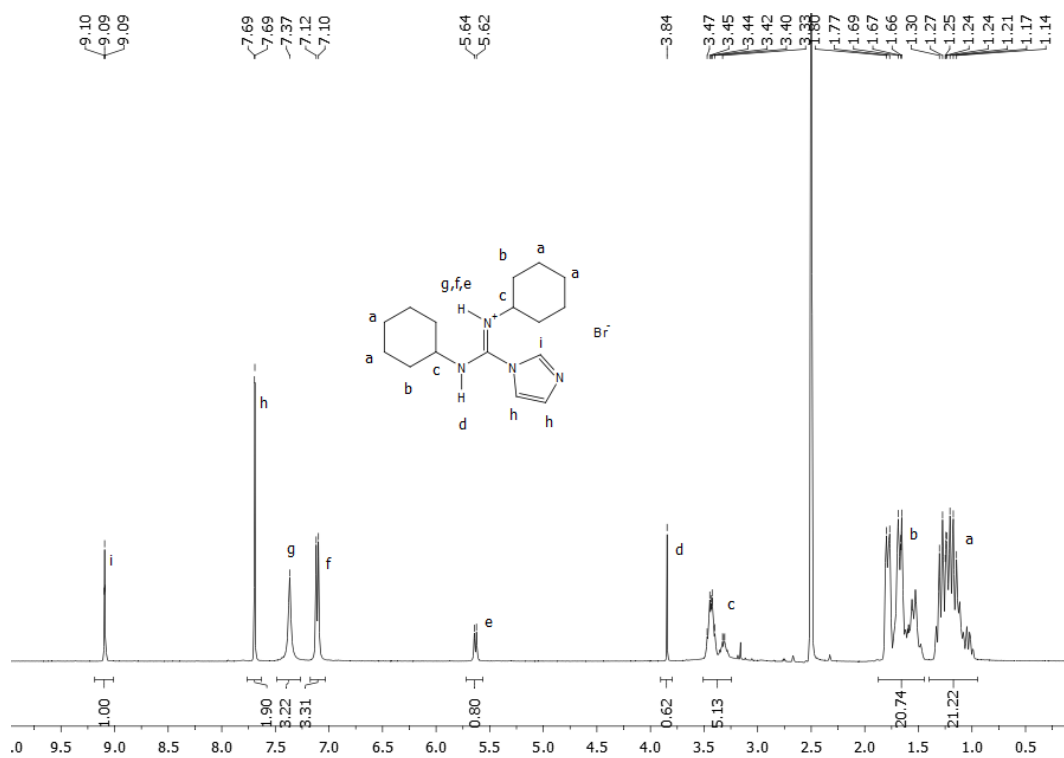


**Figure A.2.27.**  $^1\text{H}$  NMR spectrum of **14** (400 MHz, 298 K, DMSO).

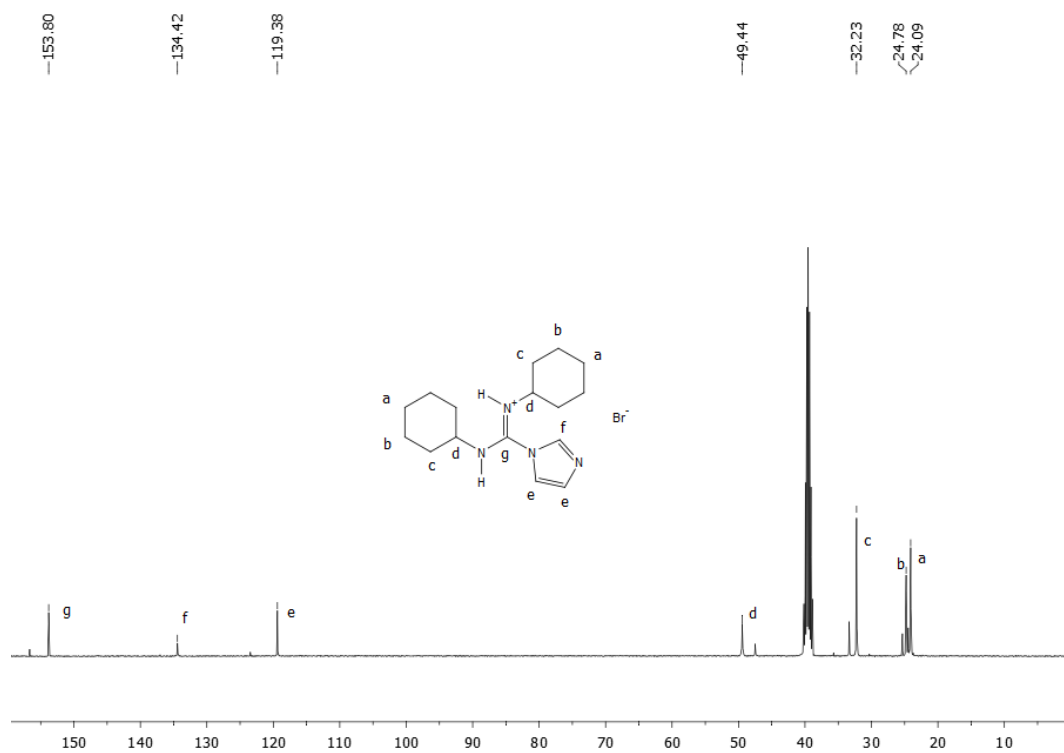


**Figure A.2.28.**  $^{13}\text{C}$  NMR spectrum of **14** (100 MHz, 298 K, DMSO).



### A.3 Supplementary NMR spectra for Chapter 4

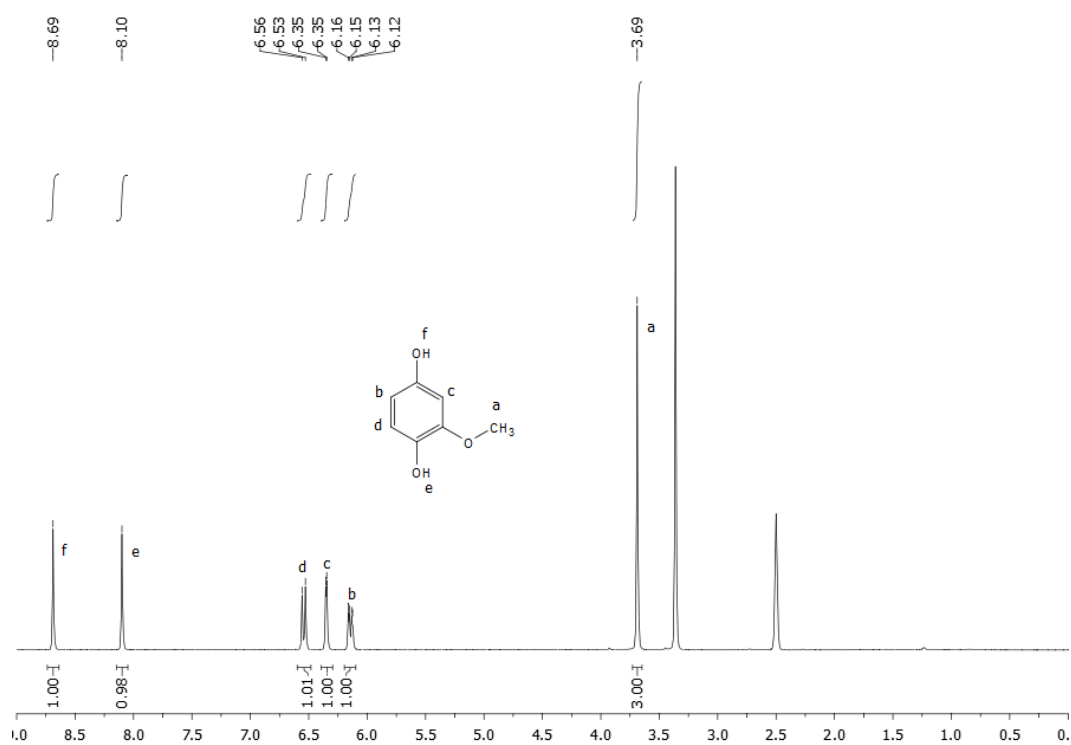


**Figure A.3.1.**  $^1\text{H}$  NMR spectrum of **2** (300 MHz, 298 K, DMSO).

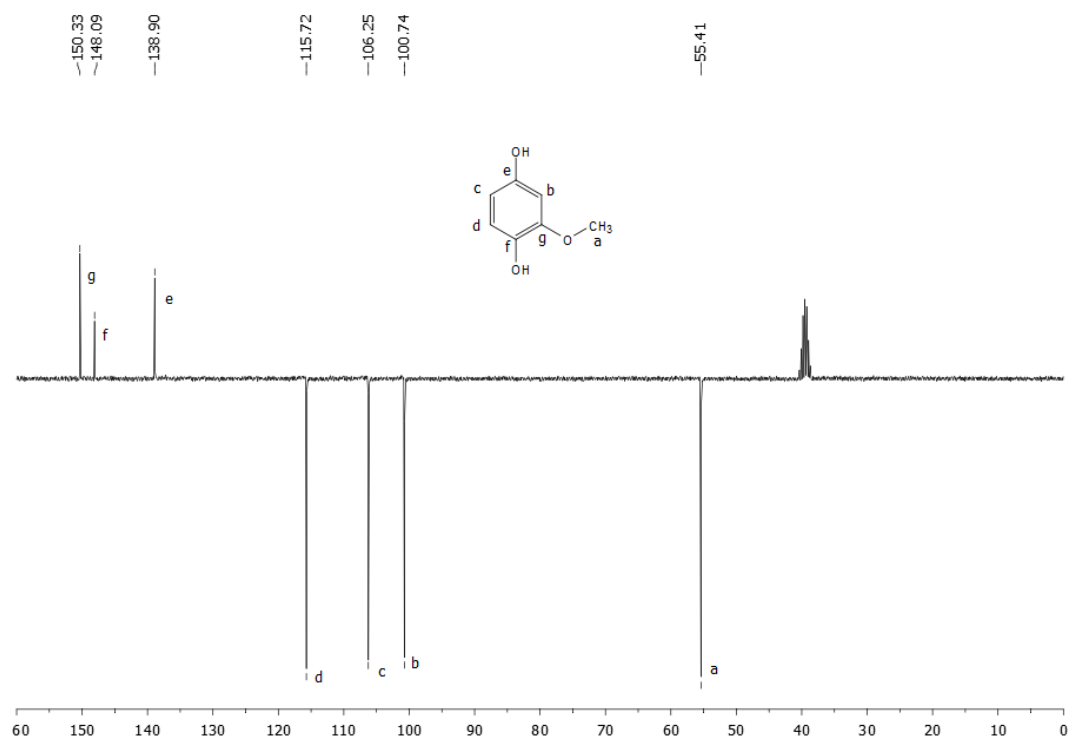


**Figure A.3.2.**  $^{13}\text{C}$  APT NMR spectrum of **2** (75 MHz, 298 K, DMSO).

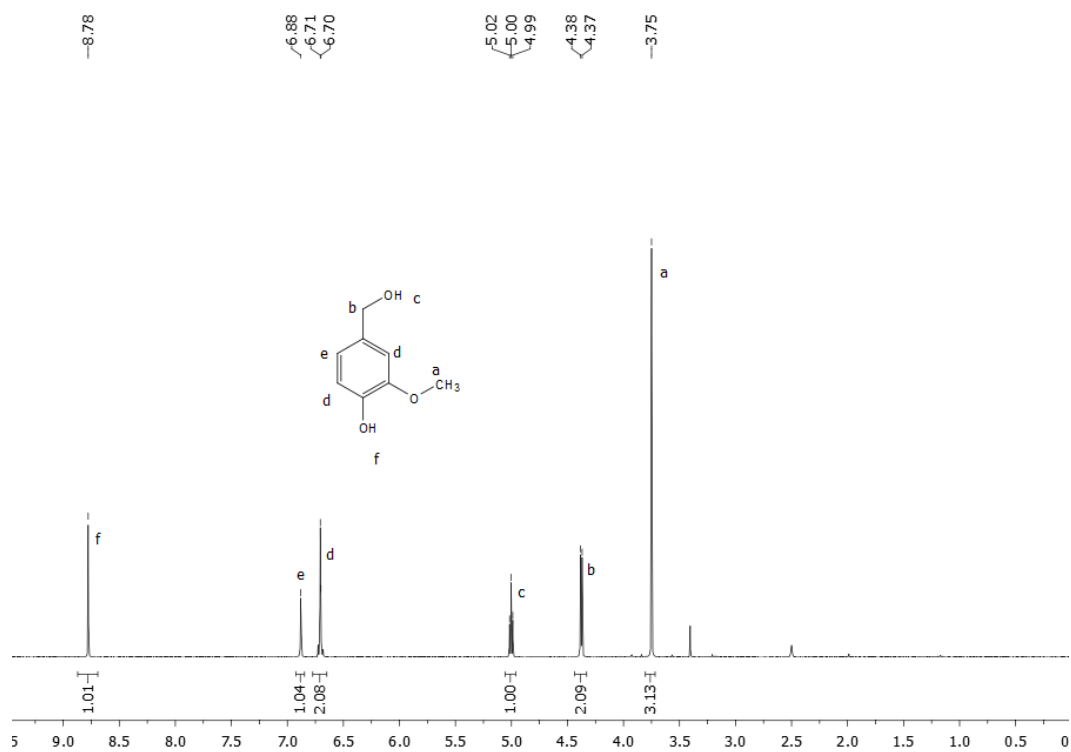


**Figure A.3.3.** <sup>1</sup>H NMR spectrum of **4** (300 MHz, 298 K, DMSO).

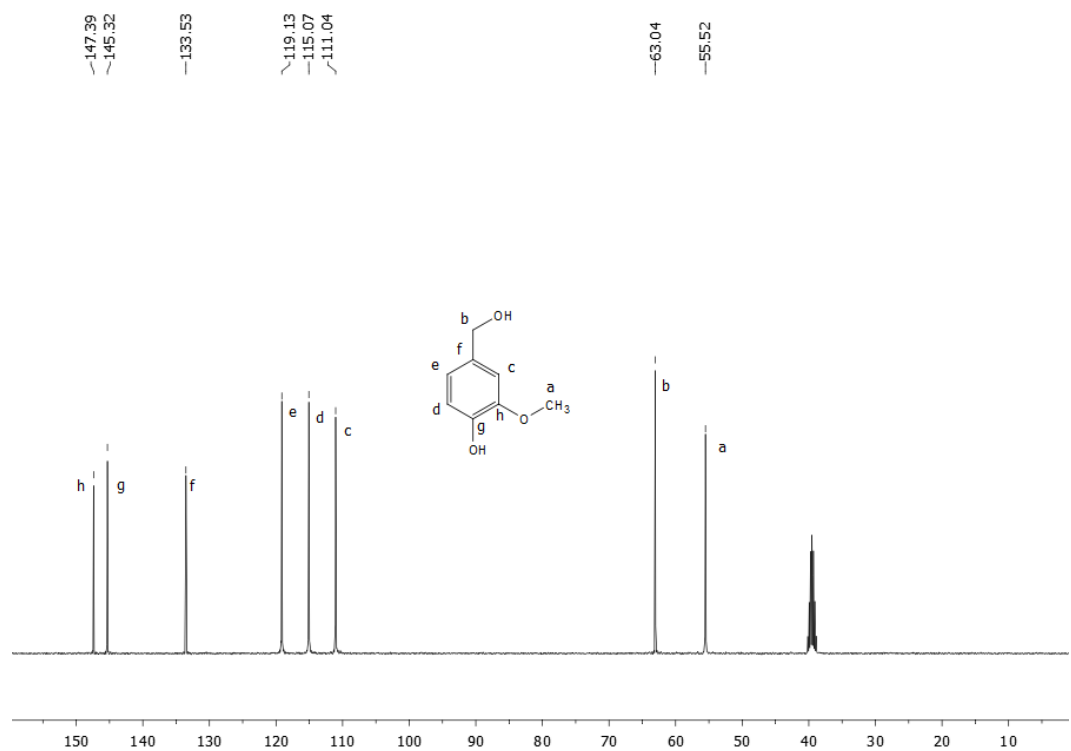


**Figure A.3.4.** <sup>13</sup>C NMR spectrum of **4** (75 MHz, 298 K, DMSO).

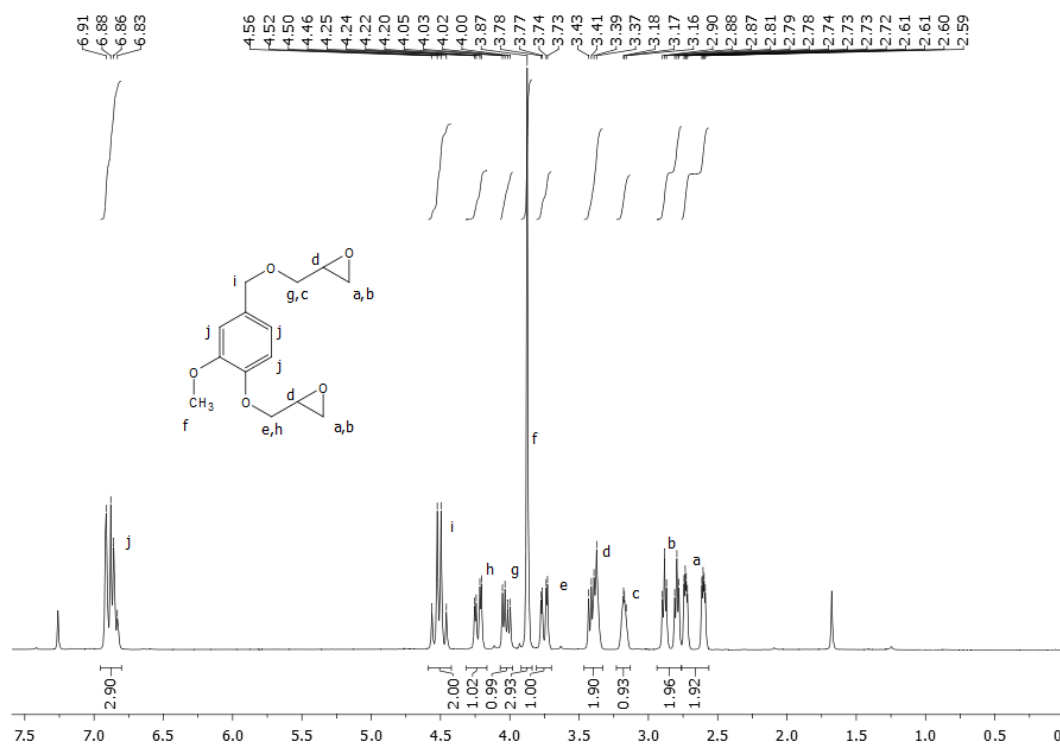


**Figure A.3.5.**  $^1\text{H}$  NMR spectrum of **5** (300 MHz, 298 K,  $\text{CDCl}_3$ ).

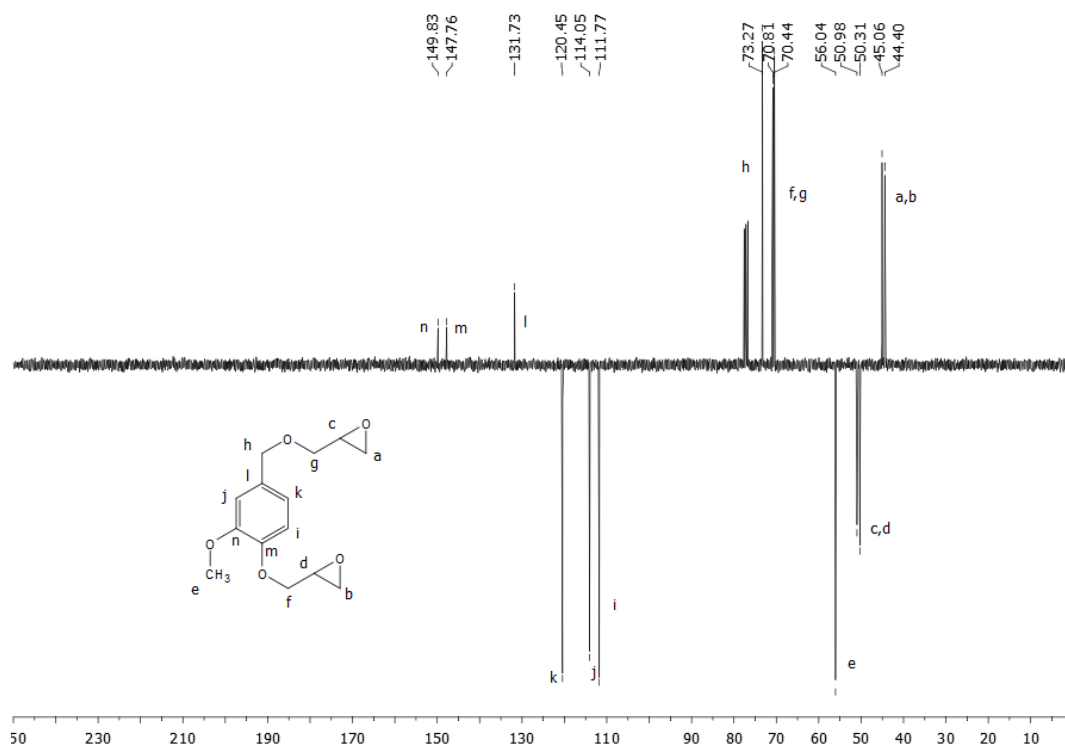


**Figure A.3.6.**  $^{13}\text{C}$  APT NMR spectrum of **5** (75 MHz, 298 K,  $\text{CDCl}_3$ ).

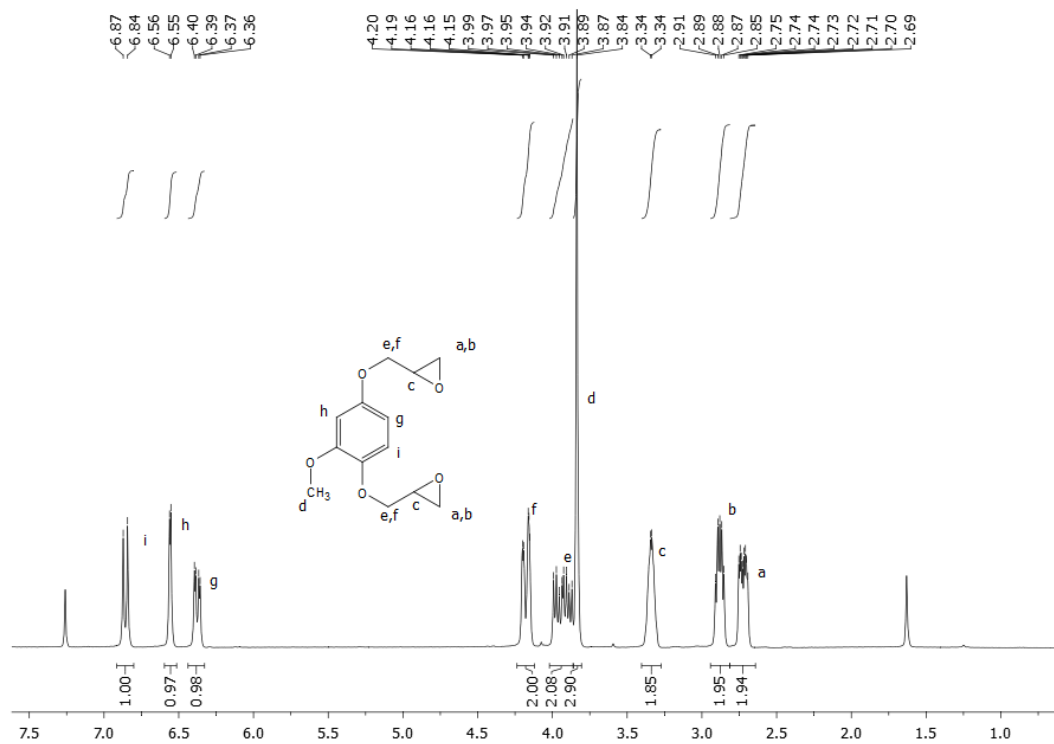


**Figure A.3.7.**  $^1\text{H}$  NMR spectrum of **6** (300 MHz, 298 K,  $\text{CDCl}_3$ ).

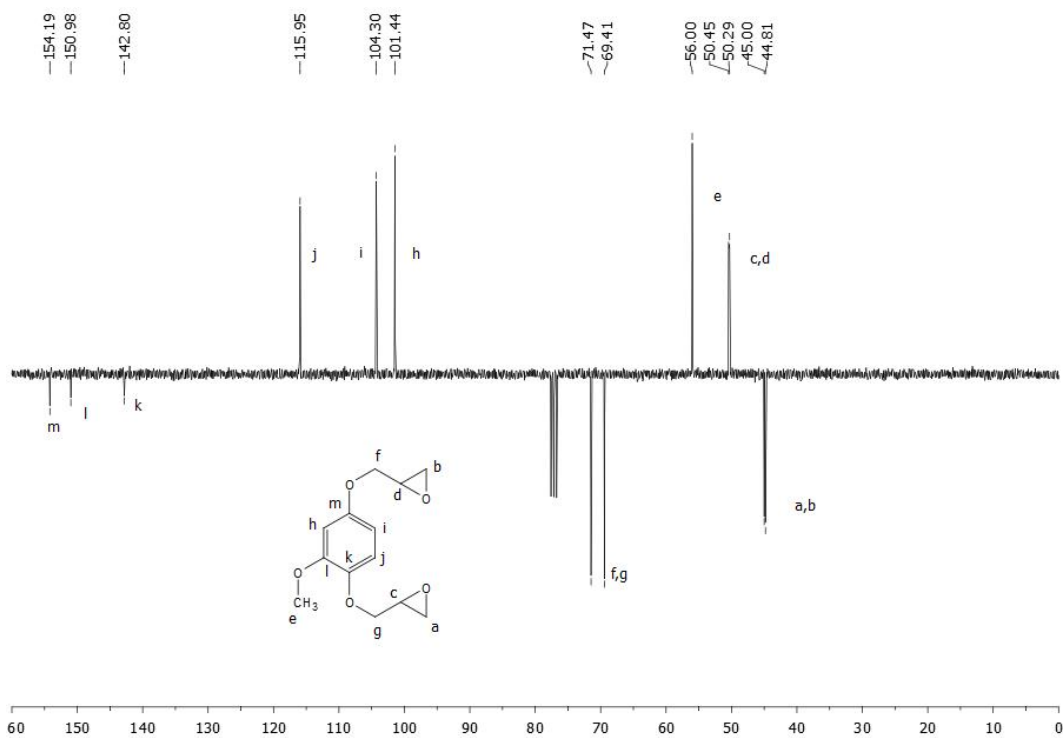


**Figure A.3.8.**  $^{13}\text{C}$  APT NMR **6** (75 MHz, 298 K,  $\text{CDCl}_3$ ).

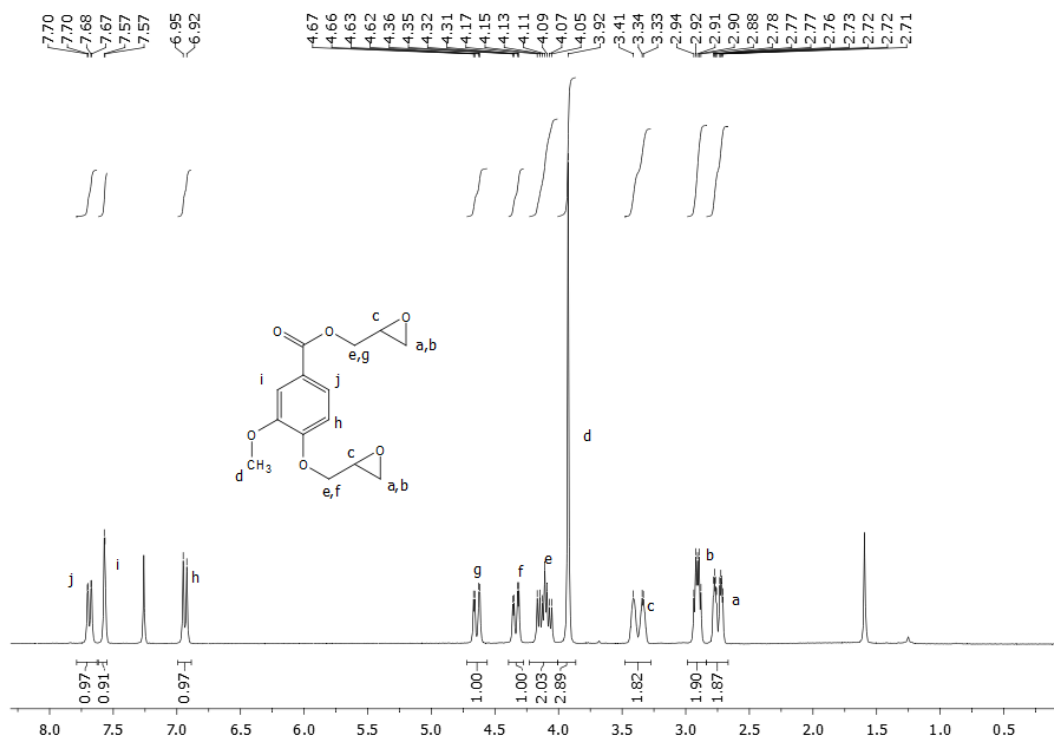


**Figure A.3.9.**  $^1\text{H}$  NMR spectrum of **7** (300 MHz, 298 K,  $\text{CDCl}_3$ ).

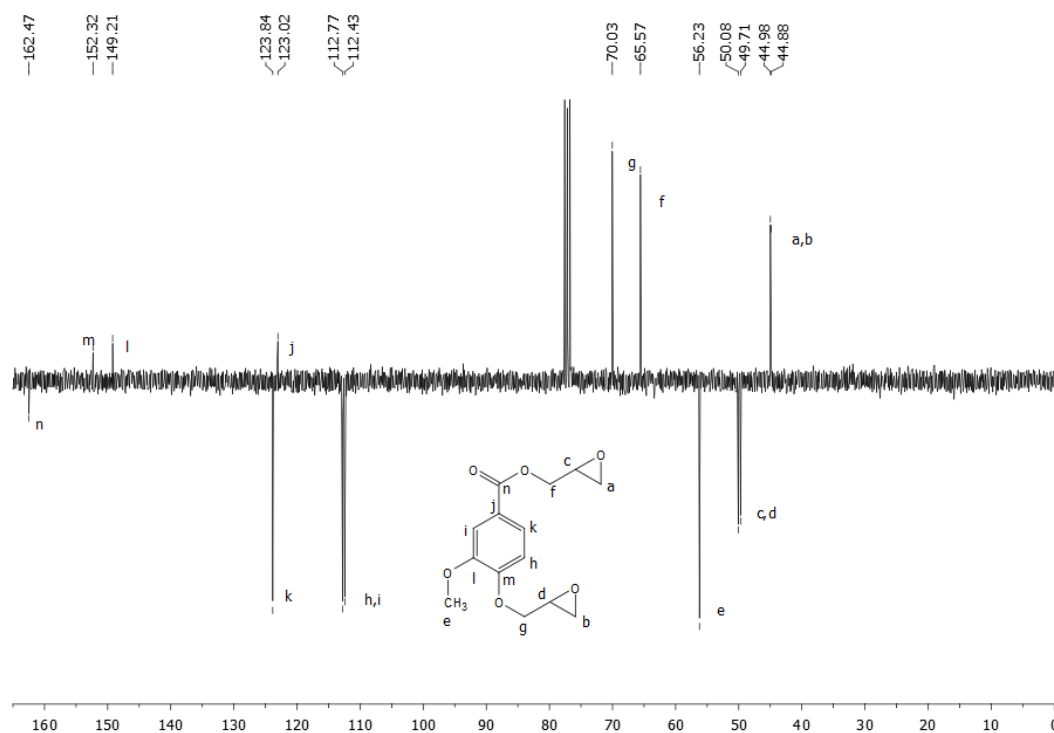


**Figure A.3.10.**  $^{13}\text{C}$  APT NMR spectrum of **7** (75 MHz, 298 K,  $\text{CDCl}_3$ ).

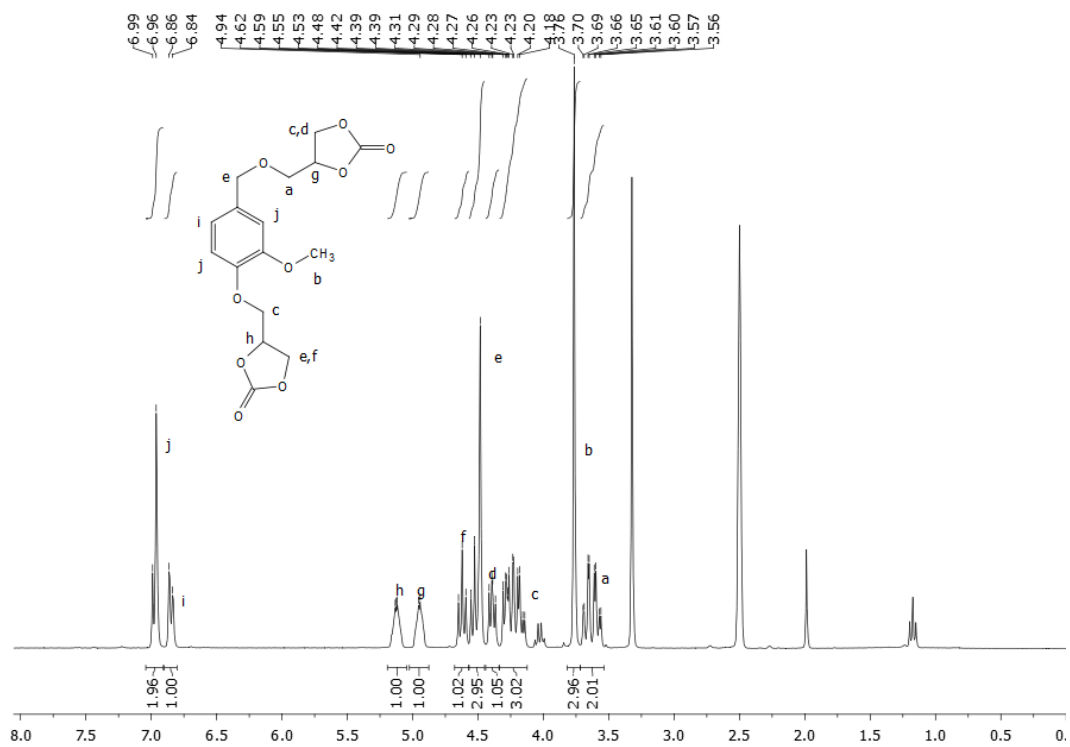


**Figure A.3.11.** <sup>1</sup>H NMR spectrum of **8** (300 MHz, 298 K, DMSO).

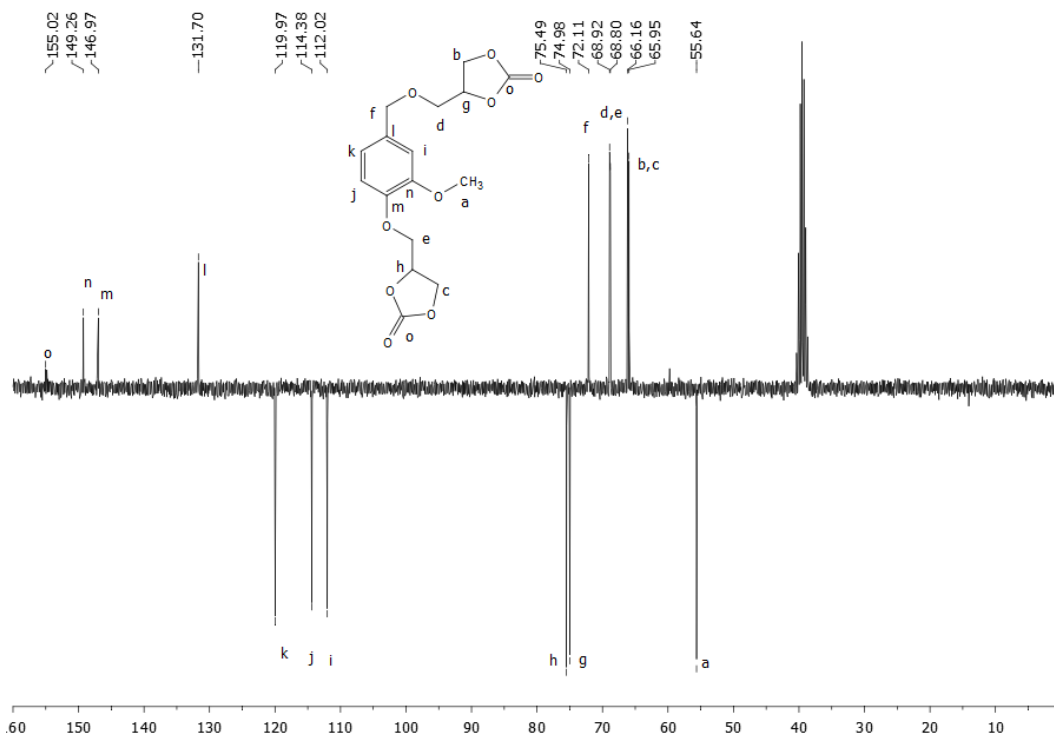


**Figure A.3.12.** <sup>13</sup>C APT NMR spectrum of **8** (75 MHz, 298 K, DMSO).

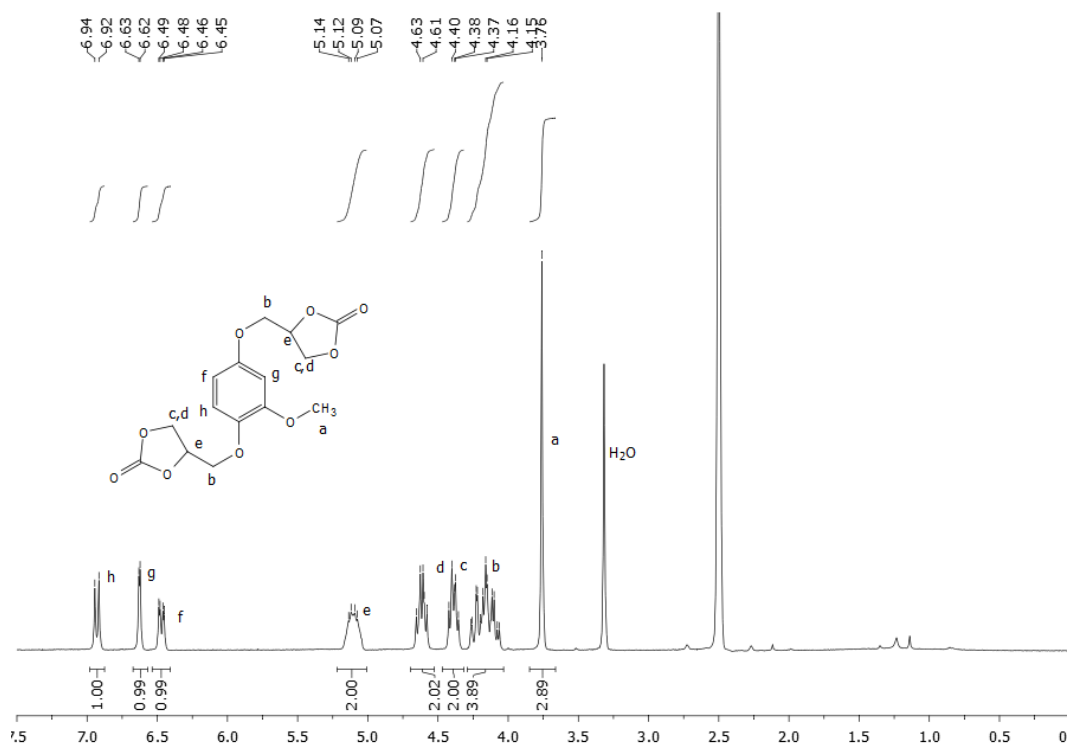


**Figure A.3.13.**  $^1\text{H}$  NMR spectrum of **9** (300 MHz, 298 K, DMSO).

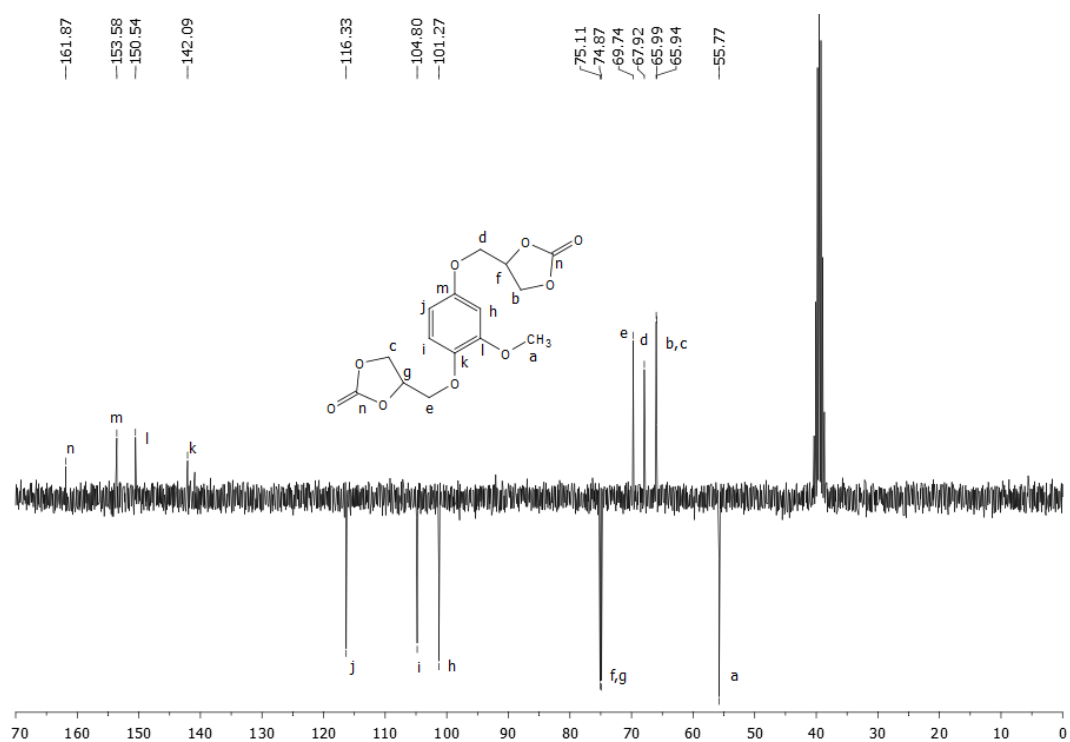


**Figure A.3.14.**  $^{13}\text{C}$  APT NMR spectrum of **9** (75 MHz, 298 K, DMSO).

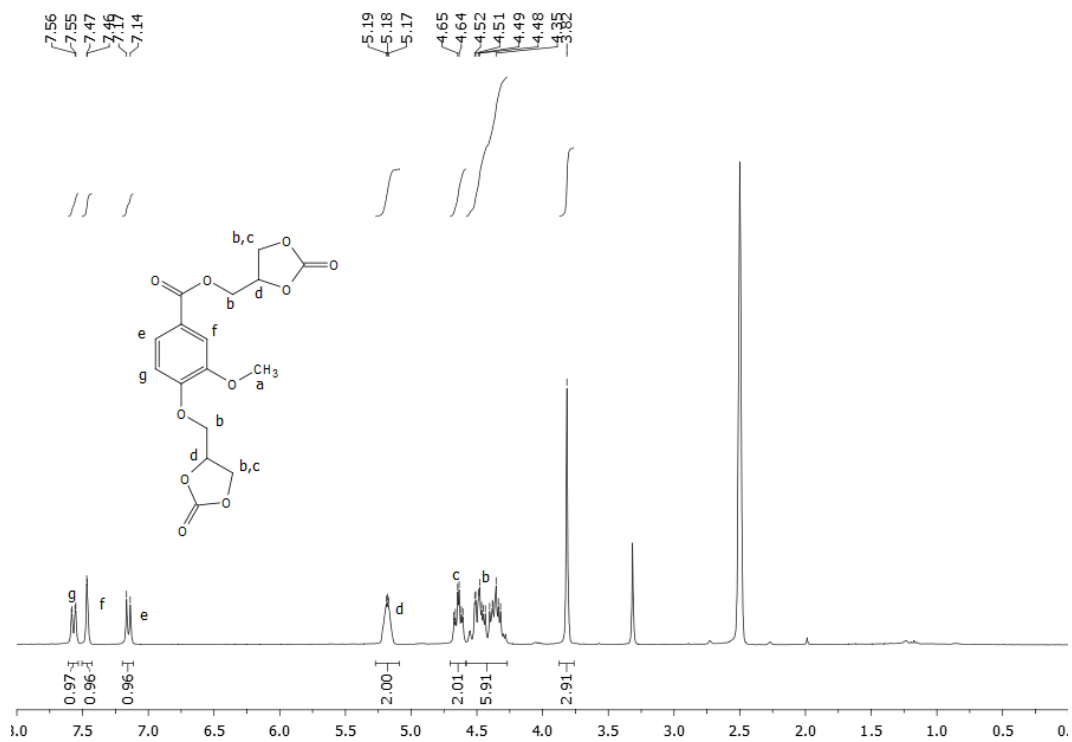


**Figure A.3.15.** <sup>1</sup>H NMR spectrum of **10** (300 MHz, 298 K, DMSO).

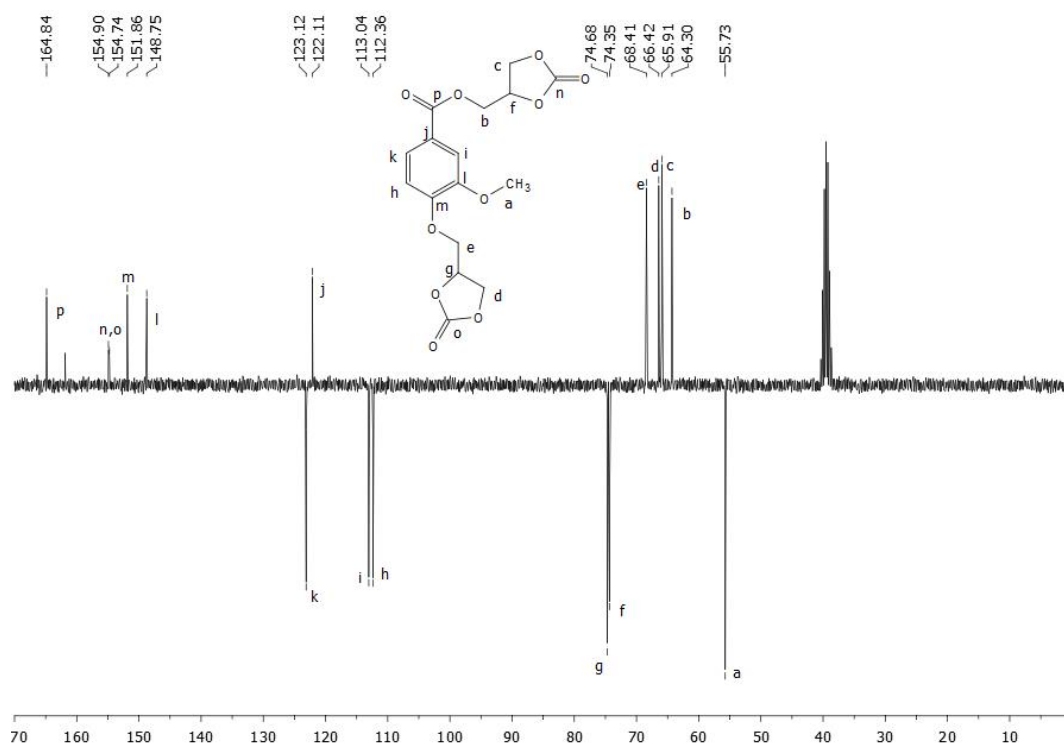


**Figure A.3.16.** <sup>13</sup>C APT NMR spectrum of **10** (75 MHz, 298 K, DMSO).



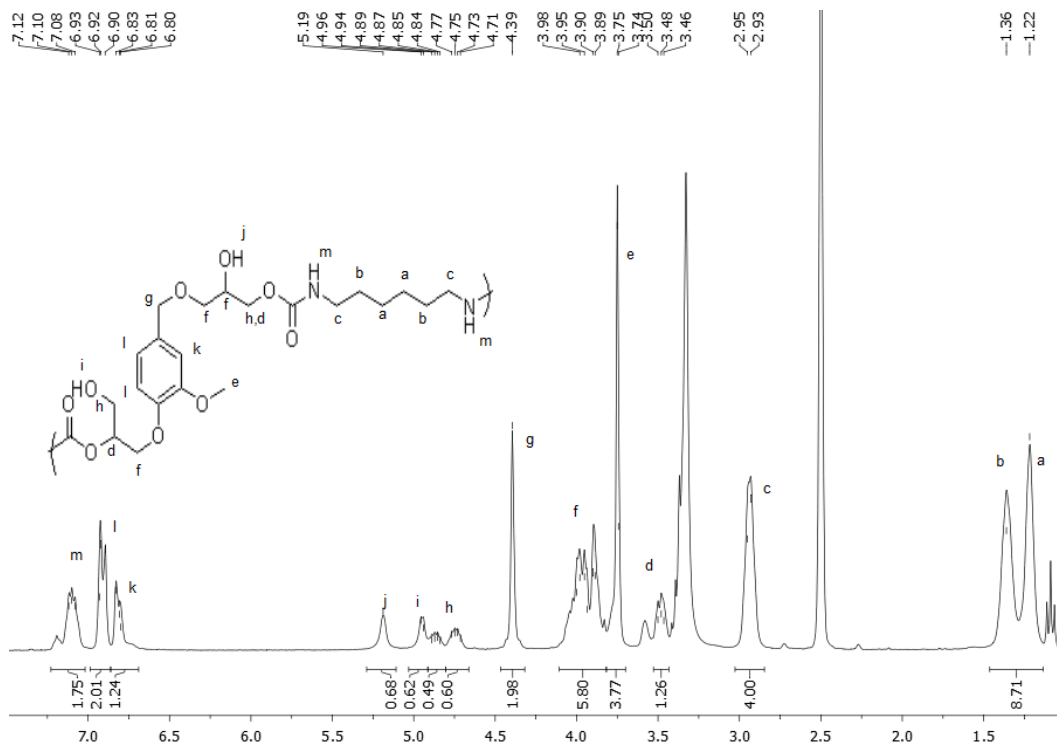


**Figure A.3.17.**  $^1\text{H}$  NMR spectrum of NIPU **11** (300 MHz, 298 K, DMSO).

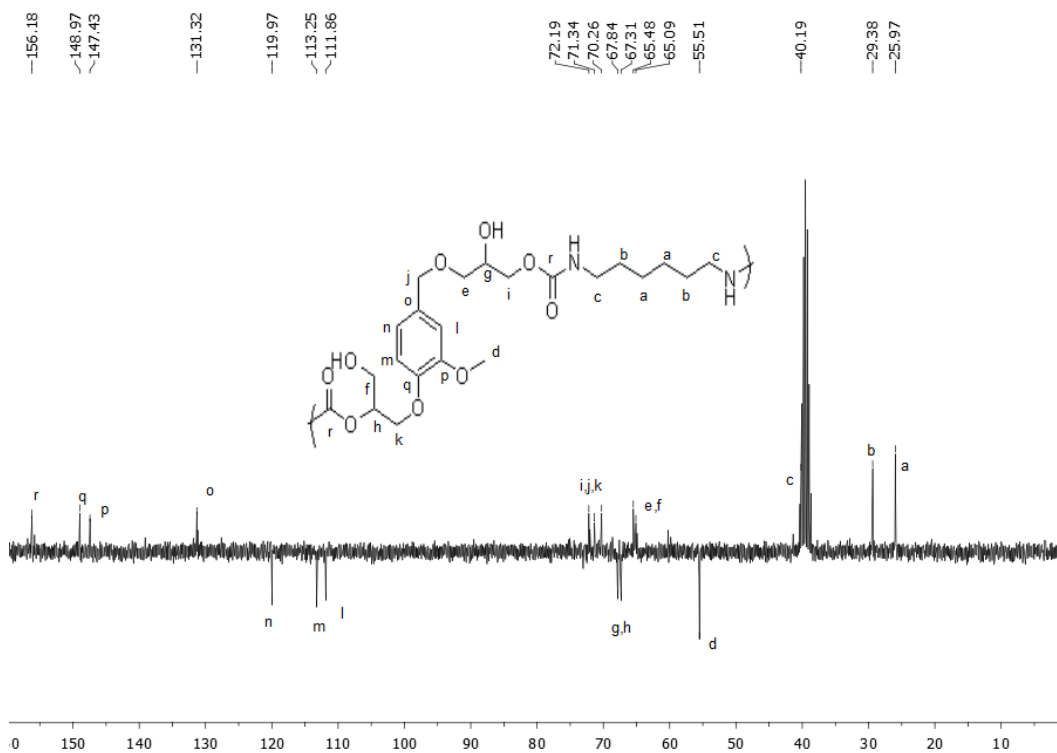


**Figure A.3.18.**  $^{13}\text{C}$  APT NMR spectrum of **11** (75 MHz, 298 K, DMSO).

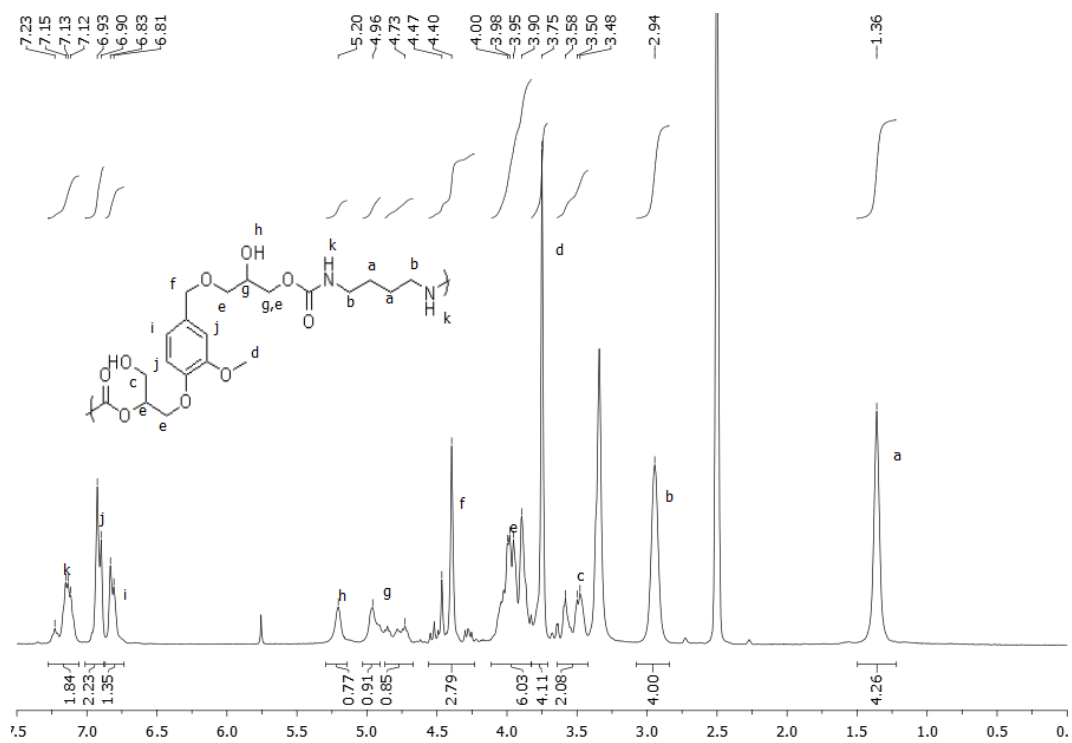


**Figure A.3.19.**  $^1\text{H}$  NMR spectrum of NIPU 12 (300 MHz, 298 K, DMSO).

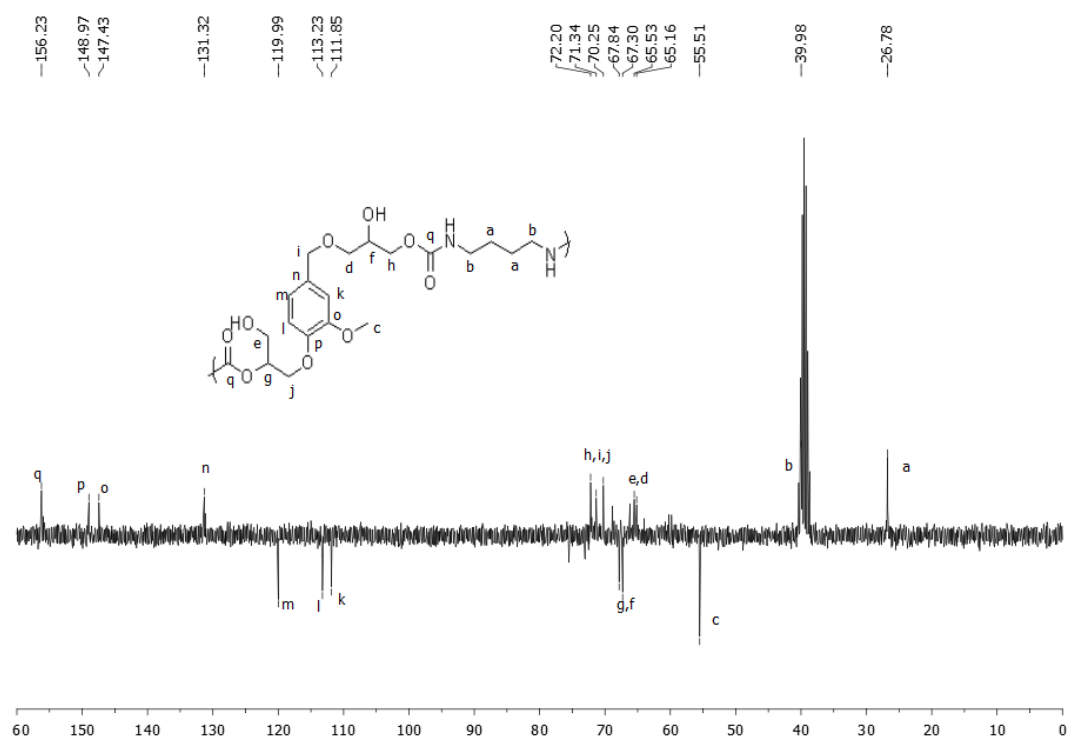


**Figure A.3.20.**  $^{13}\text{C}$  APT NMR spectrum of 12 (75 MHz, 298 K, DMSO).

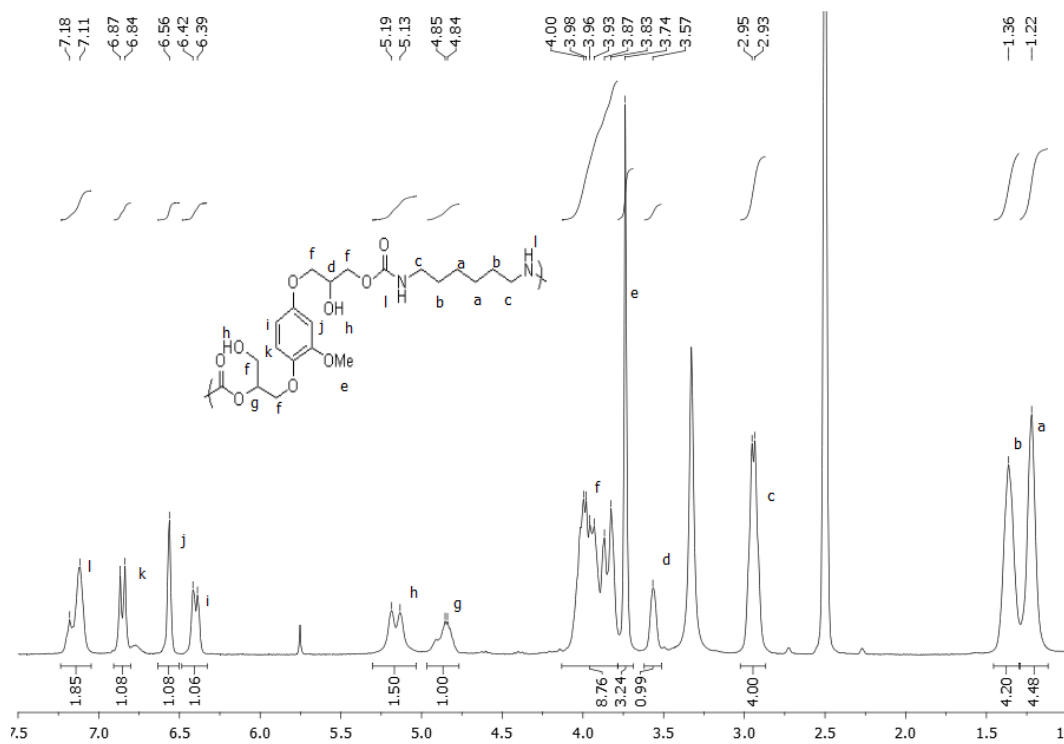


**Figure A.3.21.**  $^1\text{H}$  NMR spectrum of NIPU **13** (300 MHz, 298 K, DMSO).

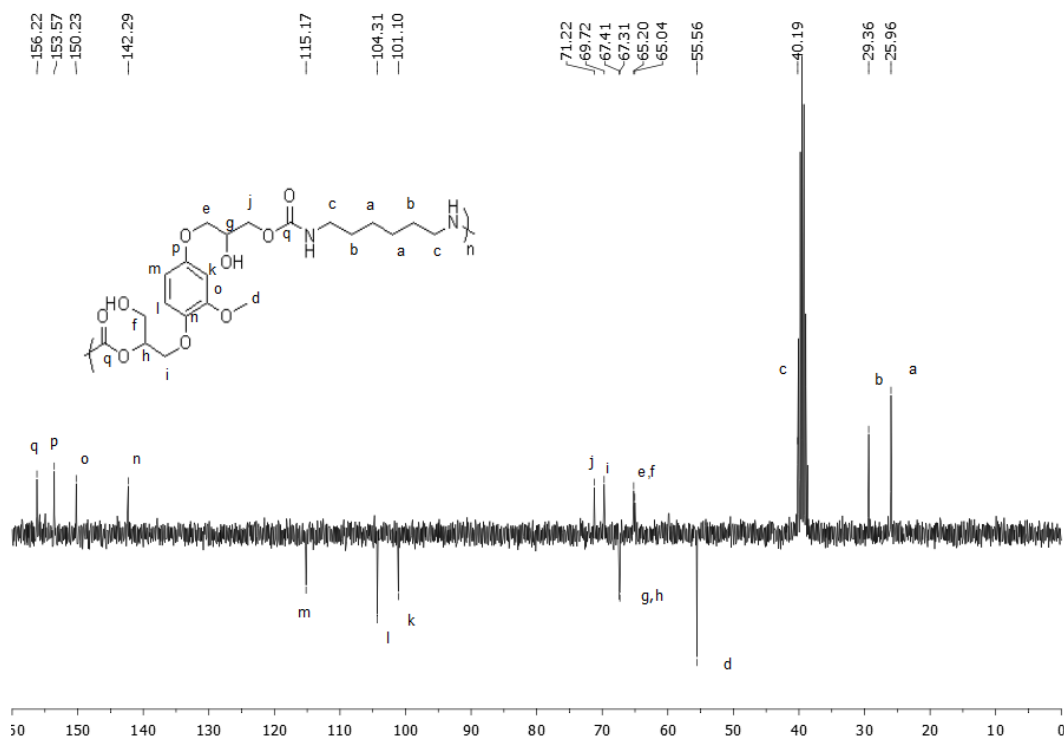


**Figure A.3.22.**  $^{13}\text{C}$  APT NMR spectrum of **13** (75 MHz, 298 K, DMSO).

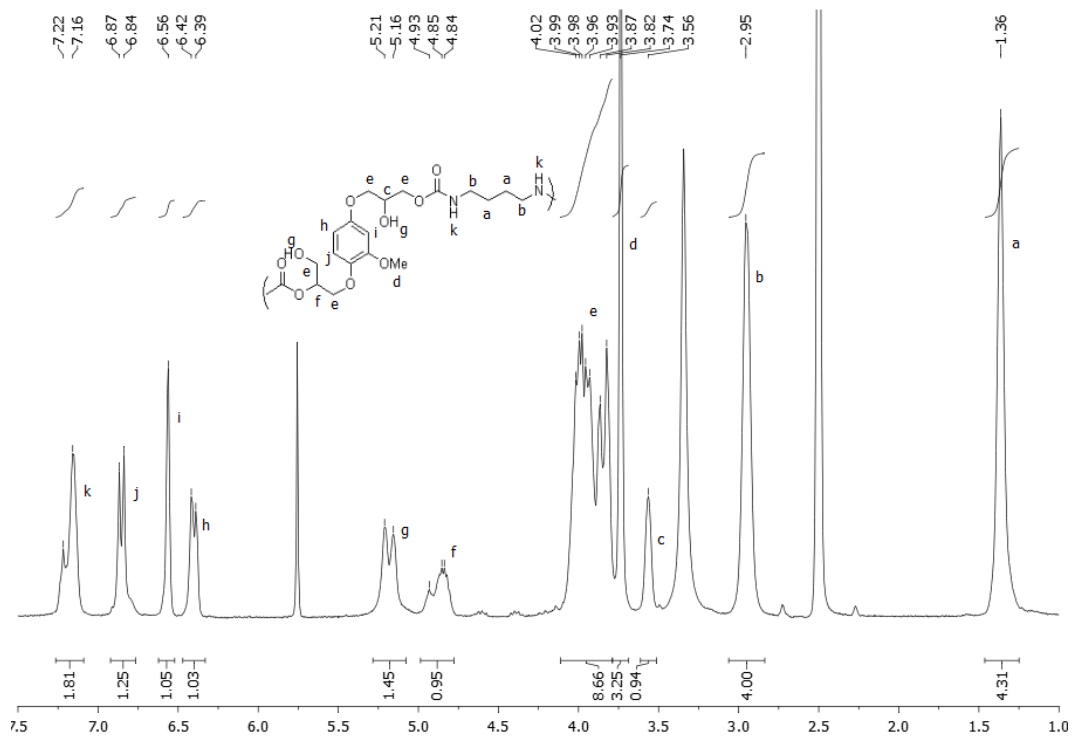


**Figure A.3.23.**  $^1\text{H}$  NMR spectrum of NIPU **14** (300 MHz, 298 K, DMSO).

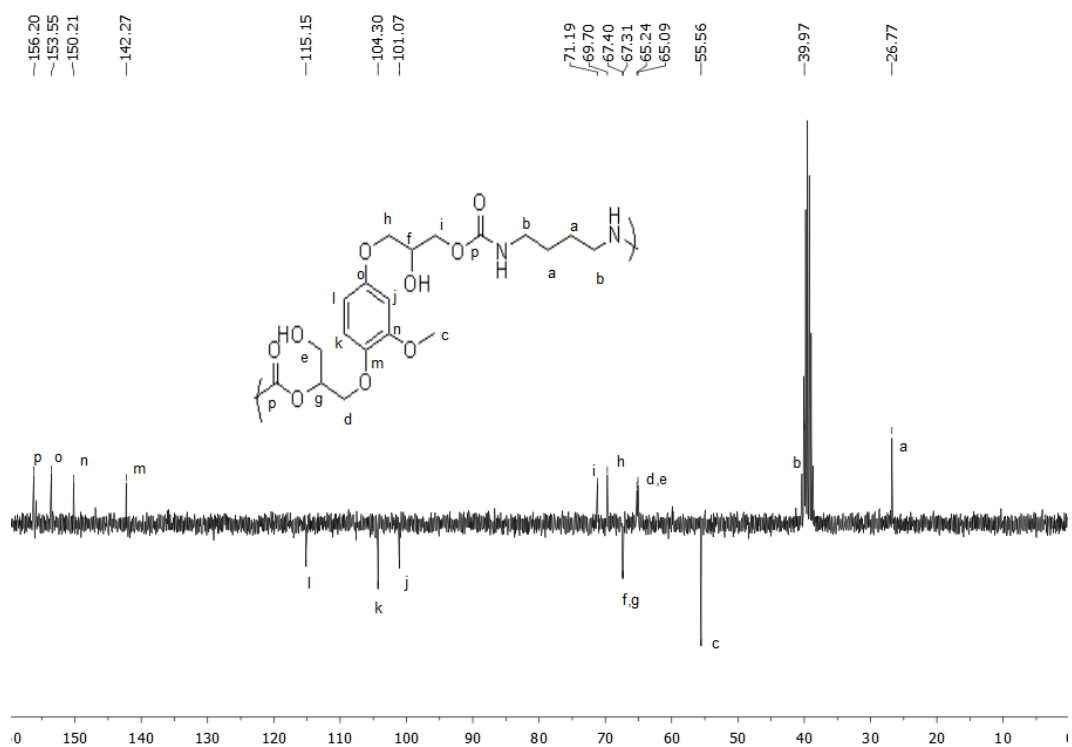


**Figure A.3.24.**  $^{13}\text{C}$  APT NMR spectrum of **14** (75 MHz, 298 K, DMSO).

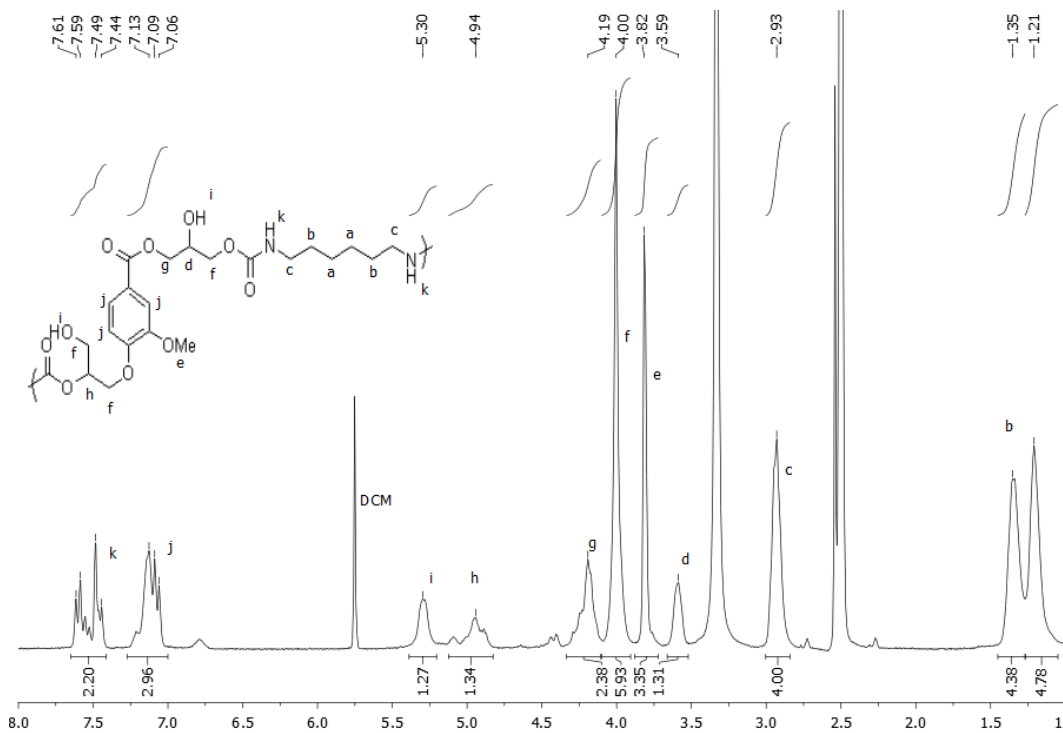


**Figure A.3.25.**  $^1\text{H}$  NMR spectrum of NIPU **15** (300 MHz, 298 K, DMSO).

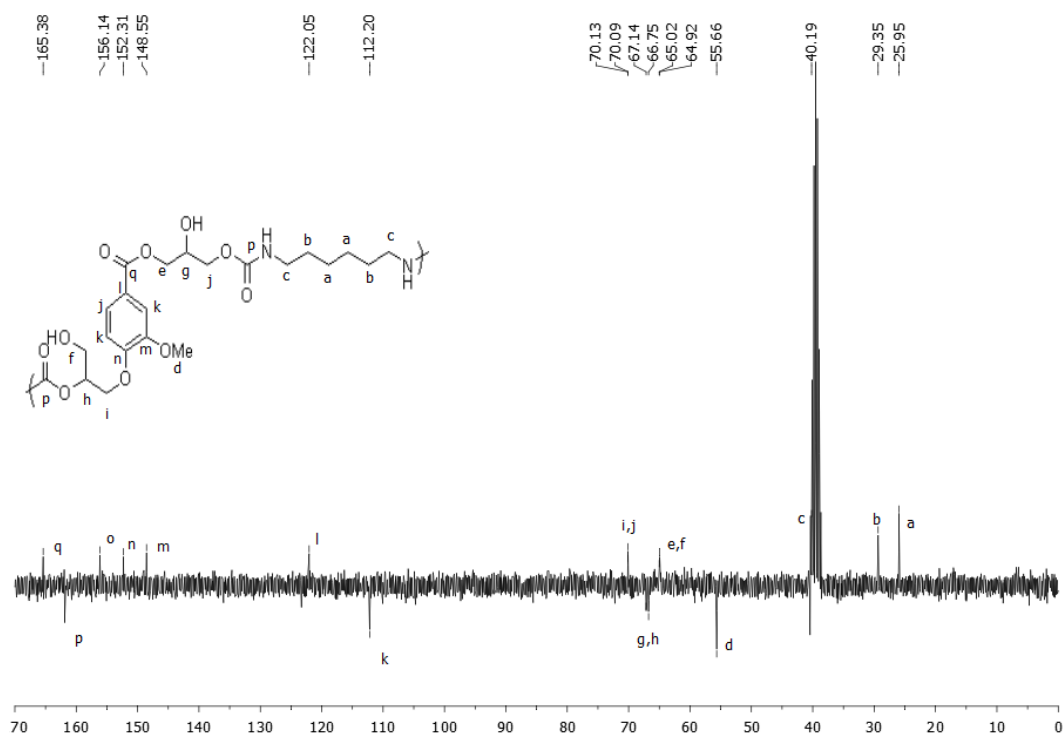


**Figure A.3.26.**  $^{13}\text{C}$  APT NMR spectrum of **15** (75 MHz, 298 K, DMSO).

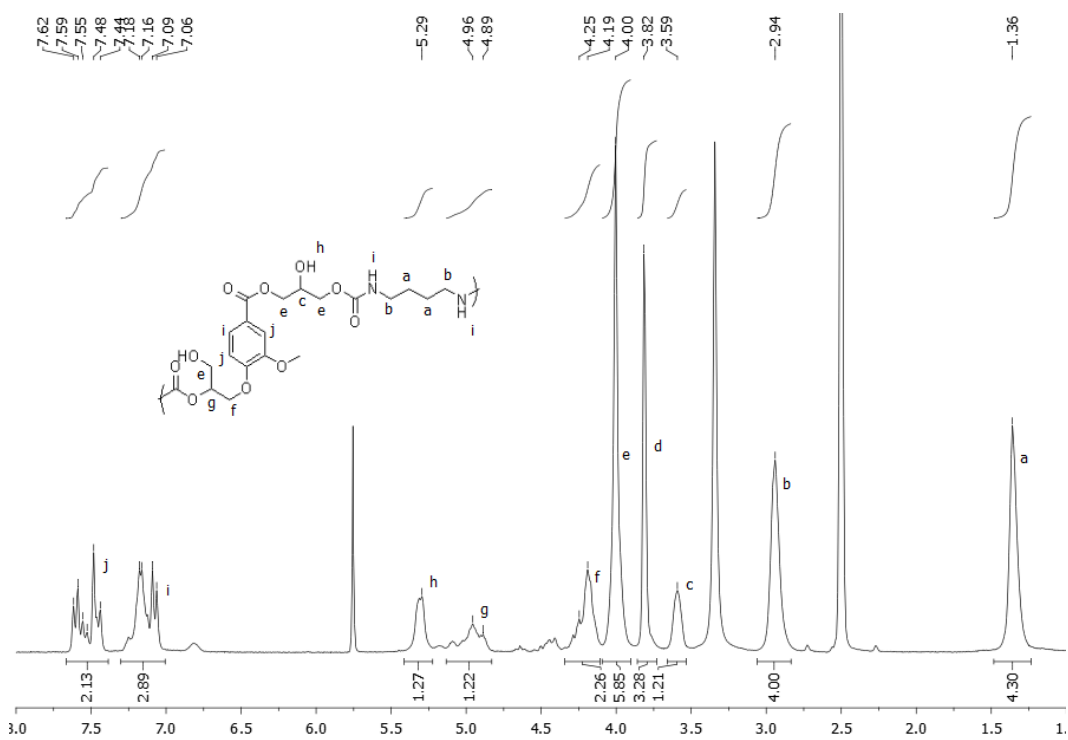


**Figure A.3.27.**  $^1\text{H}$  NMR spectrum of NIPU **16** (300 MHz, 298 K, DMSO).

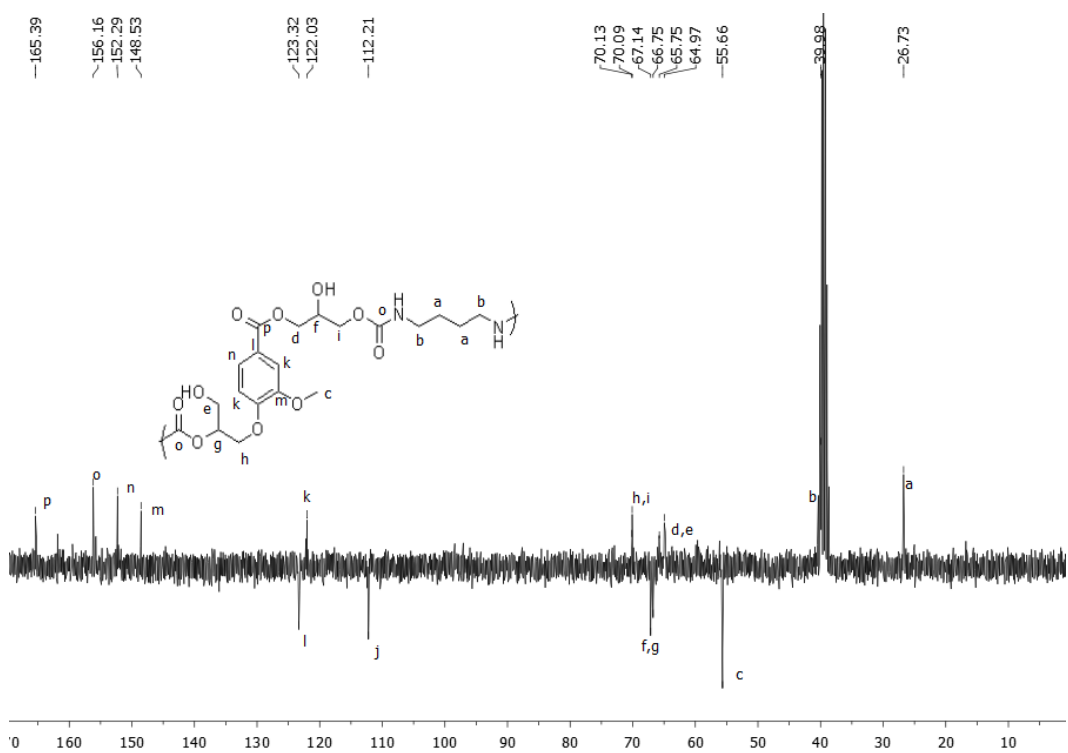


**Figure A.3.28.**  $^{13}\text{C}$  APT NMR spectrum of **16** (75 MHz, 298 K, DMSO).

## A.4 Supplementary NMR spectra for Chapter 5

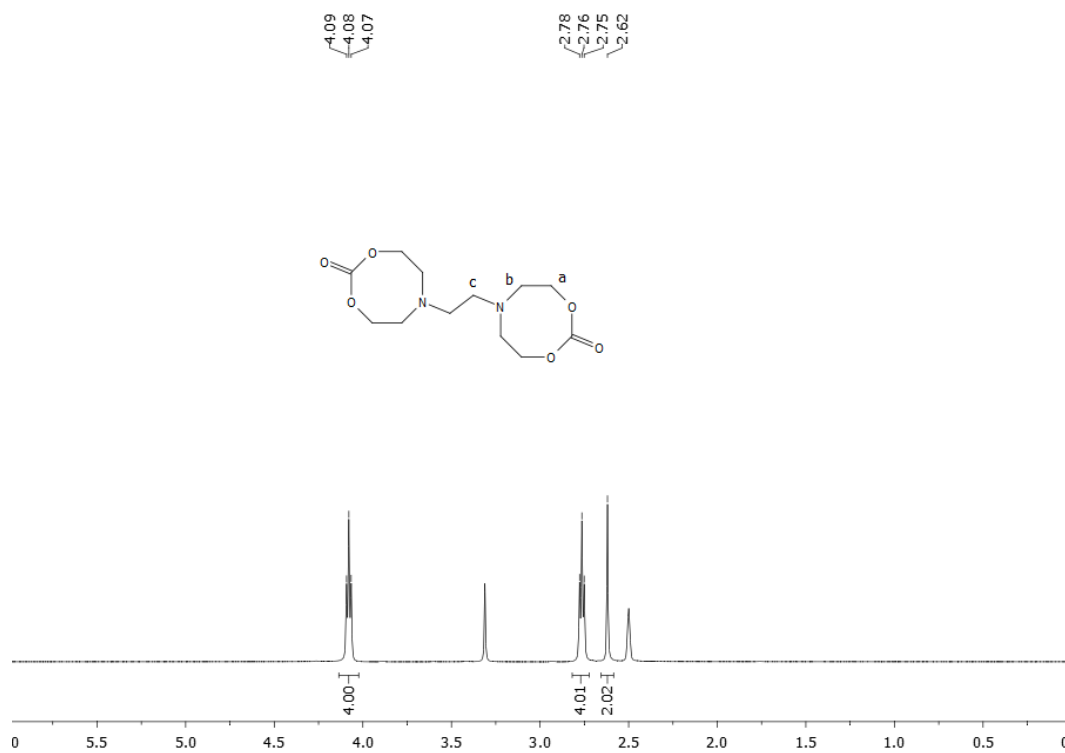


**Figure A.4.1.** <sup>1</sup>H NMR spectrum of **1** (300 MHz, 298 K, DMSO).

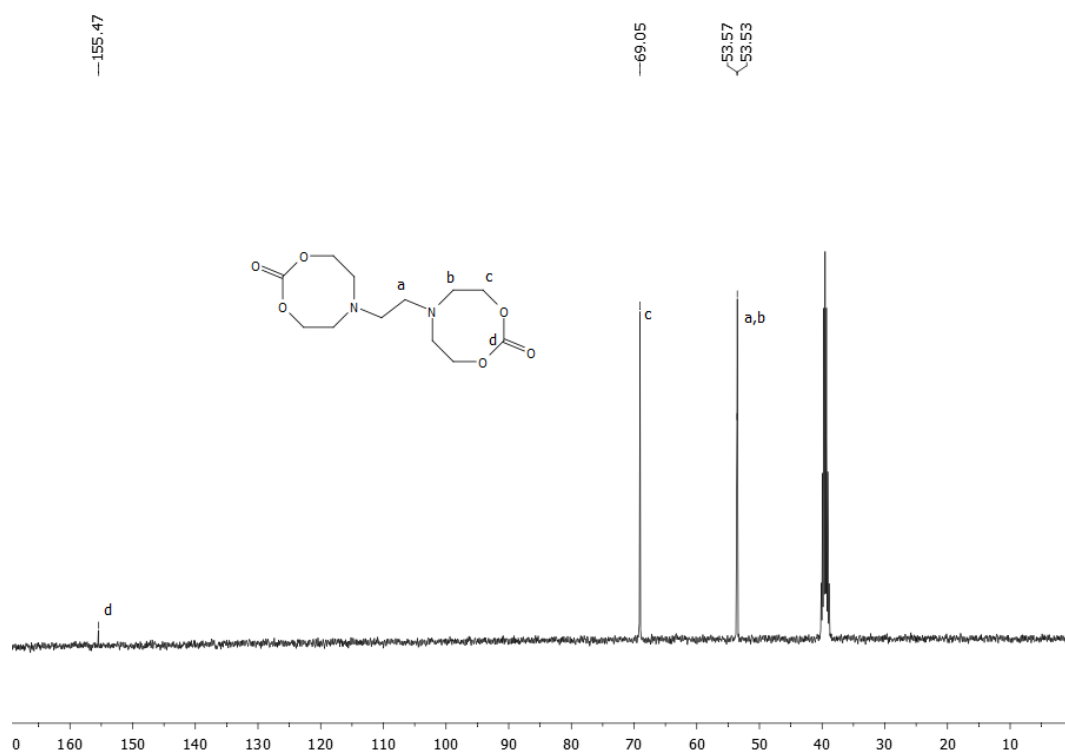


**Figure A.4.2.** <sup>13</sup>C NMR spectrum of **1** (75 MHz, 298 K, DMSO).

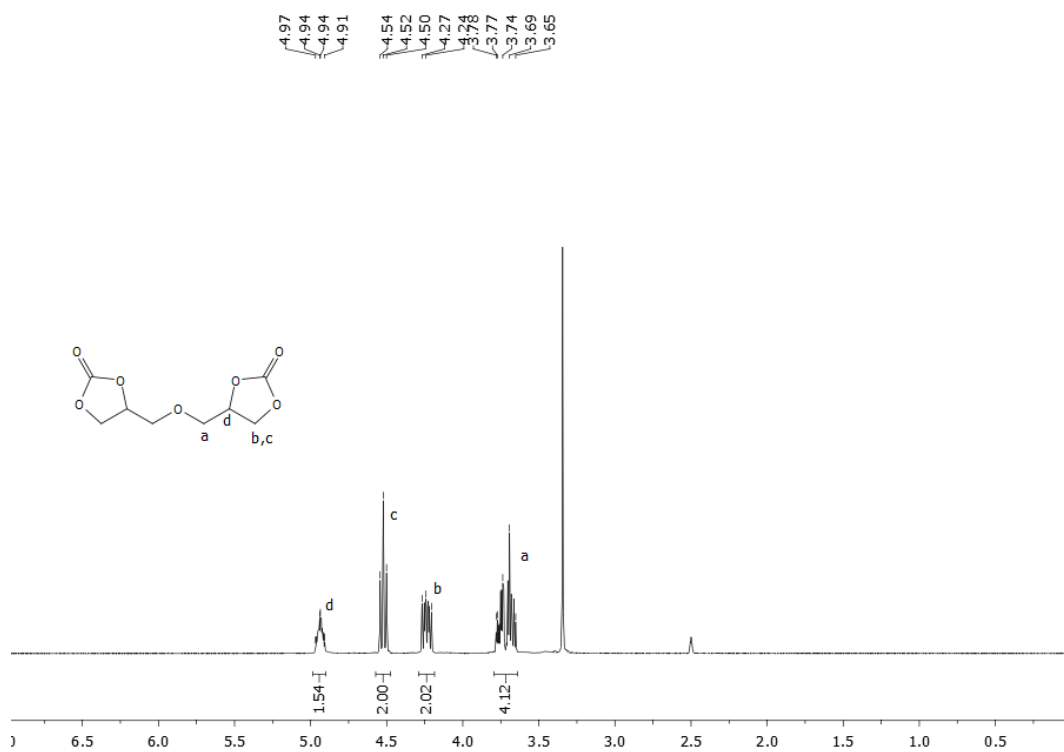


**Figure A.4.3.** <sup>1</sup>H NMR spectrum of **2** (300 MHz, 298 K, DMSO).

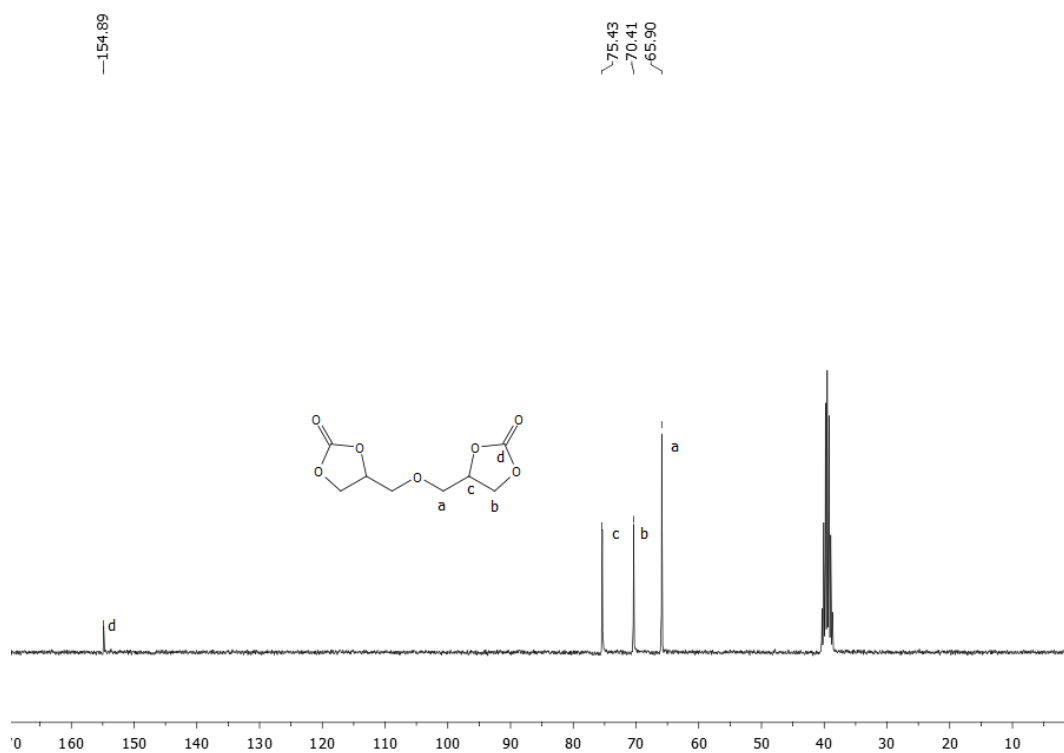


**Figure A.4.4.** <sup>13</sup>C NMR spectrum of **2** (75 MHz, 298 K, DMSO).